



**UNIVERSIDAD NACIONAL AUTÓNOMA DE MÉXICO**

**PROGRAMA DE MAESTRÍA Y DOCTORADO EN CIENCIAS QUÍMICAS**

ESTABILIDAD DE ALGUNAS BASES NITROGENADAS EN UN SISTEMA QUE  
SIMULA UNA VENTILA HIDROTHERMAL

**TESIS**

PARA OPTAR POR EL GRADO DE

**DOCTOR EN CIENCIAS**

PRESENTA

M. en C. JORGE ARMANDO CRUZ CASTAÑEDA

DRA. ALICIA NEGRÓN MENDOZA  
INSTITUTO DE CIENCIAS NUCLEARES

CIUDAD DE MÉXICO, JULIO 2019



Universidad Nacional  
Autónoma de México



**UNAM – Dirección General de Bibliotecas**  
**Tesis Digitales**  
**Restricciones de uso**

**DERECHOS RESERVADOS ©**  
**PROHIBIDA SU REPRODUCCIÓN TOTAL O PARCIAL**

Todo el material contenido en esta tesis esta protegido por la Ley Federal del Derecho de Autor (LFDA) de los Estados Unidos Mexicanos (México).

El uso de imágenes, fragmentos de videos, y demás material que sea objeto de protección de los derechos de autor, será exclusivamente para fines educativos e informativos y deberá citar la fuente donde la obtuvo mencionando el autor o autores. Cualquier uso distinto como el lucro, reproducción, edición o modificación, será perseguido y sancionado por el respectivo titular de los Derechos de Autor.



**UNIVERSIDAD NACIONAL AUTÓNOMA DE MÉXICO**

**PROGRAMA DE MAESTRÍA Y DOCTORADO EN CIENCIAS QUÍMICAS**

**ESTABILIDAD DE ALGUNAS BASES NITROGENADAS EN UN  
SISTEMA QUE SIMULA UNA VENTILA HIDROTHERMAL**

**TESIS  
PARA OPTAR POR EL GRADO DE**

**DOCTOR EN CIENCIAS**

**PRESENTA**

**M. en C. JORGE ARMANDO CRUZ CASTAÑEDA**

**DRA. ALICIA NEGRÓN MENDOZA  
INSTITUTO DE CIENCIAS NUCLEARES**



Ciudad de México, julio 2019

## **Agradecimientos**

A mi *alma mater*, mi amada Universidad Nacional Autónoma de México, por formarme académicamente y por abrirme las puertas del mundo.

A los laboratorios del Departamento de Química de Radiaciones y Radioquímica, en el Instituto de Ciencias Nucleares, por permitirme aprender, utilizando sus equipos, su infraestructura y su muy valioso personal en la elaboración de esta tesis.

A la Dra. Alicia Negrón Mendoza, por siempre darme la oportunidad de ser parte de su equipo de investigación, por su apoyo incondicional en mi formación académica, docente y personal, por su paciencia, confianza y amistad.

Al CONACyT, por la beca No. 360049, para la realización de mis estudios de Doctorado y por el apoyo en el proyecto C0011-CONACyT-ANR-188689.

A DGAPA por el apoyo 068318 otorgado a través del proyecto IN111116.

Al Programa de Maestría y Doctorado en Ciencias Químicas, UNAM.

Al Dr. Dwight Roberto Acosta Najarro por aceptar ser parte de mi jurado, por su tiempo y por sus propuestas para mejorar esta tesis.

Al Dr. Manuel Jiménez Estrada, por aceptar ser parte de mi jurado, parte de mi comité tutorial y por el tiempo invertido para la corrección y mejora a este trabajo de tesis.

A la Dra. Sofía Guillermina Burillo Amezcua, por aceptar ser parte de mi jurado, por tiempo dedicado a las correcciones y por los valiosos aportes para mejorar esta tesis.

A la Dra. María Guadalupe Cordero Tercero, por aceptar ser parte de mi jurado y por el tiempo invertido en la revisión y corrección de esta tesis.

Al Dr. Juan Manuel Navarrete Tejero, por aceptar ser parte de mi jurado y por el tiempo invertido en el mejoramiento de esta tesis.

Al Dr. Fernando Ortega Gutiérrez, por ser parte de mi comité tutorial y por el tiempo dedicado a evaluar y mejorar mi proyecto y tesis doctoral.

Al Dr. Sergio Ramos Bernal, por tomarse la atención de revisar este trabajo, por sus consejos y atenciones sobre todo y por permitirme aprender de él.

A la Dra. María Colín García, por la valiosa e importante colaboración esta tesis, pero más aún, por ser una excelente amiga.

Al Dr. Alejandro Heredia Barbero por su colaboración en el desarrollo de este proyecto y por su amistad.

A la QFB. Claudia Camargo, por apoyo otorgado para la realización de esta tesis, por su gran disposición para ayudarme, por su amistad y por sus consejos.

A el M. en C. Benjamín Leal Acevedo y el Fis. Francisco García Flores por su tiempo y apoyo en los servicios de irradiación de las muestras en el ICN, UNAM.

A la M. en C. Virginia Gómez Vidales, por el apoyo en el análisis de las muestras de EPR en el IQ, UNAM.

Al M. en C. Edgar Islas Ortiz, por su tiempo, apoyo para el análisis electroquímico y por tanto años de amistad.

A la Dra. Adriana Leticia Meléndez López, por su tiempo y aportes para mejorar esta tesis, pero principalmente por amarme y por ser mi compañera en la vida. Te amo.



*Gracias a mi familia, a las personas, a los hechos y a las experiencias que hasta ahora  
me han formado.*

Artículos obtenidos y participaciones en congresos como resultado del presente trabajo:

### **Artículos publicados:**

- 1) **J. Cruz-Castañeda**, A. L. Méndez-López, A. Heredia, S. Ramos-Bernal and A. Negrón-Mendoza. Study of Solid-State Radiolysis of Behenic, Fumaric, and Sebacic Acids for their Possible Use as Gamma Dosimeters Measured Via ATR-FT-IR Spectroscopy. *J. Nucl. Phys. Mat. Sci. Rad. A.* 6:1:81–85 (2018). DOI: [10.15415/jnp.2018.61014](https://doi.org/10.15415/jnp.2018.61014)
- 2) E. Aguilar-Ovando, **J. Cruz-Castañeda**, T. Buhse, C. Fuentes-Carreón, S. Ramos-Bernal, A. Heredia y A. Negrón-Mendoza. Irradiation of glyceraldehyde under simulated prebiotic conditions: Study in solid and aqueous state. *J Radioanal Nucl Chem* 316:3:971-979 (2018) DOI: [10.1007/s10967-018-5830-4](https://doi.org/10.1007/s10967-018-5830-4)
- 3) **J. Cruz-Castañeda**, A. L. Méndez-López, S. Ramos-Bernal and A. Negrón-Mendoza. Radiolysis of the Glycolaldehyde-Na<sup>+</sup>Montmorillonite and Glycolaldehyde-Fe<sup>3+</sup>Montmorillonite Systems in Aqueous Suspension under Gamma Radiation Fields: Implications in Chemical Evolution. *J. Nucl. Phys. Mat. Sci. Rad. A.* 5:1:137–146 (2017) DOI: [10.15415/jnp.2017.51013](https://doi.org/10.15415/jnp.2017.51013)
- 4) **J. Cruz-Castañeda**, E. Aguilar-Ovando, T. Buhse, S. Ramos-Bernal, A. Méndez-López, C. Camargo-Raya, C. Fuentes-Carreón, A. Negrón-Mendoza. The importance of glyceraldehyde radiolysis in chemical evolution. *J Radioanal Nucl Chem.* 311:1135-1141 (2017) DOI: [10.1007/s10967-016-5080-2](https://doi.org/10.1007/s10967-016-5080-2)
- 5) **J. Cruz-Castañeda**, A. Negrón-Mendoza. Radiolysis and Thermolysis of Cytosine: Importance in Chemical Evolution. *J. Nucl. Phys. Mat. Sci. Rad. A.* 4:1:183–190 (2016) DOI: [10.15415/jnp.2016.41019](https://doi.org/10.15415/jnp.2016.41019)
- 6) **J. Cruz-Castañeda**, A. Negrón-Mendoza, D. Frías, M. Colín-García A. Heredia S. Ramos-Bernal, S. Villafañe-Barajas. Chemical evolution studies: the radiolysis and thermal decomposition of malonic acid. *J Radioanal Nucl Chem.* 304:1:219-225 (2015) DOI: [10.1007/s10967-014-3711-z](https://doi.org/10.1007/s10967-014-3711-z)
- 7) **J. Cruz-Castañeda**, M. Colín-García, A. Negrón-Mendoza. The Possible Role of Hydrothermal Vents in Chemical Evolution: Succinic Acid Radiolysis and Thermolysis. *AIP Conference Proceedings* 1607:1:104-110 (2014) DOI: [10.1063/1.4890709](https://doi.org/10.1063/1.4890709)
- 8) **J. Cruz-Castañeda**, A. Negrón-Mendoza, S. Ramos-Bernal. Formation of Hydrocarbons from Acid-Clay Suspensions by Gamma Irradiation. *AIP Conference Proceedings* 1544:1:49-52 (2013) DOI: [10.1063/1.4813459](https://doi.org/10.1063/1.4813459)

### **Participación en congresos internacionales:**

- 2018 The First Billion Years: Bombardment, Flagstaff, Arizona, EE.UU
- 2018 XIV International Symposium on Radiation Physics, Puebla, México.
- 2017 Habitable Worlds 2017: A System Science Workshop, Laramie, Wy, EE.UU.
- 2017 XVIII<sup>th</sup> International Conference on the Origin of Life, San Diego, California, EE.UU.
- 2017 XIII International Symposium on Radiation Physics, Puebla, México.
- 2016 XII International Symposium on Radiation Physics, Puebla, México.
- 2015 2<sup>nd</sup> COSPAR Symposium, held in Foz do Iguacu, Brasil.
- 2015 Third International Conference on Radiation and Application in Various Fields of Research, Bunva, Montenegro.

# Índice general

<b>Resumen</b> .....	8
1. Capítulo primero .....	9
Antecedentes y generalidades .....	9
1.1. La Tierra primitiva y el origen de la vida .....	9
1.2. Evolución química y química prebiótica .....	10
1.3. Materia orgánica de importancia biológica y pre-biológica relevante en química prebiótica .....	12
1.4. Fuentes de energía probables en la Tierra primitiva .....	17
1.5. Superficies minerales relevantes en la Tierra primitiva .....	20
1.6. Ambientes geológicos probables en la Tierra primitiva .....	21
1.6.1. Manantiales hidrotermales submarinos .....	21
1.6.2. Manantiales hidrotermales subaéreos .....	25
1.7. Variables fisicoquímicas posibles en experimentos de química prebiótica simulando manantiales hidrotermales .....	28
2. Capítulo segundo. Hipótesis .....	29
3. Capítulo tercero. Objetivos .....	30
3.1. Objetivo general .....	30
3.2. Objetivos particulares .....	31
4. Capítulo cuarto. Procedimiento experimental .....	32
4.1. Preparación de materiales .....	32
4.2. Reactivos utilizados .....	33
4.3. Preparación de muestras .....	34
4.4. Termólisis de muestras .....	34
4.5. Irradiación de muestras .....	36
Cuantificación e identificación de reactivos y productos de reacción .....	37
4.6. Espectroscopía de Infrarrojo TF-ATR .....	37
4.7. Espectrofotometría de UV-Vis .....	37
4.8. Polarografía .....	37
4.9. Cromatografía de gases (GC) .....	38
4.10. GC-Espectrometría de masas (CG-EM) .....	38
4.11. Cromatografía de líquidos de ultra alta presión (UHPLC-UV) .....	39
4.12. Cromatografía de líquidos-Espectrometría de masas (LC-EM) .....	40
4.13. Resonancia paramagnética electrónica (EPR) .....	40
5. Capítulo quinto. Resultados .....	41
5.1. Citosina (base pirimidínica) .....	41
5.1.1. Experimentos de termólisis .....	43
5.1.2. Experimentos de radiólisis .....	44
5.1.3. Experimentos con suspensiones .....	45
5.2. Guanina (base púrica) .....	46
5.2.1. Experimentos de radiólisis en disolución acuosa .....	46
5.2.2. Experimentos de radiólisis en estado sólido .....	47
5.2.3. Experimentos con suspensiones .....	47
5.3. Ácido succínico (ácido carboxílico – participante en el ciclo de Krebs) .....	49
5.3.1. Experimentos de termólisis .....	49
5.3.2. Experimentos de radiólisis .....	50
5.3.3. Experimentos con suspensiones .....	53
5.4. Ácido malónico (ácido carboxílico – inhibidor del ciclo de Krebs) .....	54
5.4.1. Experimentos de termólisis .....	54

5.4.2.	Experimentos de radiólisis .....	55
5.4.3.	Experimentos con suspensiones.....	58
5.5.	Gliceraldehído (triosa - quiral) .....	59
5.5.1.	Experimentos de radiólisis en disolución acuosa.....	59
5.5.2	Experimentos de radiólisis en estado sólido .....	62
5.5.3	Experimentos con suspensiones.....	65
5.6.	Glicolaldehído (diosa – no quiral).....	66
5.6.1.	Experimentos de radiólisis .....	66
5.6.2.	Experimentos con suspensiones.....	68
6.	Capítulo sexto. Discusión de resultados.....	71
6.1.	Citosina (base pirimidínica) .....	71
6.2.	Guanina (base púrica) .....	72
6.3.	Reactividad de las bases nitrogenadas en sistemas hidrotermales .....	73
6.4.	Ácido succínico (ácido carboxílico – participante en el ciclo de Krebs).....	74
6.5.	Ácido malónico (ácido carboxílico – inhibidor del ciclo de Krebs) .....	75
6.6.	Reactividad de los ácidos carboxílicos en sistemas hidrotermales .....	76
6.7.	Gliceraldehído (triosa - quiral) .....	77
6.8.	Glicolaldehído (diosa – no quiral).....	79
6.9.	Reactividad de los carbohidratos en sistemas hidrotermales.....	80
7.	Capítulo séptimo. Conclusiones.....	81
8.	Referencias .....	82
9.	Apéndice .....	87
9.1.	Compuestos modelo - Moléculas orgánicas: .....	87
9.2.	Quiralidad .....	90
9.3.	Técnica para obtener agua tridestilada descrita por O'Donell y Sangster en 1970.....	90
9.4.	Esterificación de Fisher .....	90
9.5.	Estructura del glicolaldehído en estado sólido y en disolución acuosa .....	91
9.6.	Cadena de decaimiento del <sup>235</sup> U .....	92
10.	Índice de tablas .....	93
11.	Índice de figuras .....	94
12.	Artículos publicados .....	97

## **Resumen**

El presente proyecto se enfoca en estudiar la estabilidad de algunas moléculas orgánicas modelo de importancia pre-biológica y biológica, en condiciones que simulan aquellas probables en la vecindad de un manantial hidrotermal en la Tierra primitiva, como ejemplo de una etapa importante de la evolución química en los tiempos primordiales.

Para este propósito, se estudió la cinética de descomposición de compuestos modelo (ácidos carboxílicos, carbohidratos y bases nitrogenadas) en disolución acuosa y en estado sólido. Para este objetivo, se estudió la influencia de los gradientes de temperatura (termólisis) o radiación ionizante (radiólisis) mediante técnicas espectroscópicas, electroquímicas y cromatográficas. Se utilizaron disoluciones libres oxígeno con salinidad, presión y pH fijos, en presencia o ausencia de minerales relevantes en los manantiales hidrotermales.

Entre los resultados más importantes, se destaca que el mecanismo de formación depende del tipo de energía utilizada y puede conducir a la obtención de diferentes productos, de los cuales algunos son relevantes en el contexto de evolución química. Cuando los sistemas bajo estudio fueron expuestos a energía térmica o radiación ionizante, se formaron compuestos que pueden tener importancia como moléculas pre-biológicas. Adicionalmente, los resultados obtenidos mostraron que existe una diferencia si en los sistemas está presente un mineral ya que, por ejemplo, los minerales pueden catalizar y direccionar la reacciones químicas, además de que también pueden ser agentes concentradores y agentes protectores de materia orgánica.

## **Abstract**

This project is focused on to study the stability of some organic molecules with pre-biological and biological importance simulating those probably present in the vicinity of a hydrothermal spring on the primitive Earth, as examples of an important stage of chemical evolution in primordial times. For this purpose, the kinetics of decomposition of model compounds (carboxylic acids, carbohydrates, and nitrogenous bases) in aqueous solution and solid state, was made. To this aim, the influence of temperature gradients (thermolysis) or ionizing radiation (radiolysis) was studied through spectroscopic, electrochemical, and chromatographic techniques. The salinity, pressure, and pH and free of oxygen solutions, were fixed, in the presence or absence of relevant minerals in the hydrothermal springs.

When the systems under study were exposed to thermal energy or ionizing radiation, they formed compounds that may have importance as pre-biological molecules. The results obtained showed that there is a difference if in the systems if there is a mineral present. The mechanism of formation is dependent on the type of energy used.

# 1. Capítulo primero

## Antecedentes y generalidades

### 1.1. La Tierra primitiva y el origen de la vida

Desde su formación, la Tierra ha experimentado diversos cambios los cuales continúan hasta la actualidad. El Precámbrico constituye una de las etapas más importantes en la historia del planeta, se inicia desde la formación de la Tierra hace 4.55-4.5 Ga aproximadamente (Allègre, Manhès, y Göpel, 1995) (1 Ga=1x10<sup>9</sup> años) y concluye hasta hace unos 0.54 Ga. Durante esta etapa, particularmente en los periodos Eoarqueano y Paleoarqueano (de 4 a 3.6 y de 3.6 a 3.2 Ga, respectivamente), ocurrieron muchos de los eventos más importantes del planeta, como ejemplo el paso de un planeta estéril a un mundo lleno de vida (Brocks, Buick, Summons, y Logan, 2003). Figura 1.

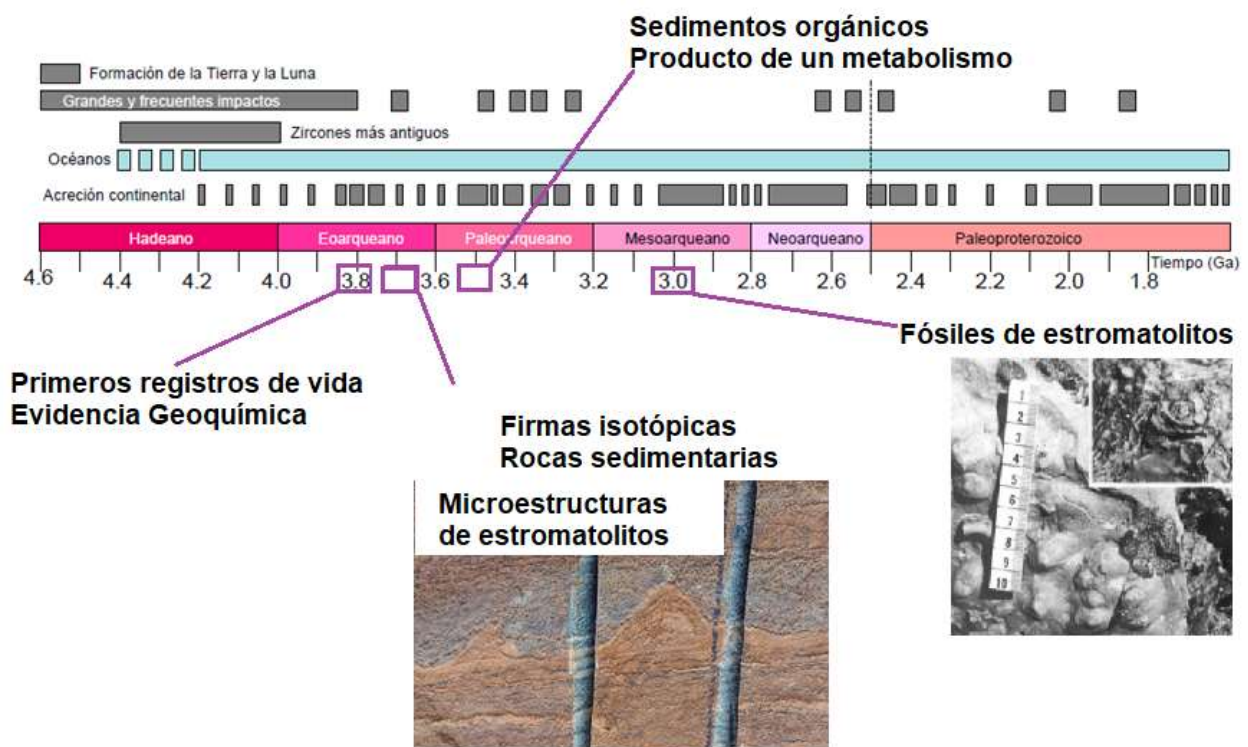


Figura 1. Primeros registros de vida (Manson y Von Brunn, 1977; Nutman *et al.*, 2016; Schidlowski, 2001; Walter, Buick, y Dunlop, 1980).

Existen diversas hipótesis que intentan explicar cómo los seres vivos pudieron emerger en la Tierra. Desde el punto de vista científico, existen dos enfoques principales en los cuales se propone cómo fue que las interacciones fisicoquímicas entre las moléculas orgánicas e inorgánicas presentes en la Tierra primitiva, pudieron originar la complejidad molecular actual. Por un lado, se encuentra el enfoque genético, que propone la gradual acumulación de compuestos orgánicos (especialmente compuestos que son parte del material genético) sintetizados en una atmósfera primitiva con grandes cantidades de dióxido de carbono, que formó lo que John. B. S. Haldane (1929) llamó la sopa primitiva (Haldane, 1929; Tirard, 2017). Por el otro, se encuentra la teoría metabólica, que propone la existencia de un metabolismo rudimentario primario (Wächtershäuser, 1988). Cualquier hipótesis en esta área de conocimiento, existente o futura, requiere considerar al menos los siguientes factores para que sea factible: 1) síntesis de materia orgánica a partir de compuestos más sencillos, 2) estabilidad de la materia orgánica sintetizada en el medio circundante, 3) fuentes de energía para promover las reacciones y 4) un ambiente geológico adecuado y probable que haya existido durante el periodo de evolución química.

## ***1.2. Evolución química y química prebiótica***

El estudio del origen de la vida se ha dividido principalmente en tres etapas: evolución nuclear, evolución química y evolución biológica (Calvin, 1956). La evolución química propuesta por Haldane en 1928 debió ocurrir en un periodo de tiempo corto en escala geológica, que va desde la formación de la Tierra hace 4.55-4.5 Ga hasta la aparición del primer ser vivo entre 3.8 y 3 Ga. El Hadeano (4.55-4.5

a 4 Ga) es el periodo de tiempo en la Tierra en donde se debió dar la mayoría de los procesos que tuvieron como consecuencia que la vida emergiera. Formalmente se define a la evolución química como la serie de procesos físicos y químicos que explican la formación abiótica de compuestos orgánicos de importancia biológica y los mecanismos por los cuales fueron aumentando su complejidad y ordenamiento, bajo condiciones que probablemente existieron en la Tierra primitiva (Negrón-Mendoza *et al.*, 1996; Orgel, 1968).

La química prebiótica, por otro lado, es una herramienta multidisciplinaria utilizada para estudiar procesos de la evolución química. En ella se proponen modelos químicos y se simulan condiciones en el laboratorio, que intentan explicar parte de los procesos que pudieron ser relevantes para que la vida emergiera en la Tierra primitiva. Uno de los experimentos más conocidos e importantes en esta área (Lazcano y Bada, 2003) fue el experimento desarrollado de por Stanley L. Miller en 1953 en el que sintetizó aminoácidos (Figura 2), en condiciones abióticas que se habían propuesto originalmente por Oparin y retomadas por H. C. Urey y J. D. Bernal (Miller, 1953).

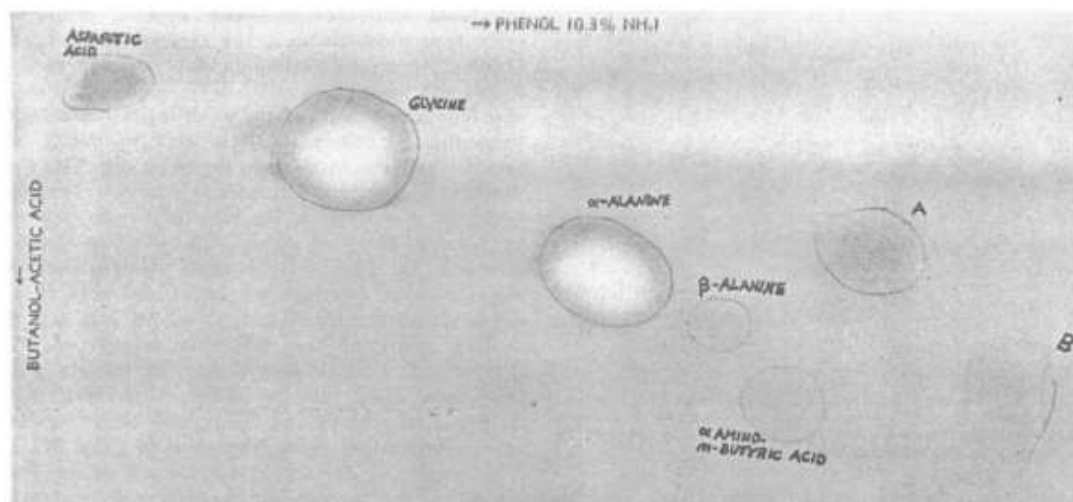


Figura 2. Cromatografía de papel para la identificación de aminoácidos en el experimento de Miller. Tomada de Miller (1953).



Cincuenta años después de la publicación de Milller, el químico Jeffrey L. Bada (estudiante de Miller) analizó muestras de viales sellados del experimento original de 1953 guardadas en el Instituto Oceanográfico de Scrips en La Jolla, EE.UU, reportando la formación de 23 aminoácidos, 4 aminas y 7 compuestos organosulfurados (Parker *et al.*, 2011).

### **1.3. Materia orgánica de importancia biológica y pre-biológica relevante en química prebiótica**

#### **1.3.1. Bases nitrogenadas**

Las bases nitrogenadas son compuestos cíclicos aromáticos que incluyen dos o más átomos de nitrógeno. Se les clasifica en dos tipos: las bases púricas (adenina y guanina), las cuales son derivados de la purina ( $C_5H_4N_4$ ) formada por dos anillos heterocíclicos, uno de seis y otro de cinco átomos (Figura 3) y las bases pirimídicas (citosina, timina y uracilo) las cuales provienen de la pirimidina ( $C_4H_4N_2$ ) formada por un anillo heterocíclico de seis átomos (Figura 4).

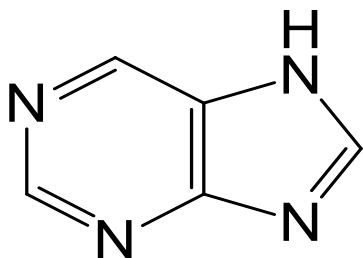


Figura 3. 9H-purina.

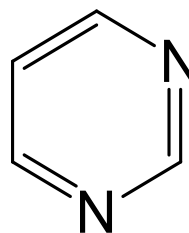


Figura 4. Pirimidina.

Las bases nitrogenadas son parte de macromoléculas orgánicas de gran importancia en química prebiótica, como el DNA (ácido desoxirribonucleico) y RNA (ácido ribonucleico), moléculas responsables de contener y transmitir la información genética; o en moléculas contenedoras de energía en diversos procesos metabólicos, como el ATP ( $C_{10}H_{16}N_5O_{13}P_3$ , adenosín trifosfato) (Figura 5) y el ADP (adenosín difosfato) o sus respectivos análogos con las diferentes bases nitrogenadas CTP, TTP, UTP, etc.

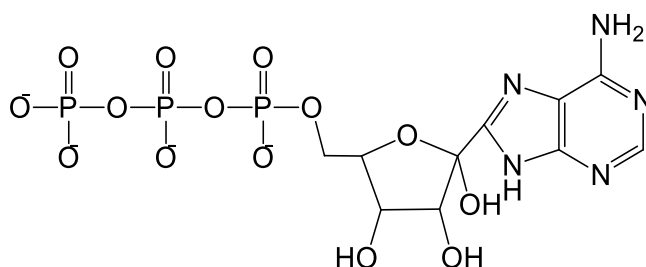


Figura 5. ATP adenosín trifosfato.

La síntesis abiótica de la adenina a partir de cianuro de amonio, propuesta por el Bioquímico Joan Oró en 1960 (Figura 6), es otro ejemplo de un experimento de química prebiótica (Oró, 1960). En 1983 Voet y Schwartz propusieron un posible mecanismo de reacción para la formación de adenina en *Bioorganic Chemistry* (Voet y Schwartz, 1983).

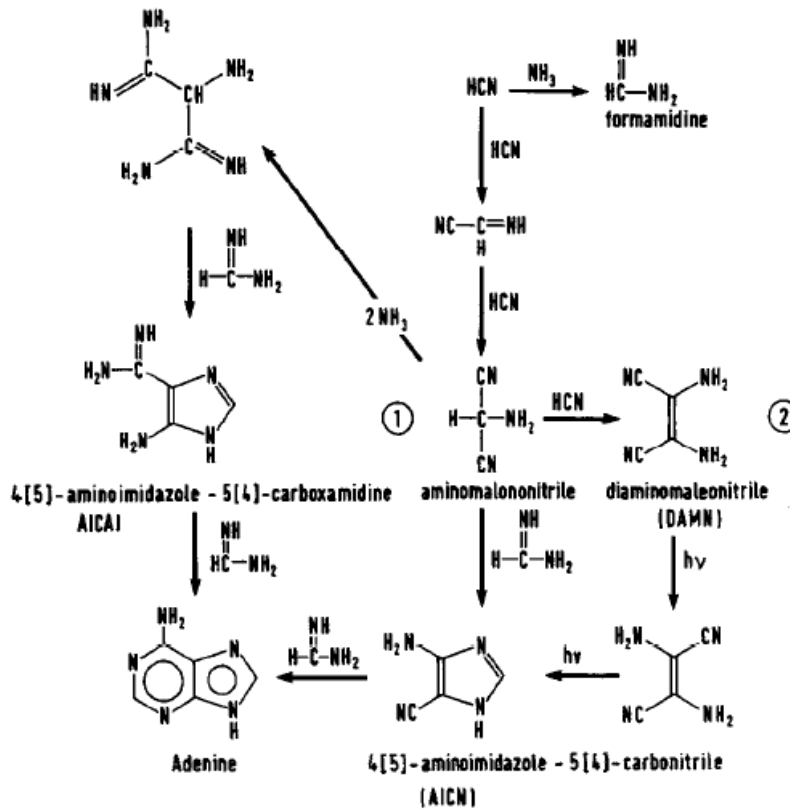


Figura 6. Mecanismo de reacción para la síntesis de adenina a partir de disoluciones acuosas de cianuro de amonio. Tomada de Voet y Schwartz (1983).

### 1.3.2. Ácidos carboxílicos

Los ácidos carboxílicos son compuestos de gran importancia biológica (Figura 7). Una de las funciones de estas moléculas es ser los intermediarios en las principales rutas metabólicas de los seres vivos (*i.e.* ciclo de Krebs). Los ácidos carboxílicos son intermediarios en las rutas de síntesis de moléculas más complejas de importancia biológica como aminoácidos, azúcares, triacilglicéridos, porfirinas y pirimidinas (*i.e.* gluconeogénesis) (Lehninger, Nelson y Cox, 2005). Por ello, el estudio en química prebiótica de estas moléculas es relevante en el periodo de evolución química. Por ejemplo, en el caso de la radiólisis del ácido acético en disolución acuosa se obtiene la síntesis abiótica de ácido succínico (Figura 8), un intermediario en el ciclo de Krebs (Garrison *et al.*, 1954).

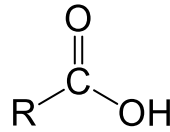


Figura 7. Estructura general de los ácidos carboxílicos<sup>1</sup>.

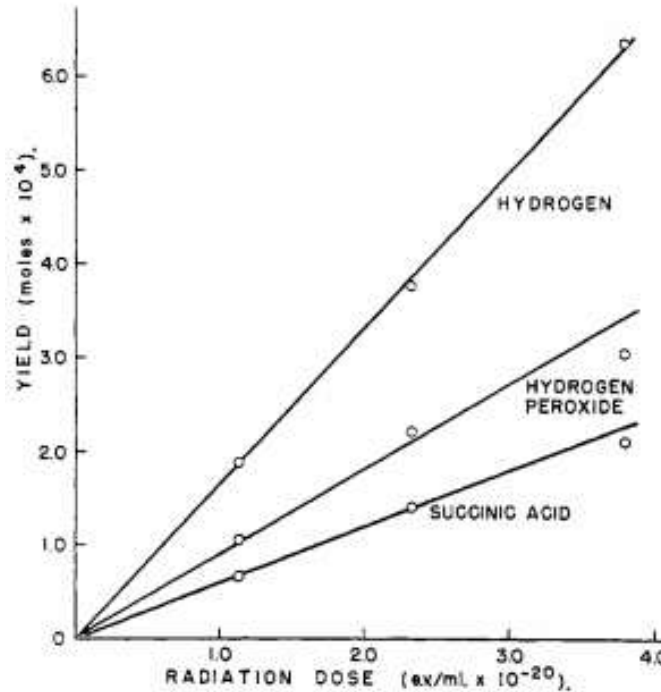


Figura 8. Producción de hidrógeno, peróxido de hidrógeno y ácido succínico en función de la dosis de radiación de disoluciones de ácido acético (Garrison *et al.*, 1954).

### 1.3.3. Carbohidratos

Los carbohidratos son moléculas orgánicas cuya fórmula mínima es  $(\text{CH}_2\text{O})_n$  (Figura 9). Son fundamentales y de gran importancia para los sistemas biológicos actuales (Gabiús, 2000; Joyce, 1989). El papel de estas moléculas en la actualidad es servir como: 1) moléculas energéticas, ya que al igual que las bases nitrogenadas son parte de la molécula de ATP la cual libera energía en la glucólisis (Figura 10) y sus análogos con otras bases nitrogenadas y 2) funcionar como moléculas

---

<sup>1</sup> R ya no es parte del grupo funcional, pero la fuerza de los ácidos carboxílicos depende del efecto electro-atractor o electro-donador de R.

estructurales en los ácidos nucleicos, particularmente en la cadena espiral de la ribosa-5-fosfato de los polímeros de DNA y RNA (Figura 11). Por todo ello, la síntesis y estabilidad de estos compuestos (*i.e.* ribosa), en condiciones primigenias es un aspecto de gran relevancia en el periodo de la evolución química terrestre.

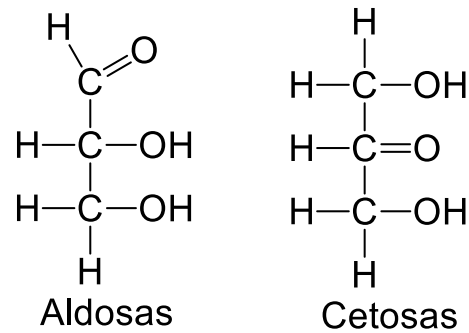


Figura 9. Estructura general para los carbohidratos dependiendo de su grupo funcional. Se muestra la forma de las aldosas y las cetosas (Morrison *et al.*, 1998).

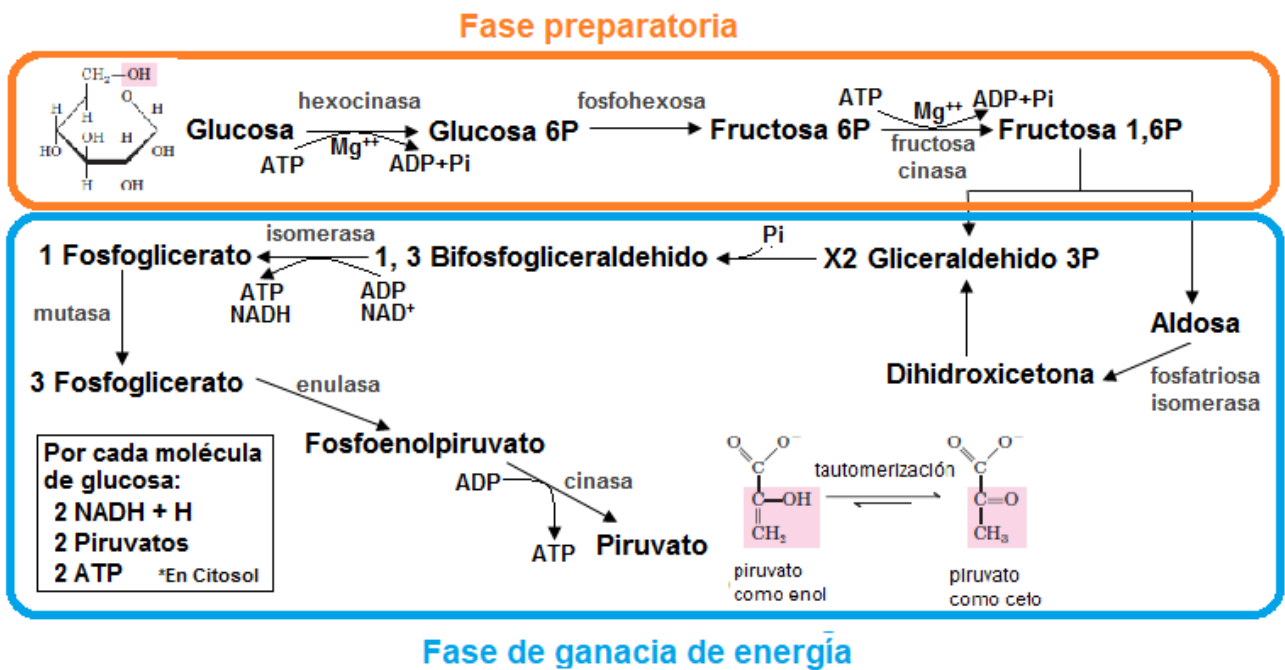


Figura 10. Diagrama general de la glucólisis.

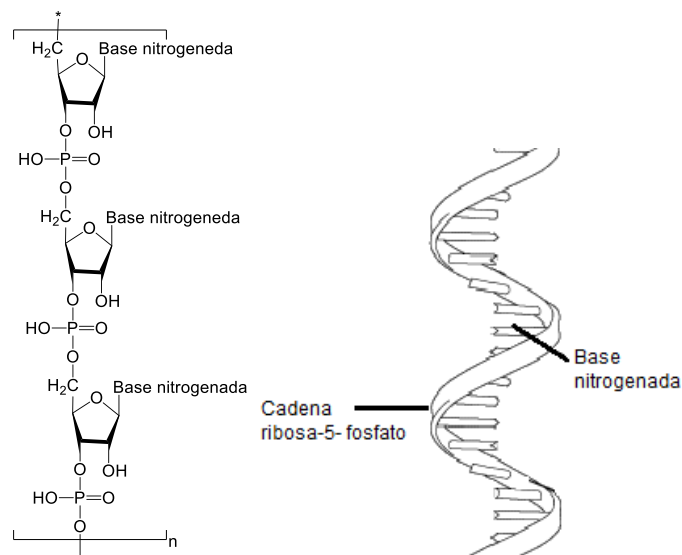


Figura 11. Cadena espiral de la ribosa-5-fosfato en el RNA.

#### 1.4. Fuentes de energía probables en la Tierra primitiva

Las fuentes y tipos de energía existentes en la Tierra primitiva son una pieza clave dentro de los procesos que ocurrieron en el periodo de evolución química, ya que la energía es la encargada de iniciar, potenciar y dirigir todos los procesos fisicoquímicos. Se han propuesto muchos procesos para generar diversos compuestos orgánicos (*i.e.* la formación de ciano-compuestos) (Ferris y Hagan, 1984) con diferentes fuentes y tipos de energía probables en la Tierra primitiva (Tabla 1) (Miller y Orgel, 1974, Garzón y Garzón, 2001). Sin embargo, no se puede afirmar que una sola fuente de energía haya sido la única o la principal responsable de producir las reacciones, ya que sólo la participación de varias o todas ellas pudo haber logrado generar todos los compuestos orgánicos de importancia biológica y pre-biológica, ya que se han reportado resultados relevantes en experimentos de química prebiótica utilizando diversas fuentes de energía. De esta premisa, surge la importancia de estudiar la síntesis y estabilidad de moléculas de importancia biológica expuestas a diferentes tipos de energía presentes en la Tierra primitiva.

**Tabla 1. Fuentes de energía en la Tierra primitiva.**

Fuente	Flujo ( $\text{Ja}^{-1}\text{m}^{-2}$ )	Intensidad ( $\text{Ja}^{-1}\text{m}^{-3}$ )	Inventario ( $\text{Ja}^{-1}$ )
Radiación solar			
UV (total)	$1.4 \times 10^8$	$1.2 \times 10^4$	$6 \times 10^{22}$
UV ( $\lambda < 150$ )	$7.1 \times 10^4$	6	$3 \times 10^{19}$
Descargas eléctricas	$1.7 \times 10^5$	14	$7 \times 10^{19}$
Rayos cósmicos	60	$5 \times 10^{-3}$	$2 \times 10^{19}$
Viento solar	$8 \times 10^3$	0.7	$3 \times 10^{18}$
Ondas de choque	$4.6 \times 10^4$	4	$2 \times 10^{19}$
Volcanes	$6 \times 10^3$	0.5	$2 \times 10^{17}$
Radioactividad	$1.17 \times 10^5$	$1.17 \times 10^2$	$10^{19}$
Corteza (huecos)	$1.5 \times 10^5$	$1.5 \times 10^{2a}$	$1.5 \times 10^{19}$ ( $5 \times 10^{20}$ )
Depósitos de U (granos)	$10^6$	$10^{3a}$	$3 \times 10^{18}$ ( $10^{20}$ )
Depósitos de U (huecos)	-	$10^5$	-

<sup>a</sup> Asumiendo una porosidad de 0.03.  
Los valores en paréntesis son de  $h = 30\text{k}$ .

Modificada de Garzón y Garzón (2001).

### 1.4.1. Energía térmica: importancia y participación en evolución química.

Un tipo de energía, ampliamente propuesta en experimentos de química prebiótica, es la energía térmica. Actualmente, se encuentra distribuida en varios y diversos ambientes; existen gradientes de temperatura en la atmósfera, en aguas termales producto de la actividad volcánica, en estanques calentados geotérmicamente, manantiales hidrotermales submarinos con temperaturas entre  $90\text{-}400^\circ\text{C}$  (Russell y Hall, 2009, Russel y Hall, 1997), manantiales hidrotermales subaéreos con temperaturas de  $48$  a  $89^\circ\text{C}$  (*i.e.* Parque Nacional de Yellowstone, EE.UU.) (Hamilton, *et al.*, 2011) además de muchas inter-fases como las formadas por roca-aire, nieve-aire, etc (Muller y Schulze-Makuch, 2006). Estos gradientes de temperatura son muy importantes desde el punto de vista de la química prebiótica, ya que estos sistemas podrían haber suministrado la energía necesaria para

promover muchas reacciones químicas importantes en el periodo de evolución química (Washington, 2000). Aunque al mismo tiempo, se debe mencionar que esa energía también podría haber promovido reacciones de termólisis, degradando los productos de síntesis (Muller y Schulze-Makuch, 2006). Así, el calor de las fuentes endógenas, además del calor generado por el impacto de cuerpos extraterrestres debieron estar presentes en la Tierra desde su formación (Oró, 1961). Por ello, la energía térmica debió ser una fuente constante que posiblemente contribuyó a la evolución química del planeta.

#### **1.4.2. Radiación ionizante: importancia y participación en la evolución química.**

El uso de energía en forma de radiación gamma en experimentos de química prebiótica tiene su base en las ventajas que tiene respecto a otras fuentes de energía como son: 1) alto poder de penetración en la mayoría de la materia orgánica, 2) independencia de la temperatura, pH, presión, concentración, humedad, estado de agregación, etc.; 3) amplia abundancia durante el periodo en el que ocurrió la evolución química (Tabla 2) (Draganic *et al.*, 1991), ya que existe en toda la corteza terrestre además de la proviene de fuentes extraterrestres en forma de partículas ionizantes como los rayos cósmicos o el viento solar (Tabla 1); 4) eficiencia en la síntesis de compuestos orgánicos (Draganic *et al.*, 1991); y finalmente 5) su capacidad de fungir como directriz de algunos procesos fisicoquímicos específicos. Por todo ello y por la gran importancia de los procesos abióticos en la Tierra primitiva en los que pudo participar la radiación ionizante, la radiación gamma ha sido propuesta como fuente de energía por muchos autores en



diferentes procesos prebióticos (Negrón-Mendoza y Ponnamperuma, 1976), algunos de los ejemplos pueden ser a) la síntesis de compuestos sencillos y macromoléculas (Ferris *et al.*, 1968), b) reacciones de polimerización (Colín-García *et al.*, 2008; Cruz-Castañeda *et al.*, 2014), condensación, descarboxilación (Negrón-Mendoza y Ramos-Bernal, 1998), desaminación (Meléndez-López *et al.*, 2014), auto-ensamblaje (Heredia *et al.*, 2017), fosforilación, ciclación (Ferris *et al.*, 1968), etc.

**Tabla 2. Fuentes radiactivas de origen terrestre.**

Fuente	Comentario
Seguras	Tiempo de vida media (x10 <sup>9</sup> años)
<sup>40</sup> K	1.25
<sup>232</sup> Th	1.39
<sup>235</sup> U	0.71
<sup>238</sup> U	4.5
<sup>244</sup> Pu	4.5
Probables Reactores nucleares naturales.	Elementos radiactivos con vida media cortas Los mismos radioelementos y radiaciones que en los reactores artificiales.

Modificada de (Draganic *et al.*, 1991) Varios reactores nucleares naturales como el de Oklo, Gabón, África pudieron estar activos desde hace 1.8 a 4.1 Ga.

### **1.5. Superficies minerales relevantes en la Tierra primitiva**

“Life, geologically speaking, consists of the interference with secondary lithosphere–atmosphere reactions so as to produce a small but ever-renewed stock of organic molecules” J. D. Bernal en Florkin (1960) p. 34.

En 1951, John D. Bernal propuso la posible participación de las arcillas y destacó su relevancia en el contexto de la evolución química. Él mismo sugirió por primera vez que las arcillas pudieron servir como: 1) agentes de adsorción de monómeros, aumentando así la concentración de éstos; 2) agentes catalizadores, y 3) como sitios de protección para evitar la degradación de moléculas necesarias para la síntesis prebiótica de moléculas más complejas (Bernal, 1951). Además,

propuso que estos procesos pudieron haber ocurrido en un ambiente formado en distintas inter-fases entre la hidrosfera y la litosfera (Ponnamperuma *et al.*, 1982). Muchos son los sólidos propuestos en experimentos de química prebiótica, considerando su posible presencia en la Tierra primitiva. Entre ellos destacan: silicatos, carbonatos, arcillas y basaltos (Hazen y Sverjensky, 2010; Otroshchenko y Vasilyeva, 1977). Un ejemplo destacado de la propuesta de participación de las superficies sólidas en la evolución química fue propuesto por Wachterhauser en 1988, en donde presenta la teoría del metabolismo de superficies como modelo antecesor de las enzimas y los templetos bioquímicos (Wachtershauser, 1988).

### **1.6. Ambientes geológicos probables en la Tierra primitiva.**

Al igual que la energía, los ambientes geológicos, en donde se desarrollaron las primeras reacciones químicas que enriquecieron la Tierra primitiva con materia orgánica, son una variable fundamental y determinante en la evolución química en la Tierra. Por ello, el determinar su posible existencia y su posible participación en procesos de evolución química es una tarea que se ha abordado desde un panorama multidisciplinario, donde disciplinas como la geoquímica, la radioquímica, la geología, etc. han propuesto posibles ambientes geológicos con diversas variables fisicoquímicas en la Tierra primitiva. Siendo estos ambientes geológicos, un conjunto de variables fisicoquímicas con las cuales se puede diseñar posibles escenarios para elaborar experimentos de química prebiótica.

#### **1.6.1. Manantiales hidrotermales submarinos**

¿Sin los océanos la vida nunca hubiera emergido en nuestro planeta?

El 71 % de la superficie terrestre actual está cubierta por agua (océanos, ríos, lagos, glaciales y acuíferos) (NASA Earth Observatory, 2010) y de ese porcentaje, el 99 %

es espacio habitable. Con menos del 10% de los océanos explorados, se estima que entre un 50-80 % de toda la vida<sup>2</sup> está bajo la superficie marina (Mora *et al.*, 2011). Esta idea ha impulsado nuevas propuestas sobre los orígenes de la vida en la Tierra proponiendo un nuevo escenario fisicoquímico para realizar experimentos en química prebiótica.

El 90 % de toda la actividad volcánica del planeta ocurre en los océanos y con el descubrimiento de los manantiales hidrotermales submarinos en la década de los 70 del siglo XX, se propuso que estos sistemas pudieron haber sido sitios relevantes en procesos de evolución química y en el origen de la vida (Russel y Hall, 1997). Una propuesta de la participación de estos sistemas en la evolución química fue presentada por el químico Günter Wächtershäuser en 1988, quien planteó la hipótesis de que los primeros organismos debieron ser de tipo termofílicos y quimioautótrofos. Estos organismos habrían estado dotados de un metabolismo que se efectuaría en la superficie de partículas sólidas de sulfuros de metales de transición, principalmente sulfuros de hierro, como los que están presentes en los manantiales hidrotermales submarinos (Wächtershäuser, 1988). Sin embargo, esta propuesta es controversial y no se han realizado experimentos que lo prueben, además que hay evidencias en contra de que los primeros organismos fueran termófilos (Miller y Lazcano, 1995).

Los manantiales hidrotermales submarinos se clasifican en dos tipos principales (Tabla 3): 1) unos profundos, de 1 a 3 kilómetros (fumarolas negras)

---

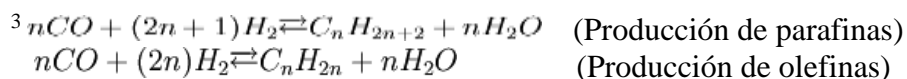
<sup>2</sup> Actualmente se han nombrado y clasificado 1.5 millones de especies de un total calculado de 8.7 millones.

(Figura 12), que emiten gases calentados directamente por el manto de la Tierra, a temperaturas superiores a 300°C; y 2) otros menos profundos menores a 1 kilómetro (fumarolas blancas) (Figura 13) con temperaturas cercanas a 90°C, donde es más probable que ocurrieran los procesos de síntesis y conservación de compuestos orgánicos. Existen hipótesis que proponen a los sistemas hidrotermales como reactores químicos donde se sintetizaron muchos compuestos orgánicos de interés pre-biológico o biológico por procesos abióticos a través de reacciones tipo Fischer-Tropsch (FTT)<sup>3</sup>, que involucran reacciones con gases a altas presiones y temperaturas, en la presencia de minerales, como la siderita, los carbonatos, óxidos de hierro o silicatos (Masters, 1979).

**Tabla 3. Comparación entre los sistemas hidrotermales submarinos más comunes.**

	<b>Fumarolas negras</b>	<b>Fumarolas blancas</b>
Profundidad (km)	1-3	<1
Montículo	sulfuros de metales	carbonatos
pH del sistema y su vecindad	2-7 hasta ~7	9-11 hasta ~7
Gradientes de Temperatura (°C)	400 a 2 en su vecindad	90 a 2 en su vecindad
CO <sub>2</sub> (mmol/kg)	4-215	~0
H <sub>2</sub> (mmol/kg)	0.1-50	0.1-50
CH <sub>4</sub> (mmol/kg)	0.05	~0
H <sub>2</sub> S(mmol/kg)	3-110	~0
Metales de transición	Fe(II) y Mn(II)	Fe(II) y Mg(II)
Presencia en el Hadeano	poco probable	probable

Entre los aportes experimentales que apoyan la participación de estos ambientes geológicos en los procesos de evolución química se encuentran: 1) el publicado por Marshall en 1994 mostrando la síntesis de aminoácidos en disolución acuosa en simulaciones hidrotermales (T=200°C) (Marshall, 1994); 2) los informes



Reacciones exotérmicas, que requieren alta presión (20-30 bar) y alta temperatura (200–350°C).

en donde se muestra la estabilidad de algunos aminoácidos solvatados en agua en contacto con fluidos supercríticos (300-400°C) (Islam *et al.*, 2003) (Alargov *et al.*, 2002); 3) en el 2009 se publicó que el equilibrio de oligomerización/hidrólisis de aminoácidos se desplaza a la oligomerización bajo condiciones hidrotermales (Lemke, Rosenbauer y Bird, 2009); y 4) en el artículo de Bada, *et al.*, 1995, publicaron que los manantiales hidrotermales submarinos no son sitios de síntesis sino de descomposición de la materia orgánica; en éste como en otros experimentos de química prebiótica se demuestra que algunos aminoácidos no podrían ser sintetizados o ser estables a temperaturas superiores a 250°C (Ito *et al.*, 2006).

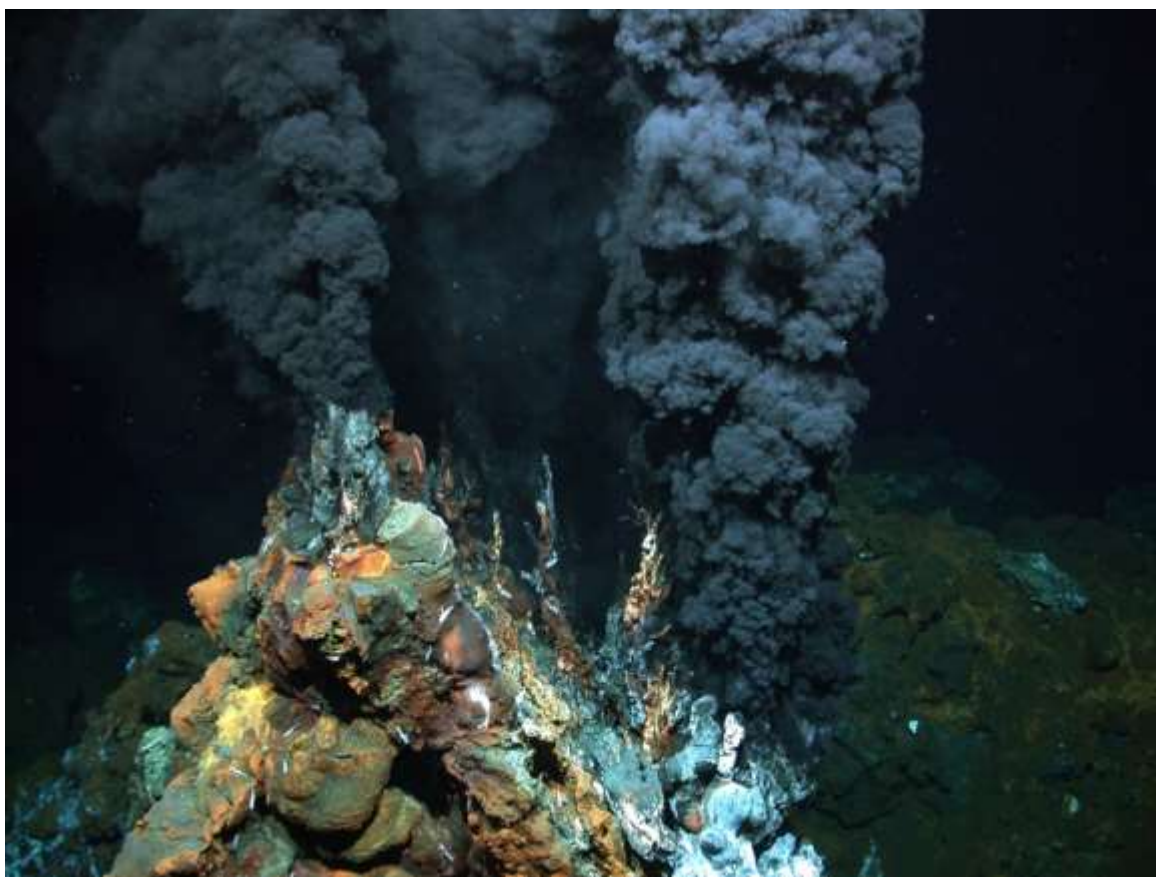


Figura 12. Fumarola negra. Tomada de <https://www.marum.de/en/Discover/Deep-Sea.html>

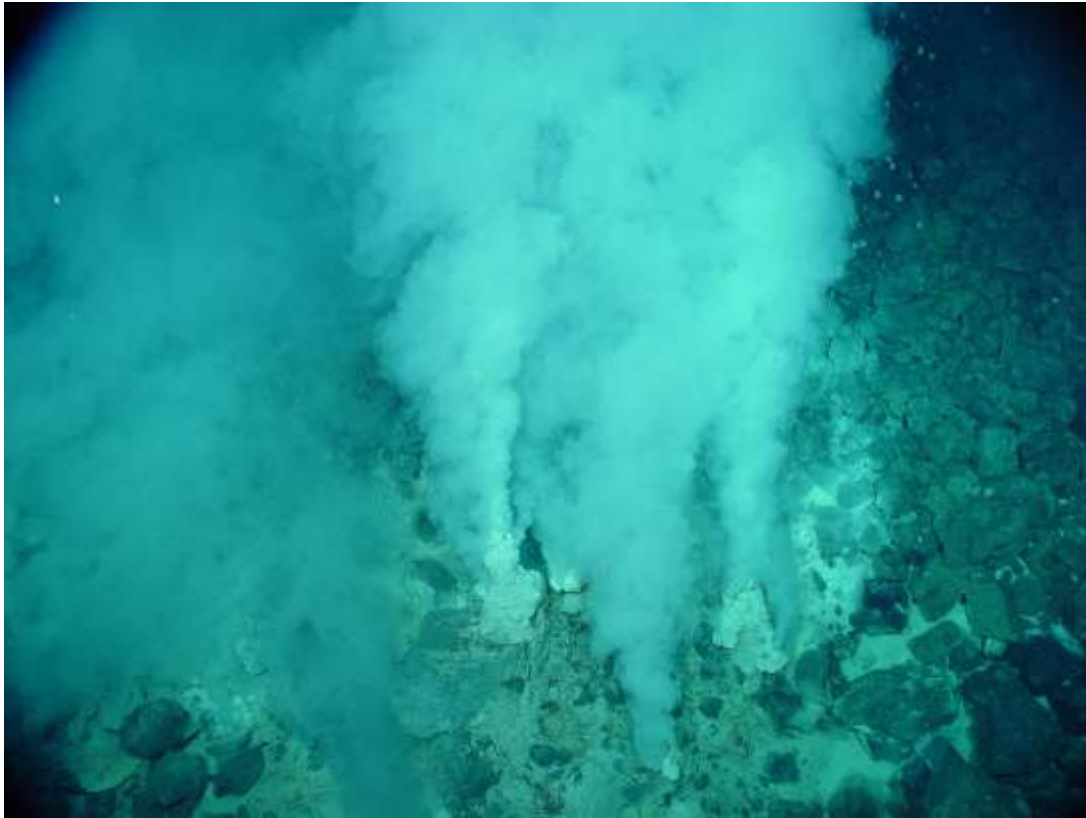


Figura 13. Fumarola blanca. Tomada de <https://sciworthy.com/are-the-building-blocks-of-life-from-a-hydrothermal-vent/>

### **1.6.2. Manantiales hidrotermales subaéreos**

Los sistemas hidrotermales subaéreos también son producto de la actividad volcánica de la Tierra, particularmente son grietas en la corteza terrestre de las cuales emana agua (magmática y meteórica) calentada geotérmicamente, rica en minerales y metales disueltos, con temperaturas de 48 a 95°C y pH desde 3 hasta 9.5, además de vapores compuestos por agua, CO<sub>2</sub> y H<sub>2</sub>S a manera de géiser, formando depósitos que pueden ser silicatos, carbonatos, boratos y/o sulfatos dependiendo de la fuente de alimentación del manantial (Campbell *et al.*, 1988).

Evidencia geoquímica indica que, a lo largo del tiempo geológico, los sistemas hidrotermales subaéreos como Yellowstone (Figura 14) han sido comunes y parecen haber sido responsables de la formación de muchos yacimientos importantes de minerales y metales (Fournier, 1989).

Ejemplos de estos sistemas hidrotermales están ampliamente distribuidos en la Tierra ya que podemos encontrar en Estados Unidos, Islandia, Rusia, India, Australia y Nueva Zelanda, pero existe evidencia geológica que indica que estos sistemas fueron abundantes en la Tierra primitiva. Como ejemplo tenemos el sistema hidrotermal sulfurado de Pilbara en Australia con una antigüedad de 3.45 Ga en el cual se ha propuesto evidencia de microfósiles de estromatolitos como una forma de vida primitiva (Djokic *et al.*, 2017).

Se ha propuesto que en estos sistemas hidrotermales, particularmente en los sedimentos, dentro de los procesos de hidratación-secado, monómeros de nucleótidos pudieron haber sido sintetizados, concentrados y estabilizados, e incluso a través de catálisis heterogénea pudieron ser polimerizados (Deamer y Georgiou, 2015).



Figura 14. Manantial hidrotermal en el parque Nacional de Yellowstone, Estados Unidos. Tomada de: <https://vivaglammagazine.com/the-best-places-to-stay-in-yellowstone-national-park/>



Se han propuestos otros posibles sistemas hidrotermales en los cuales la energía térmica para calentar el agua no proviene del calor del magma, si no de reactores nucleares naturales cuyo combustible nuclear son depósitos de naturales de  $^{235}\text{U}$  (Figura 15), los cuales pudieron ser abundantes en Hadeano (Figura 16). Siendo así la radiación ionizante<sup>4</sup> una variable adicional a las otras variables fisicoquímicas de los anteriores sistemas hidrotermales (Ebisuzaki y Maruyama, 2017).

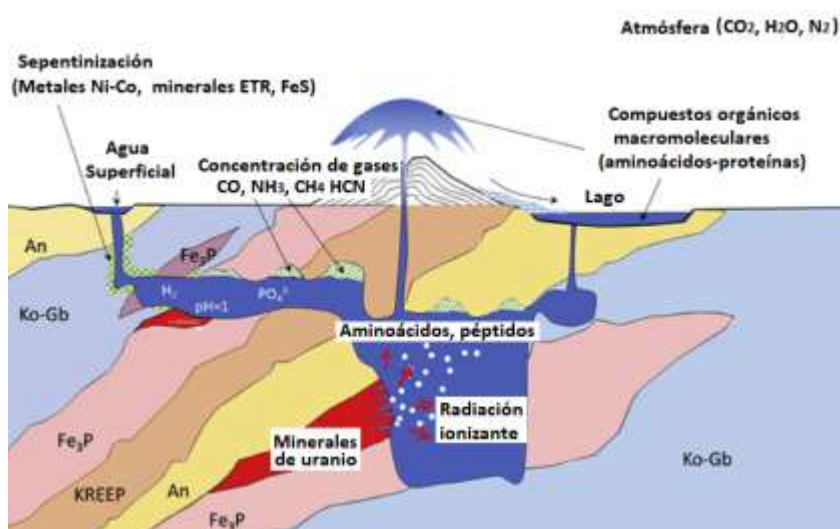


Figura 15. Manantial hidrotermal subaéreo con combustible nuclear. Tomada de Ebisuzaki y Maruyama (2017)

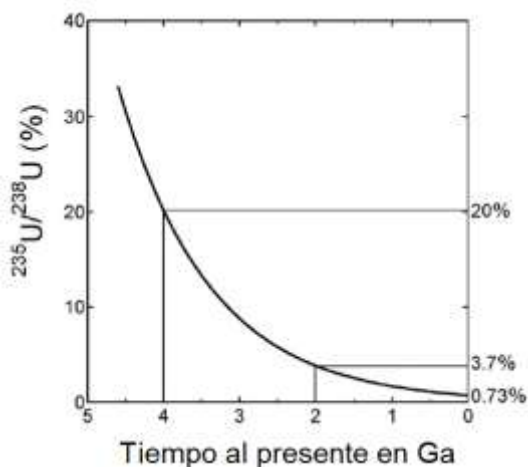


Figura 16. Abundancia del isótopo de  $^{235}\text{U}$  en el Hadeano respecto a su vida media y al isótopo  $^{238}\text{U}$ . Tomada de Ebisuzaki y Maruyama (2017)

<sup>4</sup> Véase apéndice: Cadena de decaimiento de  $^{235}\text{U}$



## 1.7. Variables fisicoquímicas posibles en experimentos de química prebiótica simulando manantiales hidrotermales

La Tabla 4 muestra la posible forma de interacción de los diversos sistemas hidrotermales con la materia orgánica.

Tabla 4. Sistemas hidrotermales y medios de reacción.

Sistema hidrotermal y sus vecindades	Estado de agregación y medio de difusión de la materia orgánica
Submarino (negras)	<ul style="list-style-type: none"> <li>Disoluciones acuosas con fluidos supercríticos</li> </ul>
Submarino (Blancas)	<ul style="list-style-type: none"> <li>Disoluciones acuosa y sólidas</li> <li>Suspensiones acuosas con minerales</li> </ul>
Subaéreos	<ul style="list-style-type: none"> <li>Disoluciones acuosas y sólidas</li> <li>Suspensiones acuosas con minerales</li> <li>Sedimentos en estado sólido</li> </ul>

La Tabla 5 muestra algunas de las posibles variables más relevantes presentes en los sistemas hidrotermales, con las cuales interactúa la materia orgánica.

Tabla 5. Posibles variables fisicoquímicas relevantes en los sistemas hidrotermales.

Sistema hidrotermal y sus vecindades	pH	Temperatura (°C)	Radiación ionizante	Fuerza iónica	Superficies minerales	Presión (atm)	Metales de transición
Submarino (negras)	2-7	2-300	gamma	si	sulfuros	200-300	si
Submarino (blancas)	7-11	2-90	gamma	si	carbonatos	90	si
Subaéreos	2-10	40-90	gamma y ultravioleta	si y/o no	carbonatos, silicatos, sulfatos, sulfuros, boratos	>1	si

En estudios de evolución química, tan importante es la síntesis de compuestos como la estabilidad de éstos en el medio ambiente prevaleciente; por ello, debe existir un balance entre la formación y destrucción de dichas moléculas para tenerlas disponibles para su posterior utilización.

## ***2. Capítulo segundo. Hipótesis***

Si la síntesis de compuestos orgánicos se puede dar en las condiciones de presión y temperatura que prevalecen en las áreas adyacentes a los cuerpos de agua que rodean a los manantiales hidrotermales subaéreos o submarinos, la presencia de sólidos como las arcillas, en particular la montmorillonita, permitirían que moléculas orgánicas como las bases nitrogenadas, los ácidos carboxílicos o los azúcares pudieran adsorberse y, así las superficies de estos sólidos contribuirían a proteger a los compuestos orgánicos de la hidrólisis y de fuentes externas de energía como el calor, o la radiación gamma, contribuyendo a incrementar la estabilidad de las moléculas en estas condiciones.

De esta manera, estos ambientes geológicos pudieron haber sido sitios idóneos para que se llevaran a cabo reacciones prebióticas, que enriquecieron con materia orgánica a la Tierra primitiva y que, por otro lado, brindaron condiciones ambientales más estables que la superficie terrestre.

### **3. Capítulo tercero. Objetivos**

#### **3.1. Objetivo general**

Estudiar la estabilidad de algunas moléculas orgánicas de importancia biológica (bases nitrogenadas, ácidos carboxílicos y carbohidratos) en condiciones que simulen las variables presentes en la vecindad de un manantial hidrotermal, como ejemplos de reacciones que pudieron ser relevantes en el contexto de la evolución química. Además, de ser posible, evaluar el posible efecto protector de los minerales hacia los compuestos modelo<sup>5</sup>:

- ✓ **citosa** (base pirimidínica)
- ✓ **guanina** (base púrica)
- ✓ **ácido succínico** (ácido carboxílico – participante en el ciclo de Krebs)
- ✓ **ácido malónico** (ácido carboxílico – inhibidor del ciclo de Krebs)
- ✓ **gliceraldehído** (triosa - quiral<sup>7</sup>)
- ✓ **glicolaldehído** (triosa – no quiral).

Para cumplir el objetivo, se estudió la cinética de descomposición de algunos compuestos orgánicos con dos tipos de energía probables en los manantiales hidrotermales (calor y radiación gamma), simulando la vecindad de un manantial hidrotermal con gradientes de temperatura o dosis de radiación, en medios de fuerza iónica, presión y pH fijos, en presencia o ausencia de minerales relevantes en estos ambientes. Monitoreando y describiendo individualmente la participación de cada una de las variables fisicoquímicas involucradas, posteriormente se evaluaron algunas posibles combinaciones de variables fisicoquímicas formando sistemas cada vez más complejos.

---

<sup>5</sup> Véase apéndice: Compuestos modelo - Moléculas orgánicas

<sup>7</sup> Véase apéndice: Quiralidad

### **3.2. *Objetivos particulares***

- 1) Evaluar la cinética de descomposición de los compuestos modelo frente a dos fuentes de energía probables en los manantiales hidrotermales:
  - a. Estudiar la termólisis de los compuestos modelo en estado sólido y en disolución acuosa.
  - b. Estudiar la radiólisis gamma de los compuestos modelo en estado sólido y en disolución acuosa.
  
- 2) Evaluar el efecto causado en la cinética de descomposición de los compuestos modelo por la presencia de superficies minerales relevantes en los manantiales hidrotermales frente a dos fuentes de energía.
  - a. Estudiar la termólisis de los compuestos modelo en presencia y ausencia de las superficies minerales.
  - b. Estudiar la radiólisis gamma de los compuestos modelo en presencia y ausencia de las superficies minerales.
  
- 3) Proponer mecanismos de reacción que describan los sistemas de reacción propuestos.

## 4. Capítulo cuarto. Procedimiento experimental

### **Modelo simple de un sistema hidrotermal (sistema químico).**

El símil del sistema hidrotermal que se utilizó consta de una **fase líquida** y una **fase mineral** en una mezcla física sometido a: 1) termólisis a diferentes temperaturas o 2) radiólisis a diferentes dosis de radiación gamma, en un sistema cerrado que en una muy primera aproximación podrían simular las condiciones de manantiales hidrotermales submarinos y subaéreos.

- ✓ **Fase líquida:** se prepararon disoluciones de los compuestos modelo, en concentraciones que pudieron existir en los océanos de la Tierra durante el periodo Hadeano ( $10^{-4}$  y  $10^{-5}$  M) (Schlesinger y Miller, 1973): **guanina** (base púrica), **citósina** (base pirimidínica), **ácido succínico y malónico** (ácidos carboxílicos), **gliceraldehído** y **glicolaldehído** (aldosas).
- ✓ **La fase mineral:** estará representada por alguna superficie mineral relevante en estos ambientes hidrotermales: **olivina** (que se transforma en **serpentina**), **montmorillonita de Na<sup>+</sup>**, **montmorillonita de Fe<sup>3+</sup>**, **atapulgita y/o hectorita.**<sup>+</sup>

Una vez terminado el proceso de termólisis o radiólisis se analizaron inmediatamente ambas fases de las muestras (líquidas y sólidas) a través de técnicas espectroscópicas, cromatográficas y espectrometría de masas.

### **4.1. Preparación de materiales**

Todo el material de vidrio que se utilizó fue tratado por 30 minutos con el ión nitronio (Figura 17) el cual es un oxidante fuerte formado *in situ* en una mezcla sulfonítrica caliente, seguido de un lavado con abundante agua bidestilada comercial y finalmente horneado por 24 horas en una mufla a 300°C (O'Donnell y Sangster, 1970).

## 4.2 Reactivos utilizados

Los reactivos utilizados en todos los experimentos fueron de la mejor calidad y mayor pureza disponible comercialmente de diversas marcas como Merck® (Alemania) o Sigma-Aldrich® (EE. UU).

Todos los disolventes utilizados son de grado HPLC de la marca Honeywell Burdick y Jacson™, adicionalmente fueron filtrados con una membrana de Nylon® de 0.25 µm de la marca Supleco®.

El agua utilizada en todas las reacciones se tridestiló para eliminar cualquier tipo de contaminación con materia orgánica según los procedimientos descritos en el apéndice<sup>10</sup> partiendo de agua bidestilada comercial y desionizada con una resistividad de 18,2 MΩ/cm en un sistema de producción de agua ultra pura de la marca Milli-Q®, Merck®.

La arcilla (montmorillonita de sodio SWy-1) utilizada en las reacciones, siempre del mismo lote, se obtuvo de “Clay Minerals Repository of the Clay Minerals Society at the University of Missouri”, y se sometió a un tratamiento con peróxido de hidrógeno con el fin de eliminar impurezas orgánicas.

La arcilla (montmorillonita de Fe<sup>3+</sup>), se obtuvo a partir de la montmorillonita de sodio SWy-1 mediante una reacción de intercambio catiónico con disoluciones de FeCl<sub>3</sub>·5H<sub>2</sub>O en concentración 1N (Gerstl y Banin, 1980) y se caracterizó mediante difracción de rayos X<sup>11</sup> y espectroscopía en el infrarrojo<sup>12</sup>.

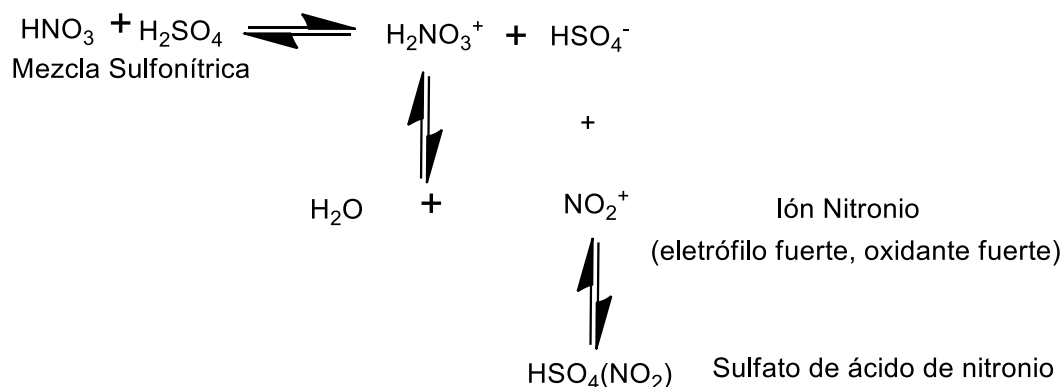


Figura 17. Formación de ión nitronio.

<sup>10</sup> Véase apéndice.

<sup>11</sup> Análisis elaborado en la USAI, Facultad de Química, UNAM.

<sup>12</sup> Análisis elaborado en el Instituto de Ciencias Nucleares, UNAM.

### **4.3. Preparación de muestras**

Todas las disoluciones y suspensiones fueron preparadas con agua tridestilada y colocadas en tubos de cultivo sellados las cuales fueron burbujeadas con argón durante cinco minutos, esto con el objetivo de desplazar el oxígeno del disolvente y saturar el sistema con el gas inerte. Las muestras en estado sólido fueron colocadas de igual forma en tubos de cultivo sellados y evacuados mediante una línea de vacío.

En los casos donde se modificó el pH de la disolución, se ajustó con ácido fórmico y/o hidróxido de amonio medido con papel pH de la marca Sigma-Aldrich®.

### **4.4. Termólisis de muestras**

Reacciones de termólisis

- En las reacciones de termólisis se calentaron los sistemas químicos entre 90 y 110°C, para ello se utilizaron dos sistemas de calentamiento: 1) un sistema de calentamiento por contacto indirecto con un disolvente orgánico en un sistema a reflujo (Figura 18), y 2) un reactor Parr<sup>13</sup> modelo 4560 de 500 mL (Figura 19) de la marca Parr Instrument Company®, operado mediante un Controlador Modular modelo 4848.

---

<sup>13</sup> Los reactores Parr están fabricados con acero inoxidable T316 y son diseñados para soportar reacciones a altas temperaturas y presiones además de ser inertes a las reacciones.

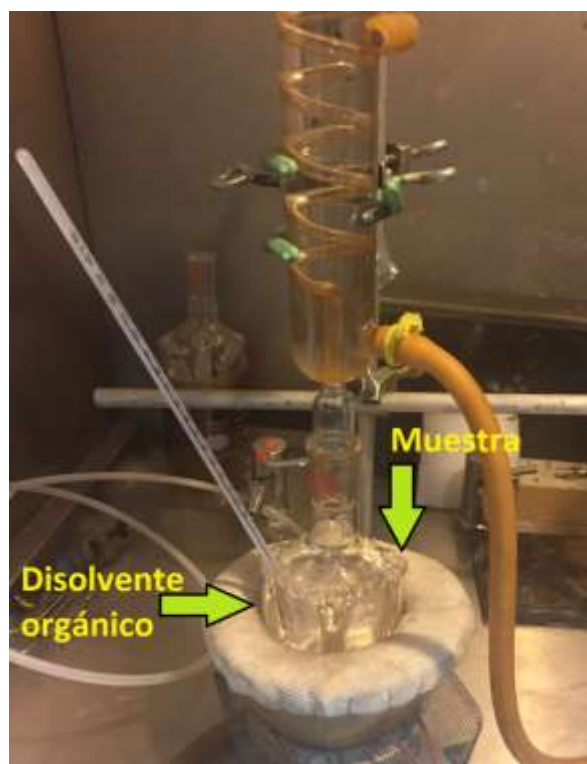


Figura 18. Sistema de calentamiento mediante contacto indirecto con disolventes orgánicos a reflujo.



Figura 19. Reactor Parr modelo 4560 de 500 mL, ICN, UNAM.



## 4.5. Irradiación de muestras

### Reacciones inducidas por radiación gamma.

La irradiación gamma de las muestras se llevó a cabo en un irradiador de tipo alberca “Gammabeam PT 651” (Figura 20) con barras de  $^{60}\text{Co}$  en distribución en “V” (Figura 21) a diferentes razones de dosis, localizado en el Instituto de Ciencias Nucleares de la UNAM

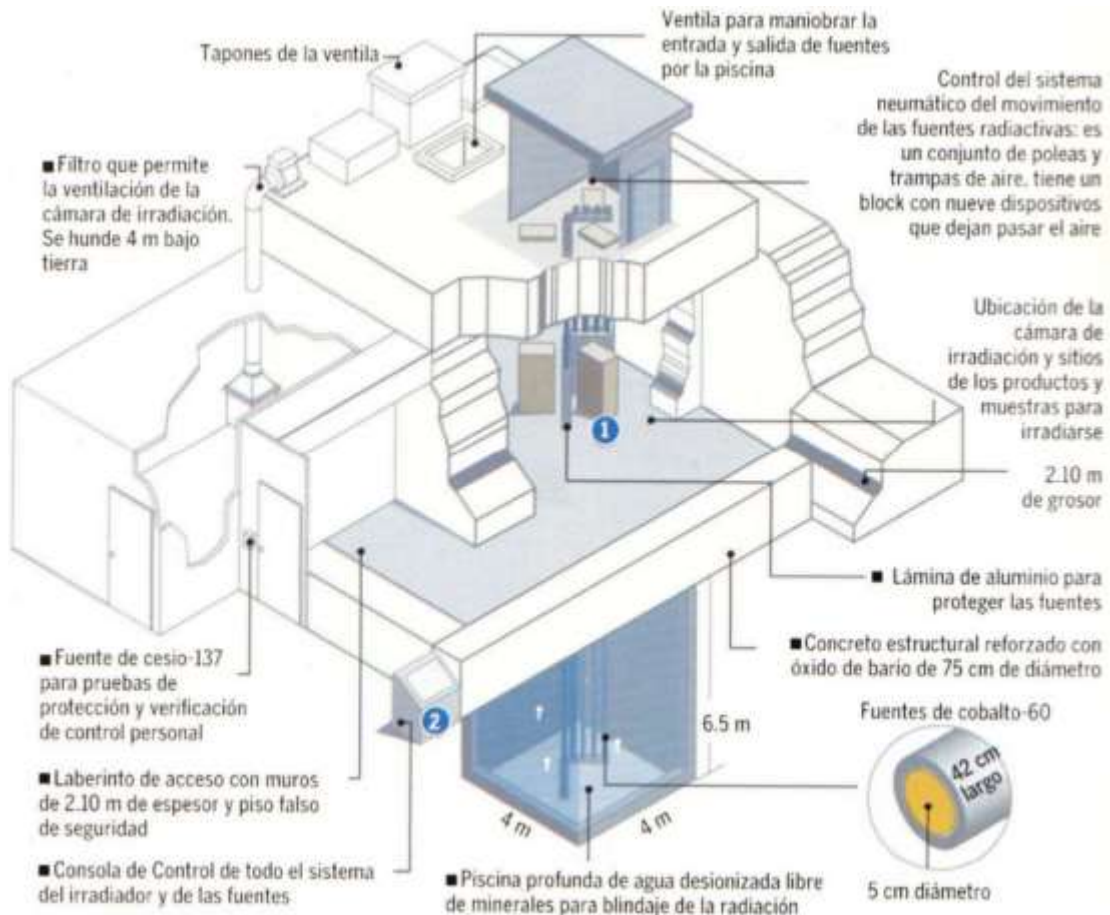


Figura 20. Irradiador Gammabeam PT 651<sup>14</sup>.

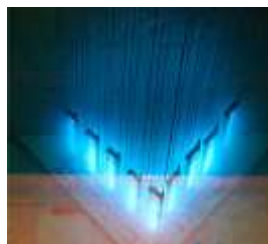


Figura 21. Disposición espacial de la barras de  $^{60}\text{Co}$  en el irradiador<sup>15</sup>.

<sup>14</sup> Fuente: Dr. Epifanio Cruz Zaragoza del Instituto de Ciencias Nucleares, UNAM

<sup>15</sup> Modificada de <http://www.alati.la/encontacto-2-mexico2.html>

## ***Cuantificación e identificación de reactivos y productos de reacción***

### ***4.6. Espectroscopía de Infrarrojo TF-ATR***

El análisis de las muestras mediante espectroscopía en el infrarrojo se llevó a cabo en un equipo Spectrum 100 FT-IR, PerkinElmer® con muestreo mediante la técnica ATR<sup>16</sup> y 16 escaneos, operado mediante el Software Spectrum™ en el Instituto de Ciencias Nucleares, UNAM.

### ***4.7. Espectrofotometría de UV-Vis***

Para análisis de las muestras mediante espectrofotometría UV-Vis se utilizó un espectrofotómetro ubicado en el Instituto de Ciencias Nucleares, UNAM de la marca Varian™ modelo Cary 100 UV-VIS operado con un el software Cary WinUV, utilizando celdas de cuarzo con 1 cm de paso óptico, variando la longitud de onda de 200 a 800 nm dependiendo del compuesto en análisis

### ***4.8. Polarografía***

Todas las medidas de polarografía para las muestras irradiadas se realizaron a temperatura ambiente (25°C) con una disolución acuosa estándar de DL-gliceraldehído en una concentración molar de  $1 \times 10^{-2}$ . Las curvas polarográficas se registraron utilizando un polarógrafo modelo 797 VA Computrace, Metrohm®, bajo las siguientes condiciones de trabajo: barrera de potencial entre 0.0 V y -1.7 V, velocidad de escaneo de 0.005 V/s, ancho de pulso de 0.05 V y tiempo de pulso de 0.04 s; como electrolitos soporte se utilizaron hidróxido de amonio y cloruro de amonio a pH 8.24. Como electrodo de trabajo se utilizó un electrodo de goteo de mercurio con un tiempo de caída de 1 s; como electrodo de referencia empleó un electrodo Ag/AgCl↓ y un electrodo auxiliar de platino. El análisis se elaboró en el laboratorio 114 de posgrado de Química (Laboratorio de Electroquímica Analítica del Departamento de Química Analítica), Facultad de Química, UNAM.

---

<sup>16</sup> ATR de la siglas en inglés Attenuated Total Reflectance

#### **4.9. Cromatografía de gases (GC)**

Los análisis de cromatografía de gases se elaboraron en dos equipos diferentes dependiendo del analito mediante los respectivos ésteres metílicos<sup>18</sup> de los ácidos carboxílicos, malónico, succínico, málico, 1, 2, 3-butanetricarboxylic, tricarbálico, aconítico, cítrico, succínico y fumárico sintetizados siguiendo el procedimiento descrito en Cruz Castañeda y Negrón Mendoza (2013) .

- A. Cromatógrafo de la marca Varian™ modelo 3700 acoplado a un detector de ionización de flama (FID), equipado con una columna empacada, OV 17 en Cromosorb W 3% 80/100 AW, con programador de temperatura de operación con intervalo de 60 a 260°C a 6°C/min, ajustando la temperatura del inyector y del detector a 250°C. Los gases empleados fueron: nitrógeno como gas acarreador con un flujo de 30 mL/min, hidrógeno con un flujo de 30 mL/min y aire con un flujo de 300mL/min. Se inyectó 1 µL de muestra por inyección. El cromatógrafo se ubica en el Instituto de Ciencias Nucleares, UNAM
- B. Cromatógrafo de la marca SRI Instruments™ modelo 8610C acoplado a un detector de ionización de flama, equipado con una columna MXT-Volátiles con un largo de 30 m, con un programa de temperatura de 80 a 200°C a 10 °C/min, seguido de una isoterma de 200°C durante 5 minutos. Los gases empleados fueron: nitrógeno como gas acarreador a 8 psi de presión; hidrógeno a 19 psi y aire 7 psi de presión para el FID. Se inyectó 1 µL de muestra por inyección. El cromatógrafo se ubica en el Instituto de Ciencias Nucleares, UNAM

#### **4.10. GC-Espectrometría de masas (CG-EM)**

Para la identificación de los analitos mediante CG-EM se utilizó un cromatógrafo modelo 6850 Agilent Technologies® equipado con una columna capilar de la marca HP™ modelo 19091S-433E de 30 m de longitud y acoplado a un detector de la marca Agilent Technologies® modelo 5975C VL MSD con un

---

<sup>18</sup> Véase apéndice: Esterificación de Fisher

detector "Triple-Axis". Se utilizó helio como gas acarreador. El programa de temperatura fue: inicio con una isoterma de 70°C por 2 minutos, seguido por una rampa en aumento de 10°C por minuto hasta 230°C y, finalizando, con otra isoterma de 230°C por 1 minuto. Se inyectó 1 µL de muestra por inyección. Éste se ubica en el Instituto de Ciencias Nucleares, UNAM

#### **4.11. Cromatografía de líquidos de ultra alta presión (UHPLC-UV)**

El análisis de cromatografía de líquidos se elaboró con un cromatógrafo modelo Ultimate 3000™ manufacturado por ThermoFisher Scientific™ conformado por una bomba isocrática UltiMate™ ISO-3100SD, un compartimiento de columna con control de temperatura UltiMate™ 3000 TCC-3000SD, acoplado con un detector de UV con longitud de onda variable ThermoFisher Scientific™ Dionex™ UltiMate™ 3000 VWD. Como fase móvil para la determinación de las bases nitrogenadas se utilizó una disolución de 0.1 moles/L de acetato de amonio disueltos en una mezcla de 80% agua y metanol 20% a pH=4, con flujo de 0.4 mL/min monitoreado a 260 nm y una columna C18 (4.6 x 75 mm, 3.5 µm con partículas esféricas) manufacturada por Waters Corp®. Se inyectaron 20 µL de muestra por inyección usando un loop y una válvula de Inyección Rheodyne. El cromatógrafo se ubica en el Instituto de Ciencias Nucleares, UNAM.

Para el caso de los azúcares o compuestos tipo azúcares se utilizó:

- A. Una disolución 70:30 metanol:agua con flujo de 1.3 mL/min monitoreado por un detector ELSD y una columna Astec CHIROBIOTIC™ T manufacturada por Sigma-Aldrich® .
- B. Una disolución 50:50 metanol:agua con flujo de 0.4 mL/min monitoreado a 260 nm y una columna C18 (4.6 x 75 mm, 3.5 µm con partículas esféricas) manufacturada por Waters Corp®.

#### **4.12. Cromatografía de líquidos-Espectrometría de masas (LC-EM)**

El análisis cromatográfico se elaboró con un sistema compuesto por una bomba isocrática modelo 515 Waters Corp®, una columna C18 (4.6 x 75 mm, 3.5 µm con partículas esféricas) manufacturada por Waters Corp® acoplada a un detector de masas de cuádruplo simple modelo SQ-2 de la marca Waters Corp® con una fuente de ionización por electrospray en modo negativo (ESI-) y modo positivo (ESI+) de la marca Waters corp®. Como fase móvil para la determinación de las bases nitrogenadas se utilizó una disolución de 0.1 moles/L de acetato de amonio disueltos en una mezcla de 80% agua y metanol 20% a pH=4, con flujo de 0.4 mL/min. Para el caso de los azúcares o compuestos tipo azúcares se utilizó como fase móvil una disolución 50:50 metanol:agua con flujo de 0.4 mL/min. El cromatógrafo se ubica en el Instituto de Ciencias Nucleares, UNAM

#### **4.13. Resonancia paramagnética electrónica (EPR)**

Para analizar las muestras mediante EPR se utilizó un espectrómetro modelo JES-TE300 Jeol Inc® en el Instituto de Química, UNAM, operando en la banda X con una frecuencia de 100 kHz de modulación y de una cavidad cilíndrica en el modo TE<sub>011</sub>. La calibración del campo magnético se hizo con un gausímetro de la marca Jeol Inc® modelo ES-FC5. Con el objetivo de lograr una geometría reproducible en la cavidad, las muestras (0.02 g) se colocaron en una celda de cuarzo tipo plana y se midió a temperatura ambiente. Los ajustes del espectrómetro para todos los espectros fueron los siguientes: 334.4 ± 10 mT; 8 mW de potencia de microondas; horno de microondas de frecuencia 9,43 GHz, modulación de ancho, 0.125 mT; constante de tiempo, 0,1 s; amplitud 200; tiempo de barrido 120 s; 13 escaneos.

## 5. Capítulo quinto. Resultados

Una vez completado el proceso de radiólisis o termólisis en la disolución acuosa para cada analito, se realizó una separación por métodos físicos. La fracción líquida se separó de la sólida para analizar posteriormente ambas fases como se muestra en la Tabla 6:

**Tabla 6. Estrategia de análisis.**

Análisis de la fase líquida	Análisis de la fase sólida
a) Analito remanente	a) Adsorción y desorción
b) Productos formados	b) Superficie

### 5.1. Citosina (base pirimidínica)

La principal reacción del proceso de termólisis y de radiólisis de la citosina en disolución acuosa ( $1 \times 10^{-4}$  M) es una reacción de desaminación de la base pirimidínica generando otra base pirimidínica: uracilo (Figura 22).

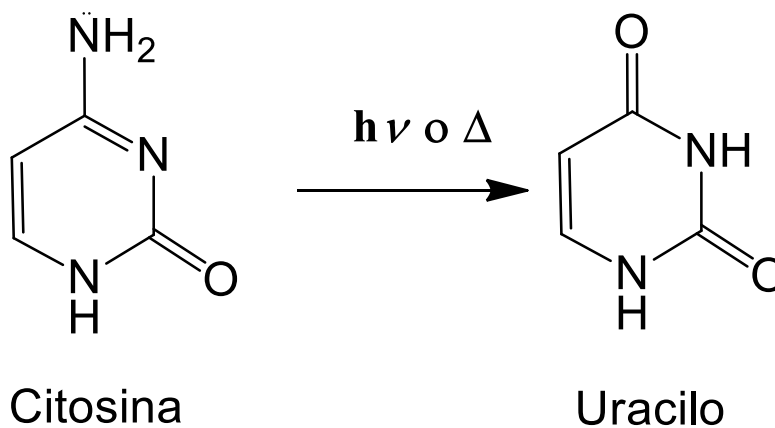


Figura 22. Reacción de desaminación de la citosina.

Como principal método para la identificación de los productos de reacción se utilizó HPLC y los respectivos espectros de fragmentación (Figura 23), la descomposición de la citosina fue cuantificada por espectrofotometría de UV a 267 nm (Figura 24) obteniendo un  $\epsilon_{267}$  experimental de  $855.84 \text{ mol}^{-1} \text{ L cm}^{-1}$  (Figura 25).

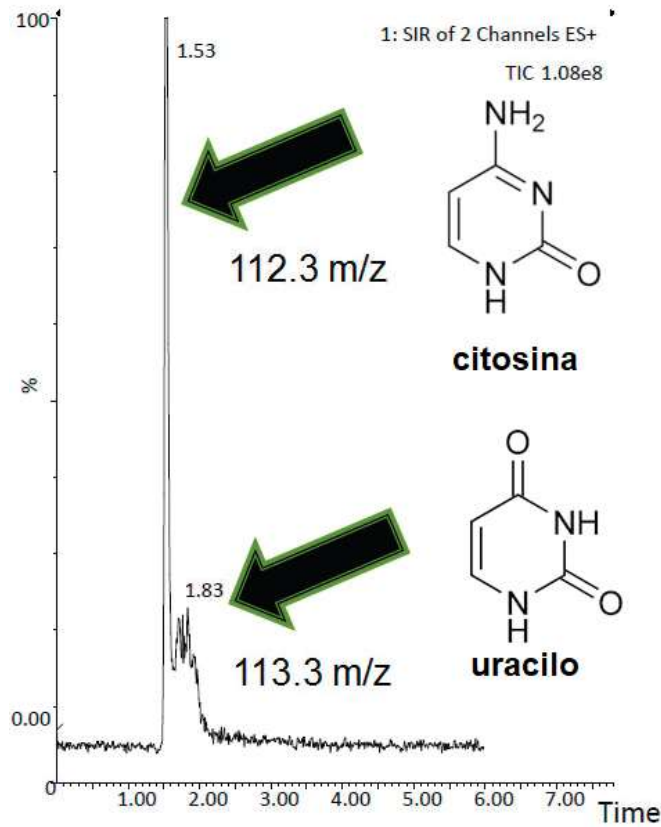


Figura 23. Análisis HPLC-MS de citosina.

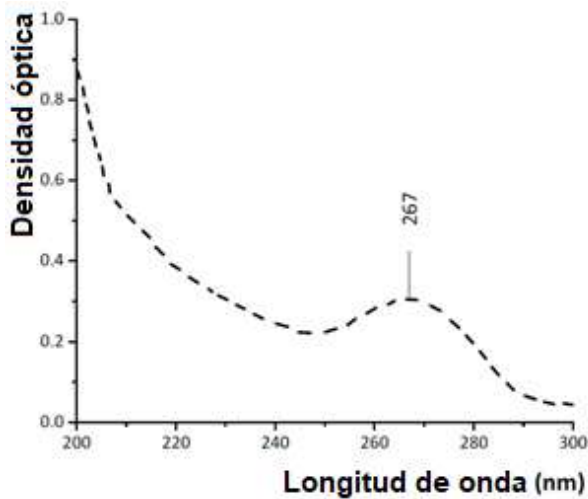


Figura 24. Análisis de espectrofotometría UV de citosina a 267 nm.

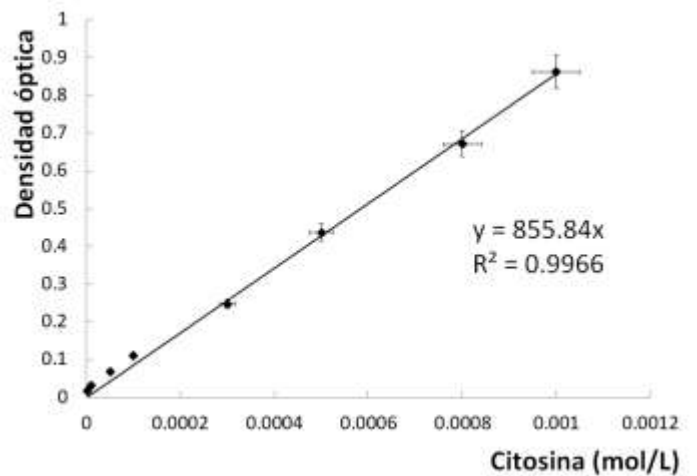


Figura 25. Curva de calibración de citosina.

La cuantificación de la producción de uracilo se hizo con espectrofotometría de UV a 258 nm.

### 5.1.1. Experimentos de termólisis

El principal producto de la termólisis de citosina en disolución acuosa ( $1 \times 10^{-4}$  M) a pH 7 a  $92^{\circ}\text{C}$  fue uracilo. La formación del uracilo es dependiente del tiempo de reacción, después de 1 026 horas el porcentaje de recuperación de citosina fue de 72 %. La Figura 26 muestra la descomposición de citosina en función del tiempo.

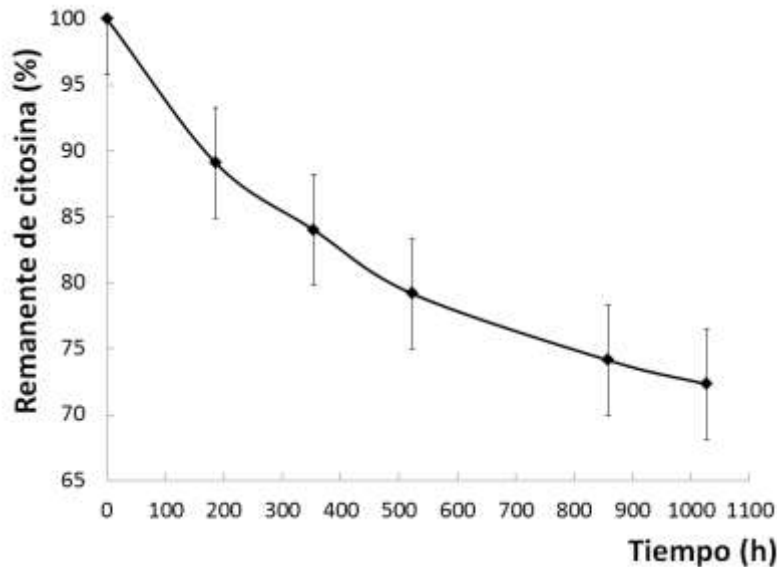


Figura 26. Termólisis de la citosina en función del tiempo.

El principal mecanismo de reacción propuesto en este trabajo para la termólisis de la citosina se muestra en la Figura 27 (Cruz-Castañeda, 2016).

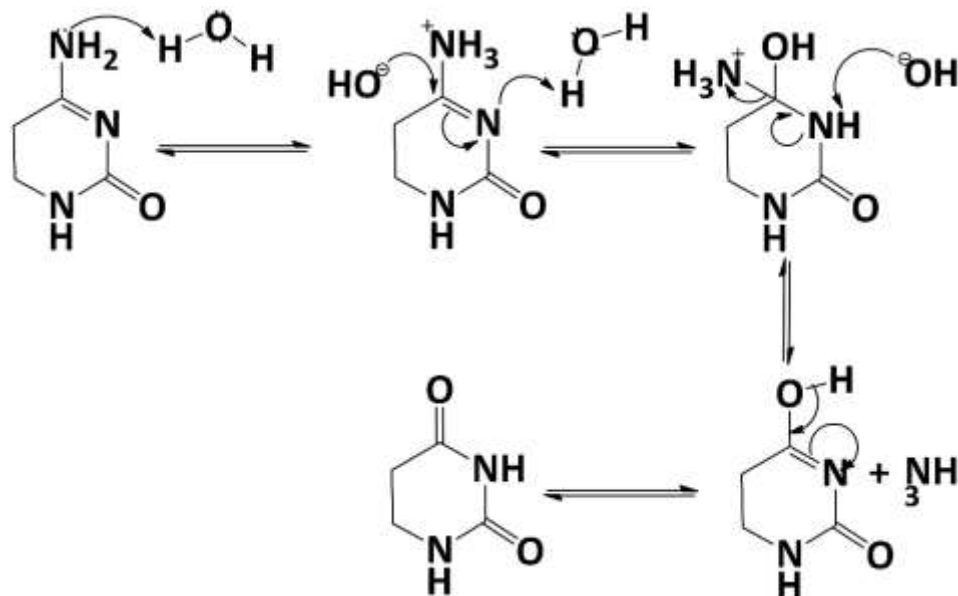


Figura 27. Mecanismo de reacción propuesto para formación de uracilo en la termólisis de citosina.



### 5.1.2. Experimentos de radiólisis

Los experimentos de radiólisis de la citosina mostraron que la molécula en disolución acuosa libre de oxígeno a pH, se descompone un 75 % a una dosis de 7.4 kGy y se descompone completamente a una dosis de 22 kGy (Figura 28). Adicionalmente se determinó que la formación de uracilo es también dependiente de la dosis (Figura 29).

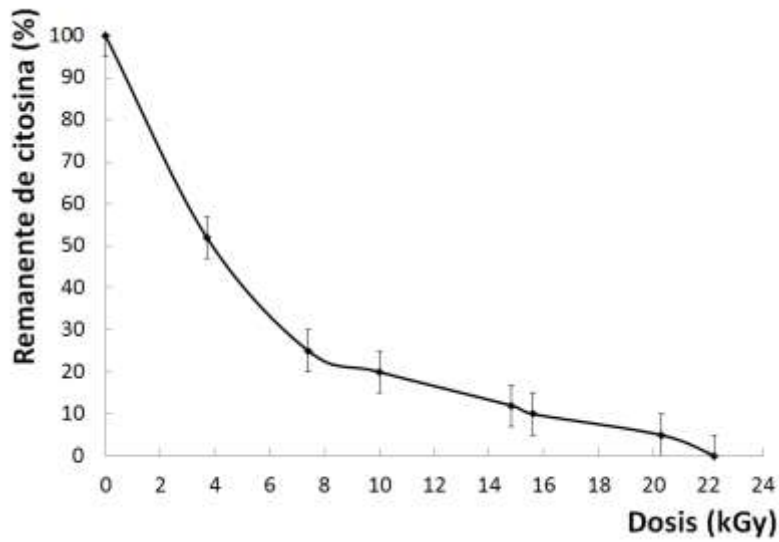


Figura 28. Descomposición de citosina en función de la dosis absorbida.

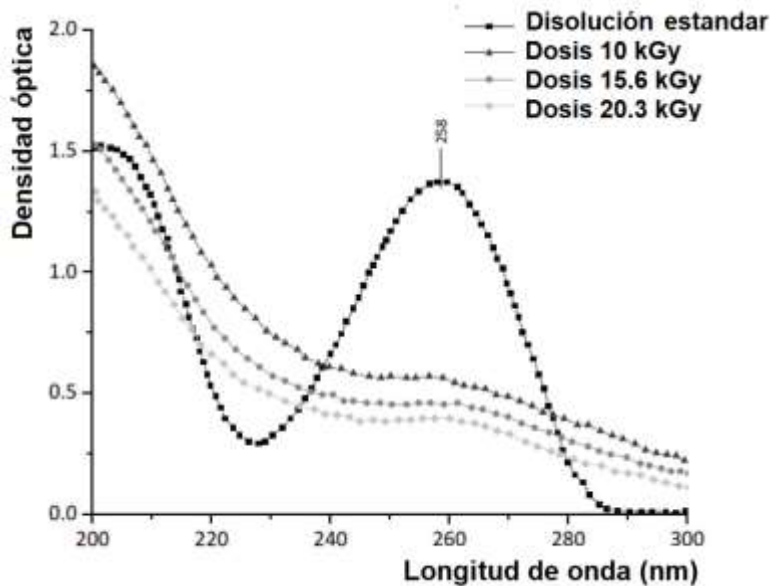


Figura 29. Análisis de espectrofotometría UV de uracilo a 258 nm.

### 5.1.3. Experimentos con suspensiones

Se elaboraron experimentos de adsorción/desorción de citosina en tres diferentes superficies sólidas (olivina, Na<sup>+</sup>-montmorillonita y Fe<sup>3+</sup>-montmorillonita) a tres diferente valores de pH (2, 7 y 11) y los resultados mostraron que la citosina en general se adsorbe preferentemente a pH ácidos (particularmente en las montmorillonita). A pH alcalinos, la adsorción es menor a 6% con las tres superficies sólidas (Figura 30).

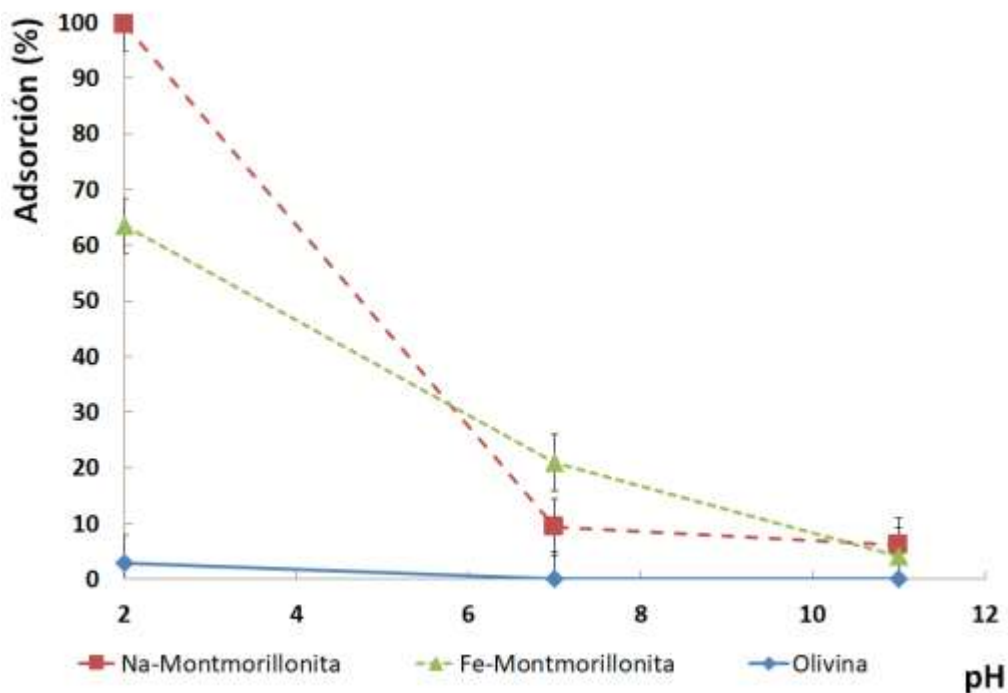


Figura 30. Experimentos de adsorción/desorción de citosina en superficies sólidas, dependiente del pH.

Adicionalmente, se determinó que, a pH alcalino, la presencia de las superficies sólidas con las que se experimentó, no modificó ni los procesos de radiólisis ni los procesos de termólisis.

## 5.2. Guanina (base púrica)

### 5.2.1. Experimentos de radiólisis en disolución acuosa

Los experimentos de la radiólisis de la guanina en disolución acuosa, libre de oxígeno, mostraron la alta inestabilidad de la base nitrogenada ante la radiación gamma, ya que a los 4 kGy se descompone más del 90% de la guanina (Figura 31) (A. L. Meléndez-López, 2018).

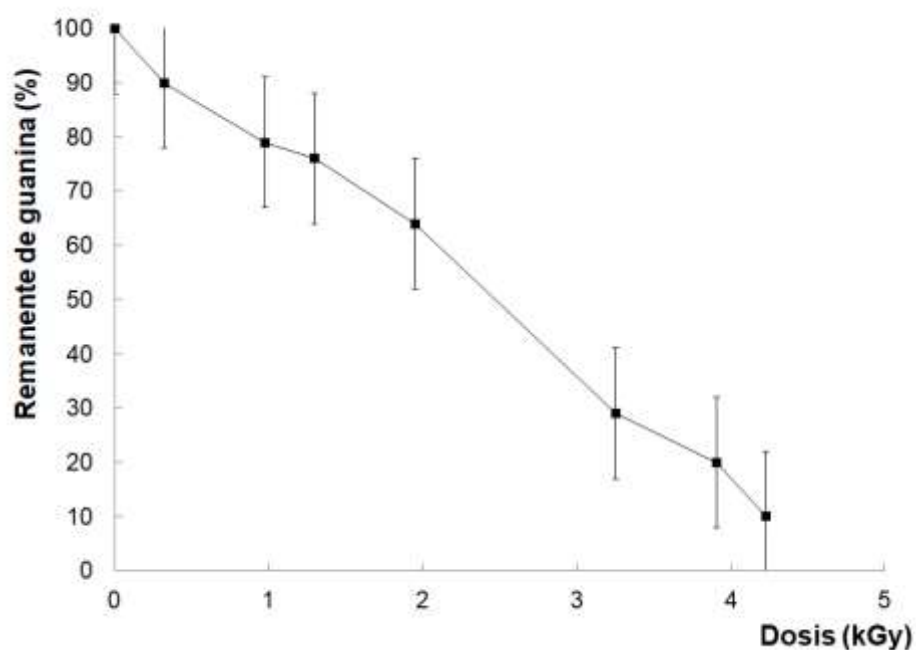


Figura 31. Descomposición de guanina en disolución acuosa, en función de la dosis absorbida.

Debido a la poca estabilidad de los productos formados ante la radiación gamma, estos compuestos no pudieron ser identificados dada su baja concentración en la disolución.

### 5.2.2. Experimentos de radiólisis en estado sólido

Experimentos previos de radiólisis de guanina en estado sólido (Meléndez-López, 2018) determinaron que la principal reacción corresponde a una dimerización, la cual fue analizada por HPLC-MS y su respectivo peso molecular (Figura 32).

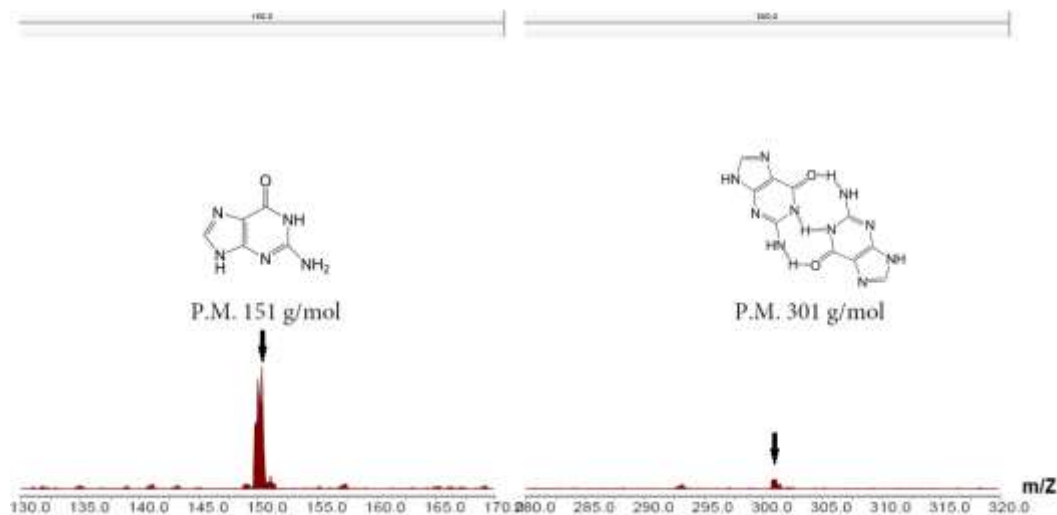


Figura 32. Análisis HPLC-MS de guanina irradiada en estado sólido. La masa de 301 g/mol corresponde al dímero. Tomada de (A. L. Meléndez-López, 2018).

### 5.2.3. Experimentos con suspensiones

Se elaboraron experimentos de adsorción/desorción de guanina en Na<sup>+</sup>-montmorillonita a tres diferentes valores de pH (2, 7 y 11). Los resultados mostraron que la guanina en general se adsorbe preferentemente a pH ácidos. A pH alcalinos la adsorción aproximada es del 20% (Figura 33).

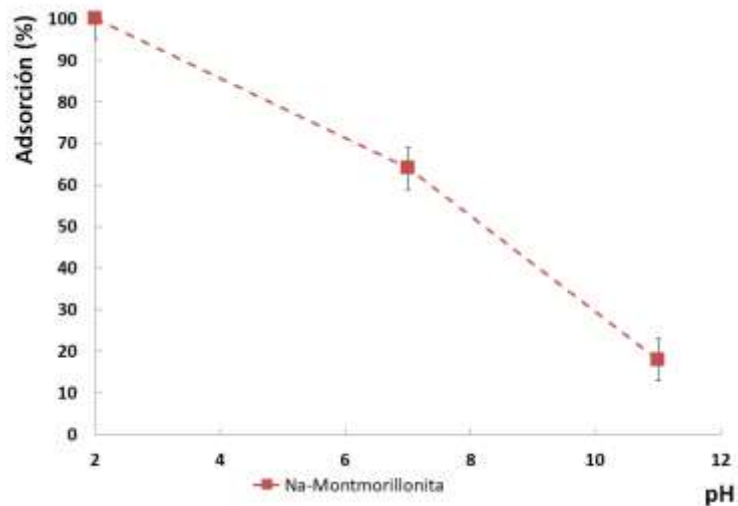


Figura 33. Adsorción/desorción de guanina en Na-montmorillonita, dependiente del pH

Los experimentos de radiólisis de guanina en suspensión acuosa con montmorillonita de sodio mostraron que la guanina aumenta su estabilidad ante la radiación gamma en comparación a los experimentos en los que hay ausencia de la arcilla, ya que a 77 kGy aún se tiene más del 60% de la guanina presente en el sistema (Figura 31)

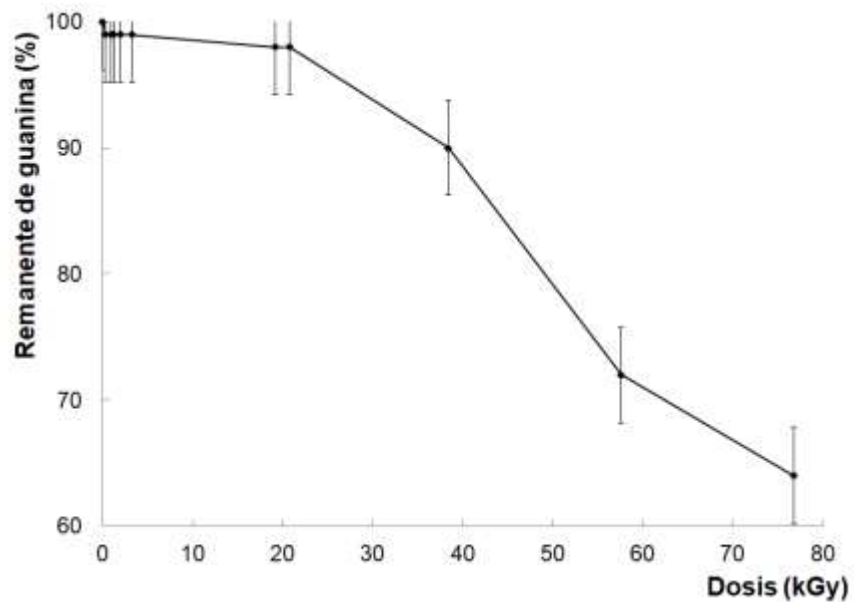


Figura 34. Descomposición de guanina en suspensión acuosa con arcilla, función de la dosis absorbida.

### 5.3. Ácido succínico (ácido carboxílico – participante en el ciclo de Krebs)

#### 5.3.1. Experimentos de termólisis

En la reacción de termólisis a 105°C en un intervalo de 0 a 100 horas del ácido succínico, se encontró que la principal reacción es una reacción de descarboxilación (Figura 35). El ácido propiónico ( $C_3H_6O_2$ ) y el dióxido de carbono ( $CO_2$ ) son los principales productos de reacción y fueron identificados por sus respectivos espectros de fragmentación en espectrometría de masas (Figura 36).

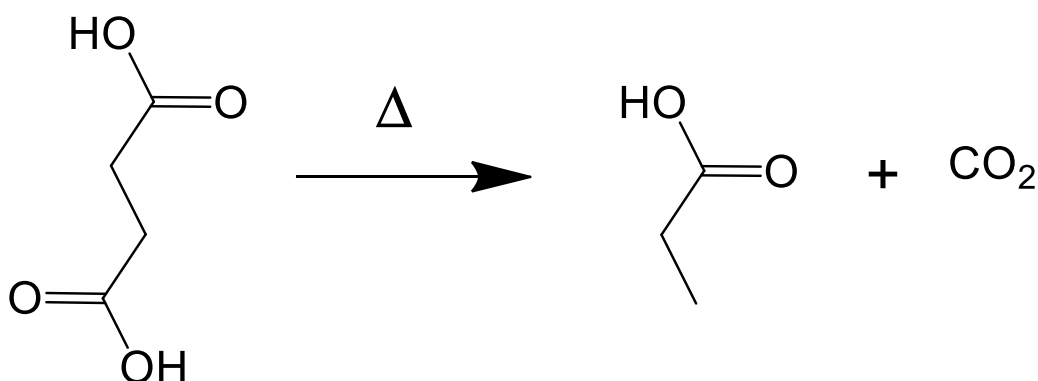


Figura 35. Reacción de descarboxilación del ácido succínico inducida por calor.

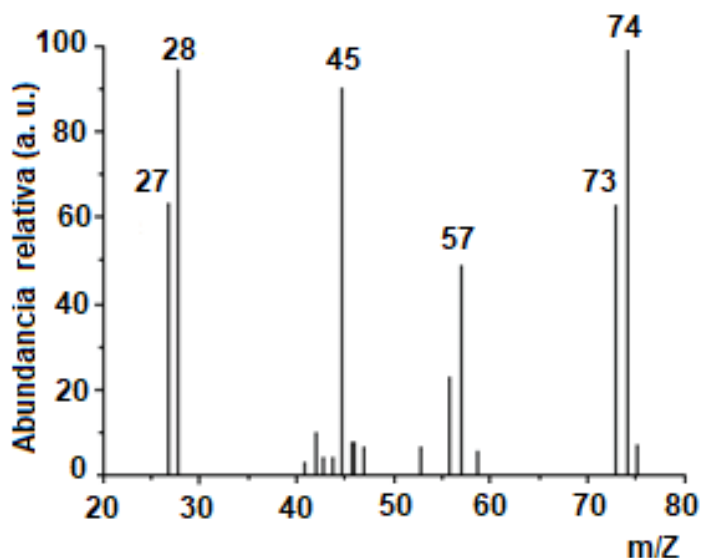


Figura 36. Espectro de fragmentación del ácido propiónico formado en la termólisis del ácido succínico.

### 5.3.2. Experimentos de radiólisis

Los experimentos de la radiólisis del ácido succínico en disolución acuosa libre de oxígeno mostraron que la principal reacción corresponde a una polimerización. El principal producto de reacción corresponde al dímero del ácido succínico (Figura 37) Adicionalmente, se determinó la formación de otros ácidos carboxílicos (Tabla 7) detectados a través de cromatografía de gases acoplado a espectrometría de masas (Figura 38).

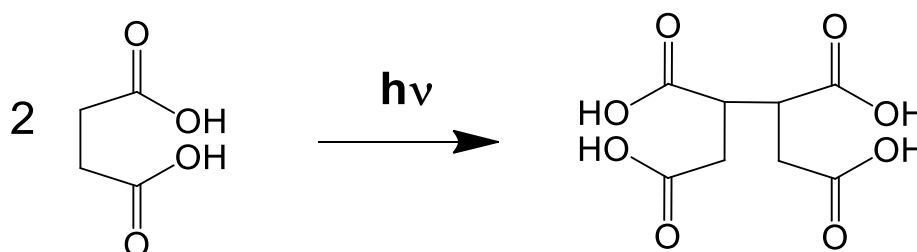


Figura 37. Radiólisis del ácido succínico en disolución acuosa. Se observa la formación del dímero.

Tabla 7. Productos de la radiólisis del ácido succínico en disolución acuosa.

Compuesto	Estructura desarrollada
Ácido málico <b>C<sub>4</sub>H<sub>6</sub>O<sub>5</sub></b>	
Ácido malónico <b>C<sub>3</sub>H<sub>4</sub>O<sub>4</sub></b>	
Ácido 1,2,3-butantricarboxílico <b>C<sub>7</sub>H<sub>10</sub>O<sub>6</sub></b>	
Ácido tricarbálico <b>C<sub>6</sub>H<sub>8</sub>O<sub>6</sub></b>	
Ácido aconítico <b>C<sub>6</sub>H<sub>6</sub>O<sub>6</sub></b>	
Ácido cítrico <b>C<sub>6</sub>H<sub>8</sub>O<sub>7</sub></b>	

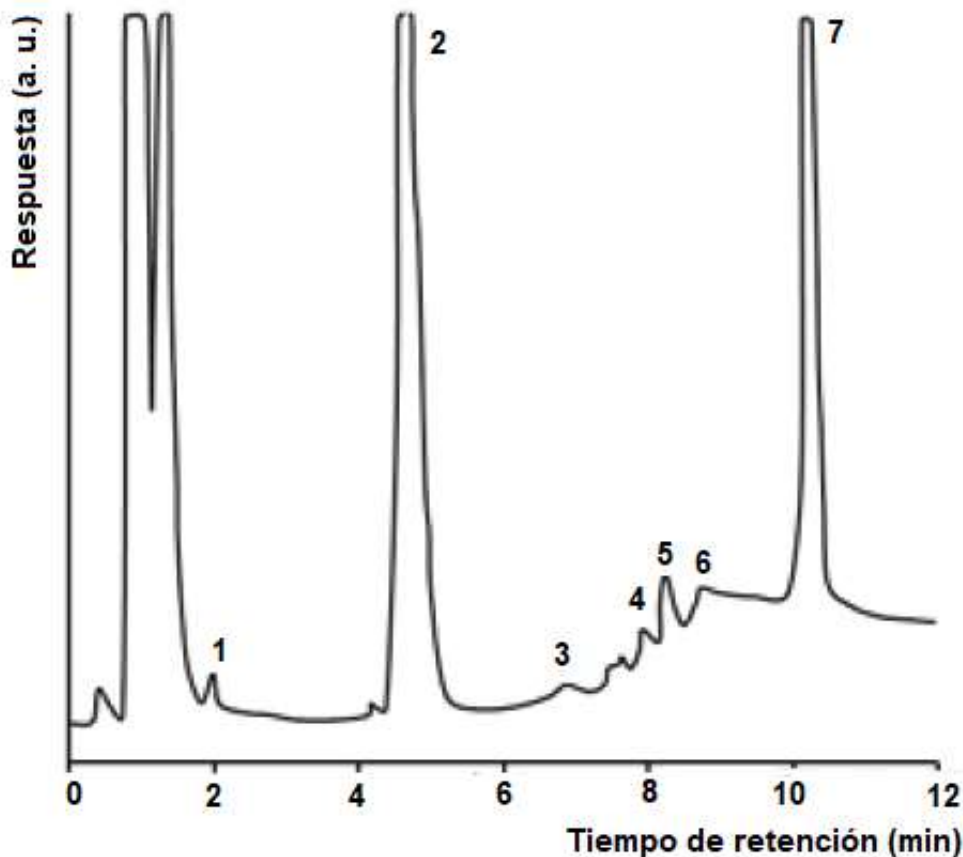


Figura 38. Cromatografía de gases de los ésteres metílicos de los ácidos carboxílicos formados por la irradiación gamma (69.4 kGy): (1) malónico, (2) succínico, (3) málico, (4) 1, 2, 3- butantricarboxílico, (5) tricarbálico + aconítico, (6) cítrico, (7) dímero del ácido succínico.

Considerando que la radiólisis se desarrolló en disolución acuosa, la principal interacción de la radiación gamma es con las moléculas de agua (Figura 39); produciendo especies altamente reactivas las cuales posteriormente reaccionan con la materia orgánica presente hasta obtener productos estables de reacción mostrados en la Figura 40.

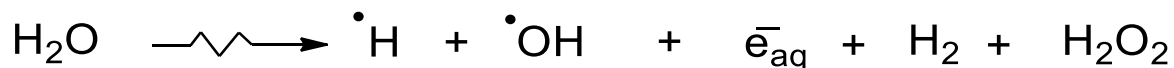


Figura 39. Radiólisis del agua.



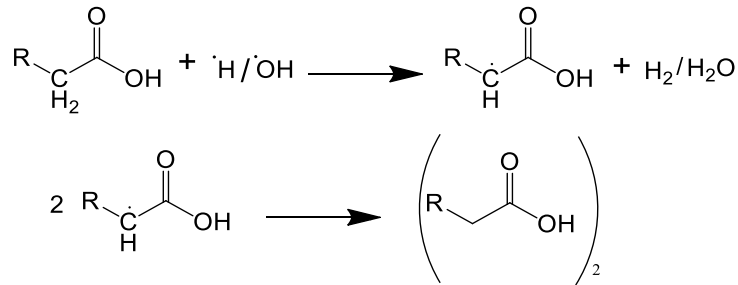


Figura 40. Reacción general entre los ácidos carboxílicos y productos de radiólisis del agua.

El mecanismo de reacción propuesto para radiólisis gamma del ácido succínico en disolución acuosa se muestra en la Figura 41 (Cruz-Castañeda, Colín-García, y Negrón-Mendoza, 2014).

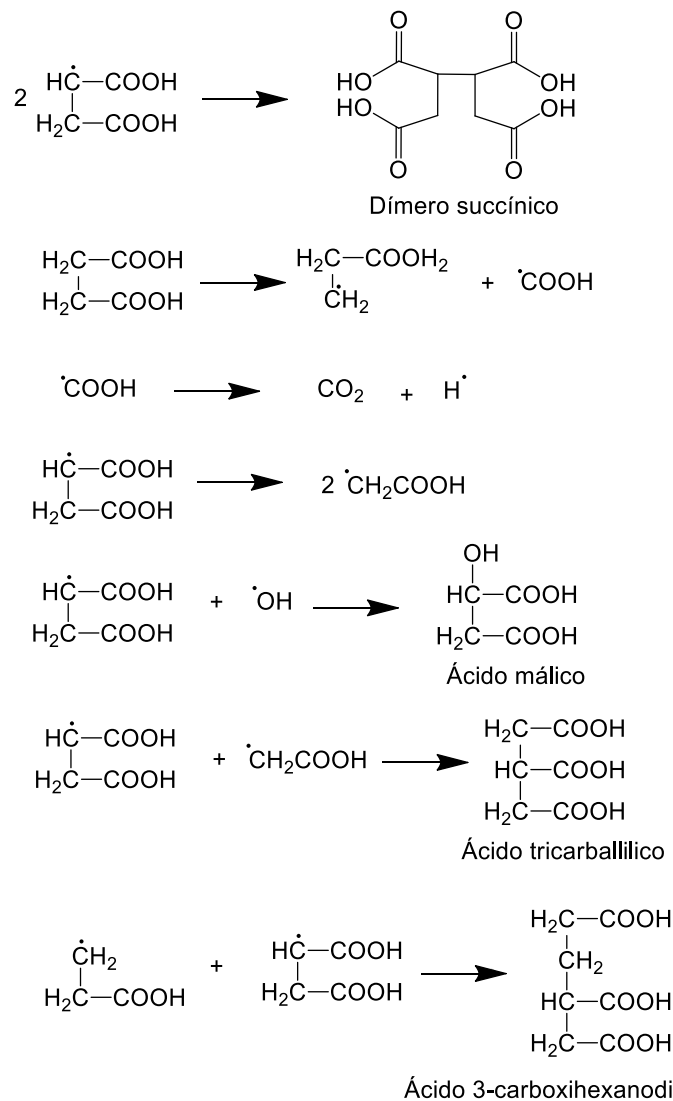


Figura 41. Mecanismo general para la radiólisis acuosa del ácido succínico.

### 5.3.3. Experimentos con suspensiones

Con el objetivo de evaluar el posible efecto causado por las superficies minerales se desarrollaron experimentos de radiólisis en suspensiones acuosas del ácido succínico utilizando montmorillonita de sodio.

Los resultados mostraron que la reacción principal es la reacción de descarboxilación (Figura 42), y no una reacción de polimerización como ocurre en la radiólisis del ácido succínico en disolución acuosa. Los productos de la reacción fueron el dióxido de carbono ( $\text{CO}_2$ ) y el ácido propiónico ( $\text{C}_3\text{H}_6\text{O}_2$ ) identificados por cromatografía de gases - espectrometría de masas (Figura 43).

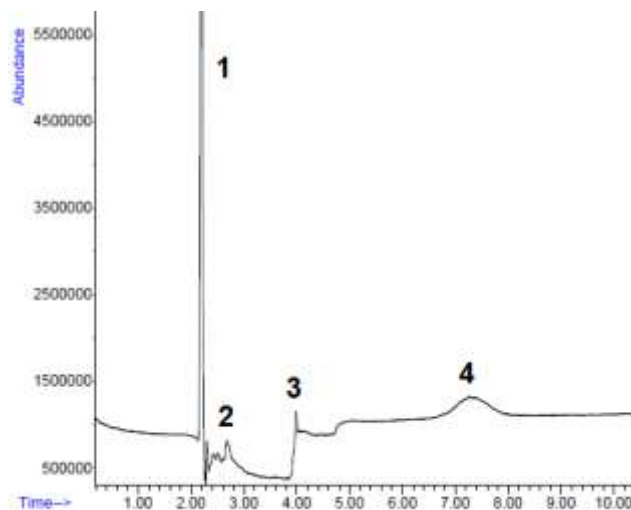


Figura 42. Cromatografía de gases de los ésteres metílicos de los ácidos carboxílicos formados por la irradiación gamma en suspensión acuosa): (1) propiónico, (2) malónico, (3) succínico, (4) málico.

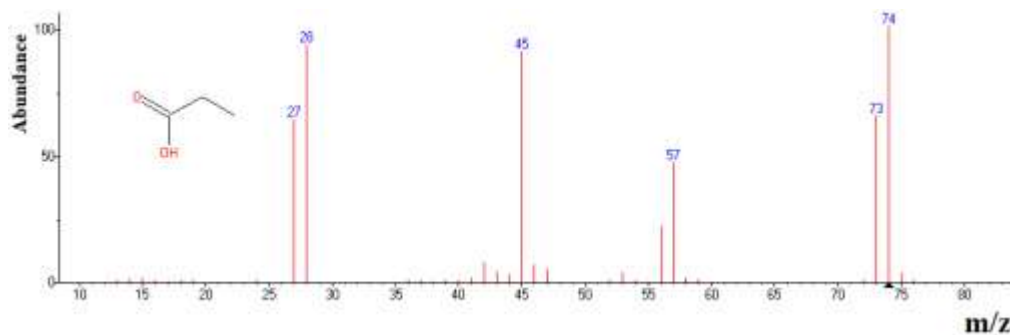


Figura 43. Espectro de fragmentación de masas del ácido propiónico formado por la radiólisis del ácido succínico en suspensión

## 5.4. *Ácido malónico (ácido carboxílico – inhibidor del ciclo de Krebs)*

### 5.4.1. *Experimentos de termólisis*

La termólisis del ácido malónico en un intervalo de 0 a 120 horas a 95°C mostró como reacción principal la de descarboxilación (Figura 44). Se identificaron como productos de reacción el ácido acético ( $C_2H_4O_2$ ) y el dióxido de carbono ( $CO_2$ ) (Figura 45) (Villafañe Barajas, 2015) (Cruz-Castañeda *et al.*, 2015).

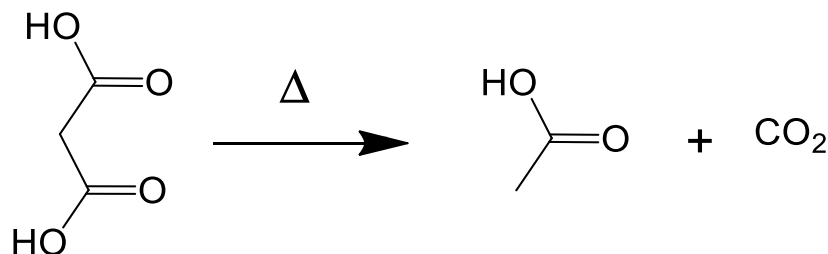


Figura 44. Reacción de descarboxilación del ácido malónico inducida por calor.

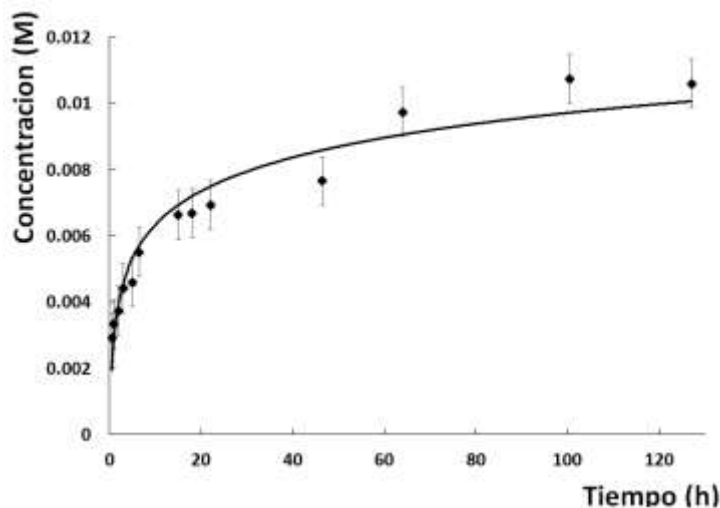


Figura 45. Formación de ácido acético por la termólisis de ácido malónico.

El mecanismo de reacción para la formación del ácido acético (Figura 46), puede ser similar al propuesto para la formación del ácido oxálico, pirúvico y oxoacético por la transferencia de un hidrógeno en un estado de transición cíclico (Back y Yamamoto, 1985; Yamamoto y Back, 1985b, 1985a).

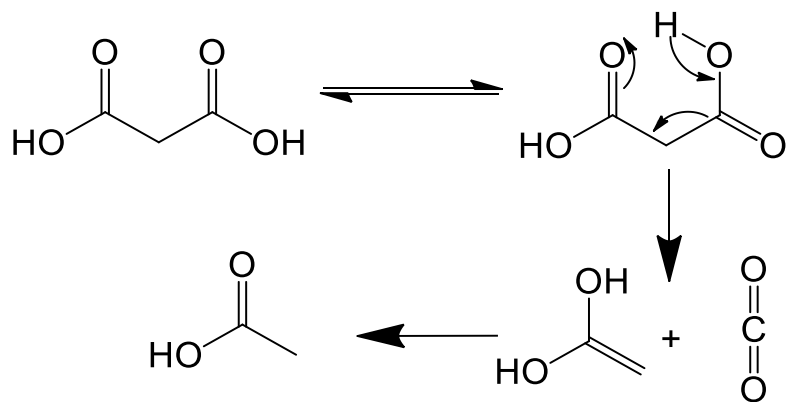


Figura 46. Mecanismo de reacción para la formación de ácido acético en la termólisis de ácido malónico.

### 5.4.2. Experimentos de radiólisis

En la radiólisis del ácido malónico en disolución acuosa libre de oxígeno la principal reacción corresponde a una descarboxilación. El principal producto de reacción corresponde al ácido acético ( $C_2H_2O_2$ ) y al dióxido de carbono ( $CO_2$ ) (Figura 47). Adicionalmente, se determinó la formación de otros ácidos carboxílicos (Tabla 8) detectados a través de cromatografía de gases acoplado a espectrometría de masas (Figura 48).

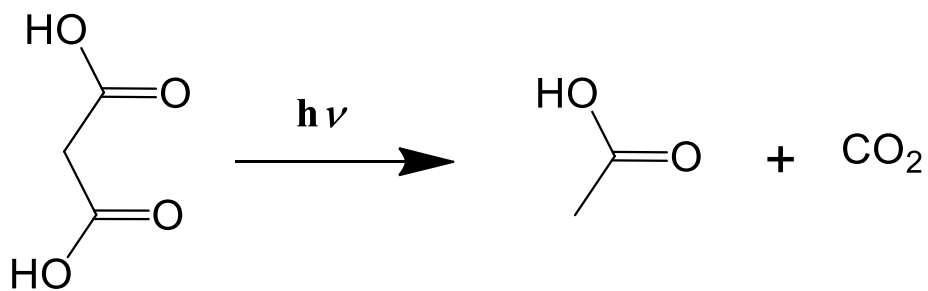


Figura 47. Radiólisis de ácido malónico en disolución acuosa.

Tabla 8. Productos de la radiólisis del ácido malónico en disolución acuosa.

Compuesto	Estructura desarrollada
Ácido oxálico <b>C<sub>2</sub>H<sub>2</sub>O<sub>4</sub></b>	
Ácido malónico <b>C<sub>3</sub>H<sub>4</sub>O<sub>4</sub></b>	
Ácido succínico <b>C<sub>4</sub>H<sub>6</sub>O<sub>4</sub></b>	
Ácido tricarbálico <b>C<sub>6</sub>H<sub>8</sub>O<sub>6</sub></b>	
Ácido 2,3 dicarboxi-succínico <b>C<sub>6</sub>H<sub>6</sub>O<sub>8</sub></b>	
Ácido cítrico <b>C<sub>6</sub>H<sub>8</sub>O<sub>7</sub></b>	

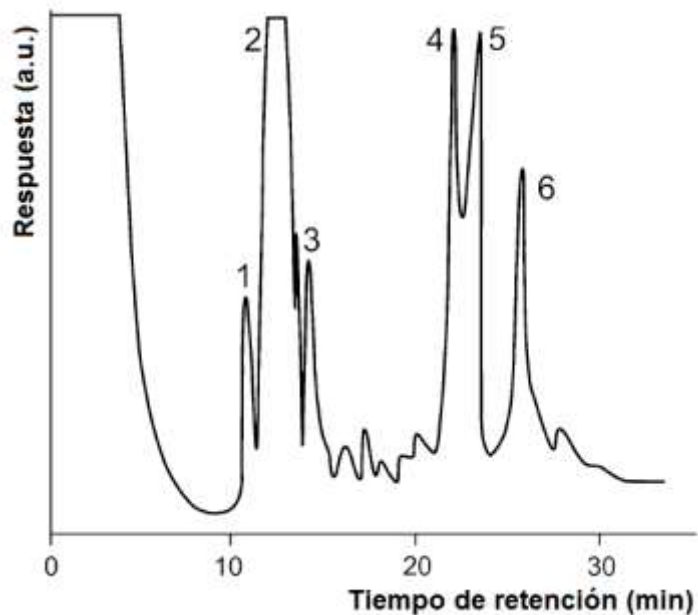
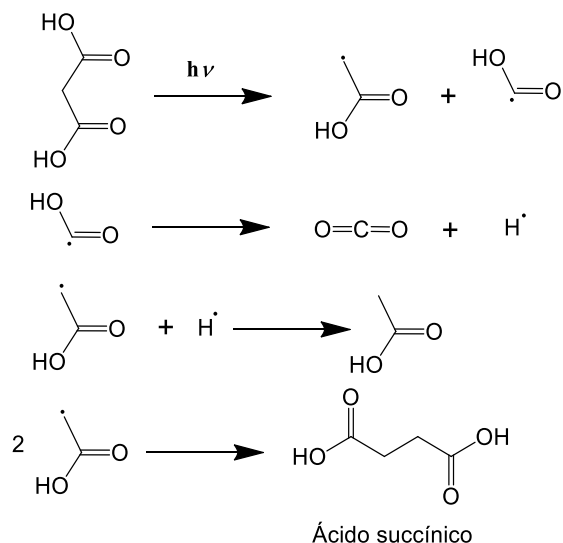
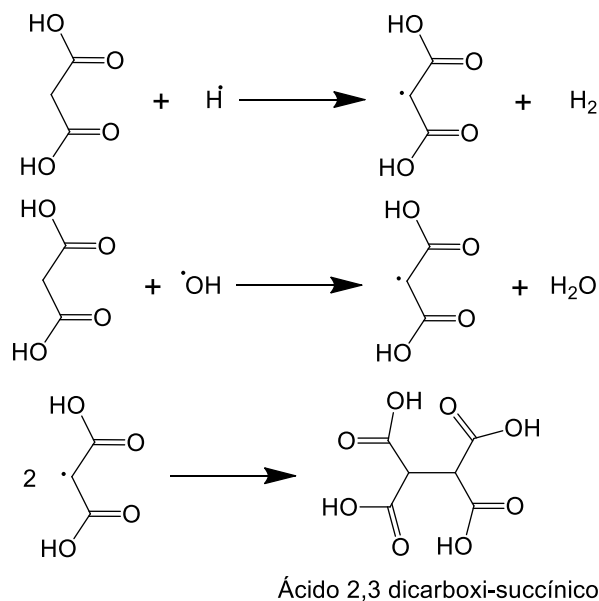


Figura 48. Cromatografía de gases de los ésteres metílicos de los ácidos carboxílicos formados por la irradiación gamma (10 kGy): (1) oxálico (2) malónico, (3) succínico, (4) tricarbálico, (5) 2,3 dicarboxi-succínico y (6) cítrico.

Debido a que la radiólisis del ácido malónico fue en disolución acuosa, la principal interacción de la radiación gamma es con las moléculas de agua (Figura 39) produciendo especies reactivas las cuales reaccionan con la materia orgánica presente en la disolución hasta obtener productos estables de reacción como el ácido succínico y el 2,3-dicarboxi-succínico . El mecanismo de reacción propuesto para la formación del ácido succínico se muestra en la Figura 49, mientras que en la Figura 50 se muestra el mecanismo de reacción del 2,3-dicarboxi-succínico.



**Figura 49. Mecanismo de reacción para la formación del ácido succínico.**



**Figura 50. Mecanismo de reacción para la formación del ácido 2,3-dicarboxi-succínico.**

### 5.4.3. Experimentos con suspensiones

Para evaluar el posible efecto causado por las superficies minerales se desarrollaron experimentos de radiólisis en suspensiones acuosas del ácido malónico utilizando montmorillonita de sodio.

Los resultados mostraron que la reacción principal es la reacción de descarboxilación (Figura 51-A). Se identificó por cromatografía de gases - espectrometría de masas, al dióxido de carbono (Figura 51-B) y al ácido acético (Figura 51-C), similar a como ocurre en la radiólisis del ácido malónico en disolución acuosa, pero en este sistema se obtuvieron menos productos secundarios de reacción.

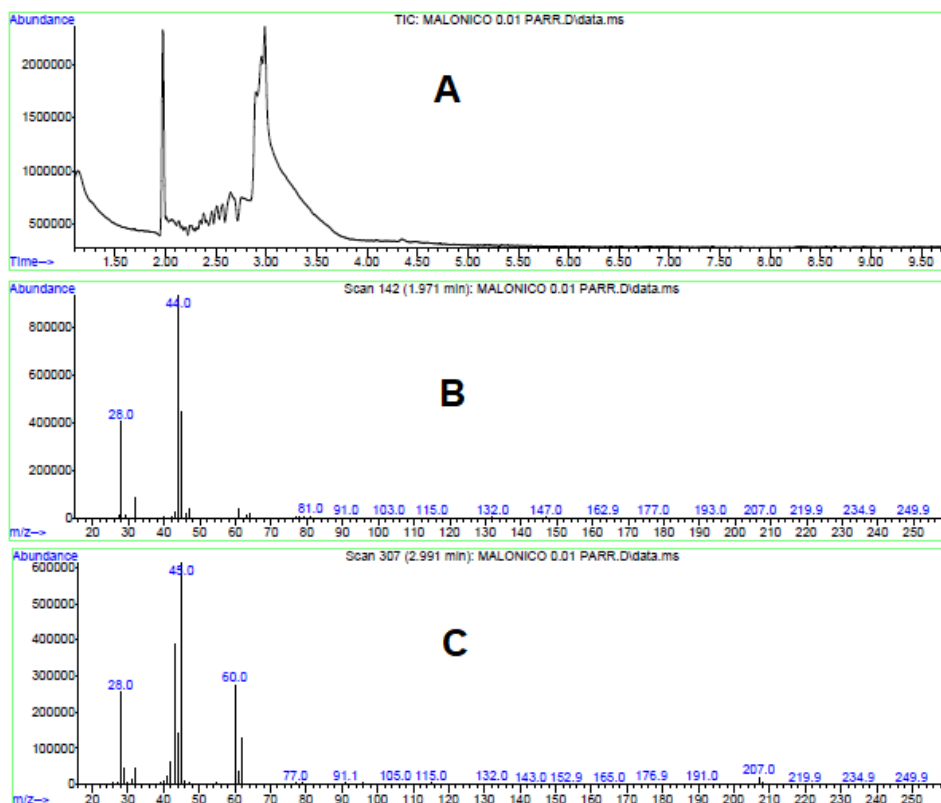


Figura 51. Cromatografía de gases de los ácidos carboxílicos formados por la irradiación gamma en suspensión acuosa (A) Espectros de masas de los productos obtenidos: (B) dióxido de carbono, (C) ácido acético.

## 5.5. Gliceraldehído (triosa - quiral)

### 5.5.1. Experimentos de radiólisis en disolución acuosa

Los experimentos de radiólisis de 0 a 60 kGy del gliceraldehído en disolución acuosa mostraron la relativa inestabilidad de gliceraldehído, con un alta tasa de reacción (determinada por polarografía, Figura 54). El gliceraldehído se descompuso más del 95% a 28 kGy (Figura 52). El principal producto de reacción (Figura 53) corresponde al malondialdehído el cual tiene un equilibrio tautomérico (Figura 55) identificado por espectrofotometría de UV a 246 nm (Figura 56), en diferentes valores de dosis de radiación (Fuentes Carreón, 2018). En la Tabla 9 se presentan los productos adicionales de la radiólisis.

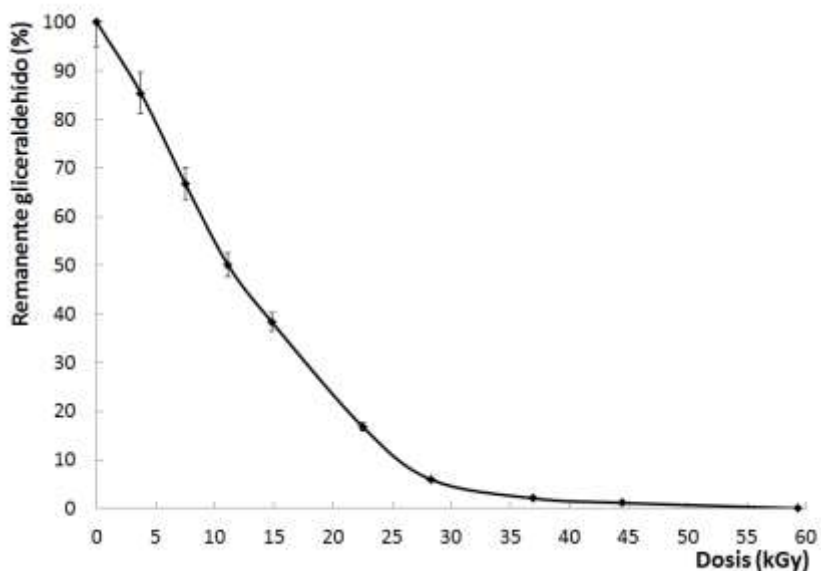


Figura 52. Descomposición de gliceraldehído en función de la dosis absorbida.

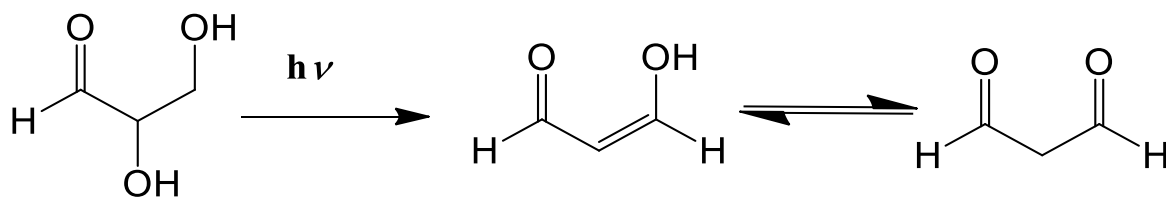


Figura 53. Radiólisis acuosa del gliceraldehído.



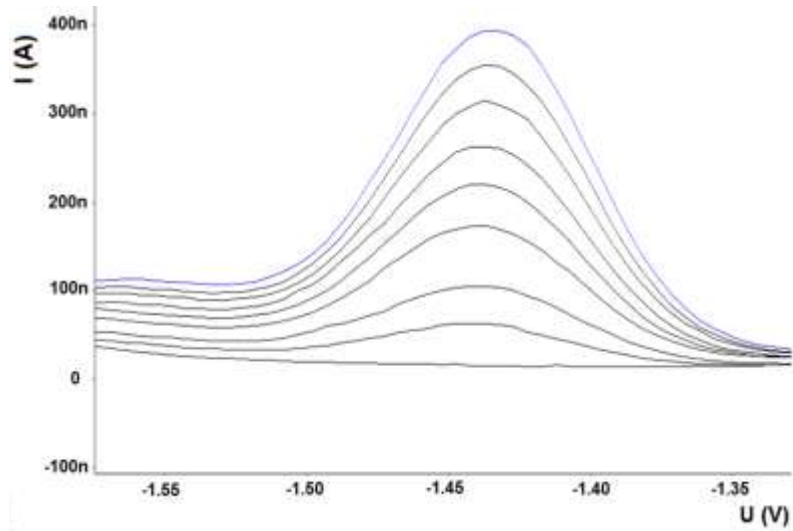


Figura 54. Análisis polarográfico del gliceraldehído.

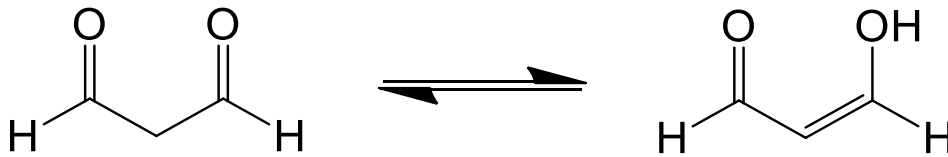


Figura 55. Equilibrio enol-cetona del malondialdehído.

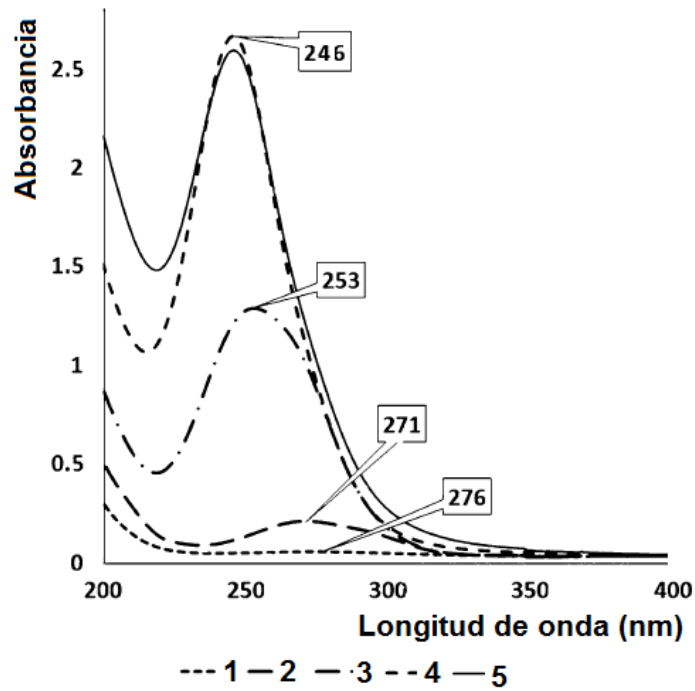


Figura 56. Espectrofotometría para la identificación de malondialdehído. Siendo 1) 0 kGy, 2) 0.22 kGy, 3) 2.2 kGy, 4) 11 kGy y 5) 20 kGy.

Tabla 9. Productos de la radiólisis del gliceraldehído en disolución acuosa.

Compuesto	Estructura desarrollada
Malondialdehído $C_3H_4O_2$	
Glicolaldehído $C_2H_4O_2$	
Metilglioxal $C_3H_4O_2$	
Glioxal $C_2H_2O_2$	
Formaldehído $CH_2O$	

Dado que la radiólisis fue en disolución acuosa, la principal interacción de la radiación gamma es con las moléculas de agua (Figura 39), produciendo especies reactivas las cuales reaccionan con el gliceraldehído presente en la disolución hasta obtener productos estables de reacción tal como se muestra en el mecanismo de reacción propuesto (Figura 57 y Figura 58).

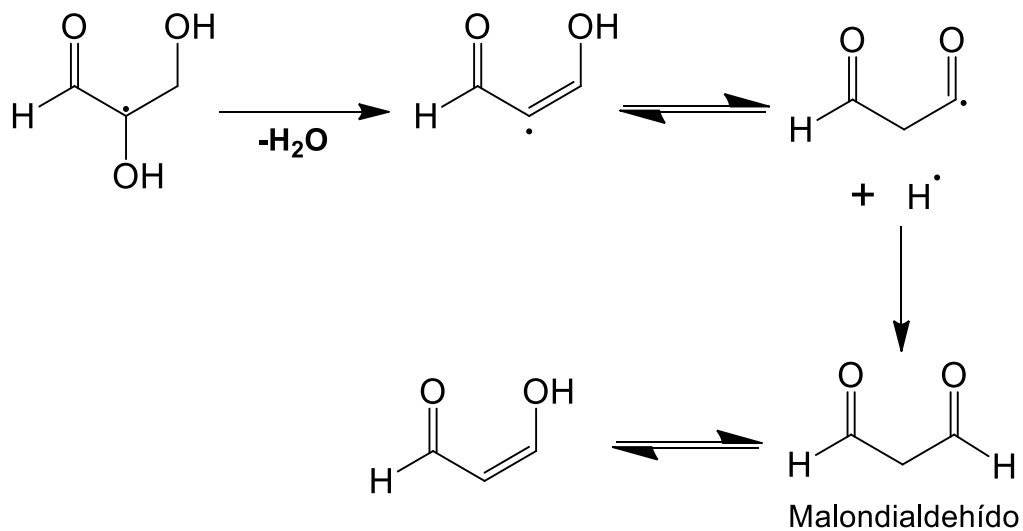


Figura 57. Mecanismo de reacción para la formación del malondialdehído.

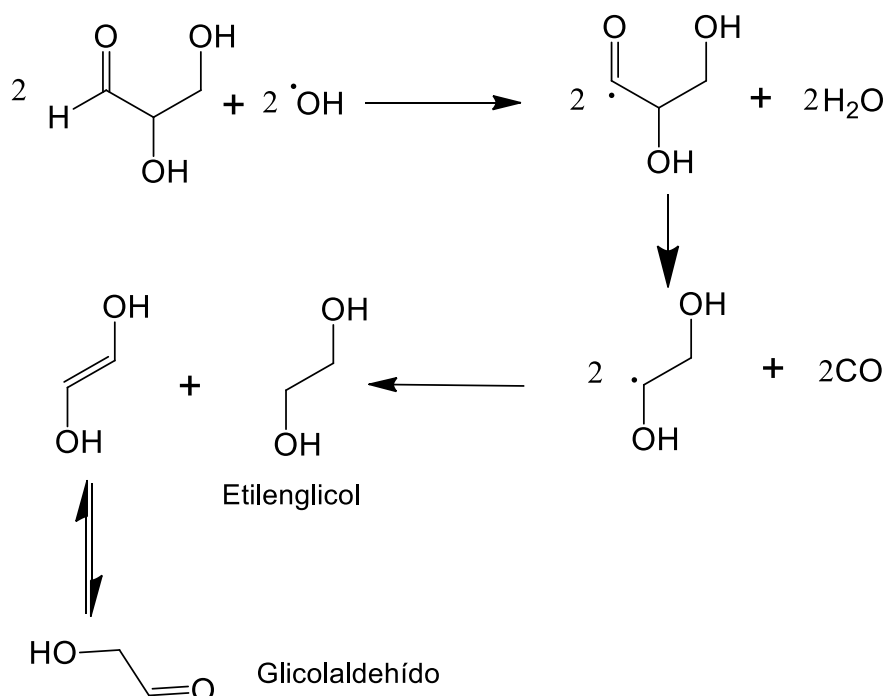


Figura 58. Mecanismo de reacción para la formación del etilenglicol y el glicolaldehído.

### 5.5.2 Experimentos de radiólisis en estado sólido

Los experimentos de radiólisis del gliceraldehído en estado sólido mostraron la estabilidad de gliceraldehído ante la radiación gamma, ya que después de 320 kGy aún se conserva aproximadamente el 82 % (Figura 60). El principal producto de reacción corresponde al dímero de etilenglicol (Figura 59). En la Tabla 10 se presentan los productos de reacción de la radiólisis del gliceraldehído en estado sólido determinados por cromatografía de gases acoplada a espectrometría de masas (Figura 61), cromatografía de líquidos acoplada a espectrometría de masas (Figura 62) y cromatografía de líquidos acoplado a espectrofotometría UV (Aguilar-Ovando *et al.*, 2018).

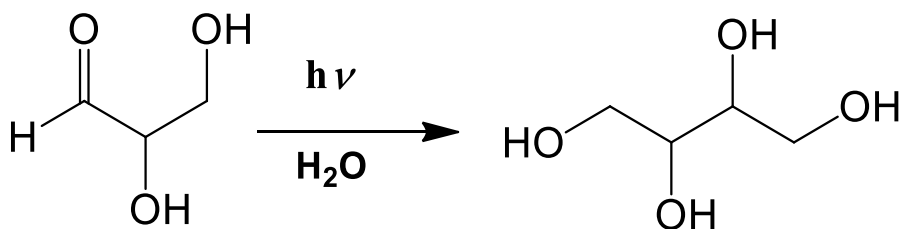


Figura 59. Radiólisis en estado sólido del gliceraldehído.

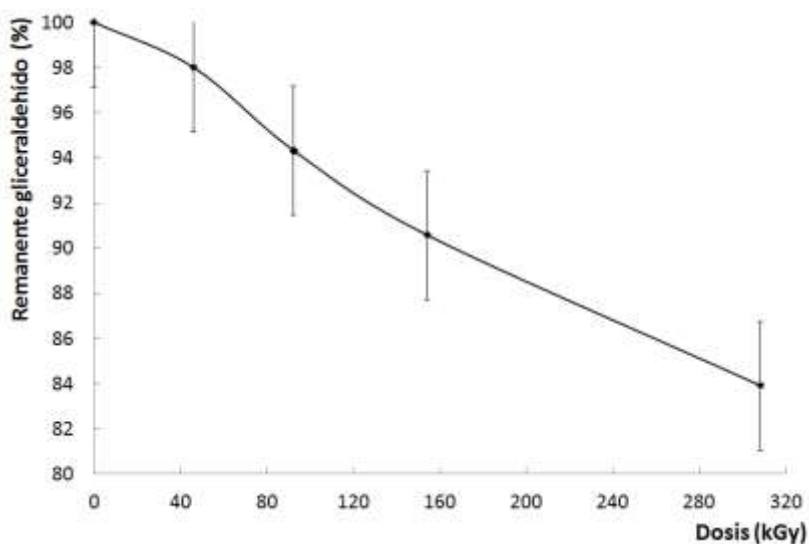


Figura 60. Descomposición de gliceraldehído en estado sólido en función de la dosis absorbida.

Tabla 10. Productos de la radiólisis del gliceraldehído en estado sólido.

Compuesto	Estructura desarrollada
Malondialdehído <b>C<sub>3</sub>H<sub>4</sub>O<sub>2</sub></b>	
Glicolaldehído <b>C<sub>2</sub>H<sub>4</sub>O<sub>2</sub></b>	
Etilenglicol <b>C<sub>2</sub>H<sub>8</sub>O<sub>2</sub></b>	
Dímero de etilenglicol <b>(C<sub>2</sub>H<sub>6</sub>O<sub>2</sub>)<sub>2</sub></b>	
2-hidroxiopropanal <b>C<sub>3</sub>H<sub>6</sub>O<sub>2</sub></b>	
Formaldehído <b>CH<sub>2</sub>O</b>	
Pentitol <b>C<sub>5</sub>H<sub>12</sub>O<sub>5</sub></b>	
Ácido fórmico <b>CH<sub>2</sub>O<sub>2</sub></b>	

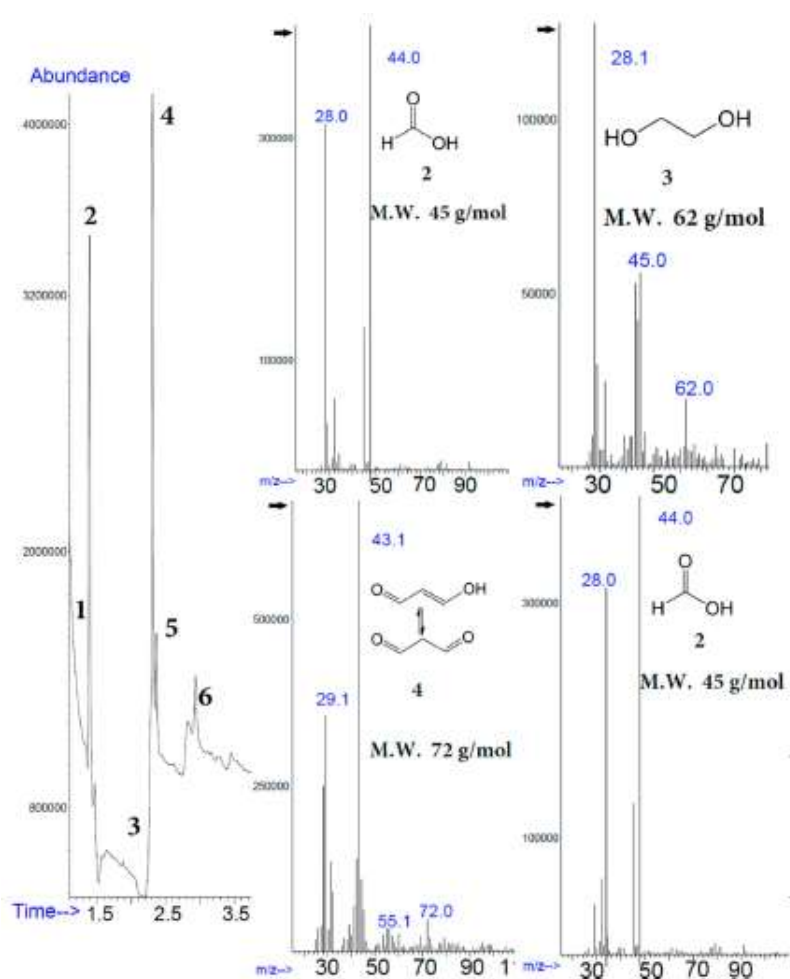


Figura 61. CG-MS de los productos formados por la radiólisis del gliceraldehído en estado sólido (1) formaldehído, (2) ácido fórmico, (3) etilenglicol, (4) malondialdehído (5) 2,3 glicolaldehído y (6) gliceraldehído.

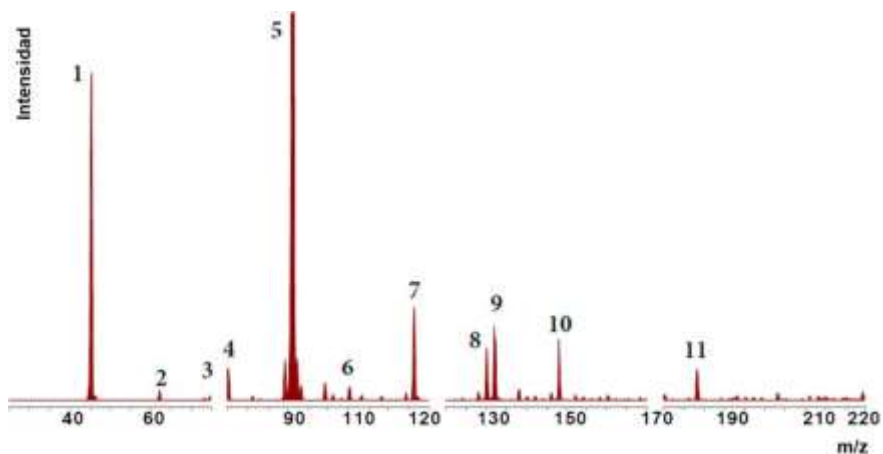


Figura 62. HPLC-MS de los productos formados por la radiólisis del gliceraldehído en estado sólido (1) ácido fórmico (reactivo) (2) glicolaldehído + etilenglicol, (3) malondialdehído, (4) 2-hidroxipropanal, (5) gliceraldehído, (7) dímero de etilenglicol, (10) pentitol, (10-12) compuestos tipo azúcares, (6, 8 y 9) desconocidos.

### 5.5.3 Experimentos con suspensiones

Se elaboraron experimentos de adsorción/desorción de gliceraldehído en tres diferentes arcillas (atapulgita, hectorita y montmorillonita) a tres diferente valores de pH (2, 7 y 11), los resultados mostraron que el gliceraldehído en general se adsorbe preferentemente a pH ácidos (especialmente en atapulgita), a pH alcalinos la adsorción es menor al 20% con las tres arcillas (Figura 63).

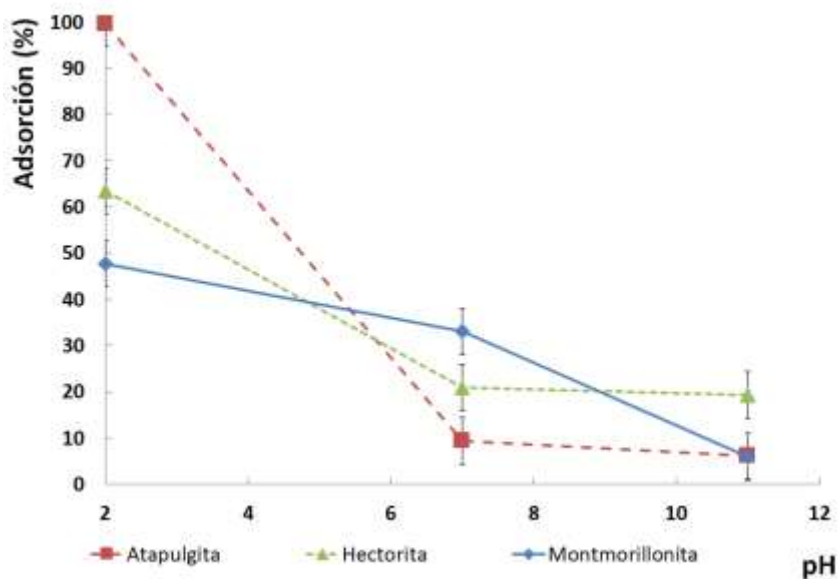


Figura 63. Experimentos de adsorción/desorción de gliceraldehído en arcillas dependiente del pH.

Los resultados de difracción de Rayos X<sup>19</sup> indican que el gliceraldehído se adsorbe preferencialmente en el canal inter-laminar de la arcilla (expansión de 11.86 a 14.59 Å), el cual tiene sitios de carácter ácido lo que puede promover reacciones (detectadas por espectrofotometría de UV a 245 nm) para la posible formación de malondialdehído de forma similar como lo hace la radiación gamma.

---

<sup>19</sup> Análisis elaborado en la Unidad de Servicios de Apoyo a la Investigación y a la Industria (USAI) de la Facultad de Química de la UNAM.

## 5.6. Glicolaldehído (diosa – no quiral)

### 5.6.1. Experimentos de radiólisis

Los experimentos de radiólisis mostraron que el glicolaldehído en disolución acuosa<sup>20</sup> libre de oxígeno corresponde a una reacción de polimerización donde los principales productos de reacción son el dímero lineal (A eritriol-122g/mol), el dímero cíclico (B 120g/mol) y un compuesto tipo azúcar de 6 carbonos (C 182 g/mol), identificados por cromatografía de líquidos y su respectivo espectro de fragmentación de masas (Figura 64). Por un análisis de HPLC-MS (Figura 65) se sabe que el rendimiento de reacción es dependiente de la dosis adsorbida.

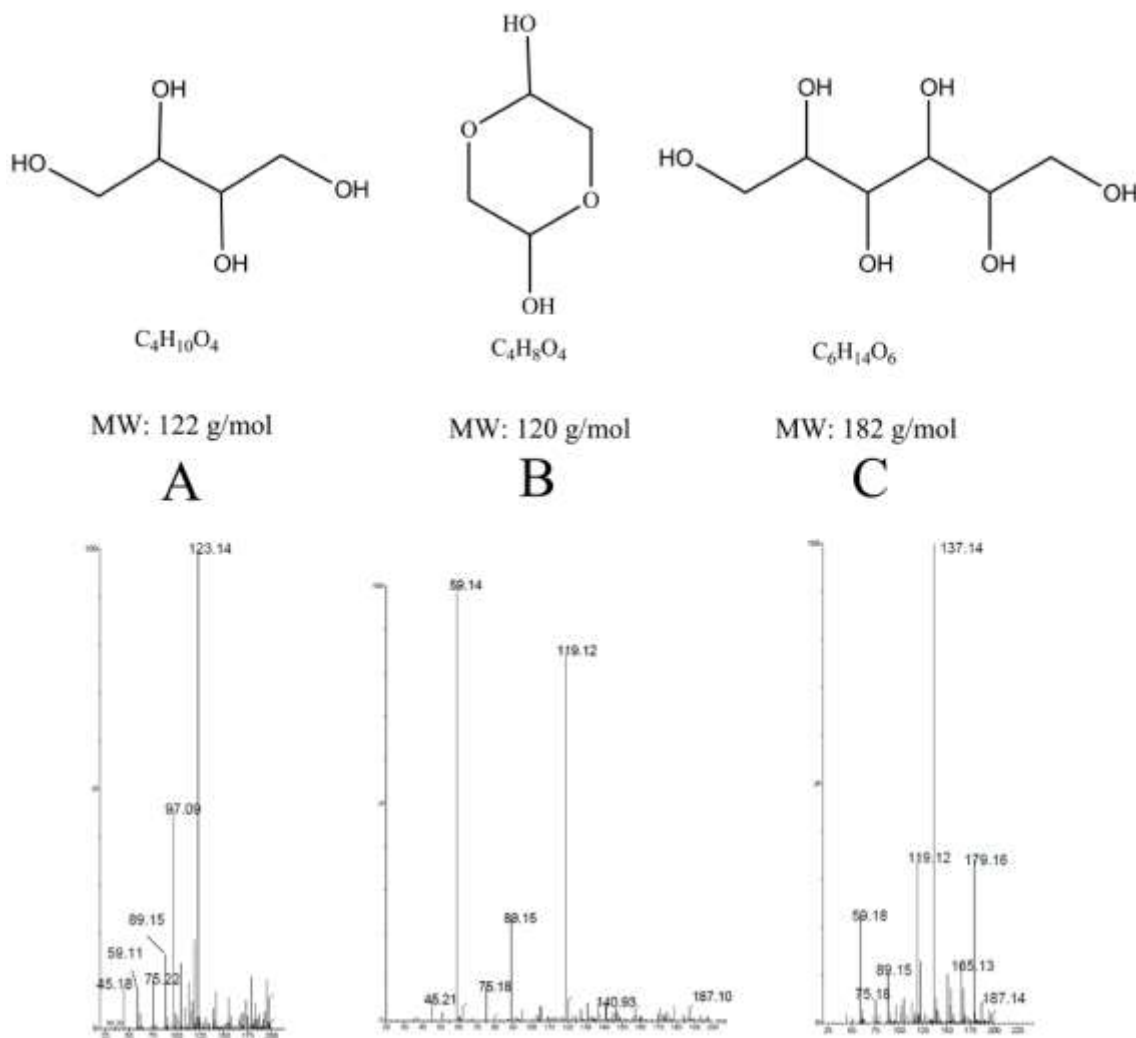


Figura 64. Espectros de fragmentación de los productos formados en la radiólisis del glicolaldehído.

<sup>20</sup> Véase apéndice: glicolaldehído en disolución acuosa

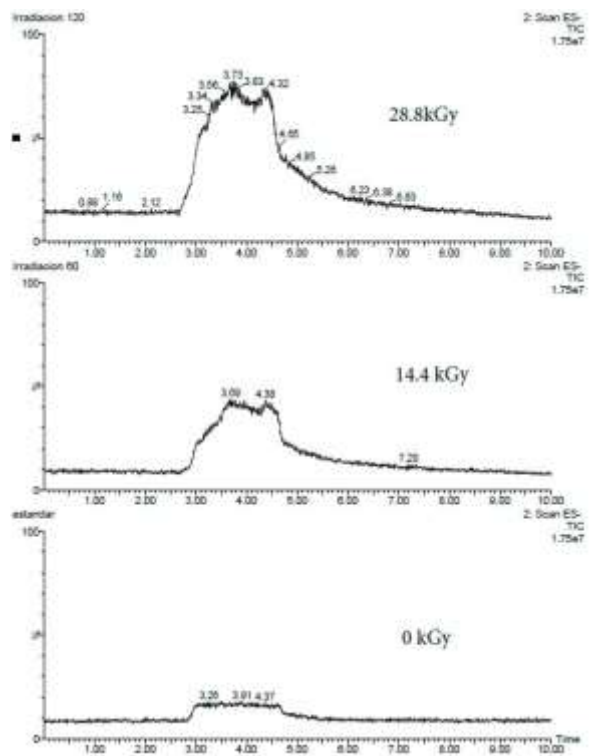


Figura 65. Análisis HPLC-MS del avance de reacción de la radiólisis del glicolaldehído.

En la Figura 66 se muestra el posible mecanismo de reacción para la polimerización de glicolaldehído (Cruz-Castañeda, *et al.*, 2017).

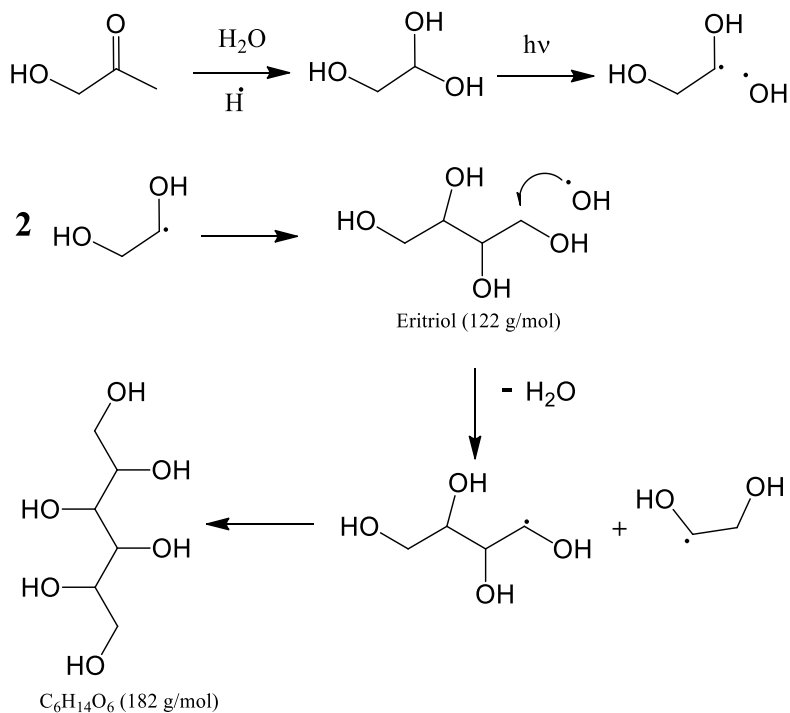


Figura 66. Mecanismo propuesto para la reacción de polimerización del glicolaldehído inducida por radiación gamma.



## 5.6.2. Experimentos con suspensiones

Con el objetivo de evaluar el posible efecto causado por las superficies minerales se desarrollaron experimentos de radiólisis en suspensiones acuosas del glicolaldehído utilizando dos arcillas: 1) montmorillonita de Na<sup>+</sup> y 2) montmorillonita de Fe<sup>3+</sup> a pH 9.

Los resultados mostraron que el monómero de glicolaldehído (1.833 minutos) es absorbido preferencialmente en la montmorillonita de hierro (97%) y que el dímero cíclico del glicolaldehído<sup>21</sup> (Figura 71) (1.7 minutos) es adsorbido preferencialmente por la montmorillonita de sodio (75%) (Figura 67).

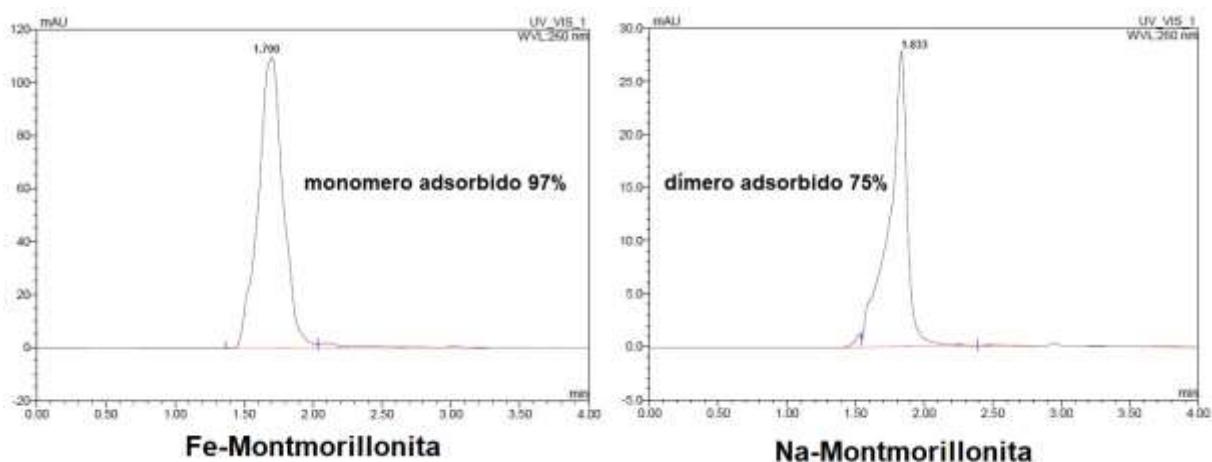


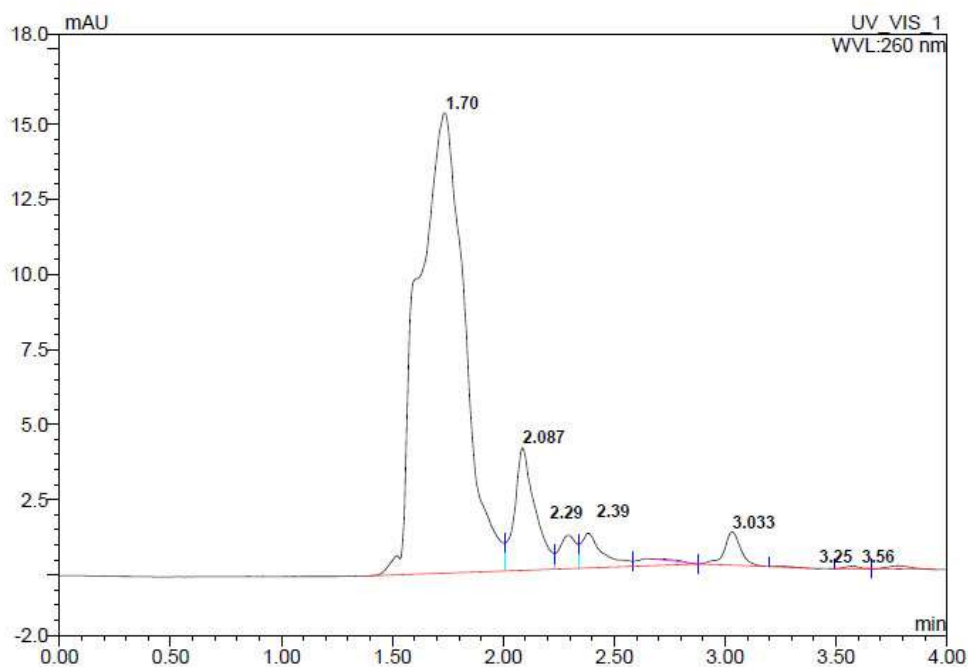
Figura 67. Experimentos adsorción/desorción de glicolaldehído en dos tipos de montmorillonita.

Ambas arcillas mostraron proteger al glicolaldehído, ya que el porcentaje de recuperación del analito fue mayor para los sistemas en suspensión respecto a su correspondiente dosis en disolución acuosa.

---

<sup>21</sup> Véase apéndice: Estructura del glicolaldehído en estado sólido y en disolución acuosa

Adicionalmente, se determinó que la montmorillonita de hierro es capaz de promover reacciones químicas en la suspensión del glicolaldehído aun sin radiación gamma, ya que se detectaron productos de reacción después de los experimentos de adsorción y desorción. Los compuestos fueron detectados por HPLC-UV (Figura 68) con tiempos de retención en 2.087, 2.28, 2.39 y 3.033 minutos. Los productos aún no se han caracterizado dada su baja concentración en la disolución.



**Figura 68. Productos detectados en los experimentos de adsorción/desorción de glicolaldehído en montmorillonita de hierro.**

Tabla 11. Resumen de algunos resultados relevantes en simulaciones hidrotermales.

Compuesto modelo	Importancia biológica y/o pre-biológica	Antecedentes de resultados relevantes en experimentos de química prebiótica de los compuestos modelo	Algunos resultados experimentales relevantes respecto a las principales variables fisicoquímicas en las simulaciones del presente trabajo.			
			Fuente de energía		Fase mineral	
			Radiólisis y productos	Termólisis y productos	pH óptimo de adsorción	Efecto principal de la superficie sólida en el sistema
Citosina	<ul style="list-style-type: none"> <li>• Presente en ADN y ARN</li> <li>• Componente de CTP, CDP y CMP</li> </ul>	-Síntesis abiótica <sup>1</sup> -Sus precursores abióticos han sido detectados en el Medio Interestelar <sup>2</sup>	<b>Desaminación:</b> <ul style="list-style-type: none"> <li>• Uracilo</li> </ul>	<b>Desaminación:</b> <ul style="list-style-type: none"> <li>• Uracilo</li> </ul>	ácido	Ninguno
Guanina	<ul style="list-style-type: none"> <li>• Presente en ADN y ARN</li> <li>• Componente de GTP, GDP y GMP</li> </ul>	-Síntesis abiótica <sup>3</sup> -Sus precursores abióticos han sido detectados en el Medio Interestelar <sup>2</sup>	<b>Hidroxilación:</b> <ul style="list-style-type: none"> <li>• 8 hidroxiguanina<sup>5</sup></li> </ul>		ácido	Protector ante fuentes de energía como agente adsorbente
Ácido succínico	<ul style="list-style-type: none"> <li>• Participante en el ciclo de Krebs</li> <li>• Reactante para la síntesis de otras macromoléculas</li> </ul>	-Síntesis abiótica <sup>6</sup> -Detectado en meteoritas <i>i. e.</i> Murchinson <sup>7</sup>	<b>Polimerización:</b> <ul style="list-style-type: none"> <li>• Ácido málico</li> <li>• Ácido malónico</li> <li>• Ácido 1,2,3-butantricarbónico</li> <li>• Ácido tricarbálico</li> <li>• Ácido aconítico</li> <li>• Ácido cítrico</li> </ul>	<b>Descarboxilación:</b> <ul style="list-style-type: none"> <li>• Ácido propiónico</li> <li>• Dióxido de carbono</li> </ul>	ácido	Dirige la radiólisis hacia la reacción de descarboxilación
Ácido malónico	<ul style="list-style-type: none"> <li>• Inhibidor del ciclo de Krebs</li> <li>• Reactante para la síntesis de otras macromoléculas</li> </ul>	-Síntesis abiótica -Detectado en meteoritas <i>i. e.</i> Murchinson <sup>8</sup>	<b>Polimerización</b> <ul style="list-style-type: none"> <li>• Ácido oxálico</li> <li>• Ácido succínico</li> <li>• Ácido tricarbálico</li> <li>• Ácido 2,3-dicarboxi-succínico</li> <li>• Ácido cítrico</li> </ul>	<b>Descarboxilación:</b> <ul style="list-style-type: none"> <li>• Ácido acético</li> <li>• Dióxido de carbono</li> </ul>	ácido	Dirige la radiólisis hacia la reacción de descarboxilación
Gliceraldehído	<ul style="list-style-type: none"> <li>• Participante en la glucólisis</li> <li>• Reactante para la síntesis de otros azúcares</li> </ul>	-Síntesis abiótica <sup>9</sup> -Primeros sistemas auto-catalíticos abióticos <sup>10</sup>	<b>Descomposición vía radicales libres</b> <ul style="list-style-type: none"> <li>• Malondialdehído</li> <li>• Glicolaldehído</li> <li>• Metilglioxal</li> <li>• Glioxal</li> <li>• Formaldehído</li> </ul>	<b>Descomposición vía radicales libres</b>	ácido	Promover procesos similares a los inducidos por radiación gamma
Glicolaldehído	<ul style="list-style-type: none"> <li>• Reactante para la síntesis de otros azúcares</li> </ul>	-Síntesis abiótica <sup>11</sup> -Detectado en el Medio Interestelar <sup>12</sup> -Primeros sistemas auto-catalíticos abióticos <sup>13</sup>	<b>Polimerización</b> <ul style="list-style-type: none"> <li>• Malondialdehído</li> <li>• Etilenglicol</li> <li>• Dímero de etilenglicol</li> <li>• 2-hidroxiopropanal</li> <li>• Formaldehído</li> <li>• Pentiol</li> <li>• Ácido fórmico</li> </ul>	<b>Descomposición vía radicales libres</b>	ácido	-Promover procesos similares a los inducidos por radiación gamma -Protector ante fuentes de energía como agente adsorbente

1. (Kobayashi *et al.*, 1986), 2, 4. (Rank, Townes, y Welch, 1971), 3. (Miyakawa *et al.*, 2000), 5. (A. L. Meléndez-López, 2018), 6. (Garrison *et al.*, 1954), 7, 8. (Pizzarello y Shock, 2010), 9, 11. (Weber y Pizzarello, 2006), 10, 12. (Parmon, 2008) y 11 (Hollis, Lovas, y Jewell, 2000)

## **6. Capítulo sexto. Discusión de resultados**

### **6.1. Citosina (base pirimidínica)**

Los resultados obtenidos muestran, para el caso particular de la descomposición de la citosina (radiólisis y termólisis), que el producto principal de la degradación de la citosina es otra base nitrogenada (el uracilo) formada a través de una reacción de desaminación dependiente de la dosis adsorbida. El uracilo tiene un gran interés pre-biológico y biológico pues el uracilo sólo está presente en el polímero de RNA y no el de DNA, siendo este hecho, un resultado relevante en los procesos de evolución química y evolución biológica en la Tierra primitiva.

Los experimentos mostraron que la citosina se adsorbe en algunas superficies minerales principalmente cuando el pH del medio es ácido y no se adsorbe en pH alcalinos. Por ello, en los experimentos en que se simula un sistema hidrotermal blanco, con pH's alcalinos (pH 9), la citosina está principalmente en la disolución acuosa y no adsorbida en la superficie mineral. En consecuencia, los sólidos solo podrían modificar el sistema por proceso de catálisis heterogénea. Sin embargo, es importante resaltar que la presencia de los sólidos utilizados en estos experimentos (olivina, Na<sup>+</sup>-montmorillonita y Fe<sup>3+</sup>-montmorillonita), en este proceso no modifican los mecanismos de reacción ni la estabilidad de la citosina en la disolución acuosa a pH alcalino.

## **6.2. Guanina (base púrica)**

Los experimentos de radiólisis de guanina en disolución acuosa demostraron que esta base nitrogenada, es extremadamente lábil y reactiva cuando se expone a fuentes de alta energía (*i.e.* radiación gamma); a 4 kGy la guanina se descompone en más del 90 %. Dada la alta reactividad de la guanina y la cinética de descomposición de sus productos de degradación, no se logró identificar los productos de la degradación de la guanina.

La radiólisis de la guanina en estado sólido mostró que la principal reacción en este sistema es una reacción de polimerización, en la cual el principal producto de reacción es el dímero de la guanina.

Los experimentos de adsorción/desorción de la guanina en Na<sup>+</sup>-montmorillonita mostraron que la guanina se adsorbe al 100 % a pH ácidos en el canal inter-laminar y aproximadamente en un 20 % a pH alcalino en la orillas de la arcilla.

Los experimentos de radiólisis del sistema en suspensión, comparando con el sistema de citosina, mostraron que la guanina aumenta su estabilidad ante la radiación gamma, ya que a 77 kGy aún se tiene un 60 % de guanina. Este hecho es relevante en los procesos de evolución química, ya que no sólo es importante la síntesis de materia orgánica, si no también es importante la preservación de la materia orgánica, para así, poco a poco y por diversos mecanismos, conseguir un aumento en la complejidad de la materia orgánica.

### **6.3. Reactividad de las bases nitrogenadas en sistemas hidrotermales**

Comparando los resultados de la cinética de descomposición de la citosina y de la guanina, podemos resaltar que la aromaticidad de los dos anillos adyacentes presentes en las bases púricas le otorga mayor estabilidad ante mecanismos de descomposición de vía radicales libres, tales como los que son generados por la radiación ionizante o el calor.

La diferencia en la estereoquímica es otro factor relevante en los procesos de adsorción-desorción de las bases nitrogenadas en diversas superficies sólidas, ya que, aunque las bases púricas y pirimidínicas se pueden adsorber-desorber, los porcentajes y las velocidades de los procesos son muy diferentes entre ellas. Adicionalmente, las constantes de acidez (estrechamente relacionadas con la estructura) también son un factor que puede marcar la diferencia fisicoquímica en los procesos de adsorción ya que, según los resultados, dependiendo del pH el sistema se puede modificar, por ejemplo, ambas bases nitrogenadas se pueden adsorber a pH ácido, pero a pH alcalino solo las bases púricas se adsorben aunque en un porcentaje menor y las pirimidínicas no.

#### **6.4. *Ácido succínico (ácido carboxílico – participante en el ciclo de Krebs)***

Los experimentos para estudiar la descomposición del ácido succínico mostraron que el sistema es dependiente del tipo de energía. Para el caso de la termólisis, el ácido succínico se descompone principalmente en ácido propiónico y dióxido de carbono a través de una reacción de descarboxilación. Mientras que en la radiólisis gamma, la principal reacción es una reacción de polimerización para formar el dímero del ácido succínico; adicionalmente, en la radiólisis también se forman otros productos de reacción, principalmente ácidos carboxílicos (Tabla 7), los cuales tienen relevancia en diversos procesos de evolución química.

Los experimentos con suspensiones acuosas de ácido succínico en Na<sup>+</sup>-montmorillonita mostraron que las superficies sólidas son capaces de modificar y redirigir los mecanismos de reacción, además pueden aumentar la eficiencia en la formación de un producto. En los experimentos de radiólisis de la suspensión, se determinó que los principales productos de reacción son el ácido propiónico y el dióxido de carbono, a través de una reacción de descarboxilación, similar a la termólisis y completamente opuesto a la radiólisis de la disolución acuosa. De esta manera, se muestra la importancia de la fuente de energía en las reacciones y procesos que tuvieron lugar en la Tierra primitiva en la etapa de evolución química.

### **6.5. *Ácido malónico (ácido carboxílico – inhibidor del ciclo de Krebs)***

Los resultados de los experimentos para estudiar la cinética de descomposición del ácido malónico mostraron un comportamiento general similar al del ácido succínico. En la termólisis del ácido malónico, también la principal reacción es la descarboxilación, pero en este caso se produce ácido acético y dióxido de carbono. Para el sistema de la radiólisis acuosa del ácido malónico, al igual que en el sistema con ácido succínico, se forman diversos ácidos carboxílicos relevantes en evolución química, pero a diferencia del ácido succínico, en el sistema del ácido malónico adicionalmente se forman ácido acético y dióxido de carbono, como en su respectiva termólisis.

Respecto a los resultados de la radiólisis de suspensiones acuosas de ácido malónico con Na<sup>+</sup>-montmorillonita mostraron un comportamiento análogo al sistema con ácido succínico. La presencia de la superficie sólida también modifica los mecanismos de reacción, aumentando para este caso la reacción de descarboxilación del ácido malónico.

Como una primera aproximación, se puede proponer que la presencia de montmorillonita modifica la degradación de los ácidos carboxílicos direccionando la reacción hacia un mecanismo de descarboxilación (A Negrón-Mendoza y Ramos-Bernal, 1998).



## **6.6. Reactividad de los ácidos carboxílicos en sistemas hidrotermales**

La diferencia principal entre los diferentes ácidos carboxílicos es básicamente el tamaño de la cadena hidrocarbonada o el número de grupos ácido carboxílico presentes, y dado que no se cambia ningún grupo funcional la reactividad de los ácidos carboxílicos es muy similar entre todos ellos, con algunas diferencias, consecuencia de fuerzas intermoleculares o configuraciones estereoquímicas.

Los resultados de los experimentos mostraron que, en general, los ácidos carboxílicos en presencia de fuentes de energía se descomponen principalmente mediante una reacción de descarboxilación siguiendo una cinética de primer orden, formando hidrocarburos o ácidos carboxílicos más pequeños. Adicionalmente se determinó que la presencia de superficies minerales puede catalizar la reacción de descarboxilación.

Una reacción secundaria que también pueden llevar a cabo los ácidos carboxílicos son reacciones de polimerización vía radicales libres, en las cuales el producto principal corresponde al dímero, pero al ser vía radicales libres se forman otros productos entre los cuales están presentes otros ácidos carboxílicos.

### **6.7. Gliceraldehído (triosa - quiral)**

Los resultados obtenidos de los experimentos de la radiólisis acuosa mostraron la relativa inestabilidad del gliceraldehído ante la radiación gamma, ya que a los 28 kGy se descompone más del 95 %, obteniendo como producto principal el malondialdehído (MDA), además de otros cuatro productos de reacción (Tabla 9). Los productos obtenidos (malondialdehído, glicolaldehído, metilglioxal, glioxal, y formaldehído) tienen gran interés en experimentos de química prebiótica, ya que son compuestos tipo azúcares con relevancia en evolución química debido a su gran utilidad para los sistemas biológicos actuales.

La radiólisis del gliceraldehído en estado sólido, por otro lado, mostró que este compuesto es estable ante la radiación gamma, ya que a los 320 kGy aún se tiene más del 82 % como remanente. El principal producto de reacción es el dímero del etilenglicol. Sin embargo, al igual que en la radiólisis en disolución acuosa también se forman otros siete compuestos tipo azúcares como productos de reacción (Tabla 10), los cuales también son relevantes en procesos de evolución química. En particular el glicolaldehído ha sido detectado en el Medio Interestelar (Remijan, 2004), por lo cual es relevante en otras hipótesis en el contexto de química prebiótica. Además, el gliceraldehído es precursor de otras aldosas y cetosas más complejas de interés pre-biológico (Mizuno y Weiss, 1974).

Se realizaron experimentos de adsorción/desorción de gliceraldehído en tres diferentes sólidos (atapulgita, hectorita y montmorillonita). Los resultados indican que para los tres sólidos la adsorción se da principalmente a pH ácidos (100 % para el caso con atapulgita), y para el caso de pH alcalino se absorbe como máximo un 20 % para las tres superficies sólidas utilizadas.

Un resultado importante de resaltar es el hecho de que la montmorillonita es capaz de promover la formación de malondialdehído a partir de gliceraldehído, de forma similar a la radiación gamma.

## 6.8. Glicolaldehído (diosa – no quiral)

Los resultados obtenidos para la radiólisis acuosa del glicolaldehído indican como principal mecanismo de reacción las reacciones de polimerización, formando azúcares o compuestos tipo azúcares, *i.e.* eritriol, (Figura 64 A). Dichos compuestos son importantes intermediarios en la síntesis de otros compuestos más complejos relevantes en evolución química. El rendimiento de reacción es proporcional a la dosis adsorbida por el sistema (Figura 65).

Para evaluar el efecto causado por la presencia de algunas superficies sólidas en el sistema, se elaboraron experimentos de adsorción/desorción de glicolaldehído en dos arcillas ( $\text{Na}^+$ -montmorillonita y  $\text{Fe}^{3+}$ -montmorillonita), estos experimentos mostraron un adsorción preferencial entre el monómero y el dímero cíclico del gliceraldehído: el monómero se adsorbe preferencialmente por la  $\text{Na}^+$ -montmorillonita y el dímero se adsorbe preferencialmente por la  $\text{Fe}^{3+}$ -montmorillonita. Adicionalmente, se identificó que la  $\text{Fe}^{3+}$ -montmorillonita, al igual que lo ocurrido con el gliceraldehído, es capaz de promover reacciones químicas en el glicolaldehído, este proceso es probablemente iniciado por el carácter de “ácido de Lewis” del catión de la arcilla. Este hecho es relevante en experimentos de química prebiótica, pues ayuda a explicar algunos procesos importantes en evolución química.

Respecto a la radiólisis gamma de suspensiones acuosas de glicolaldehído, los resultados muestran una mayor recuperación del analito en comparación con la radiólisis acuosa, mostrando así un efecto protector de las arcillas para la materia orgánica ante la radiación gamma.

## **6.9. Reactividad de los carbohidratos en sistemas hidrotermales**

La química de los carbohidratos es muy diversa y por tanto compleja. Aunque en principio todos los carbohidratos poseen los mismos grupos funcionales, el tamaño y la estereoquímica juegan un papel fundamental en la reactividad de los diversos carbohidratos ya que, dependiendo de su tamaño, los carbohidratos se pueden ciclar en anillos de 5 o 6 miembros, se pueden polimerizar mediante reacciones de eterificación, pueden tener equilibrios tautoméricos, e incluso pueden formar redes cristalinas. Esto hace que los carbohidratos sean muy reactivos y puedan formar muchos productos de reacción ya que cualquier variable fisicoquímica puede modificar el mecanismo de reacción haciendo que éste se dirija a productos completamente diferentes.

Los resultados de los experimentos resaltaron la alta reactividad de los carbohidratos ya que ambos azúcares mostraron ser lábiles a la radiación ionizante y al calor, incluso a la presencia de las superficies minerales ya que en disolución acuosa las arcillas promueven reacciones químicas en los carbohidratos.

Entre los productos obtenidos en los procesos de radiólisis se determinaron otros compuestos tipo azúcares de mayor y/o menor peso molecular de azúcar reagente, indicando que los procesos son mediante un mecanismo vía radicales libres.

## **7. Capítulo séptimo. Conclusiones**

Los mecanismos de síntesis, condensación y polimerización de la materia orgánica, al igual que los mecanismos de preservación y acumulación de la misma, son completamente dependientes de las condiciones fisicoquímicas presentes en los muy diversos ambientes geológicos en el periodo de evolución química en la Tierra. Por ello, el determinar la posible participación de las múltiples variables fisicoquímicas es sin duda, el objetivo principal de todos los experimentos de química prebiótica

En este proyecto se estudió la cinética de descomposición (termólisis y radiólisis) de compuestos modelo, simulando la vecindad de distintos sistemas hidrotermales en medios de salinidad, presión y pH fijos, en presencia de superficies minerales relevantes en estos ambientes geológicos, esto con el objetivo de evaluar en primera instancia, si estos ambientes pudieron haber sido sitios idóneos para que se llevaran a cabo procesos y reacciones prebióticas relevantes para la evolución química en la Tierra primitiva.

De acuerdo con los resultados obtenidos, podemos concluir en una primera aproximación que:

- 1) el tipo de energía utilizada para la degradación, es el agente detonante y directriz en muchos procesos fisicoquímicos importantes para la evolución química.
- 2) la radiación ionizante es un factor determinante en los mecanismos de reacción de los diferentes sistemas.
- 3) los gradientes de temperatura pueden favorecer la síntesis de muchos compuestos orgánicos.
- 4) la presencia de superficies minerales en los sistemas pueden catalizar y direccionar las reacciones químicas. Los minerales además pueden ser agentes concentradores y agentes protectores de la materia orgánica ante diferentes fuentes de energía, contribuyendo a incrementar la estabilidad de las moléculas en condiciones adversas.
- 5) La vecindad de los manantiales hidrotermales se puede proponer cautelosamente, como reactores químicos naturales contemporáneos al periodo Hadeano, en los cuales se pudo sintetizar, condensar y polimerizar de forma abiótica materia orgánica en el periodo de evolución química en la Tierra primitiva.

## 8. Referencias

- Aguilar-Ovando, E., Cruz-Castañeda, J., Buhse, T., Fuentes-Carreón, C., Ramos-Bernal, S., Heredia, A., & Negrón-Mendoza, A. (2018). Irradiation of glyceraldehyde under simulated prebiotic conditions: Study in solid and aqueous state. *Journal of Radioanalytical and Nuclear Chemistry*, 316(3), 971–979. <https://doi.org/10.1007/s10967-018-5830-4>
- Alargov, D. K., Deguchi, S., Tsujii, K., & Horikoshi, K. (2002). Reaction Behaviors of Glycine under Super- and Subcritical Water Conditions. *Origins of Life and Evolution of the Biosphere*, 32(1), 1–12. <https://doi.org/10.1023/A:1013906319253>
- Allègre, C. J., Manhès, G., & Göpel, C. (1995). The age of the Earth. *Geochimica et Cosmochimica Acta*, 59(8), 1445–1456. [https://doi.org/10.1016/0016-7037\(95\)00054-4](https://doi.org/10.1016/0016-7037(95)00054-4)
- Back, R. A., & Yamamoto, S. (1985). The gas-phase photochemistry and thermal decomposition of glyoxylic acid. *Canadian Journal of Chemistry*, 63(2), 542–548. <https://doi.org/10.1139/v85-088>
- Bada, J. L., Miller, S. L., & Zhao, M. (1995). The stability of amino acids at submarine hydrothermal vent temperatures. *Origins of Life and Evolution of the Biosphere*, 25(1–3), 111–118. <https://doi.org/10.1007/BF01581577>
- Bernal, J. D. (1951). *The physical basis of life*. Routledge and Paul. Retrieved from <https://books.google.com.mx/books?id=nPE5AAAAMAAJ>
- Brocks, J. J., Buick, R., Summons, R. E., & Logan, G. A. (2003). A reconstruction of Archean biological diversity based on molecular fossils from the 2.78 to 2.45 billion-year-old Mount Bruce Supergroup, Hamersley Basin, Western Australia. *Geochimica et Cosmochimica Acta*, 67(22), 4321–4335. [https://doi.org/10.1016/S0016-7037\(03\)00209-6](https://doi.org/10.1016/S0016-7037(03)00209-6)
- Calvin, M. (1956). *Chemical Evolution and the origin of life*. Source: *American Scientist* (Vol. 44). Retrieved from <https://www.jstor.org/stable/pdf/27826801.pdf?refreqid=excelsior%3A1f64dc29801c69dd6a6560d572292fc7>
- Campbell, A. C., Palmer, M. R., Klinkhammer, G. P., Bowers, T. S., Edmond, J. M., Lawrence, J. R., ... Karson, J. A. (1988). Chemistry of hot springs on the Mid-Atlantic Ridge. *Nature*, 335(6190), 514–519. <https://doi.org/10.1038/335514a0>
- Colín-García, M., Negrón-Mendoza, A., Ramos-Bernal, S., & Chacón, E. (2008). Irradiation of Icy Cometary Analogs: Its Relevance in Reference to Chemical Evolution and the Origin of Life BT - From Fossils to Astrobiology: Records of Life on Earth and Search for Extraterrestrial Biosignatures. In J. Seckbach & M. Walsh (Eds.) (pp. 425–442). Dordrecht: Springer Netherlands. [https://doi.org/10.1007/978-1-4020-8837-7\\_21](https://doi.org/10.1007/978-1-4020-8837-7_21)
- Cruz-Castañeda, J., Meléndez-López, A. L., Ramos-Bernal, S., Negrón-Mendoza, A. (2017). Stability of the Glycolaldehyde-Na+Montmorillonite and Glycolaldehyde-Fe3+Montmorillonite Systems in Aqueous Suspension under Gamma Radiation Fields: Implications in Chemical Evolution. *Journal of Nuclear Physics, Material Sciences, Radiation and Applications*, 5(1), 137–146. <https://doi.org/10.15415/jnp.2017.51013>
- Cruz-Castañeda, J. (2016). Radiolysis and Thermolysis of Cytosine: Importance in Chemical Evolution. *Journal of Nuclear Physics, Material Sciences, Radiation and Applications*, 4(1), 183–190. <https://doi.org/10.15415/jnp.2016.41019>
- Cruz-Castañeda, J., Colín-García, M., & Negrón-Mendoza, A. (2014a). The possible role of hydrothermal vents in chemical evolution: Succinic acid radiolysis and thermolysis, 104, 104–110. <https://doi.org/10.1063/1.4890709>
- Cruz-Castañeda, J., Colín-García, M., & Negrón-Mendoza, A. (2014b). The possible role of hydrothermal vents in chemical evolution: Succinic acid radiolysis and thermolysis. *AIP Conference Proceedings*, 1607(1), 104–110. <https://doi.org/10.1063/1.4890709>
- Cruz-Castañeda, J., Negrón-Mendoza, A., Frías, D., Colín-García, M., Heredia, A., Ramos-Bernal, S., & Villafañe-Barajas, S. (2015). Chemical evolution studies: the radiolysis and thermal decomposition of malonic acid. *Journal of Radioanalytical and Nuclear Chemistry*, 304(1), 219–225. <https://doi.org/10.1007/s10967-014-3711-z>
- Cruz Castañeda, J. A., & Negrón Mendoza, A. (2013). *Reacciones del acido fumarico en presencia de montmorillonita*. Programa de Posgrado en Ciencias Químicas. Universidad Nacional Autónoma de México, México.

- Cytosine. (2018). Retrieved from <http://www.chemspider.com/Chemical-Structure.577.html>
- Deamer, D. W., & Georgiou, C. D. (2015). Hydrothermal Conditions and the Origin of Cellular Life. *Astrobiology*, 15(12), 1091–1095. <https://doi.org/10.1089/ast.2015.1338>
- Djokic, T., Van Kranendonk, M. J., Campbell, K. A., Walter, M. R., & Ward, C. R. (2017). Earliest signs of life on land preserved in ca. 3.5 Ga hot spring deposits. *Nature Communications*, 8, 16149. <https://doi.org/10.1038/ncomms16149>
- Draganic, I., Bjergbake, E., Draganic, Z., & Sehested, K. (1991). Decomposition of ocean archeon waters by 40K radiation 3800 Ma ago as a source of oxygen and oxidizing species. *Precambrian Res.*, 52, 337–345.
- Ebisuzaki, T., & Maruyama, S. (2017). Nuclear geyser model of the origin of life: Driving force to promote the synthesis of building blocks of life. *Geoscience Frontiers*, 8(2), 275–298. <https://doi.org/10.1016/J.GSF.2016.09.005>
- Ferris, J. P., & Hagan, W. J. (1984). HCN and chemical evolution: The possible role of cyano compounds in prebiotic synthesis. *Tetrahedron*, 40(7), 1093–1120. [https://doi.org/10.1016/S0040-4020\(01\)99315-9](https://doi.org/10.1016/S0040-4020(01)99315-9)
- Ferris, J. P., Sanchez, R. A., & Orgel, L. E. (1968). Studies in prebiotic synthesis: III. Synthesis of pyrimidines from cyanoacetylene and cyanate. *Journal of Molecular Biology*, 33(3), 693–704. [https://doi.org/10.1016/0022-2836\(68\)90314-8](https://doi.org/10.1016/0022-2836(68)90314-8)
- Fischer, E., & Speier, A. (1895). Darstellung der Ester. *Berichte Der Deutschen Chemischen Gesellschaft*, 28(3), 3252–3258. <https://doi.org/10.1002/cber.189502803176>
- Florkin, M. (1960). *Aspects of the Origin of Life: International Series of Monographs on Pure and Applied Biology*. Elsevier Science. Retrieved from [https://books.google.com.mx/books?id=QwPLBAAAQBAJ&dq=The+problem+of+stages+in+biopoesis+bernal&source=gbs\\_navlinks\\_s](https://books.google.com.mx/books?id=QwPLBAAAQBAJ&dq=The+problem+of+stages+in+biopoesis+bernal&source=gbs_navlinks_s)
- Fournier, R. O. (1989). Geochemistry and Dynamics of the Yellowstone National Park Hydrothermal System. *Annual Review of Earth and Planetary Sciences*, 17(1), 13–53. <https://doi.org/10.1146/annurev.earth.17.050189.000305>
- Fuentes Carreón, C. A. (2018). *Estudio de la estabilidad de gliceraldehído en campos altos de radiación gamma: relevancia en la tierra primitiva y en cuerpos extraterrestre*. Universidad Nacional Autónoma de México.
- Gabius, H.-J. (2000). Biological Information Transfer Beyond the Genetic Code: The Sugar Code. *Naturwissenschaften*, 87(3), 108–121. <https://doi.org/10.1007/s001140050687>
- Garrison, W. M., Bennett, W., Cole, S., Haymond, H. R., & Weeks, B. M. (1954). Indirect and Direct Action of Heavy Particle Radiation on Acetic Acid in Aqueous Solutions. *Journal of the American Chemical Society*, 77, 2720–2727.
- Garzón, L., & Garzón, M. L. (2001). Radioactivity as a Significant Energy Source in Prebiotic Synthesis. *Origins of Life and Evolution of the Biosphere*, 31(1/2), 3–13. <https://doi.org/10.1023/A:1006664230212>
- Gerstl, Z., & Banin, A. (1980). Fe (super 2+) -Fe (super 3+) transformations in clay and resin ion-exchange systems. *Clays and Clay Minerals*, 28(5), 335–345.
- Glyceraldehyde. (2018). Retrieved from <http://www.chemspider.com/Chemical-Structure.731.html>
- Glycolaldehyde. (2018). Retrieved from <http://www.chemspider.com/Chemical-Structure.736.html>
- Guanine. (2018). Retrieved from <http://www.chemspider.com/Chemical-Structure.744.html>
- Haldane, J. B. S. (1929). The origin of life. *Rationalist Annual*, 148, 3–10.
- Hamilton, T. L., Lange, R. K., Boyd, E. S., & Peters, J. W. (2011). Biological nitrogen fixation in acidic high-temperature geothermal springs in Yellowstone National Park, Wyoming. *Environmental Microbiology*, 13(8), 2204–2215. <https://doi.org/10.1111/j.1462-2920.2011.02475.x>
- Hazen, R. M., & Sverjensky, D. A. (2010). Mineral surfaces, geochemical complexities, and the origins of life. *Cold Spring Harbor Perspectives in Biology*, 2(5), a002162. <https://doi.org/10.1101/cshperspect.a002162>
- Heredia, A., Colín-García, M., Puig, T. P. i., Alba-Aldave, L., Meléndez, A., Cruz-Castañeda, J. A., ... Mendoza, A. N. (2017). Computer simulation and experimental self-assembly of irradiated glycine amino acid under magnetic fields: Its possible significance in prebiotic chemistry. *BioSystems*. <https://doi.org/10.1016/j.biosystems.2017.08.008>
- Hollis, J. M., Lovas, F. J., & Jewell, P. R. (2000). Interstellar Glycolaldehyde: The First Sugar. *The Astrophysical Journal*, 540(2), L107–L110. <https://doi.org/10.1086/312881>



- Islam, M. N., Kaneko, T., & Kobayashi, K. (2003). Reaction of Amino Acids in a Supercritical Water-Flow Reactor Simulating Submarine Hydrothermal Systems. *Bulletin of the Chemical Society of Japan*, 76(6), 1171–1178. <https://doi.org/10.1246/bcsj.76.1171>
- Ito, M., Gupta, L. P., Masuda, H., & Kawahata, H. (2006). Thermal stability of amino acids in seafloor sediment in aqueous solution at high temperature. *Organic Geochemistry*, 37(2), 177–188. <https://doi.org/10.1016/J.ORGGEOCHEM.2005.09.004>
- Joyce, G. F. (1989). RNA evolution and the origins of life. *Nature*, 338(6212), 217–224.
- Kelvin, W. T. B. (1894). *The Molecular Tactics of a Crystal*. London: Clarendon Press.
- Kobayashi, K., Hua, L.-L., Gehrke, C. W., Gerhardt, K. O., & Ponnampertuma, C. (1986). Abiotic synthesis of nucleic acid bases by electric discharge in a simulated primitive atmosphere. *Origins of Life and Evolution of the Biosphere*, 16(3–4), 299–300. <https://doi.org/10.1007/BF02422036>
- Lazcano, A., & Bada, J. L. (2003). The 1953 Stanley L. Miller Experiment: Fifty Years of Prebiotic Organic Chemistry. *Origins of Life and Evolution of the Biosphere*, 33(3), 235–242. <https://doi.org/10.1023/A:1024807125069>
- Lehninger, A. L., Nelson, D. L., & Cox, M. M. (2005). *Lehninger Principles of Biochemistry*. W. H. Freeman. Retrieved from <https://books.google.com.mx/books?id=7chANOUY0LYC>
- Lemke, K. H., Rosenbauer, R. J., & Bird, D. K. (2009). Peptide Synthesis in Early Earth Hydrothermal Systems. *Astrobiology*, 9(2), 141–146. <https://doi.org/10.1089/ast.2008.0166>
- Malonic acid. (2018). Retrieved from <http://www.chemspider.com/Chemical-Structure.844.html>
- Manson, T. R., & Von Brunn, V. (1977). 3-Gyr-old stromatolites from South Africa. *Nature*, 266(5597), 47–49. <https://doi.org/10.1038/266047a0>
- Marshall, W. L. (1994). Hydrothermal synthesis of amino acids. *Geochimica et Cosmochimica Acta*, 58(9), 2099–2106. [https://doi.org/10.1016/0016-7037\(94\)90288-7](https://doi.org/10.1016/0016-7037(94)90288-7)
- Masters, C. (1979). The Fischer-Tropsch Reaction. *Advances in Organometallic Chemistry*, 17, 61–103. [https://doi.org/10.1016/S0065-3055\(08\)60321-4](https://doi.org/10.1016/S0065-3055(08)60321-4)
- Meléndez-López, A. L. (2018). *Simulación de ambientes primigenios para la formación y estabilidad de compuestos de importancia biológica: relevancia en evolución química*. Universidad Nacional Autónoma de México.
- Meléndez-López, A., Negrón-Mendoza, A., Gómez-Vidales, V., Uribe, R. M., & Ramos-Bernal, S. (2014). Study of l-aspartic acid for its possible use as a dosimeter in the interval of 3.4–20 kGy at different irradiation temperatures. *Radiation Physics and Chemistry*, 104, 230–234. <https://doi.org/http://dx.doi.org/10.1016/j.radphyschem.2014.03.012>
- Miller, S. L. (1953). A Production of Amino Acids under Possible Primitive Earth Conditions Author ( s ): Stanley L . Miller Published by: American Association for the Advancement of Science Stable URL : <http://www.jstor.org/stable/1680569> A Production of Amino Acids Under Po, 117(3046), 528–529.
- Miller, S. L., & Lazcano, A. (1995). The origin of life—did it occur at high temperatures? *Journal of Molecular Evolution*, 41(6), 689–692. <https://doi.org/10.1007/bf00173146>
- Miller, S., & Orgel, L. (1974). *The origins of life on the Earth*. New Jersey: Prentice-Hall.
- Miyakawa, S., Murasawa, K.-I., Kobayashi, K., & Sawaoka, A. B. (2000). Abiotic Synthesis of Guanine with High-Temperature Plasma. *Origins of Life and Evolution of the Biosphere*, 30(6), 557–566. <https://doi.org/10.1023/A:1026587607264>
- Mizuno, T., & Weiss, A. H. (1974). Synthesis and Utilization of Formose Sugars. *Advances in Carbohydrate Chemistry and Biochemistry*, 29, 173–227. [https://doi.org/10.1016/S0065-2318\(08\)60250-4](https://doi.org/10.1016/S0065-2318(08)60250-4)
- Mora, C., Tittensor, D. P., Adl, S., Simpson, A. G. B., & Worm, B. (2011). How Many Species Are There on Earth and in the Ocean? *PLoS Biology*, 9(8), e1001127. <https://doi.org/10.1371/journal.pbio.1001127>
- Morrison, R. T., Boyd, R. N., Zugazagoitia Herranz, R., & Fiedler, P. (1998). *Química orgánica*. Addison Wesley Longman.
- Muller, A. W. J., & Schulze-Makuch, D. (2006). Thermal Energy and the Origin of Life. *Origins of Life and Evolution of Biospheres*, 36(2), 177–189. <https://doi.org/10.1007/s11084-005-9003-4>
- NASA Earth Observatory. (2010). How much water is there on Earth, from the USGS Water Science School. Retrieved from <https://water.usgs.gov/edu/earthhowmuch.html>
- Negrón-Mendoza, A., & Ramos-Bernal, S. (1998). Radiolysis of carboxylic acids adsorbed in clay

- minerals. *Radiation Physics and Chemistry*, 52(1), 395–399. [https://doi.org/https://doi.org/10.1016/S0969-806X\(98\)00059-0](https://doi.org/https://doi.org/10.1016/S0969-806X(98)00059-0)
- Negrón-Mendoza, A., & Ramos-Bernal, S. (1998). Radiolysis of carboxylic acids adsorbed in clay minerals. *Radiation Physics and Chemistry*, 52(1), 395–399. [https://doi.org/https://doi.org/10.1016/S0969-806X\(98\)00059-0](https://doi.org/https://doi.org/10.1016/S0969-806X(98)00059-0)
- Negrón-Mendoza, Alicia, & Ponnampereuma, C. (1976). Formation of biologically relevant carboxylic acids during the gamma irradiation of acetic acid. *Origins of Life*, 7(3), 191–196. <https://doi.org/10.1007/BF00926937>
- Negrón Mendoza, A., Albarrán, G., Ramos Bernal, S., Chela flores, J., & Raulin, F. (1996). Clays as natural catalyst in Prebotic Processes. In *Chemical Evolution: Physics of the Origin and Evolution* (pp. 97–106). Holanda: Academic publishers.
- Nutman, A. P., Bennett, V. C., Friend, C. R. L., Van Kranendonk, M. J., & Chivas, A. R. (2016). Rapid emergence of life shown by discovery of 3,700-million-year-old microbial structures. *Nature*, 537(7621), 535–538. <https://doi.org/10.1038/nature19355>
- O'Donnell, J. H., & Sangster, D. F. (1970). *Principles of Radiation Chemistry. Other Information: Orig. Receipt Date: 31-DEC-70; Bib. Info. Source: UK (United Kingdom (sent to DOE from))*. United Kingdom: Edward Arnold.
- Orgel, L. E. (1968). Evolution of the genetic apparatus. *Journal of Molecular Biology*, 38(3), 381–393. [https://doi.org/https://doi.org/10.1016/0022-2836\(68\)90393-8](https://doi.org/https://doi.org/10.1016/0022-2836(68)90393-8)
- Oró, J. (1960). Synthesis of adenine from ammonium cyanide. *Biochemical and Biophysical Research Communications*, 2(6), 407–412. [https://doi.org/10.1016/0006-291X\(60\)90138-8](https://doi.org/10.1016/0006-291X(60)90138-8)
- Oró, J. (1961). Comets and the Formation of Biochemical Compounds on the Primitive Earth. *Nature*, 190, 389. Retrieved from <http://dx.doi.org/10.1038/190389a0>
- Otroshchenko, V. A., & Vasilyeva, N. V. (1977). The role of mineral surfaces in the origin of life. *Origins of Life*, 8(1), 25–31. <https://doi.org/10.1007/BF00930936>
- Parker, E. T., Cleaves, H. J., Dworkin, J. P., Glavin, D. P., Callahan, M., Aubrey, A., ... Bada, J. L. (2011). Primordial synthesis of amines and amino acids in a 1958 Miller H<sub>2</sub>S-rich spark discharge experiment. *Proceedings of the National Academy of Sciences of the United States of America*, 108(14), 5526–5531. <https://doi.org/10.1073/pnas.1019191108>
- Parmon, V. N. (2008). The Prebiotic Phase of the Origin of Life as Seen by a Physical Chemist. In *Biosphere Origin and Evolution* (pp. 89–101). Boston, MA: Springer US. [https://doi.org/10.1007/978-0-387-68656-1\\_6](https://doi.org/10.1007/978-0-387-68656-1_6)
- Pizzarello, S., & Shock, E. (2010). The organic composition of carbonaceous meteorites: the evolutionary story ahead of biochemistry. *Cold Spring Harbor Perspectives in Biology*, 2(3), a002105. <https://doi.org/10.1101/cshperspect.a002105>
- Ponnampereuma, C., Shimoyama, A., & Friebele, E. (1982). Clay and the origin of life. *Origins of Life*, 12(12), 9–40.
- Rank, D. M., Townes, C. H., & Welch, W. J. (1971). Interstellar Molecules and Dense Clouds. *Science*, 174(4014), 1083–1101. Retrieved from <http://www.jstor.org/stable/1733439>
- Remijan, J. M. H. and P. R. J. and F. J. L. and A. (2004). Green Bank Telescope Observations of Interstellar Glycolaldehyde: Low-Temperature Sugar. *The Astrophysical Journal Letters*, 613(1), L45. Retrieved from <http://stacks.iop.org/1538-4357/613/i=1/a=L45>
- Russel, M. J., & Hall, A. J. (1997). The emergence of life from iron monosulphide bubbles at a submarine hydrothermal redox and pH front. *Journal of the Geological Society*, 154(3), 377–402. <https://doi.org/10.1144/gsjgs.154.3.0377>
- Russell, M. J., & Hall, A. J. (2009). The Hydrothermal Source of Energy and Materials at the Origin of Life. In *Chemical Evolution II: From the Origins of Life to Modern Society* (Vol. 1025, pp. 45–62). American Chemical Society. <https://doi.org/doi:10.1021/bk-2009-1025.ch00310.1021/bk-2009-1025.ch003>
- Schidlowski, M. (2001). Carbon isotopes as biogeochemical recorders of life over 3.8 Ga of Earth history: evolution of a concept. *Precambrian Research*, 106(1–2), 117–134. [https://doi.org/10.1016/S0301-9268\(00\)00128-5](https://doi.org/10.1016/S0301-9268(00)00128-5)
- Schlesinger, G., & Miller, S. L. (1973). Equilibrium and kinetics of glyconitrile formation in aqueous solution. *Journal of the American Chemical Society*, 95(11), 3729–3735. <https://doi.org/10.1021/ja00792a043>
- Succinic acid. (2018). Retrieved from <http://www.chemspider.com/Chemical-Structure.1078.html>

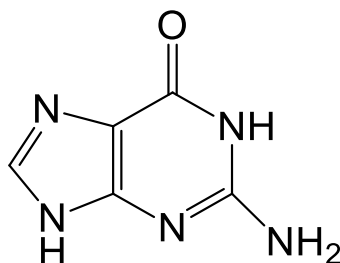
- Tirard, S. (2017). J. B. S. Haldane and the origin of life. *Journal of Genetics*, 96(5), 735–739. Retrieved from <http://www.ncbi.nlm.nih.gov/pubmed/29237880>
- Villafañe Barajas, S. A. (2015). *Estabilidad del ácido malónico bajo las condiciones presentes en manantiales hidrotermales blancos*. Universidad Nacional Autónoma de México,.
- Voet, A. B., & Schwartz, A. W. (1983). Prebiotic adenine synthesis from HCN—Evidence for a newly discovered major pathway. *Bioorganic Chemistry*, 12(1), 8–17. [https://doi.org/10.1016/0045-2068\(83\)90003-2](https://doi.org/10.1016/0045-2068(83)90003-2)
- Wächtershäuser, G. (1988). *Before Enzymes and Templates: Theory of Surface Metabolism*. *MICROBIOLOGICAL REVIEWS* (Vol. 52). Retrieved from <http://mmbbr.asm.org/>
- Walter, M. R., Buick, R., & Dunlop, J. S. R. (1980). Stromatolites 3,400–3,500 Myr old from the North Pole area, Western Australia. *Nature*, 284(5755), 443–445. <https://doi.org/10.1038/284443a0>
- Washington, J. (2000). The Possible Role of Volcanic Aquifers in Prebiologic Genesis of Organic Compounds and RNA. *Origins of Life and Evolution of the Biosphere*, 30(1), 53–79. <https://doi.org/10.1023/A:1006692606492>
- Weber, A. L., & Pizzarello, S. (2006). The peptide-catalyzed stereospecific synthesis of tetroses: a possible model for prebiotic molecular evolution. *Proceedings of the National Academy of Sciences of the United States of America*, 103(34), 12713–12717. <https://doi.org/10.1073/pnas.0602320103>
- Yamamoto, S., & Back, R. A. (1985a). The gas-phase photochemistry of oxalic acid. *The Journal of Physical Chemistry*, 89(4), 622–625. <https://doi.org/10.1021/j100250a014>
- Yamamoto, S., & Back, R. A. (1985b). The photolysis and thermal decomposition of pyruvic acid in the gas phase. *Canadian Journal of Chemistry*, 63(2), 549–554. <https://doi.org/10.1139/v85-089>
- Yaylayan, V. A., Harty-Majors, S., & Ismail, A. A. (1998). Investigation of the mechanism of dissociation of glycolaldehyde dimer (2,5-dihydroxy-1,4-dioxane) by FTIR spectroscopy. *Carbohydrate Research*, 309(1), 31–38. [https://doi.org/https://doi.org/10.1016/S0008-6215\(98\)00129-3](https://doi.org/https://doi.org/10.1016/S0008-6215(98)00129-3)

## 9. Apéndice

### 9.1. Compuestos modelo - Moléculas orgánicas:

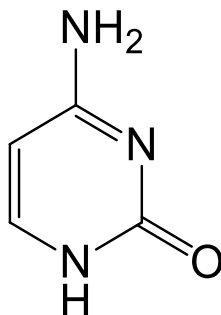
A continuación se presentan algunas propiedades fisicoquímicas para los analitos:

- ✓ **guanina** (base púrica) (“Guanine,” 2018)



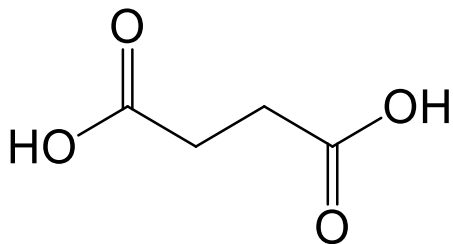
- IUPAC: 2-amino-1H-purina-6(9H)-ona
- Fórmula molecular:  $C_5H_5N_5O$
- Peso molecular: 151.126 g/mol
- Apariencia: sólido amorfo blanco

- ✓ **citosa** (base pirimidínica) (“Cytosine,” 2018)



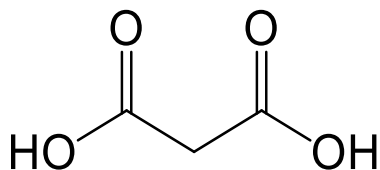
- IUPAC: 4-amino-2-ona-pirimidina
- Fórmula molecular:  $C_4H_5N_3O$
- Peso molecular: 111.102 g/mol
- Apariencia: sólido amorfo blanco

- ✓ **ácido succínico** (ácido carboxílico – participante en el ciclo de Krebs)  
("Succinic acid," 2018)



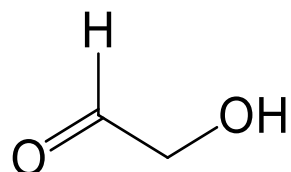
- IUPAC: Ácido butanodioico
- Fórmula molecular:  $C_4H_6O_4$
- Peso molecular: 118.088 g/mol
- Apariencia: sólido cristalino blanco.
- $pK_{a1}$  4.2,  $pK_2$  5.6
- ácido dicarboxílico

- ✓ **ácido malónico** (ácido carboxílico – inhibidor del ciclo de Krebs) ("Malonic acid," 2018)



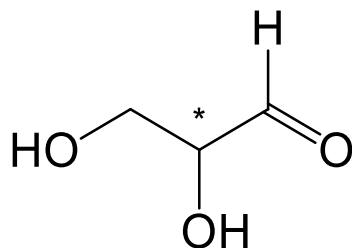
- IUPAC: Ácido propanodioico
- Fórmula molecular:  $C_3H_4O_4$
- Peso molecular: 104.062 g/mol
- Apariencia: sólido cristalino blanco.
- $pK_{a1}$  2.83,  $pK_2$  5.69
- Ácido dicarboxílico

- ✓ **glicolaldehído** (diosa – no quiral) (“Glycolaldehyde,” 2018) .



- IUPAC: 2-hidroxi-etanal
- Fórmula molecular:  $C_2H_4O_2$
- Peso molecular: 60.052 g/mol
- Apariencia: sólo existe en disolución acuosa al disolver el dímero el cual es sólido cristalino blanco.

- ✓ **gliceraldehído** (triosa - quiral) (“Glyceraldehyde,” 2018)



- UPAC: 2,3-Dihidroxi-propanal
- Fórmula molecular:  $C_3H_6O_3$
- Peso molecular: 90.078 g/mol
- El carbono  $\alpha$  al grupo carbonilo es quiral
- Apariencia mezcla racémica: sólido amorfo blanco.
- Apariencia de los isómeros aislados: líquidos amarillento

## 9.2. Quiralidad

El término quiralidad fue propuesto por primera vez por William Thomson (Lord Kelvin), en su libro de 1854 titulado "The Molecular Tactics of a Crystal", y refiere a los objetos que no son superponibles con su imagen especular:

"I call any geometrical figure, or group of points, *chiral*, and say that it has chirality, if its image in a plane mirror, ideally realized, cannot be brought to coincide with itself. Two equal and similar right hands are homochirally similar. Equal and similar right and left hands are heterochirally similar or 'allochirally' similar (but heterochirally is better). These are also called 'enantiomorphs,' after a usage introduced, I believe, by German writers. Any chiral object and its image in a plane mirror are heterochirally similar" (Kelvin, 1894) .

En química, particularmente en la estereoquímica, la quiralidad es fundamental ya que existe una gran cantidad de reacciones las cuales son estereoselectivas y/o estereoespecíficas, por ejemplo, en bioquímica la estereoselectividad de las enzimas hace que sólo uno de los enantiómeros de los aminoácidos o de los carbohidratos sea partícipe en rutas metabólicas.

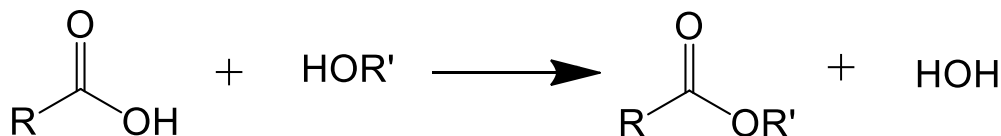
## 9.3. Técnica para obtener agua tridestilada descrita por O'Donell y Sangster en 1970

Para obtener el agua tridestilada empleada en química de radiaciones, se parte de agua bidestilada comercial, la cual se somete a tres destilaciones consecutivas con diferentes compuestos. La primera se realiza colocando 1 g de  $\text{KMnO}_4$  y 1 g de  $\text{NaOH}$  por cada litro de agua, la segunda destilación contiene 0.5 mL de  $\text{H}_2\text{SO}_4$  y 1 g de  $\text{K}_2\text{Cr}_2\text{O}_7$  por cada litro de agua y por último se destila sin ningún compuesto.

## 9.4. Esterificación de Fisher

Una esterificación de Fischer (

**Figura 69**) es una reacción catalizada por un ácido de tipo ataque nucleofílico al carbono del grupo carbonilo de un ácido carboxílico por el átomo de oxígeno de un alcohol formando un enlace éster y moléculas de agua como producto de reacción, descrita por primera vez por Emil Fischer y Arthur Speier en 1895 (Fischer y Speier, 1895) .



**Figura 69.** Reacción general de la esterificación de Fischer.

## 9.5. Estructura del glicolaldehído en estado sólido y en disolución acuosa

El glicolaldehído en estado sólido se encuentra principalmente en su forma dimérica (Figura 70) con un peso molecular de 120 g/mol y un punto de fusión de 85°C.

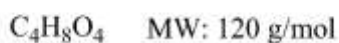
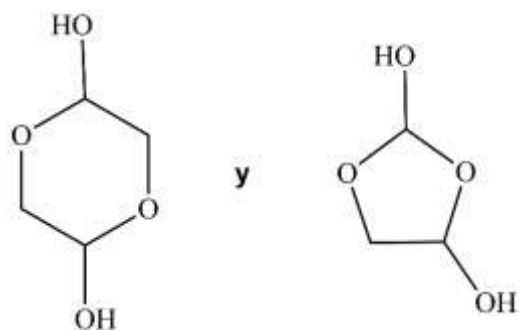


Figura 70. Estructura cíclica de los dímeros de glicolaldehído.

Sin embargo en disolución acuosa el glicolaldehído se encuentra en cuatro posibles formas las cuales fueron identificadas por un detector de masas (Figura 71) (Yaylayan, Harty-Majors y Ismail, 1998).

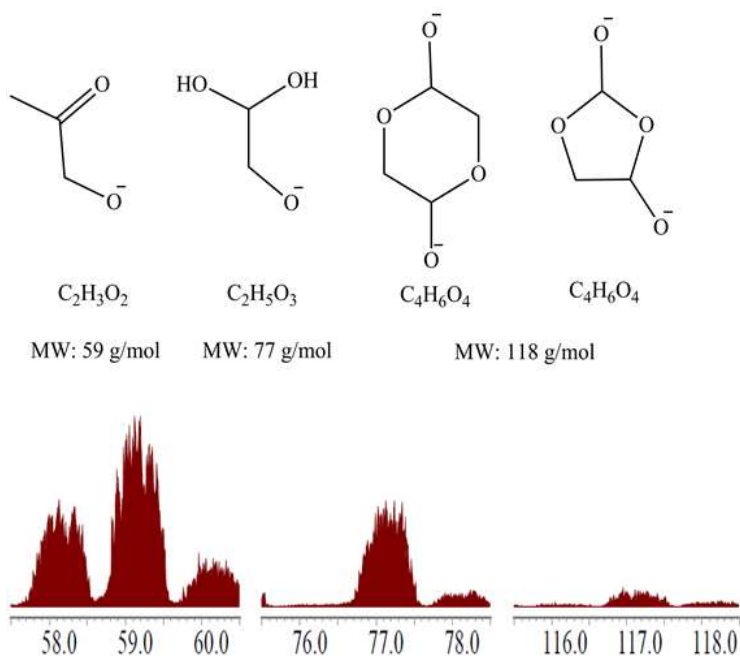


Figura 71. Formas monoméricas del glicolaldehído en disolución acuosa.



### 9.6. Cadena de decaimiento del $^{235}\text{U}$

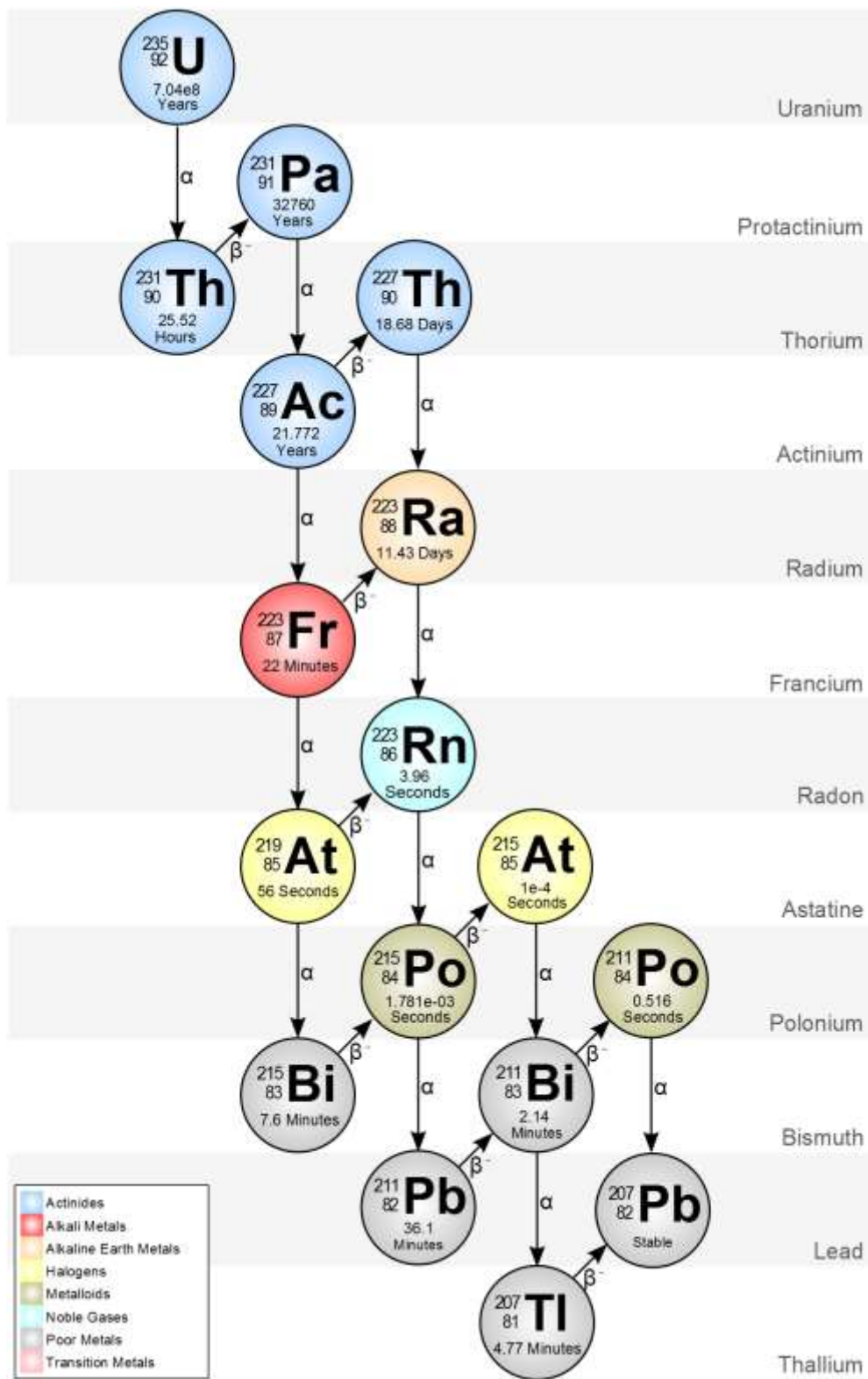


Figura 72. Cadena de decaimiento del isótopo  $^{235}\text{U}$  a  $^{207}\text{Pb}$ . Tomada de <http://metadata.berkeley.edu/nuclear-forensics/Decay%20Chains.html>

## **10. Índice de tablas**

Tabla 1. Fuentes de energía en la Tierra primitiva. ....	18
Tabla 2. Fuentes radiactivas de origen terrestre.....	20
Tabla 3. Comparación entre los sistemas hidrotermales submarinos más comunes.....	23
Tabla 4. Sistemas hidrotermales y medios de reacción. ....	28
Tabla 5. Posibles variables fisicoquímicas relevantes en los sistemas hidrotermales. ....	28
Tabla 6. Estrategia de análisis. ....	41
Tabla 7. Productos de la radiólisis del ácido succínico en disolución acuosa. ....	50
Tabla 8. Productos de la radiólisis del ácido malónico en disolución acuosa. ....	56
Tabla 9. Productos de la radiólisis del gliceraldehído en disolución acuosa. ....	61
Tabla 10. Productos de la radiólisis del gliceraldehído en estado sólido. ....	63
Tabla 11. Resumen de algunos resultados relevantes en simulaciones hidrotermales. ....	70

## 11. Índice de figuras

Figura 1. Primeros registros de vida(Manson y Von Brunn, 1977; Nutman <i>et al.</i> , 2016; Schidlowski, 2001; Walter, Buick, y Dunlop, 1980).....	9
Figura 2. Cromatografía de papel para la identificación de aminoácidos en el experimento de Miller. Tomada de Miller (1953). .....	11
Figura 3. 9H-purina. ....	12
Figura 4. Pirimidina. ....	12
Figura 5. ATP adenosín trifosfato.....	13
Figura 6. Mecanismo de reacción para la síntesis de adenina a partir de disoluciones acuosas de cianuro de amonio. Tomada de Voet y Schwartz (1983). .....	14
Figura 7. Estructura general de los ácidos carboxílicos . ....	15
Figura 8. Producción de hidrógeno, peróxido de hidrógeno y ácido succínico en función de la dosis de radiación de disoluciones de ácido acético (Garrison <i>et al.</i> , 1954).....	15
Figura 9. Estructura general para los carbohidratos dependiendo de su grupo funcional. Se muestra la forma de las aldosas y las cetosas (Morrison <i>et al.</i> , 1998). .....	16
Figura 10. Diagrama general de la glucólisis. ....	16
Figura 11. Cadena espiral de la ribosa-5-fosfato en el RNA. ....	17
Figura 12. Fumarola negra. Tomada de <a href="https://www.marum.de/en/Discover/Deep-Sea.html">https://www.marum.de/en/Discover/Deep-Sea.html</a> .....	24
Figura 13. Fumarola blanca. Tomada de <a href="https://sciworthy.com/are-the-building-blocks-of-life-from-a-hydrothermal-vent/">https://sciworthy.com/are-the-building-blocks-of-life-from-a-hydrothermal-vent/</a> .....	25
Figura 14. Manantial hidrotermal en el parque Nacional de Yellowstone, Estados Unidos. Tomada de: <a href="https://vivaglammagazine.com/the-best-places-to-stay-in-yellowstone-national-park/">https://vivaglammagazine.com/the-best-places-to-stay-in-yellowstone-national-park/</a> .....	26
Figura 15. Manantial hidrotermal subaéreo con combustible nuclear. Tomada de Ebisuzaki y Maruyama (2017) .....	27
Figura 16. Abundancia del isotopo de <sup>235</sup> U en el Hadeano respeto a su vida media y al isotopo <sup>238</sup> U. Tomada de Ebisuzaki y Maruyama (2017) .....	27
Figura 17. Formación de ión nitronio. ....	33
Figura 18. Sistema de calentamiento mediante contacto indirecto con disolventes orgánicos a reflujo. ....	35
Figura 19. Reactor Parr modelo 4560 de 500 mL, ICN, UNAM.....	35
Figura 20. Irradiador Gammabeam PT 651. ....	36
Figura 21. Disposición espacial de la barras de <sup>60</sup> Co en el irradiador. ....	36
Figura 22. Reacción de desaminación de la citosina.....	41
Figura 23. Análisis HPLC-MS de citosina. ....	42
Figura 24. Análisis de espectrofotometría UV de citosina a 267 nm. ....	42
Figura 25. Curva de calibración de citosina. ....	42
Figura 26. Termólisis de la citosina en función del tiempo. ....	43
Figura 27. Mecanismo de reacción propuesto para formación de uracilo en la termólisis de citosina. ....	43
Figura 28. Descomposición de citosina en función de la dosis absorbida. ....	44
Figura 29. Análisis de espectrofotometría UV de uracilo a 258 nm.....	44
Figura 30. Experimentos de adsorción/desorción de citosina en superficies sólidas, dependiente del pH. ....	45
Figura 31. Descomposición de guanina en disolución acuosa, en función de la dosis absorbida. ..	46
Figura 32. Análisis HPLC-MS de guanina irradiada en estado sólido. La masa de 301 g/mol corresponde al dímero. Tomada de (A. L. Meléndez-López, 2018). ....	47
Figura 33. Adsorción/desorción de guanina en Na-montmorillonita, dependiente del pH.....	48

Figura 34. Descomposición de guanina en suspensión acuosa con arcilla, función de la dosis absorbida.....	48
Figura 35. Reacción de descarboxilación del ácido succínico inducida por calor.....	49
Figura 36. Espectro de fragmentación del ácido propiónico formado en la termólisis del ácido succínico.....	49
Figura 37. Radiólisis del ácido succínico en disolución acuosa. Se observa la formación del dímero. ....	50
Figura 38. Cromatografía de gases de los ésteres metílicos de los ácidos carboxílicos formados por la irradiación gamma (69.4 kGy): (1) malónico, (2) succínico, (3) málico, (4) 1, 2, 3-butantricarboxílico, (5) tricarbálico + aconítico, (6) cítrico, (7) dímero del ácido succínico.....	51
Figura 39. Radiólisis del agua.....	51
Figura 40. Reacción general entre los ácidos carboxílicos y productos de radiólisis del agua.....	52
Figura 41. Mecanismo general para la radiólisis acuosa del ácido succínico.....	52
Figura 42. Cromatografía de gases de los ésteres metílicos de los ácidos carboxílicos formados por la irradiación gamma en suspensión acuosa): (1) propiónico, (2) malónico, (3) succínico, (4) málico. ....	53
Figura 43. Espectro de fragmentación de masas del ácido propiónico formado por la radiólisis del ácido succínico en suspensión.....	53
Figura 44. Reacción de descarboxilación del ácido malónico inducida por calor.....	54
Figura 45. Formación de ácido acético por la termólisis de ácido malónico.....	54
Figura 46. Mecanismo de reacción para la formación de ácido acético en la termólisis de ácido malónico.....	55
Figura 47. Radiólisis de ácido malónico en disolución acuosa.....	55
Figura 48. Cromatografía de gases de los ésteres metílicos de los ácidos carboxílicos formados por la irradiación gamma (10 kGy): (1) oxálico (2) malónico, (3) succínico, (4) tricarbálico, (5) 2,3 dicarboxi-succínico y (6) cítrico.....	56
Figura 49. Mecanismo de reacción para la formación del ácido succínico.....	57
Figura 50. Mecanismo de reacción para la formación del ácido 2,3-dicarboxi-succínico.....	57
Figura 51. Cromatografía de gases de los ácidos carboxílicos formados por la irradiación gamma en suspensión acuosa (A) Espectros de masas de los productos obtenidos: (B) dióxido de carbono, (C) ácido acético.....	58
Figura 52. Descomposición de gliceraldehído en función de la dosis absorbida.....	59
Figura 53. Radiólisis acuosa del gliceraldehído.....	59
Figura 54. Análisis polarográfico del gliceraldehído.....	60
Figura 55. Equilibrio enol-cetona del malondialdehído.....	60
Figura 56. Espectrofotometría para la identificación de malondialdehído. Siendo 1) 0 kGy, 2) 0.22 kGy, 3) 2.2 kGy, 4) 11 kGy y 5) 20 kGy.....	60
Figura 57. Mecanismo de reacción para la formación del malondialdehído.....	61
Figura 58. Mecanismo de reacción para la formación del etilenglicol y el glicolaldehído.....	62
Figura 59. Radiólisis en estado sólido del gliceraldehído.....	62
Figura 60. Descomposición de gliceraldehído en estado sólido en función de la dosis absorbida.....	63
Figura 61. CG-MS de los productos formados por la radiólisis del gliceraldehído en estado sólido (1) formaldehído, (2) ácido fórmico, (3) etilenglicol, (4) malondialdehído (5) 2,3 glicolaldehído y (6) gliceraldehído.....	64
Figura 62. HPLC-MS de los productos formados por la radiólisis del gliceraldehído en estado sólido (1) ácido fórmico (reactivo) (2) glicolaldehído + etilenglicol, (3) malondialdehído, (4) 2-hidroxiopropanal, (5) gliceraldehído, (7) dímero de etilenglicol, (10) pentitol, (10-12) compuestos tipo azúcares, (6, 8 y 9) desconocidos.....	64

Figura 63. Experimentos de adsorción/desorción de gliceraldehído en arcillas dependiente del pH. ....	65
Figura 64. Espectros de fragmentación de los productos formados en la radiólisis del glicolaldehído. ....	66
Figura 65. Análisis HLPC-MS del avance de reacción de la radiólisis del glicolaldehído. ....	67
Figura 66. Mecanismo propuesto para la reacción de polimerización del glicolaldehído inducida por radiación gamma. ....	67
Figura 67. Experimentos adsorción/desorción de glicolaldehído en dos tipos de montmorillonita. .	68
Figura 68. Productos detectados en los experimentos de adsorción/desorción de glicolaldehído en montmorillonita de hierro. ....	69
Figura 69. Reacción general de la esterificación de Fischer. ....	90
Figura 70. Estructura cíclica de los dímeros de glicolaldehído. ....	91
Figura 71. Formas monoméricas del glicolaldehído en disolución acuosa. ....	91
Figura 72. Cadena de decaimiento del isótopo $^{235}\text{U}$ a $^{207}\text{Pb}$ . Tomada de <a href="http://metadata.berkeley.edu/nuclear-forensics/Decay%20Chains.html">http://metadata.berkeley.edu/nuclear-forensics/Decay%20Chains.html</a> .....	92

## ***12. Artículos publicados***



## Study of Solid-State Radiolysis of Behenic, Fumaric, and Sebacic Acids for their Possible Use as Gamma Dosimeters Measured Via ATR-FT-IR Spectroscopy

J. Cruz-Castañeda<sup>1,2</sup>, A. L. Meléndez-López<sup>1,2</sup>, A. Heredia<sup>1</sup>, S. Ramosbernal<sup>1</sup>, and A. Negrón-Mendoza<sup>1\*</sup>

<sup>1</sup>*Institute of Nuclear Sciences, National Autonomous University of Mexico (UNAM), PO Box 70-543, 04510 Mexico City, Mexico*

<sup>2</sup>*Master's and PhD Program in Chemical Sciences, National Autonomous University of Mexico (UNAM). PO Box 70-543, 04510 Mexico City, Mexico*

\*Email: [negron@nucleares.unam.mx](mailto:negron@nucleares.unam.mx)

### ARTICLE INFORMATION

Received: June 15, 2018

Revised: July 03, 2018

Accepted: July 19, 2018

Published online: August 6, 2018

#### Keywords:

dosimeter, carboxylic acid, gamma radiation, ATR-FT-IR spectroscopy

DOI: [10.15415/jnp.2018.61014](https://doi.org/10.15415/jnp.2018.61014)

### ABSTRACT

The intensive use of ionizing radiation has promoted the constant investigation of adequate dosimetric systems in the measurement of doses applied in irradiated products. The objective of this work is to propose gamma dosimetric systems, using carboxylic acids in a solid state and measuring the change via infrared spectroscopy (carboxylic acid/ATR-FT-IR<sup>1</sup>). We worked with three systems: (1) behenic acid/ATR-FT-IR, (2) sebacic acid/ATR-FT-IR, and (3) fumaric acid/ATR-FT-IR. The change in absorbance corresponding to the stretching vibration frequency of the carbonyl group to the absorbed dose (in the range of kGy) was measured. The results showed that the acid/ATR-FT-IR systems have a linear response with respect to the absorbed dose, for behenic acid/ATR-FT-IR from 0 to 122 kGy, for ATR-FT-IR sebacic acid from 0 to 61 kGy, and for fumaric acid/ATR-FT-IR from 0 to 34 kGy. The results indicated that the linear response of the absorbance dose in the three systems allows us to continue studying other variables to be able to propose them as chemical dosimeters.

## 1. Introduction

Different chemical dosimetry systems have been proposed. The most popular is the Fricke dosimeter, measured via UV-VIS spectrophotometry at 304 nm [1]. Other dosimeters are based on the use of amino acid films on PET<sup>2</sup> measured by EPR<sup>3</sup>, such as the alanine dosimeter [2] or the aspartic acid dosimeter [3]. However, no universal dosimeter exists due to the different physical and chemical variables of each dosimetric system—for example, temperature, sensitivity, linear response interval, analysis time, type of radiation, etc. For this reason, it is crucial to investigate diverse possible dosimetry systems to be able to measure doses in various circumstances. Several authors studied the stability of carboxylic acids against gamma radiation. Their primary decomposition in the solid state via gamma radiolysis is a decarboxylation reaction, forming a corresponding hydrocarbon with one fewer carbon atom and carbon dioxide (CO<sub>2</sub>) [4-5], with radiochemical yield G (CO<sub>2</sub>) values of about 3 [6]. The objective of this work is to propose dosimetric systems for gamma radiation using carboxylic acids, specifically behenic acid (C<sub>22</sub>H<sub>44</sub>O<sub>2</sub>), sebacic acid (C<sub>10</sub>H<sub>18</sub>O<sub>4</sub>), and fumaric acid (C<sub>4</sub>H<sub>4</sub>O<sub>4</sub>), measuring in the signal corresponding to the carbonyl bond stretch (C = O)

monitored by ATR-FT-IR spectroscopy. For this purpose, the change in absorbance corresponding to the stretching of the carbonyl bond (C = O) was measured via ATR-FT-IR spectroscopy at 1700 cm<sup>-1</sup> for behenic acid, 1685 cm<sup>-1</sup> for sebacic acid, and 1660 cm<sup>-1</sup> for fumaric acid. The results indicated that carboxylic acid-ATR-FT-IR systems show a linear response to the dose of gamma radiation from Gy to the order of kGy at room temperature (20°C).

## 2. Experimental

### 2.1 Chemicals and Materials

The reagents used were purchased from Sigma-Aldrich® (USA) and were of a higher commercially available purity. To avoid contamination in the glass vials, they were treated with a hot mixture of HNO<sub>3</sub> and H<sub>2</sub>SO<sub>4</sub> for 30 minutes, followed by a wash with distilled water. Then, they were heated at 300 °C for 24 hours.

### 2.2 Irradiation of Samples

The gamma irradiation of the samples was carried out at room temperature with a dose rate of 170 Gy/min in a

“Gammabeam PT 651” irradiator equipped with a high-intensity  $^{60}\text{Co}$  source, at Instituto de Ciencias Nucleares, UNAM.

### 3. Analysis of Samples

#### 3.1 ATR-FT-IR

The analysis of the samples via infrared spectrometry was performed in a PerkinElmer® Spectrum 100 FT-IR spectrometer with ATR sampling operated by the Spectrum™ software v.10.0, in absorbance mode from 650 to 4000  $\text{cm}^{-1}$ , using 50-gauge pressure and 16 scan, at Instituto de Ciencias Nucleares, UNAM.

### 4. Results

The main pathway of decomposition in the solid-state gamma radiolysis of carboxylic acids was the decarboxylation reaction of the acid, forming as the main product hydrocarbon with one less carbon atom and  $\text{CO}_2$  [3].

#### 4.1 Behenic Acid

##### 4.1.1 Infrared spectroscopy analysis

Behenic acid ( $\text{C}_{21}\text{H}_{43}\text{COOH}$ ) is a monocarboxylic acid with a molecular weight of 340.59 g/mol characterized by infrared spectroscopy, mainly by bands at 2915 and 2850  $\text{cm}^{-1}$  that correspond to the frequency of stretching of the methylene group, and a band at 1700  $\text{cm}^{-1}$  that corresponds to the stretching frequencies of the carbonyl group (Figure 1). After the irradiation, the results showed a

linear dependence between the band intensity at 1700  $\text{cm}^{-1}$  with respect to the absorbed dose in a range of 0 to 120 kGy (Figure 2 and Figure 3).

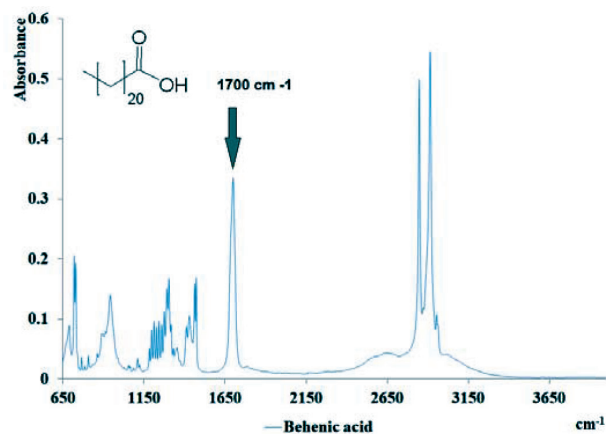


Figure 1. Infrared spectrum of behenic acid.

#### 4.2 Sebacic Acid

##### 4.2.1 Infrared spectroscopy analysis

Sebacic acid ( $\text{C}_{10}\text{H}_{18}\text{O}_4$ ) is a dicarboxylic acid with a molecular weight of 202.25 g/mol characterized by infrared spectroscopy, mainly by bands at 2915 and 2850  $\text{cm}^{-1}$  that correspond to the frequency of the stretching of the methylene group, and a band at 1685  $\text{cm}^{-1}$  that corresponds to the stretching frequencies of the carbonyl group (Figure 4). The results showed a linear dependence between band intensity at 1685  $\text{cm}^{-1}$  with respect to the absorbed dose in a range of 0 to 61 kG (Figure 5 and Figure 6).

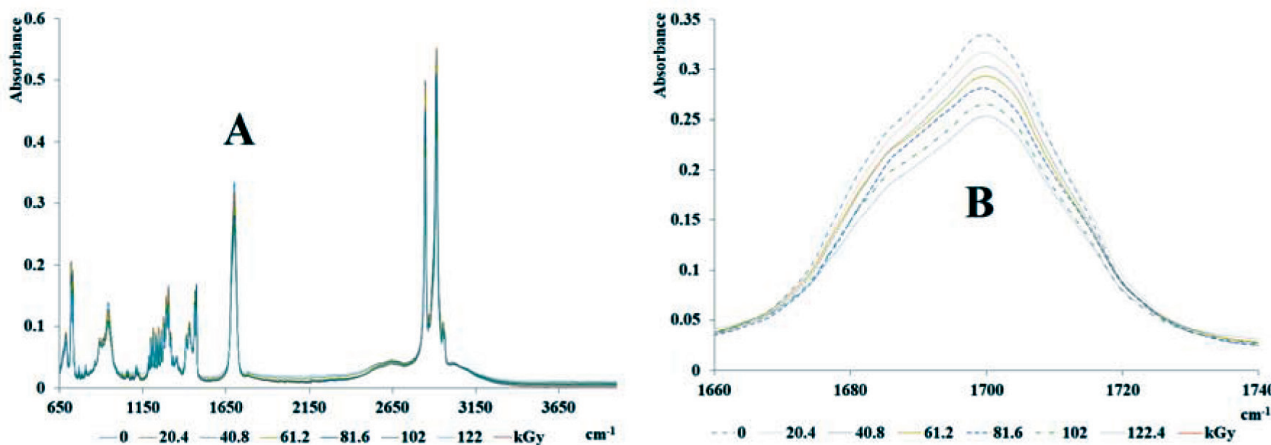


Figure 2. “A” corresponds to the infrared spectrums of behenic acid at various doses. “B” corresponds to the stretching band of the carbonyl group at 1700 $\text{cm}^{-1}$ .



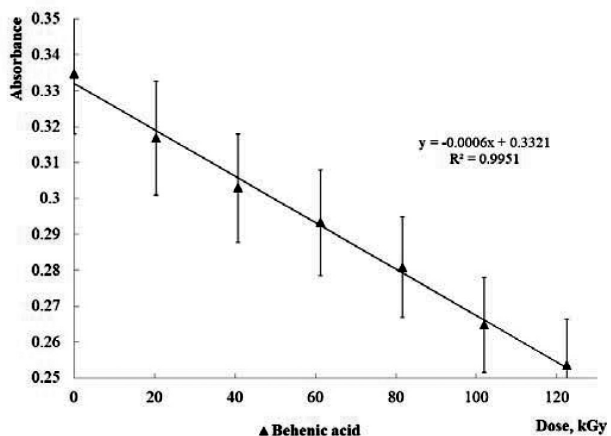


Figure 3. Relationship between the absorbance of the carbonyl group band and the absorbed dose.

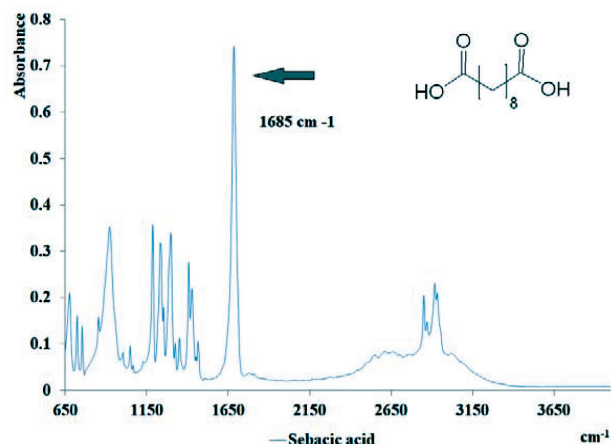


Figure 4. Infrared spectrum of sebacic acid.

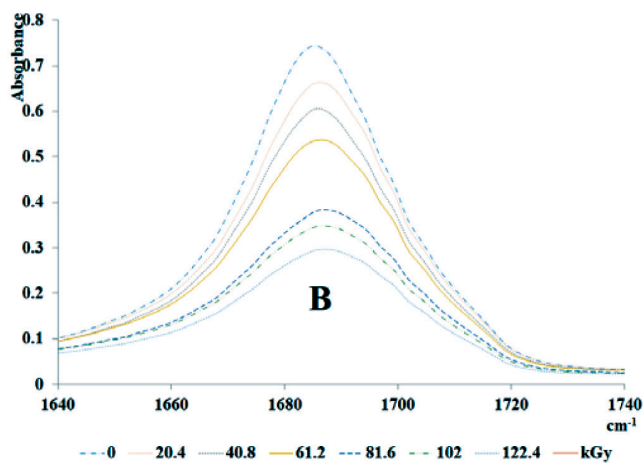
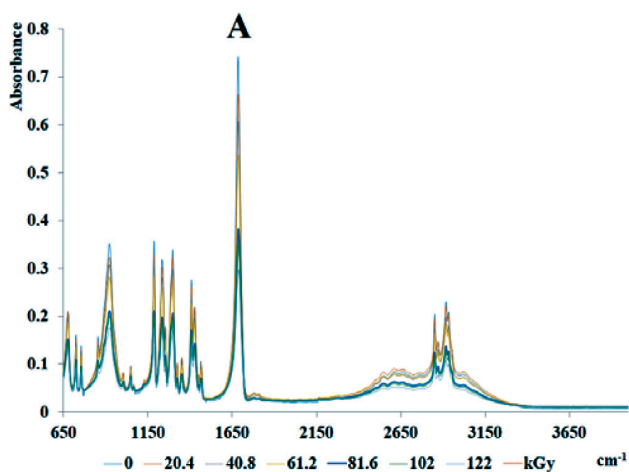


Figure 5. “A” corresponds to the infrared spectrums of sebacic acid at various doses. “B” corresponds to the stretching band of the carbonyl group at 1685cm<sup>-1</sup>.

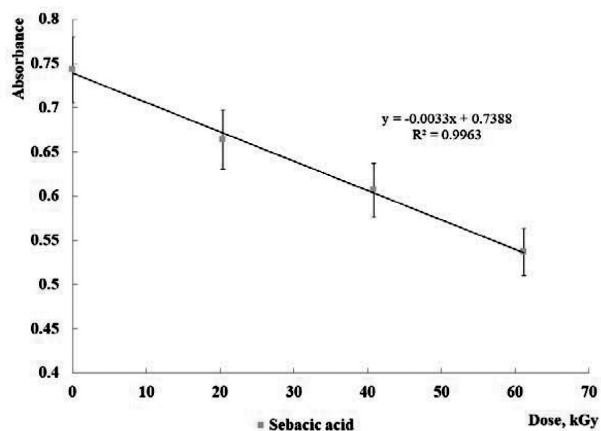


Figure 6. Relationship between the absorbance of the carbonyl group band and the absorbed dose.

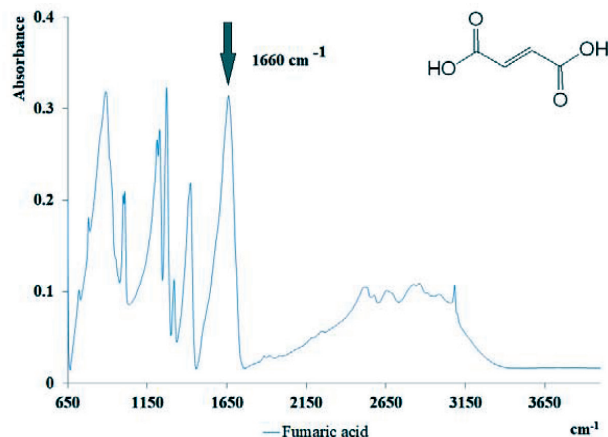


Figure 7. Infrared spectrum of fumaric acid.

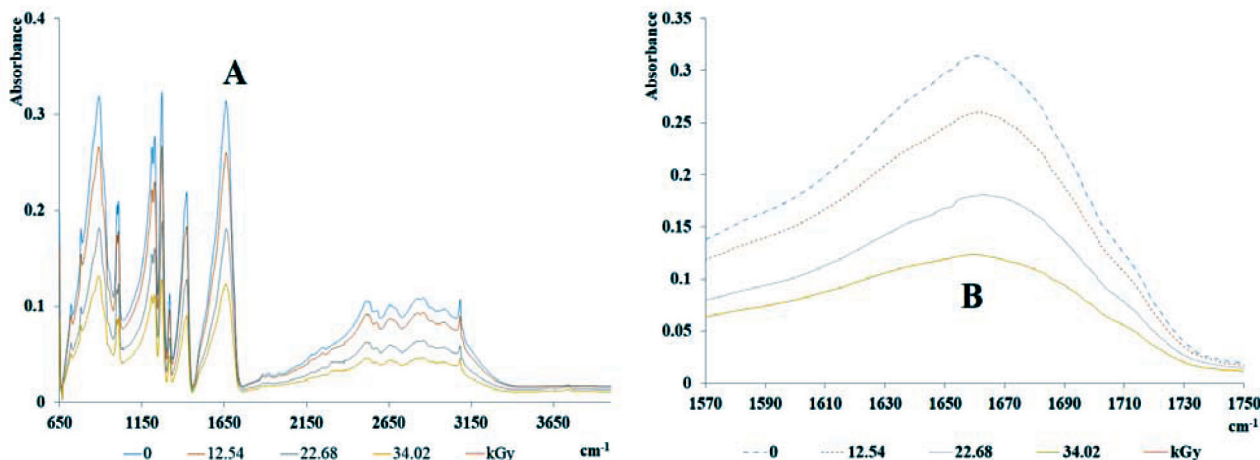


Figure 8. “A” corresponds to the infrared spectra of fumaric acid at various doses. “B” corresponds to the stretching band of the carbonyl group at 1660 cm<sup>-1</sup>.

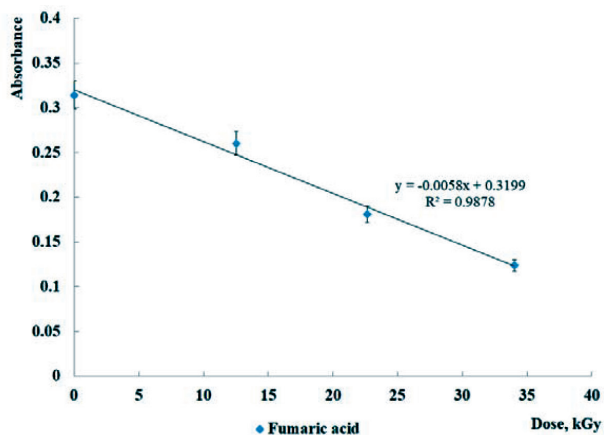


Figure 9. Relationship between the absorbance of the carbonyl group band and the absorbed dose.

### 4.3 Fumaric Acid

#### 4.3.1 Infrared spectroscopy analysis

Fumaric acid (C<sub>4</sub>H<sub>4</sub>O<sub>4</sub>) is an unsaturated dicarboxylic acid with a molecular weight of 116.07 g/mol characterized by infrared spectroscopy, mainly by bands at 3150 cm<sup>-1</sup> that correspond to the frequency of stretch bond C-H sp<sup>2</sup>, and a band at 1665 cm<sup>-1</sup> that corresponds to the stretch frequencies of the carbonyl group. The results showed a linear dependence between band intensity at 1660 cm<sup>-1</sup> with respect to the absorbed dose in a range of 0 to 34 kG and Figure 6.

## 5. Remarks

The results indicated that the studied carboxylic acids show a linear response in different dose intervals up to the order

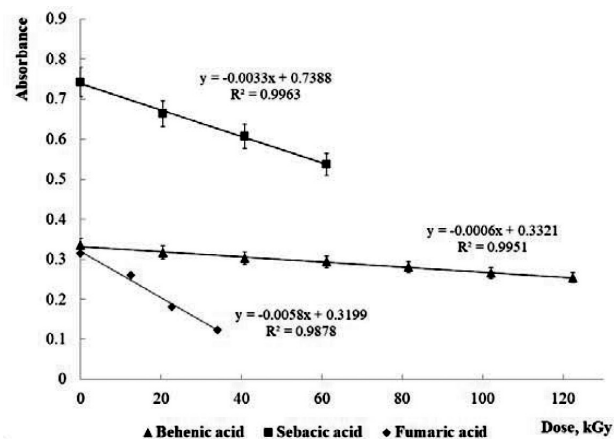


Figure 10. Range of linear response absorbance *vs* absorbed dose for various carboxylic acids.

of the kGy depending on the structure of the carboxylic acid (Figure 10), which suggests that these acids in conjunction with infrared spectroscopy can be proposed as a dosimetric systems for gamma radiation. However, more studies are still needed to determine if this system is independent of other physicochemical variables, such as dose intensity, temperature, etc.

## Acknowledgments

Support was received from C001–Ciencia y Tecnología y la Agencia Nacional de la Investigación–188689, Dirección General de Asuntos del Personal Académico grant IN11116, and the Programa de Maestría y Doctorado en Ciencias Químicas-UNAM.

---

**References**

- [1] K. Van Laere, J. Buysse, and P. Berkvens, *Int. J. Radiat. Appl. Instrumentation. Part A. Appl. Radiat. Isot.* **40**, 885 (1989).  
[https://doi.org/10.1016/0883-2889\(89\)90012-9](https://doi.org/10.1016/0883-2889(89)90012-9)
- [2] A. R. Jones, *Radiat. Res.* **47**, 35 (1971).  
<https://doi.org/10.2307/3573286>
- [3] A. Negron-Mendoza and S. Ramos-Bernal, *Radiat. Phys. Chem.* **52**, 395 (1998).  
[https://doi.org/10.1016/S0969-806X\(98\)00059-0](https://doi.org/10.1016/S0969-806X(98)00059-0)
- [4] J. Cruz-Castañeda, A. Negron-Mendoza, and S. Ramos-Bernal, *AIP Conf. Proc.* **49**, 49 (2013).
- [5] H. Fricke and E. J. Hart, in *Radiat. Dosim.*, edited by F. H. Attix; W. C Roesch, 2nd ed. (Academic Press, New York, 1966).
- [6] A. Meléndez-López, A. Negrón-Mendoza, V. Gómez-Vidales, R. M. Uribe, and S. Ramos-Bernal, *Radiat. Phys. Chem.* **104**, 230 (2014).  
<https://doi.org/10.1016/j.radphyschem.2014.03.012>



# Irradiation of glyceraldehyde under simulated prebiotic conditions: Study in solid and aqueous state

E. Aguilar-Ovando<sup>1,2</sup> · J. Cruz-Castañeda<sup>1,3</sup> · T. Buhse<sup>2</sup> · C. Fuentes-Carreón<sup>1,4</sup> · S. Ramos-Bernal<sup>1</sup> · A. Heredia<sup>1</sup> · A. Negrón-Mendoza<sup>1</sup>

Received: 21 September 2017  
© Akadémiai Kiadó, Budapest, Hungary 2018

## Abstract

We investigated the radiolysis of DL-glyceraldehyde in a solid state and in an aqueous solution. The catalytic effect of a clay onto glyceraldehyde was also studied. We carried out the irradiation in a <sup>60</sup>Co gamma ray source (Gammabeam 650 PT), with doses up to 360 kGy, at three temperatures (77, 198 and 295 K). For the analysis, we used various spectroscopic and chromatographic analytical methods. The results show that this compound is labile under irradiation and that it forms malondialdehyde, glycolaldehyde and other sugar-like compounds that are important in chemical-evolution studies.

**Keywords** Radiolysis · Chemical evolution · Origin of life · Malondialdehyde · Glyceraldehyde

## Introduction

The study of the interactions between ionizing radiation and complex organic substances, particularly biopolymers, is important for the understanding of biochemical processes, chemical evolution and the origin of life. Carbohydrates, as well as proteins and nucleic acids, play an important role in biological systems. Carbohydrates are the cell's construction materials and an energy source. Studies indicate that carbohydrates' radiation transformations are important in biological processes in modern technology and in everyday life [1]. The radiation chemistry of carbohydrates is peculiar due to these compounds' versatility to produce a variety of other organic compounds (e.g., aldehydes, ketones and hydroxy groups), and even the

simplest carbohydrates present great chemical complexity [1, 2].

The data about the transformation of aldehydes through ionizing radiation are very scarce. Many carbohydrates react under ionizing radiation with complex mechanisms that are not completely understood; even the simplest carbohydrates, when irradiated, produce complicated mixtures of products, which illustrates the multiplicity of radiation-induced degradation pathways [1].

## Chemical evolution

An important step toward the origin of life on Earth was the transition from inorganic molecules to the compounds that would form parts of living forms. The common approach to understanding this step has been to simulate the processes that might have taken place on the primitive Earth leading to the formation of complex molecules and, eventually, living cells. These physical and chemical processes are the so-called chemical evolution.

A simulation of the possible environments on the primitive Earth require the consideration of different interfaces combined, including minerals in contact with aqueous solutions that may contain biologically related organic compounds under the influence of different energy sources. Glyceraldehyde is important in this type of study because it may form complex sugars of biological

✉ A. Negrón-Mendoza  
negron@nucleares.unam.mx

<sup>1</sup> Instituto de Ciencias Nucleares, Universidad Nacional Autónoma de México, 04510 Coyoacán, CDMX, México

<sup>2</sup> Centro de Investigaciones Químicas, Universidad Autónoma del Estado de Morelos, Cuernavaca, Mor, México

<sup>3</sup> Posgrado en Ciencias Químicas, Universidad Nacional Autónoma de México, 04510 Coyoacán, CDMX, México

<sup>4</sup> Facultad de Ciencias, Universidad Nacional Autónoma de México, 04510 Coyoacán, CDMX, México

importance [3–7]. Glyceraldehyde is considered the simplest triose and is readily formed in prebiotic experiments that simulate the presence of extraterrestrial ices [3] or other primitive terrestrial conditions [4]. The stability of glyceraldehyde in the surrounding environment and the feasible chemical reactions in which it participates are the relevant factors in describing how the first self-replicable systems might have emerged.

The synthesis of organic matter is essential to chemical evolution. For this synthesis, energy initiates, promotes and directs all physicochemical processes; therefore, the sources of energy that existed on the early Earth were useful in the abiotic synthesis of organic matter.

Ionizing radiation energy may have been of great importance in the chemical reactions that occurred on the early Earth [8–10], and, as such, energy has high efficiency in inducing the synthesis of organic compounds. It can penetrate into matter and is relatively abundant. There were two sources of ionizing radiation on the early Earth: the radionuclides in the Earth's crust and extraterrestrial sources such as cosmic rays and the solar wind [8, 9].

Extraterrestrial bodies are exposed to various types of high-energy radiation, mainly in the form of cosmic rays (high-speed particles), ultraviolet (UV) rays and gamma photons [10]. As Cataldo et al. [11] described, the decay of radionuclides in comets, asteroids, meteorites and the larger bodies of the solar system, across the age of the solar system (i.e.,  $4.69 \times 10^9$  years), deposited a dose about  $\sim 14$  MGy [11]. The minerals and other inorganic solids in these bodies might have also influenced the behavior of the organic molecules by acting as catalysts, concentrators or protecting agents [12]. On the primitive Earth and on these small bodies, the most relevant minerals were carbonates, sulfides and silicates such as clays [12].

In this work, our aim is to stress the relevance of ionizing radiation as a tool for studying the stability of glyceraldehyde under high-radiation fields. To this end, we investigate the radiolysis of racemic glyceraldehyde at various temperatures, simulating primitive conditions. We study glyceraldehyde in three forms, in a solid state, in an aqueous solution and adsorbed in a clay mineral (Na-montmorillonite), to study the stability of this compound in several environments.

## Experimental

### Chemicals and glassware

The chemicals were prepared and the glassware was cleaned in accordance with the standard procedures used in radiation chemistry. The glassware was cleaned with a sulfo-nitric solution [13].

DL-glyceraldehyde of the highest purity available was purchased from the Sigma Chemical Company USA. For this study, Na-montmorillonite of Wyoming bentonite (Crook County, Wyoming, USA), from clay mineral standard batch SWY-1, was used.

### Preparation of samples

Solid samples were prepared in glass tubes in a vacuum. Standard-stock aqueous solutions of glyceraldehyde (i.e.,  $1 \times 10^{-2}$  M) were prepared using triple-distilled water, either in an Ar atmosphere or in the presence of  $N_2O$ . Another set of samples were adsorbed in Na-montmorillonite according to the procedure from Ramos and Negron-Mendoza [12]. All solutions were stored in a refrigerator at 4 °C while not in use.

### Irradiation of samples

All samples were irradiated at Instituto de Ciencias Nucleares, Universidad Nacional Autonoma de Mexico (UNAM) using a high-intensity  $^{60}Co$  gamma ray source (Gammabeam 651 PT). Sealed vials containing the solid samples were irradiated at room temperature (298 K), at the temperatures of dry ice (198 K) and at liquid nitrogen (77 K), with doses up to 386 kGy. The samples were irradiated with a dose rate of 257 Gy/min. This dose rate was measured using a Fricke dosimeter [13].

### Analysis of samples

The effect of  $\gamma$ -irradiation on glyceraldehyde was investigated using various spectroscopic and chromatographic analytical methods: UV spectroscopy, ultra-high-performance liquid chromatography (UHPLC), gas chromatography coupled to a mass detector (GC–MS) and liquid chromatography coupled to a mass detector (HPLC–MS). For the solid samples, both Fourier-transform infrared spectroscopy (FT-IR) and electron paramagnetic resonance (EPR) were used. The samples were analyzed immediately after irradiation.

### UV spectroscopy

To determine how the irradiation affects the compound under study, UV spectroscopy was performed using a Cary 100 spectrometer (USA) in the range of 200–350 nm.

### ATR–FT-IR analysis

Infrared spectra were recorded using the attenuated total reflection sampling technique on a Spectrum 100 FT-IR spectrometer (PerkinElmer, USA).

## EPR analysis

After irradiation, the solid samples were analyzed using EPR. The samples (each  $30 \pm 0.1$  mg) were placed in a quartz tubes and analyzed with a JEOL JES-TE300 spectrometer operating in the X band at a 100-kHz modulation frequency. They were also analyzed using the TE<sub>011</sub> mode in a cylindrical cavity that was equipped with a variable temperature unit. The magnetic field was externally calibrated with a precision gaussmeter, JEOL ES-FC5. The spectrometer settings for all spectra were as follows: microwave power, 1 mW; center field,  $334 \pm 10$  mT; microwave frequency, 9.44 GHz; modulation width, 0.025 mT; time constant, 0.1 s; amplitude, 125; sweep time, 120 s; and 13 scans. The readings used the vertical peak-to-peak method, and the analyses were done at room temperature (298 K) and at the temperatures of liquid nitrogen (77 K) and dry ice (198 K). The EPR spectra present broad lines because of the radicals' many possible orientations in the magnetic field.

To observe the evolution of the signals with the temperatures, one sample was irradiated at 4 kGy and at 77 K, and it was measured as the temperature in the spectrometer was raised from 113 to 293 K. Some irradiated samples were measured by changing the microwave power to observe the behavior of the peaks. The EPR analysis was carried out at Instituto de Química, UNAM.

## UHPLC–UV analysis

The ultra-high-pressure liquid chromatography analysis was performed on an UltiMate 3000 UHPLC system (Thermo Fisher Scientific) equipped with an UltiMate ISO-3100SD standard isocratic pump and an UltiMate 3000 TCC-3000SD standard thermostated column compartment. This system was coupled with a variable-wavelength UV–Vis detector (Thermo Fisher Scientific, Dionex UltiMate 3000 VWD). Analysis was done on a Symmetry C18 column ( $4.6 \times 75$  mm, 3.5  $\mu$ m spherical particle size; Waters Corp. USA) at 50 °C under an isocratic elution of a mobile phase (0.1 M ammonium acetate solution; 80% methanol, 20% water at pH 4) with a constant flow of 0.4 mL/min and monitored at 260 nm. The solid samples were dissolved in distilled water (0.01 M). A sample volume (20  $\mu$ L) was injected using a loop.

## HPLC–ESI–MS analysis

The liquid chromatographic analysis was performed on an HPLC system (515-pump from Waters Corp.) coupled with a single-quadrupole mass-detection system (SQ-2, Waters Corp.), with electrospray ionization in negative (ESI–) and

positive (ESI+) modes, source cone energy of 15 V and capillary energy of 3 kV. The analysis was done as described above.

## Gas chromatography–mass spectrometry (GC–MS)

Gas chromatography-mass spectrometry (CG-MS) was also used for identification of radiolytic products. The system has a chromatograph Agilent Technologies 6850 with a capillary column of 30 m HP-5MS coupled to a mass detector Agilent Technologies 5975C VL MSD, Triple-Axis Detector, using He as a carrier gas. A temperature program was used with an initial temperature of 75 °C, followed by a ramp increasing 25 °C per minute up to 200 °C. This temperature was held for 1 min.

## Formation of 2,4-dinitrophenylhydrazones and their analysis by thin-layer chromatography (TLC) and UHPLC–UV

The carbonyl-contained compounds formed by irradiation were also identified using TLC. For this technique, 2,4-dinitrophenylhydrazine (2,4-DNPH) was prepared by adding 2,4-DNPH to a hot mixture of H<sub>2</sub>SO<sub>4</sub>, ethanol and distilled water. The resulting 0.15 M concentration solution was filtered and stored. Then, 2,4-DNPH in an acidic solution was added to a solution of the carbonyl-containing compounds. The 2,4-dinitrophenylhydrazones precipitated as yellow-orange crystals. The precipitate was filtered, dried and stored for subsequent analysis.

For TLC analysis, the hydrazones were separated by using aluminum plates (20  $\times$  5 cm) coated with Silica Gel H (E. Merck AG, Darmstadt, Germany), with ethyl acetate/toluene as the eluent.

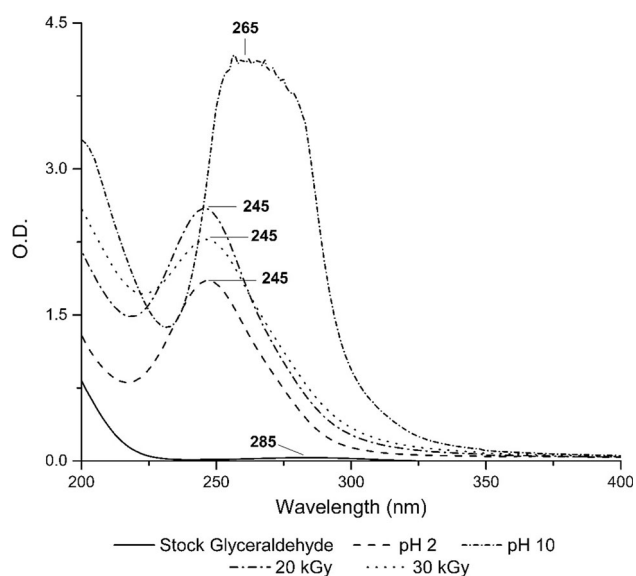
The radiolytic products were also identified via the formation of 2,4-dinitrophenylhydrazones followed by UHPLC-UV.

## Results

### UV analysis

The formation of UV-absorbing compounds in glycer-aldehyde considerably increased upon irradiation for both the solid-state and aqueous-solution samples. Figure 1 shows the UV spectra of the irradiated solid-state glycer-aldehyde dissolved in distilled water (0.01 M). The samples were analyzed at pH 2 and 10. This figure shows strong changes in the UV spectra that increase in intensity with the absorbed doses. The maximum band shifted to a shorter wavelength (from 276 to 245 nm), and the main

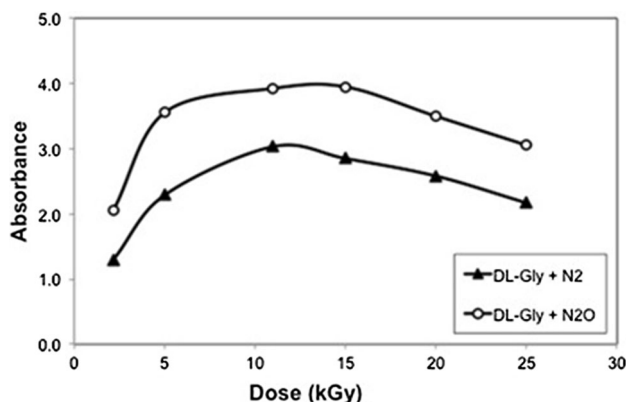




**Fig. 1** UV spectra of irradiated solid state glyceraldehyde, dissolved in distilled water (0.01 M) at different doses and pH. (1) Stock solution 0 kGy (pH 2), (2) 8 kGy (pH2), (3) 8 kGy (pH 10), (4) 20 kGy (pH 2), (5) 30 kGy (pH2)

product responsible for the absorption was malondialdehyde (MDA), which has a high extinction coefficient at 245 nm ( $1.34 \times 10^4$ ) and at 267 nm ( $3.18 \times 10^4$ ) [14]. The same behavior was observed with the change of pH, due to the formation of the enol form of MDA. The experimental value registered for  $\lambda$  agrees with the reported values in the literature [14].

MDA was also formed during the irradiation of the glyceraldehyde aqueous solution 0.01 M [15 and the references therein]. In aqueous samples, the peak at 245 nm increased its intensity considerably when the irradiation was in the presence of  $N_2O$  (Fig. 2) or at a basic pH. As previously mentioned, the molar absorptivity of MDA is very high. Even low concentrations provided high absorbance, as it was reported [15].

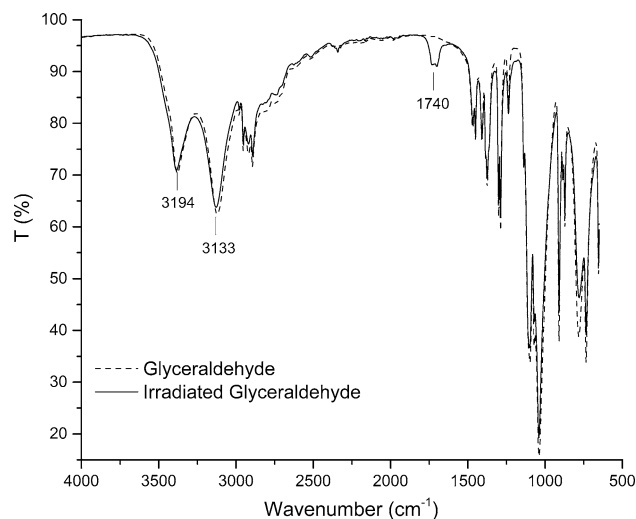


**Fig. 2** UV spectra of aqueous solution of glyceraldehyde (0.01 M) irradiated at different doses (a) saturated with Ar and (b) saturated with  $N_2O$

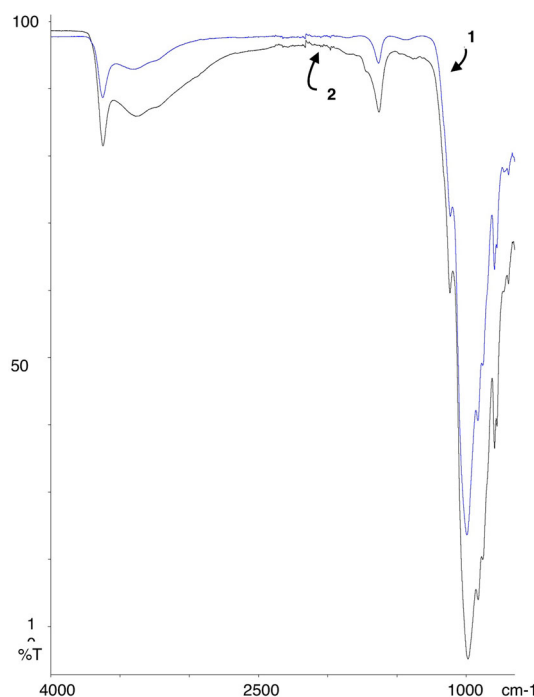
For the samples that were adsorbed in clay, after the centrifugation of the suspension, the solution showed the same changes in the UV spectra, which indicates that the clay catalyzes the decomposition of glyceraldehyde, forming MDA in a similar way as in the irradiated samples.

### FT-IR spectra

The IR spectrum of glyceraldehyde shows two bands at 3394 and 3133  $cm^{-1}$ . Notoriously, the carbonyl group



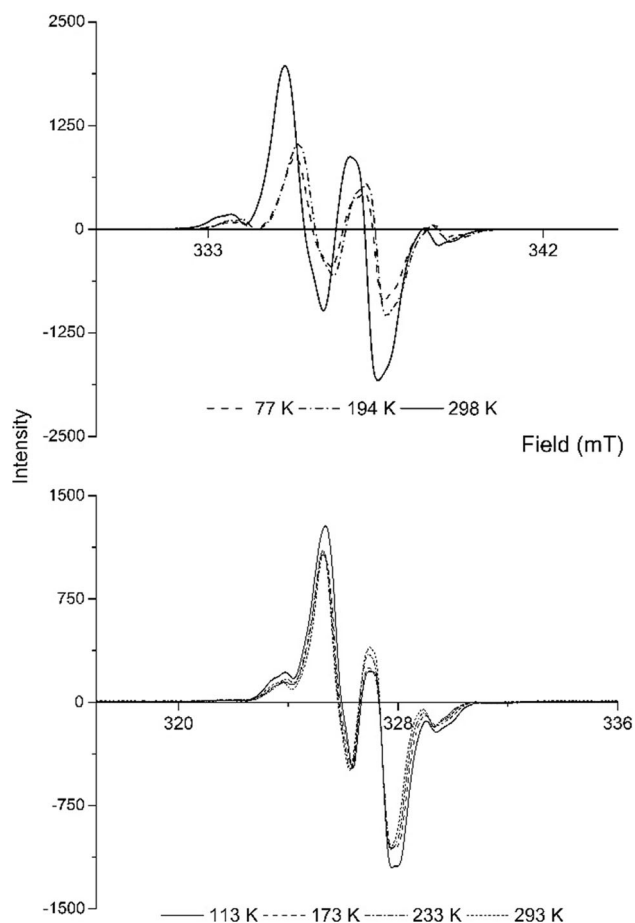
**Fig. 3** Infrared spectra for glyceraldehyde: solid line standard (cyclic hemiacetal form) and irradiated at 38 kGy



**Fig. 4** FT-IR spectra of (1) Na-montmorillonite and (2) Na-montmorillonite-glyceraldehyde

stretching vibration in the  $1740\text{--}1720\text{ cm}^{-1}$  range and the  $2800\text{--}2700\text{ cm}^{-1}$  range (characteristic of aldehydes) is missing, which suggest that in crystalline solid-state glyceraldehyde exists as the cyclic hemiacetal dimer. The bands in the  $3394\text{--}3133\text{ cm}^{-1}$  region correspond to the OH stretching vibration of the hemiacetal OH groups, as reported previously [16]. After irradiation, the carbonyl band is detected, its formation the consequence of either the formation of carbonyl-containing compounds or the breakup of the cyclic hemiacetal dimer (Fig. 3).

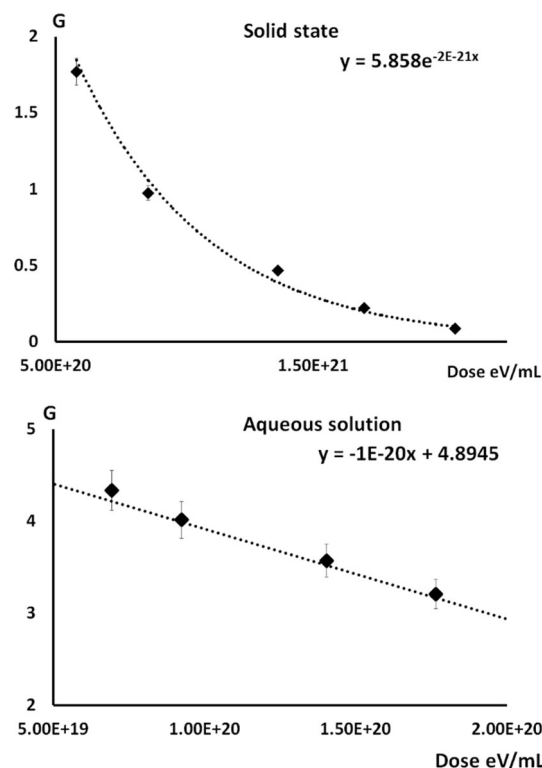
The samples treated with clay were analyzed by FT-IR; for this purpose, the clay was separated from the suspension by means of centrifugation. The clay was dried in an oven at  $40\text{ }^{\circ}\text{C}$  and then analyzed, as described previously. The spectrum showed only the bands' characteristics of the Na-montmorillonite but not of glyceraldehyde (Fig. 4), possibly due to the low concentration of this molecule in the clay.



**Fig. 5** EPR spectra of irradiated glyceraldehyde **a** at the same irradiation time changing the irradiation temperature, **b** sample irradiated 4 kGy at 77 K and heated in the cavity of the spectrometer from 113 to 293 K

## EPR analysis

The obtained EPR signal consisted of composite spectra caused by the formation of various free radicals, which created broad and overlapping lines, regardless of irradiation temperature or microwave power. No signal was observed when the material was not exposed to gamma radiation. The EPR spectra for the samples irradiated at 77, 195 and 298 K showed the same pattern. Figure 5 shows the EPR spectra of the glyceraldehyde irradiated at the same irradiation time at various temperatures. The signal at  $g = 2.0090$  was the most representative line in the spectrum. This  $g$  value remains constant at 77, 195 and 298 K, which indicates that the nature of the free radicals formed by gamma irradiation is not affected by temperature variations. Also, this behavior is observed with glyceraldehyde irradiated at 77 K with an absorbed dose of 4 kGy. The spectra were recorded as the temperature was changed from 113 to 293 K. The EPR of samples irradiated at 308 kGy at different microwave power show that there is no appreciable change in the saturated peaks to be suppressed; therefore, they correspond to the same radicals that can still be observed more than 6 months after irradiation.



**Fig. 6** G of decomposition of glyceraldehyde as function of irradiated dose for solid state and aqueous samples



## UHPLC and HPLC–ESI–MS: mass spectrometry analysis

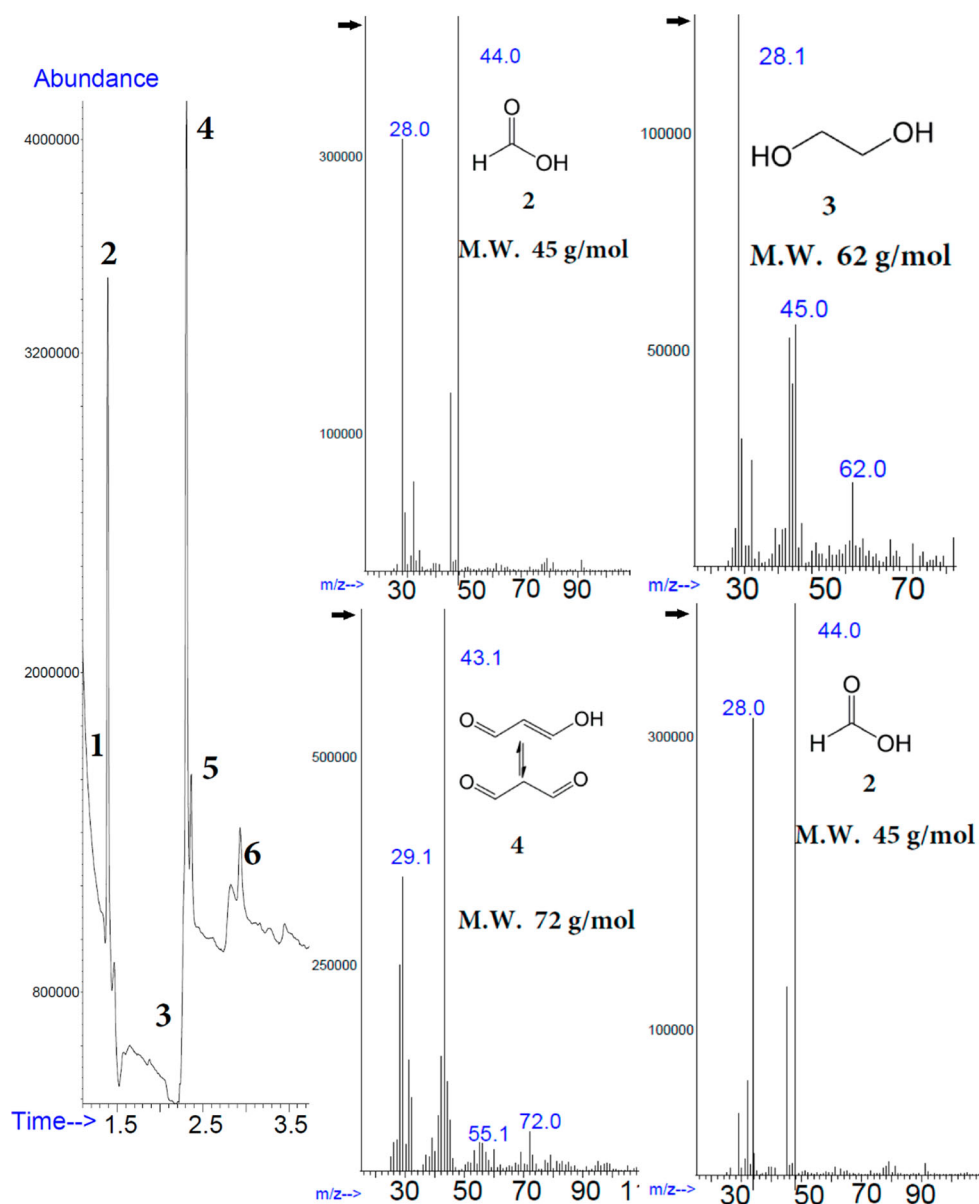
The decomposition of glyceraldehyde was analyzed using UHPLC. For the solid samples, after irradiation, 0.01 M aqueous solutions were prepared. The decomposition yield was found to be dose-dependent, and a yield-dose plot was used to derive an initial yield of decomposition with  $G = 2.2$  for the solid samples and  $G = 4.9$  for the aqueous solutions. Figure 6 shows that glyceraldehyde in an aqueous solution is labile under irradiation. Glyceraldehyde, in a solid state, is moderately stable under irradiation, and more than 80% remained at 329 kGy. The products formed by gamma radiation were analyzed via HPLC–ESI–MS analysis, and non-irradiated glyceraldehyde

presented a molecular weight corresponding to the 90 m/z monomer and the 180 m/z for the dimer. The irradiated solid samples show the formation of glycolaldehyde (60 m/z), malondialdehyde (72 m/z), ethylene glycol (62 m/z), glyceric acid (106 m/z) and sugar-like compounds, all of which increased with the doses but decreased afterward.

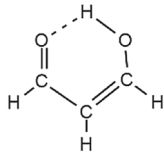

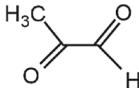
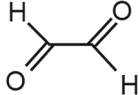
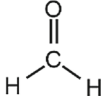
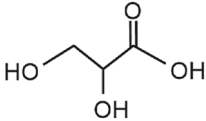
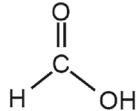
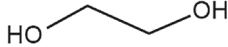
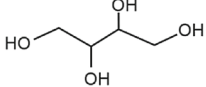
## Gas chromatography–mass spectrometry analysis

The confirmation of the radiolytic products was made by gas chromatography–mass spectrometry. For a solid-state glyceraldehyde irradiated at 8 kGy, Fig. 7 shows the total ion chromatogram and the fragmentation patterns for some

**Fig. 7** Total ion chromatogram and mass spectra for a solid-state sample of glyceraldehyde irradiated 8 kGy. After irradiation the sample was dissolved in distilled water (0.01 M). Legend: (1) formaldehyde, (2) formic acid, (3) ethylene glycol, (4) MDA, (5) glycolaldehyde, (6) glyceraldehyde



**Table 1** Identified compounds in different irradiated systems

Molecule	Chemical Structure	Irradiation in:		Detection Technique
		Solid state	Aqueous solution	
Malondialdehyde		x	x	* ✓ ▲
Glycolaldehyde		x	x	* ✓ * ▲
Methylglyoxal			x	✓
Glyoxal			x	✓
Formaldehyde		x	x	▲ ✓ *
Glyceric Acid		x		*
Formic Acid		x		▲
Ethylene Glycol		x		▲ *
Ethylene Glycol (dimer)		x		▲

HPLC-Mass Spectroscopy	*
GC-Mass Spectroscopy	▲
2,4-dinitrophenylhydrazones (detected by HPLC-UV)	✓
2,4-dinitrophenylhydrazones (detected by TLC)	*

of the identified compounds. For the analysis, the sample was dissolved in distilled water to make a 0.01 M solution.

The analysis of 2,4-dinitrophenylhydrazones by UHPLC and TLC also showed similar radiolytic products, thus complementing the results. Table 1 summarizes the identified compounds in the different systems exposed to gamma radiation.

## Discussion

We studied the response of glyceraldehyde after exposure to gamma radiation at various doses and, in the case of solid-state glyceraldehyde, at three temperatures (77, 195 and 295 K). The formation of UV-absorbing compounds increases considerably upon irradiation for both solid-state and aqueous-solution glyceraldehyde, producing simple

compounds relevant in chemical evolution [3–7]. MDA is also formed from glyceraldehyde in contact with Namontmorillonite, indicating that the clay catalyzes the decomposition of glyceraldehyde.

Glyceraldehyde's radiation-induced free-radical formation exhibits very complex chemical behavior due to its multiple functional groups and the possibility of forming hemiacetals. The same EPR spectra pattern for the radicals formed from the irradiation was presented in all solid samples, only with less intensity at the lower temperatures and doses. The registered EPR spectra are a composite because they simultaneously trap several free radicals, regardless of the irradiation temperature. These radicals' signals remained for more than 6 months.

In an aqueous system, the radiation interacts with water molecules and, through an indirect effect, the water's radiolytic products attack the organic one, giving rise to the observed products. MDA increases when the irradiation is in the presence of  $N_2O$ , which means that OH radicals from the water radiolysis are involved in this process. The OH radical is a powerful oxidizing agent and is very reactive with aldehydes [17–19].

The photolysis of glyceraldehyde produced two secondary radicals derived from the primary radical at C-1, according to Steenken and Schulte-Frohlinde [17, 19]:  $CH_2OH \cdot CHCOOH$  from 1,2-eliminations of water and  $\cdot CHOCH_2OH$  from 1,1-eliminations of water and decarbonylation. These authors did not detect a secondary radical from primary radicals at C-2. The major reactions include the fission of the C–H bonds attached to the carbonyl group and to the H of the secondary alcohol, resulting in a hydrogen atom and a radical in the monomeric form.

MDA was formed in all the studied samples. In aqueous solutions, the irradiation of sugars produces MDA as a product [1, 2]. In a solid state, the formation of MDA can be related to small changes induced by radiation that starts from the breaking of the cyclic hemiacetal dimer, the stable form in which glyceraldehyde is present in a solid state.

Glyceraldehyde's radiation chemistry at large doses and large decompositions, such as those used in this work, is important in chemical evolution [3, 4]. The ionizing radiation from natural nuclear reactors [8] and the chemical action of cosmic radiation and radioactive decay were important sources of energy on the early Earth and in extraterrestrial bodies such as comets [9].

## Conclusion

One set of biologically relevant organic compounds comprises the sugars and their precursors, including glyceraldehyde, the simplest triose. The presence of these

compounds in prebiotic environments is critical for the formation of more complex molecular systems. These compounds might have been carried to Earth on extraterrestrial bodies such as comets or meteorites, but the compounds in an aqueous solution or in a solid state must have been sufficiently stable to persist in hostile environments. In this work, we studied radiation-induced changes in solid and aqueous-solution glyceraldehyde.

According to this study's results, the degree of glyceraldehyde alteration was noticeable, even at the lowest radiation dose used. Many compounds were formed as a result of irradiation, although they had low yields. The mass spectra of the irradiated samples showed the formation of malondialdehyde, glyceric acid, ethylene glycol, glycolaldehyde and other sugar-like products. The formation of malondialdehyde produced a change in the UV spectra upon irradiation, with a shifted wavelength and increased intensity absorbance. The formation of glycolaldehyde (which can be considered the simplest sugar) is very important. This compound has been detected in interstellar space. These results are in agreement with the results obtained in recent research by other groups in the area of chemical evolution [3].

This work's preliminary results reveal ionizing radiation's role as a driving force in prebiotic processes. On the early Earth, ionizing radiation may have been important for the reactions during the period of chemical evolution in which complex molecules first formed. Hence, regardless of the nature of this energy, it can induce complex chemical changes in organic compounds.

**Acknowledgements** This work was supported by CONACyT (Grant No. C001-CONACyT-ANR-188689) and PAPIIT (Grant No. IN226817). J.C. received supported from a CONACyT fellowship and from the Posgrado en Ciencias Químicas. We thank Chem. Claudia Camargo, M.Sc. Benjamin Leal, and Phys. Francisco Flores for their technical assistance.

## References

1. Kochetkov NK, Kudrjashov LI, Chlenov MA (1979) Radiation chemistry of carbohydrates. Elsevier Ltd, Amsterdam
2. von Sonntag C, Tipson RS (2013) In: Horton D (ed) Advances in carbohydrate chemistry and biochemistry, 1st edn. Academic Press, New York
3. Meinert C, Myrgorodska I, De Marcellus P, Buhse T, Nahon L, Hoffmann SV, Lle d'Hendecourt, Meierhenrich UJ (2016) Ribose and related sugars from ultraviolet irradiation of interstellar ice analogs. *Science* 352:208–212
4. Weber A, Pizzarello LS (2006) The peptide-catalyzed stereospecific synthesis of tetroses: a possible model for prebiotic molecule evolution. *PNAS* 103:12713–12717
5. Kofoed J, Reymond JL, Darbre T (2005) Prebiotic carbohydrates synthesis: zinc-proline catalyzes direct aqueous aldol reactions of  $\alpha$ -hydroxy aldehydes and ketones. *Org Biomol Chem* 3:1850–1855

6. Chen MC, Cafferty BJ, Mamajanov I, Gállego I, Khanam J, Krishnamurthy R, Hud NV (2014) Spontaneous prebiotic formation of a  $\beta$ -ribofuranoside that self-assembles with a complementary heterocycle. *J Am Chem Soc* 136:5640–5646
7. Jalbout AF, Abrell L, Adamowicz L, Polt R, Apponi AJ, Ziurys LM (2007) Sugar synthesis from a gas-phase formose reaction. *Astrobiology* 7(3):433–442
8. Draganic IG, Draganic ZD, Adloff JP (1990) Radiation and radioactivity on Earth and beyond. CRC Press Inc, Boca Raton
9. Draganic I, Draganic Z (1998) Radiation-chemical approaches to comets and interstellar dust. *J Chim Phys* 85:55–61
10. Mosqueira FG, Albarrán G, Negrón-Mendoza A (1996) A review of conditions affecting the radiolysis due to  $^{40}\text{K}$  on nucleic acid bases and their derivatives adsorbed on clay minerals: implications in prebiotic chemistry. *Orig Life Evol Bios* 26:75–94
11. Cataldo F, Ursini O, Angelini G, Iglesias-Groth S, Manchado A (2011) Radiolysis and radioracemization of 20 amino acids from the beginning of the solar system. *Rend Fis Acc Lincei* 22:81–94
12. Ramos-Bernal S, Negrón-Mendoza A (1992) A radiation heterogeneous processes of  $^{14}\text{C}$ -acetic acid adsorbed in Namontmorillonite. *J Radioanal Nucl Chem* 160:487
13. Draganic IG, Draganic ZD (1971) The radiation chemistry of water. Academic Press, New York
14. Kwon TW, Watts BM (1963) Determination of malonaldehyde by ultraviolet spectrophotometry. *J Food Sci* 28:627–630
15. Cruz-Castañeda J, Aguilar-Ovando E, Buhse T, Ramos-Bernal S, Meléndez-López A, Camargo-Raya C, Fuentes-Carreón C, Negrón-Mendoza A (2017) The importance of glyceraldehyde radiolysis in chemical evolution. *J Radioanal Nucl Chem* 311:1135–1141
16. Kobayashi Y, Igarashi T, Takahashi H, Higasi K (1976) Infrared and Raman studies of the dimeric structures of 1,3-dihydroxyacetone, D (+)- and DL-glyceraldehyde. *J Mol Struct* 35:85–99
17. Steenken S, Schulte-Frohlinde D (1973) Fragmentation of radical derived from glycolaldehyde and glyceraldehyde in aqueous solution: an EPR study. *Tetrahedron Lett* 9:653–654
18. Steenken S (1979) Oxidation of phenolates and phenylenediamines by 2-alkononyl radicals produced from 1,2-dihydroxy- and 1-hydroxy-2-alkoxyalkyl radicals. *Phys Chem* 83:595–599
19. Fuchs E, Heusinger H (1995) Sonolysis and radiolysis of glyceraldehyde deaerated aqueous solution. *Ultrason Sonochem* 2:S105–S109

# Radiolysis of the Glycolaldehyde-Na<sup>+</sup>Montmorillonite and Glycolaldehyde-Fe<sup>3+</sup>Montmorillonite Systems in Aqueous Suspension under Gamma Radiation Fields: Implications in Chemical Evolution

J. CRUZ-CASTAÑEDA<sup>1,2</sup>, A. L. MELÉNDEZ-LÓPEZ<sup>1,2</sup>, S. RAMOS-BERNAL<sup>1</sup>  
AND A. NEGRÓN-MENDOZA<sup>1\*</sup>

<sup>1</sup>Instituto de Ciencias Nucleares, Universidad Nacional Autónoma de México, UNAM. Cd. Universitaria, A. P. 70-543, 04510 México, D. F. México

<sup>2</sup>Programa de Maestría y Doctorado en Ciencias Químicas, UNAM. Cd. Universitaria, A. P. 70-543, 04510 México, D. F. México

\*Email: [negron@nucleares.unam.mx](mailto:negron@nucleares.unam.mx)

Published online: August 07, 2017

The Author(s) 2017. This article is published with open access at [www.chitkara.edu.in/publications](http://www.chitkara.edu.in/publications)

**Abstract** The stability and reactivity of organic molecules with biological and pre-biological significance in primitive conditions are of paramount importance in chemical evolution studies. Sugars are an essential component in biological systems for the different roles that they play in living beings. The objective of the present work is to study the gamma radiolysis of aqueous solutions of glycolaldehyde, the simplest sugar and aqueous suspensions of glycolaldehyde-Na<sup>+</sup>-montmorillonite and glycolaldehyde-Fe<sup>3+</sup>Montmorillonite. Our results indicate that the radiolysis of the aqueous solutions of glycolaldehyde (0.03M), oxygen free, mainly produce the linear dimer known as eritriol (122 g/mol) and a sugar-like compound with six carbon atoms (180 g/mol). The experiments with the clay suspensions show that clays can adsorb glycolaldehyde and protect it from gamma irradiation. Additionally, it was observed that depending on the cation present in the clay, the percentage and the product (monomer or cyclic dimer) adsorption was different. In the case of Fe<sup>3+</sup> Montmorillonite, this clay catalyzed the decomposition of glycolaldehyde, forming small amounts non-identified products. The analysis of these systems was performed by ATR-FTIR, UV spectroscopy, liquid chromatography (UHPLC-UV), and HPLC coupled to a mass spectrometry.

**Keywords:** Glycolaldehyde, gamma radiation, chemical evolution, clay

Journal of Nuclear  
Physics, Material  
Sciences, Radiation and  
Applications  
Vol-5, No-1,  
August 2017  
pp. 137-146

---

Cruz-Castañeda, J  
Meléndez-López, AL  
Ramos-Bernal, S  
Negrón-Mendoza, A

---

## 1. INTRODUCTION

Carbohydrates are compounds with a minimal formula  $(\text{CH}_2\text{O})_n$  that play a paramount role in biological systems [2,6] since they participate in several essential functions like (1) the energetic metabolism and (2) as structural molecules in the ribose-phosphate backbone in DNA or RNA. For these roles, sugars are compounds of high interest in the context of the chemical evolution. Their abiotic synthesis, the stability of these in the surrounding environment, and the types of reactions that can participate are important steps in trying to describe how the first self-replicable systems emerged. Glycolaldehyde ( $\text{C}_2\text{H}_4\text{O}$ ) is the simplest sugar that has been detected in the interstellar medium [4, 5]. Also, it is intermediate for the synthesis of more complex sugars in abiotic reactions.

In chemical evolution, the stability of bio-organic compounds, like carbohydrates, in the surrounding geological environment is crucial, especially in the presence of an external energy source (e.g. ionizing radiation, thermal energy, etc.) [1]. Among the proposed mechanism for increasing the stability of organic compounds, in a plausible geological scenario is their adsorptions onto mineral surfaces [7, 8]. Several solid surfaces may have been relevant in this context: sulfides, carbonates, and clays [9].

In this work, we highlight the type of reactions that sugars can have under gamma irradiation, and the possible role of clay minerals as a protecting agent for the bio-organic molecules adsorbed. Clay minerals are relevant due to their adsorption capacity, ancient origin, and their broad geological distribution. This work is focused on the radiolysis of glycolaldehyde adsorbed in two clay minerals:  $\text{Na}^+$ -montmorillonite and  $\text{Fe}^{3+}$ -montmorillonite under a high radiation field. To this end, the radiolysis of both systems was carried out by exposing them to a different irradiation dose. The analysis of these systems was performed by ATR- FTIR, UV spectroscopy, liquid chromatography (UHPLC-UV), and HPLC-coupled to a mass spectrometry.

## 2. EXPERIMENTAL

### 2.1 Chemicals and Materials

The chemicals were purchased from Sigma-Aldrich Co. (USA) and were of the highest purity available in the market (glycolaldehyde dimer, ammonium acetate,  $\text{FeCl}_3 \cdot 5\text{H}_2\text{O}$ ). The HPLC-grade solvents (water and methanol) were purchased from Honeywell Burdick & Jackson (NJ, USA). The glassware was treated with a warm mixture of  $\text{HNO}_3$  and  $\text{H}_2\text{SO}_4$  for 20 minutes, followed by a wash with distilled water and heating in an oven at  $300^\circ\text{C}$  overnight. All of the chemical and glassware were handled to minimize contamination [11].

---

---

The clay used in the reactions (Na<sup>+</sup>-montmorillonite SWy-1) was obtained from Clay Minerals Repository of the Clay Minerals Society at the University of Missouri. It was treated with hydrogen peroxide to remove organic impurities; the same lot was used in all the experiments. Fe<sup>3+</sup>-montmorillonite was prepared from Na<sup>+</sup>-montmorillonite by an ion exchange reaction [3]. For this, 1N solutions of FeCl<sub>3</sub>·5H<sub>2</sub>O were prepared to exchange the Na<sup>+</sup> cations in the clay with the desired Fe<sup>3+</sup> ions.

## 2.2 Preparation of samples

Standard stock solutions of glycolaldehyde were prepared using triple distilled water, oxygen-free by bubbling Ar for 20 minutes. Then, 3 mL of the solution (0.03 M) and 100 mg of clay were placed in sealed culture tubes followed by shaking at 250 rpm for 20 minutes. All of the solutions were stored in a refrigerator at 4°C while not in use.

## 2.3 Irradiation of Samples

All samples were irradiated at room temperature using a high-intensity <sup>60</sup>Co gamma source (Gammabeam 651 PT) at ICN-UNAM, at two different doses (14 and 29 kGy), and with a dose rate of 240 Gy/min. The dose was evaluated using a ferrous sulfate, copper sulfate dosimeter [10]. The samples were analyzed immediately after irradiation.

## 2.4 Analysis of samples

### 2.4.1 HPLC-ESI-MS analysis

The liquid chromatographic analysis was performed on an HPLC system (515-pump from Waters Corp.), coupled with a Single Quadrupole Mass Detection system (SQ-2 manufactured by Waters Corp.), with an electrospray ionization negative mode (ESI-), a positive mode (ESI+) source cone energy of 15V, and a capillary energy of 3kV. The analysis was done in Symmetry C18 column (4.6 x 75mm, 3.5 μm spherical particle size, by Waters Corp.) under an isocratic elution of a mobile phase (0.1M ammonium acetate solution; 80% methanol and 20% water at pH=4), and at a constant flow of 0.4 mL/min. A sample volume (20 μL) was injected using a loop.

### 2.4.2 UHPLC-UV analysis

The ultra high-pressure liquid chromatography analysis was performed on an UHPLC system Ultimate 3000, manufactured by ThermoFisher Scientific (UltiMate™ ISO-3100SD standard isocratic pump and an UltiMate™ 3000 TCC-3000SD Standard Thermostatted Column Compartment), and coupled

Radiolysis of the  
Glycolaldehyde-  
Na<sup>+</sup>Montmor-  
illonite and  
Glycolaldehyde-  
Fe<sup>3+</sup>Montmorillonite  
Systems in Aqueous  
Suspension under  
Gamma Radiation  
Fields: Implications  
in Chemical  
Evolution

---

---

Cruz-Castañeda, J  
Meléndez-López, AL  
Ramos-Bernal, S  
Negrón-Mendoza, A

with Variable Wavelength UV-Vis Detectors, Thermo Scientific™ Dionex™ UltiMate™ 3000 VWD. The analysis was done on a Symmetry C18 column (4.6 x 75 mm, 3.5 μm spherical particle size by Waters Corp), at 50°C under an isocratic elution of mobile phase (0.1 M ammonium acetate solution; 80% methanol, 20% water at pH=4), at a constant flow of 0.4 mL/min, monitored at 260 nm. A sample volume (20 μL) was injected using a loop.

---

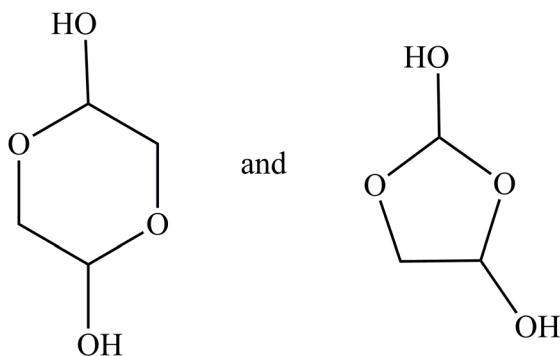
### 2.4.3 ATR-FTIR

Infrared spectra were obtained by the attenuated total reflection (ATR) sampling technique on Spectrum 100 spectrometer FTIR equipment manufactured by PerkinElmer (USA).

## 3. RESULTS

Glycolaldehyde in solid state is mainly found as a dimer (Figure 1) with a molecular weight of 120 g/mol and melting point of 85°C. It was identified by its IR spectrum (Figure 2) due to the presence of the characteristic band of alcohols at 3394 cm<sup>-1</sup>, band of ethers at 1134 cm<sup>-1</sup>, and by the absence of the carbonyl group tension bands in 1740–1720 cm<sup>-1</sup> and in 2800 and 2700 cm<sup>-1</sup> (Fermi resonance) characteristic of aldehydes.

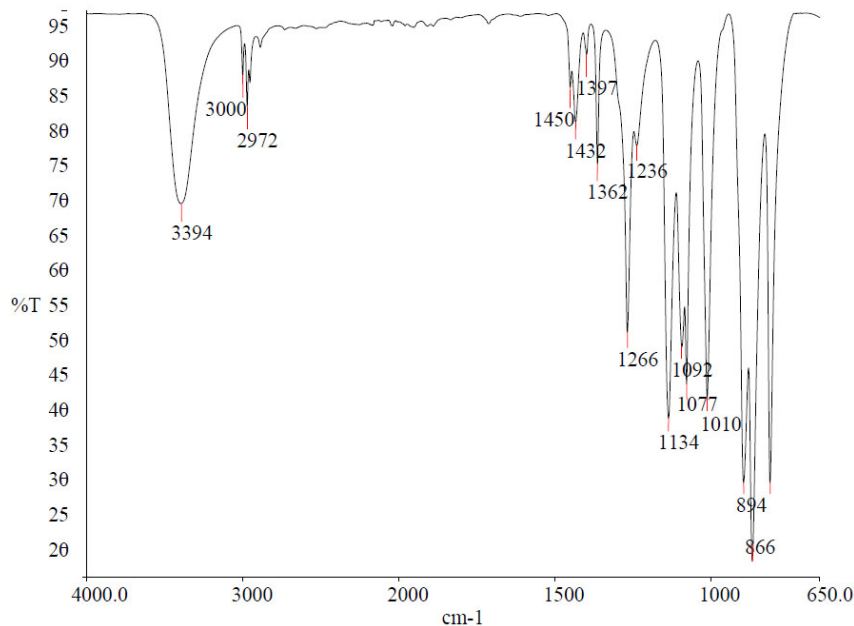
The results indicate that the cyclic dimer of glycolaldehyde in aqueous solution is hydrolyzed to form four species that are in chemical equilibrium (Figure 3A) [11], which were identified by their molecular ions in an MS detector by direct infusion with an ESI-source (Figure 3B).



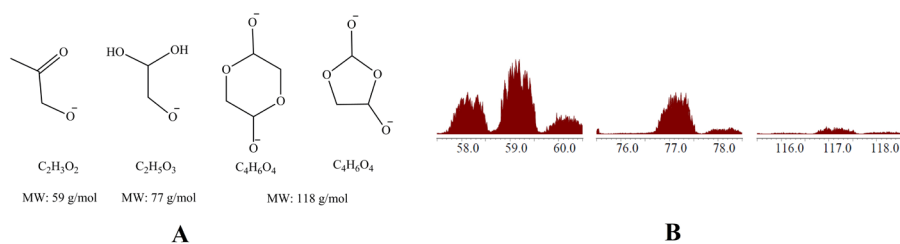
**Figure 1:** Structure of cyclic dimers of glycolaldehyde in aqueous solution  $3 \times 10^{-2}M$ .

---





**Figure 2:** ATR-FTIR spectrum of glycolaldehyde.

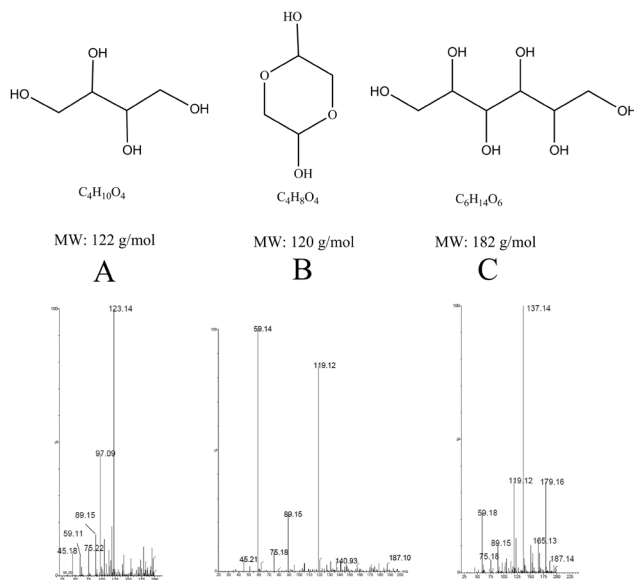


**Figure 3:** Chemical species of glycolaldehyde in aqueous solution identified by MS detector ESI-source.

The main reaction of glycolaldehyde in aqueous solution under gamma irradiation is the polymerization in which the main products are the linear dimer (Figure 4A) known as eritriol (122 g/mol) and the cyclic dimer (120 g/mol) Figure 4B. Also, a higher molecular weight molecule was detected, and it is a sugar-like compound, with six carbon atoms (180 g/mol) Figure 4C. Identified by their respective fragmentation spectra obtained by the HPLC-ESI-MS analysis.

The polymerization reaction of glycolaldehyde was monitored by UHPLC-UV analysis with the retention times: 1.7 minutes for the dimer and

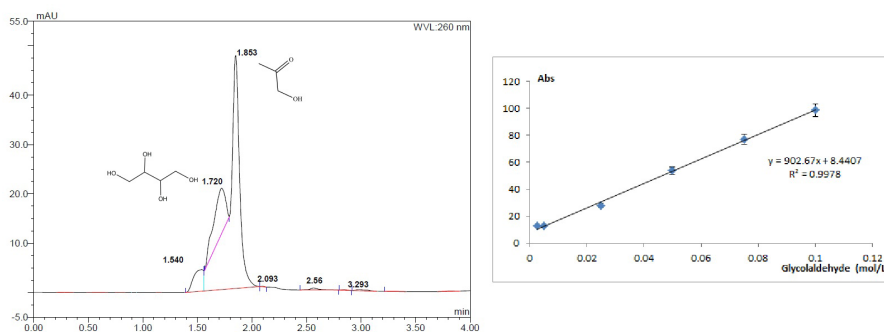
Cruz-Castañeda, J  
Meléndez-López, AL  
Ramos-Bernal, S  
Negrón-Mendoza, A



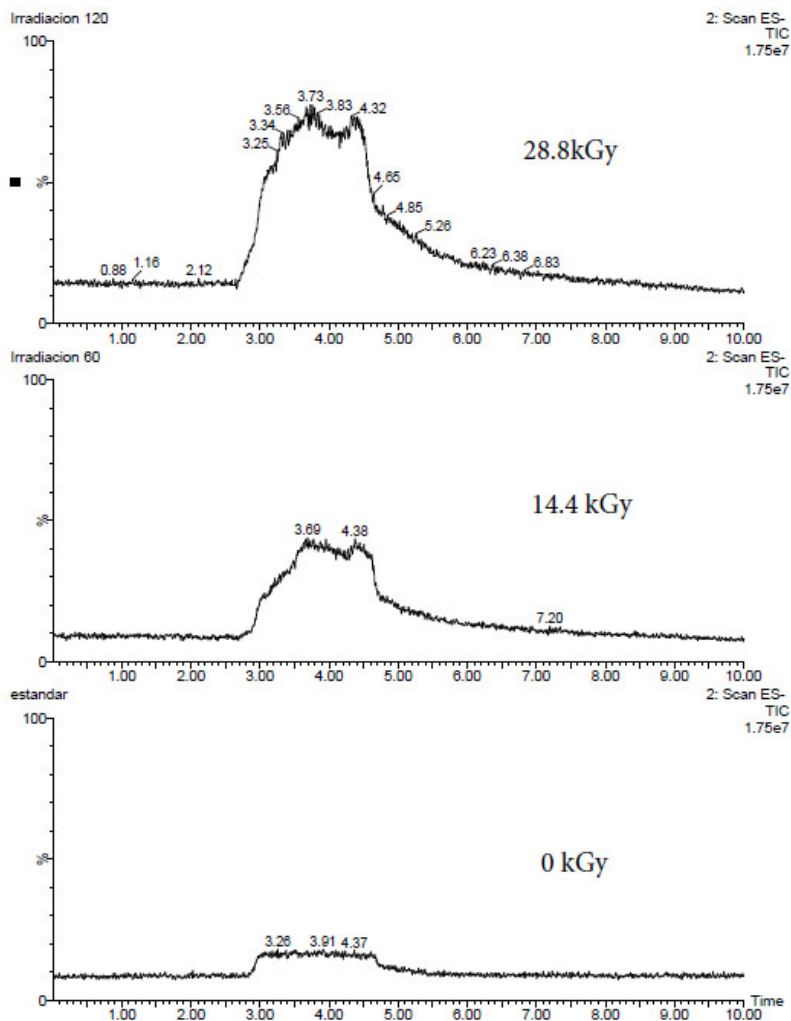
**Figure 4:** MS fragmentation spectra products of radiolysis.

1.8 minutes for the monomer (Figure 5); the formation of the dimers and other polymers is dependent on the irradiation dose; if it is high, the irradiation dose also increases (Figure 6).

The possible reaction mechanism for the radiolysis is shown in Fig. 7. The results of UHPLC-UV analysis show that  $\text{Fe}^{3+}$ -montmorillonite preferentially adsorbed the glycolaldehyde monomer by 97% (retention time: 1.7 minutes) to the cyclic dimer (retention time: 1.8 minutes). However,  $\text{Na}^+$  montmorillonite



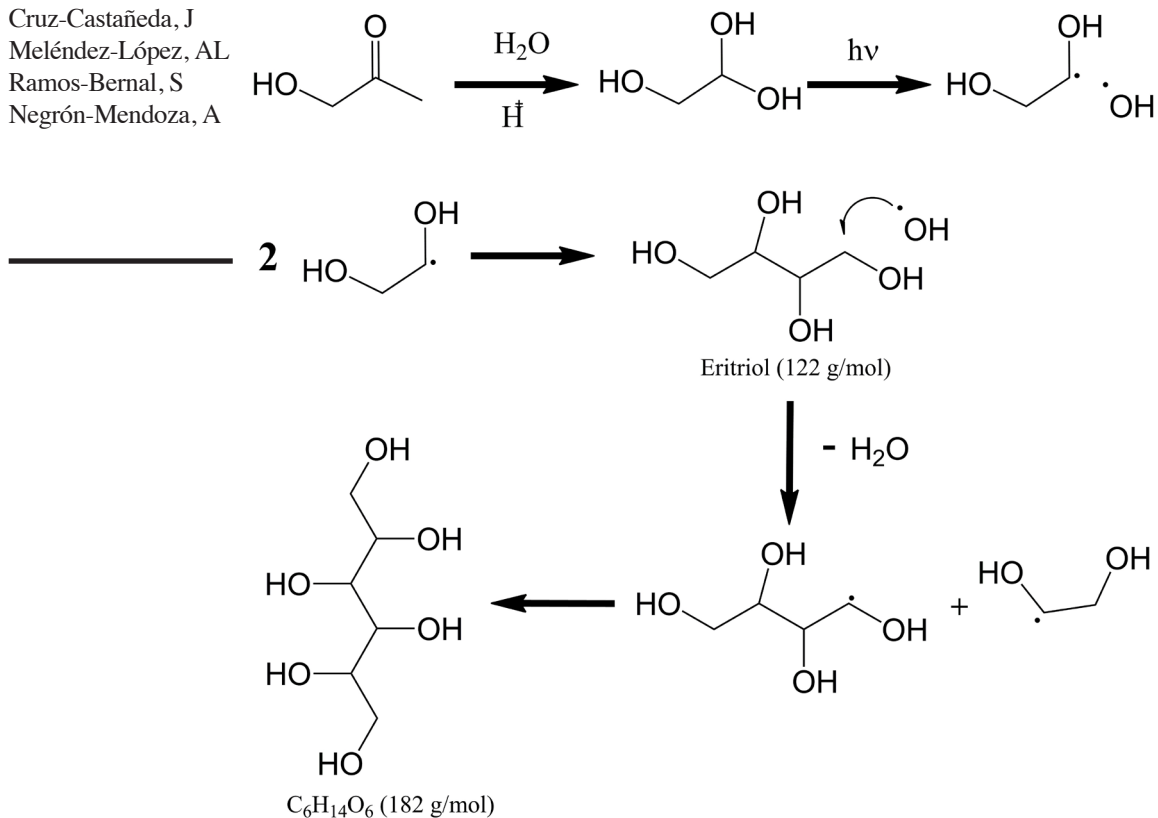
**Figure 5:** HPLC-UV analysis of glycolaldehyde at 260nm.



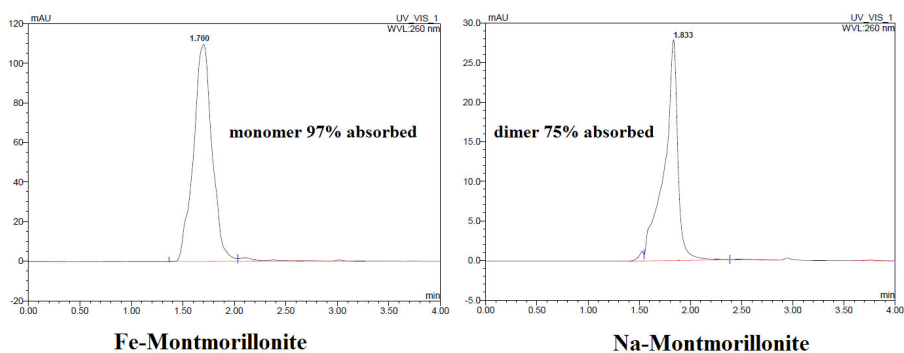
**Figure 6:** TIC HPLC-MS analysis of glycolaldehyde.

adsorbs the cyclic dimer preferentially (75%, retention time 1.8 minutes), as it is showed in Figure 8. Both clays were able to protect the glycolaldehyde adsorbed onto them when the clay-organic systems were exposed to gamma radiation, since the recovery of glycolaldehyde after the irradiation and desorption processes was higher, and the polymers were formed in smaller quantities than those in the experiments without clay.

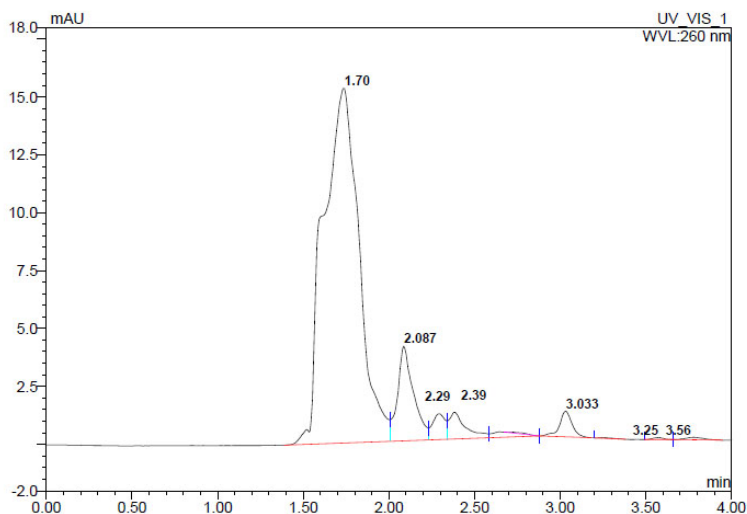
Cruz-Castañeda, J  
 Meléndez-López, AL  
 Ramos-Bernal, S  
 Negrón-Mendoza, A



**Figure 7:** The suggested mechanism for the formation of polymers from the glycolaldehyde radiolysis Radiolysis of glycolaldehyde-clay suspensions.



**Figure 8:** Adsorption experiments analyzed by UHPLC-UV in the aqueous phase.



**Figure 9:** Adsorption experiments analyzed by UHPLC-UV.

Additionally, it was found that Fe<sup>3+</sup> montmorillonite promotes chemical reactions in the aqueous suspension with glycolaldehyde without gamma radiation, since, after the adsorption and desorption experiments, low-yield reaction products were detected by UHPLC-UV. These products are not yet identified, and they presented retention times of 2.087, 2.29, 2.39, and 3.033 minutes (Figure 9).

## REMARKS

The sugars are bio-compounds of paramount importance in biological systems. For this reason, it is relevant to find the possible physicochemical and geological conditions of its possible abiotic synthesis and the mechanisms of its polymerization in chemical evolution studies. Sugar-like compounds may have been important intermediates in the reaction mechanisms for the synthesis and polymerization of sugars used by early biological systems. The results obtained indicate that the glycolaldehyde in aqueous solution in the presence of a high energy source is polymerized forming sugar-like compounds.

Glycolaldehyde adsorbed onto clays minerals and exposed to gamma irradiation presented a higher yield of recovery in comparison with the samples without clay. Also, it was found a preferential adsorption of the monomer and cyclic dimer of glycolaldehyde by the different clays used in these experiments. Energy sources, as well as the presence of solid surfaces, played diverse roles

---

Cruz-Castañeda, J in the chemical evolution, such as catalysts, reaction directing agents, and  
Meléndez-López, AL especially as protective agents for compounds of biological significance.  
Ramos-Bernal, S  
Negrón-Mendoza, A

### ACKNOWLEDGMENTS

The support from C001-CONACYT-ANR-188689, DGAPA grant IN111116, is acknowledged. J.C. was supported by a CONACyT fellowship and Programa de Maestría y Doctorado en Ciencias Químicas-UNAM.

---

### REFERENCES

- [1] Draganić, I. G., Draganić, Z. D., and Adloff, J. P. (1990). Radiation and radioactivity on earth and beyond: CRC Press.
  - [2] Gabius, H.-J. Biological Information Transfer Beyond the Genetic Code: The Sugar Code. [Journal article]. *Naturwissenschaften*, **87(3)**, 108–121 (2000).
  - [3] Gerstl, Z., & Banin, A. Fe (super 2<sup>+</sup>) -Fe (super 3<sup>+</sup>) transformations in clay and resin ion-exchange systems. *Clays and clay Minerals*, **28(5)**, 335–345 (1980).
  - [4] Hollis, J. M., Lovas, F. J., & Jewell, P. R. Interstellar Glycolaldehyde: The First Sugar. *The Astrophysical Journal Letters*, **540(2)**, L107 (2000).
  - [5] Jes, K. J., Cécile, F., Suzanne, E. B., Tyler, L. B., Ewine, F. v. D., and Markus, S. Detection of the Simplest Sugar, Glycolaldehyde, in a Solar-type Protostar with ALMA. *The Astrophysical Journal Letters*, **757(1)**, L4 (2012).
  - [6] Joyce, G. F. RNA evolution and the origins of life. *Nature*, **338(6212)**, 217–224 (1989).
  - [7] Meléndez-López, A. L., Ramos-Bernal, S., and Ramírez-Vázquez, M. L. Stability of guanine adsorbed in a clay mineral under gamma irradiation at temperatures (77 and 298 K): Implications for chemical evolution studies. *AIP Conference Proceedings*, **1607(1)**, 111–115 (2014).
  - [8] Negrón-Mendoza, A., and Albarran, G. Chemical effects of ionizing radiation and sonic energy in the context of chemical evolution. In: *Chemical Evolution. Origin of life*, 147-235 (1993).
  - [9] Negrón Mendoza, A., Albarrán, G., and Ramos Bernal, S. (1996). Clays as natural catalyst in Prebiotic Processes *Chemical Evolution: Physics of the Origin and Evolution* (pp. 97-106). Springer Netherlands: Academic publishers.
  - [10] O'Donnell, J. H., & Sangster, D. F. (1970). *Principles of radiation chemistry*, New York: Elsevier.
  - [11] Yaylayan, V. A., Harty-Majors, S., and Ismail, A. A. Investigation of the mechanism of dissociation of glycolaldehyde dimer (2,5-dihydroxy-1,4-dioxane) by FTIR spectroscopy. *Carbohydrate Research*, **309(1)**, 31–38 (1998).
-

# The importance of glyceraldehyde radiolysis in chemical evolution

J. Cruz-Castañeda<sup>1,2</sup> · E. Aguilar-Ovando<sup>1,3</sup> · T. Buhse<sup>3</sup> · S. Ramos-Bernal<sup>1</sup> ·  
A. Meléndez-López<sup>1,2</sup> · C. Camargo-Raya<sup>1</sup> · C. Fuentes-Carreón<sup>1,4</sup> · A. Negrón-Mendoza<sup>1</sup>

Received: 27 May 2016

© Akadémiai Kiadó, Budapest, Hungary 2016

**Abstract** Studies in chemical evolution are intended to demonstrate how compounds of biological importance are generated from substances that could have been found in abiotic conditions on the primitive Earth or in extraterrestrial environments. In this context, the aim of the present work was to examine the behavior of DL-glyceraldehyde in both aqueous solution and solid samples under gamma irradiation. We irradiated DL-glyceraldehyde at different doses and temperatures with a gamma source; even at low doses and temperature (77 K), free radicals were detected. Among the products formed were ethylene glycol and glycolaldehyde. Some sugar-like compounds were also detected.

**Keywords** Gamma irradiation · Glyceraldehyde · Chemical evolution · Primitive Earth

## Introduction

The field of chemical evolution encompasses the formation of biologically relevant compounds under primitive-earth conditions; in this context, life arose from inorganic

molecules, which became organic molecules and eventually biological ones. In addition to the nucleic acids and proteins that provide the foundations of life, sugar plays a critical role, as it is part of nucleic acid components (e.g., RNA) and is linked to almost every life process in biological systems [1].

The synthesis of organic matter in a simulated primitive environment (terrestrial or extraterrestrial) has been widely studied [1]. An important aspect of chemical evolution is the stability of the organic molecules that have biological significance under primitive conditions, especially in the presence of constant energy sources. Some protective mechanisms may be enacted to ensure that important compounds endure these primitive conditions.

One set of biologically relevant organic compounds comprises the sugars and their precursors, such as glyceraldehyde, the simplest triose. The presence of these compounds in prebiotic environments is critical in the formation of more complex systems. These compounds, which might have been carried to Earth by extraterrestrial bodies such as comets or meteorites, must be sufficiently stable to persist in hostile environments whether they are in an aqueous solution or a dry state. According to Weber and Pizzarello [2], glyceraldehyde was probably present on the prebiotic Earth, as it has been synthesized under prebiotic conditions [2 and the references therein].

Sources of energy that existed on the early Earth and that were useful in the abiotic synthesis of organic matter are essential parts of chemical evolution because energy is responsible for initiating, promoting, and directing all physicochemical processes. Energy in the form of ionizing radiation was probably of great importance in the chemical reactions that occurred on the early Earth and in extraterrestrial environments [3–6] due to its high efficiency in inducing the synthesis of organic compounds, its

✉ A. Negrón-Mendoza  
negrón@nucleares.unam.mx

<sup>1</sup> Instituto de Ciencias Nucleares, Universidad Nacional Autónoma de México, Mexico City, México

<sup>2</sup> Programa de Maestría y Doctorado en Ciencias Químicas, UNAM, Mexico City, México

<sup>3</sup> Centro de Investigaciones Químicas, Universidad Autónoma del Estado de Morelos, Cuernavaca, Morelos, México

<sup>4</sup> Facultad de Ciencias, Universidad Nacional Autónoma de México, Mexico City, México

penetration into matter, and its relative abundance. Two sources contributed to this type of energy: ionizing radiation from radionuclides in the Earth's crust and radiation from extraterrestrial sources such as cosmic rays or the solar wind [3, 4].

Extraterrestrial bodies are exposed to various types of high-energy radiation, mainly in the form of cosmic rays (high-speed particles), ultraviolet (UV) rays, and gamma photons [3]. Cataldo et al. [7] described calculations related to the energy deposited by the decay of radionuclides in comets, asteroids, meteorites and larger bodies of the solar system on the time scale of the age of the solar system (i.e.,  $4.69 \times 10^9$  years about 14 MGy) [7]. In these bodies, the presence of minerals and other solid surfaces may influence the behavior of organic molecules by acting as catalysts, concentrators or protecting agents [5]. On the primitive Earth and on small bodies, the most relevant minerals were carbonates, sulfides and, in particular, clays and silicates [5].

The aim of this work is to study the stability of prebiotic organic molecules such as glyceraldehyde under ionizing radiation (gamma rays of  $^{60}\text{Co}$ ). The study was carried out on aqueous solutions and solid samples at 298, 198 and 77 K, thus simulating the environments of prebiotic Earth and a comet's core, which has an icy phase consisting of water mixed with glyceraldehyde.

## Experimental

### Reagents and glassware

High-purity DL-glyceraldehyde (Merck Co., USA) was employed in all of the experiments. Sodium-montmorillonite, hectorite, and attapulgite (from the Clay Mineral Society's Source of Clay Minerals Repository) were used to anchor the aldehyde. The glassware was treated with a warm mixture of  $\text{HNO}_3$  and  $\text{H}_2\text{SO}_4$  for 60 min, rinsed with bi-distilled water, and heated in a 350 °C oven overnight. Triple-distilled water was used for all aqueous solutions, according to the standards of radiation chemistry [8].

### Preparation of samples

Three types of samples were prepared: aqueous solutions of glyceraldehyde, aqueous solutions of glyceraldehyde in the presence of a clay mineral and solid samples with only powdered glyceraldehyde. Aqueous solutions of glyceraldehyde from  $1 \times 10^{-1}$  to  $2 \times 10^{-4}$  mol/L were saturated with argon and prepared with triple-distilled water in sealed glass tubes. The pH of this solution was 6.9.

For the solid samples, the DL-glyceraldehyde powder was placed inside of a glass tube and evacuated for 20 min.

### Sorption experiments

Three clays were used for adsorption experiments: Sodium-montmorillonite, attapulgite and hectorite. To prepare the clay-glyceraldehyde system, 0.1 g of clay was mixed with 3 mL of the glyceraldehyde standard solution ( $1 \times 10^{-2}$  mol/L). The pH was adjusted with formic acid and ammonium hydroxide, and left on a plate undergoing continuous agitation at 150 rpm for 30 min. After this time, a Beckman Allegra XL-90 centrifuge was used (for 30 min at 25,000 rpm and 20 °C) to separate the fine-particle solids from the liquid phases. High-performance liquid chromatography (HPLC) mass spectroscopy was employed to determine the percentage of glyceraldehyde that adsorbed onto the clay, relative to the amount available in the standard solution.

A desorption test was carried out to determine how much glyceraldehyde could be recovered from the mineral; this was done by changing the pH of the solid previously separated by centrifugation from 2 to 11. Glyceraldehyde was recovered after three cycles of treatment with KOH (0.1 mol/L). The clay was dried at 80 °C overnight and then ground in an agate mortar for X-ray diffraction analysis. The solution was analyzed using HPLC mass spectrometry.

### Radiolysis experiments

The irradiation was carried out at Institute de Ciencias Nucleares-UNAM using a high-intensity radiation source,  $^{60}\text{Co}$  (Gammabeam 651PT). The samples were irradiated at room temperature (298 K). The dose rate was determined to be  $221 \pm 3$  Gy/min using the ferrous ammonium sulfate-cupric sulfate dosimeter [8]. The samples were bubbled with argon for 20 min in a warm container to eliminate dissolved oxygen.

### Aqueous solution

The aqueous samples without clay were irradiated from 0 to 25 kGy and pH 6.9.

### Solid samples

These samples were irradiated for 0.5–10 h in liquid nitrogen (77 K), in dry ice (195 K), and at room temperature (298 K) using the same position at the source. These samples were analyzed using electronic paramagnetic resonance (EPR). Another set of solid samples was irradiated from 0 to 308 kGy and analyzed using polarography.



## Analysis

The compounds were analyzed using HPLC coupled with mass spectrometry detector. Other analyses were performed using UV spectroscopy, polarography, and EPR spectroscopy. The samples were analyzed immediately after irradiation. The clays were analyzed using X-ray diffraction spectroscopy.

## UV–Vis spectroscopy

After irradiation, the aqueous samples were analyzed using UV spectroscopy with a Carry 100 spectrometer in the range of 200–350 nm. The samples with clay were separated beforehand by centrifugation.

## Polarography

All polarography measurements for the irradiated samples were performed at room temperature (25 °C) with an initial  $1 \times 10^{-2}$  mol/L DL-glyceraldehyde aqueous solution. Polarographic curves were registered on a Metrohm polarography Model 797 VA Computrace, The working conditions included a start potential of 0.0 V, a final potential of  $-1.7$  V, a scan rate of 0.005 V/s, a pulse width of 0.05 V, a pulse time of 0.04 s, and support electrolytes of ammonium hydroxide and ammonium chloride (pH 8.24). The working electrode was dropping mercury with a drop time of 1 s; the reference electrode used Ag and AgCl, and the counter electrode used platinum. The program (797 VA Computrace Version 1.2) controlled the potential of the mercury cathode.

## HPLC–MS analysis

Direct analysis of liquid samples was performed using electrospray-ionization negative-mode (ESI-) mass spectrometry with a Single Quadrupole Mass Detector (SQ-2, manufactured by Waters Corp., USA). The working conditions included a capillary of 2.1 kV, a cone of 10 V, a source temperature of 150 °C, a desolvation temperature of 350 °C, a desolvation gas flow of 650 L/h, and a sample rate of 100  $\mu$ L/min. The samples were analyzed at 18 °C. In addition, the samples were introduced to the mass detector via HPLC using a HPLC Column XBridge C18 measuring 3.5  $\mu$ m 3.0  $\times$  100 mm (WT186003027) with a liquid phase of methanol and water (50:50 ratio) at 0.4 mL/min. Some samples were analyzed by HPLC coupled to an ELSD detector. The column used was a Chirobiotic T, and the liquid phase was methanol and water (70:30 ratio) at 1.3 mL/min.

## EPR analysis

EPR measurements were performed at Instituto de Química-UNAM, using  $30 \pm 0.1$  mg of the sample in a quartz tube at room temperature and a JEOL JES-TE300 spectrometer, which was operating on the X-band at a 100 kHz modulation frequency and which had a cylindrical cavity in the TE<sub>011</sub> mode. The external calibration of the magnetic field was made using a precision JEOL ES-FC5 gauss meter. The spectrometer was set to measure all spectra with a center field of 335.0 mT, a microwave power of 1 mW, a microwave frequency of 9.43 GHz, a modulation width of 0.079 mT, a time constant of 0.1 s, an amplitude of  $1 \times 100$ , and a sweep time of 120 s; two scans were completed. The readings were made at the vertical peak-to-peak height of the line. Spectral acquisitions and manipulations were performed using the ES-IPRITS/TE program. The EPR spectra were recorded as a first derivative.

## X-ray diffraction spectroscopy

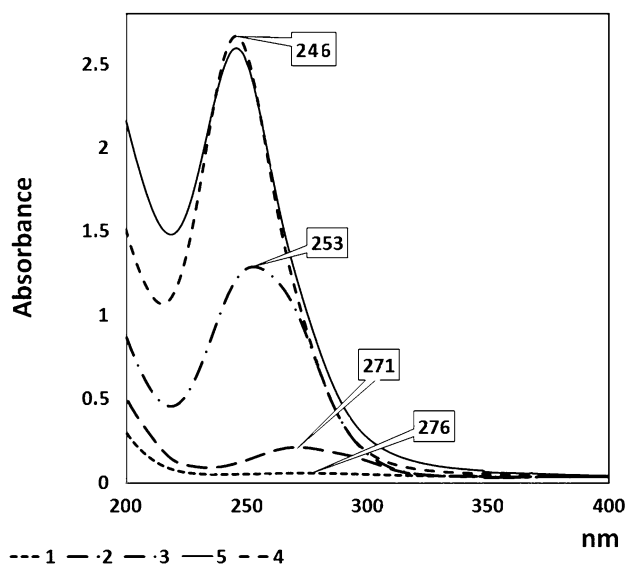
The adsorption of glyceraldehyde by montmorillonite was followed by X-ray diffraction spectroscopy using a Bruker 08 Advance diffractometer, with filtered CuK $\alpha$  radiation ( $\lambda = 1.5406$  Å) Ni filter; 40 kV, 40 mA, at  $2\theta$  angles from 2 to 90° during 30 min. Specimens were prepared by pressing the organic adsorbed montmorillonite on the diffractometer's plastic holder (polymethylmethacrylate). The spectrometer was calibrated using Si, quartz, and kaolinite reference materials.

## Results and discussion

### Aqueous and solid samples without clay minerals

The glyceraldehyde molecule contains both an aldehyde group and two hydroxyl groups. It is highly reactive and occurs in the biosphere [2, 9, 10]. Preliminary results show that glyceraldehyde is unstable under irradiation in aqueous solutions; even at low doses, it starts to decompose rapidly. It forms a compound that has a much higher absorption coefficient in the UV spectra, accompanied by a hypsochromic shift in the maximum absorption from 274 to 246 nm, which can indicate the formation of a product with a new chromophore or functional group (Fig. 1). The adsorption increases with the dose, and the maximum absorption changes with the pH at the same dose.

This shift probably corresponds to the formation of malonaldehyde (also known as malondialdehyde, MDA), which has a UV absorption spectrum pH-dependent. It presents a maximum at 245 nm (molar absorptivity,  $\epsilon = 1.34 \times 10^4$ ) below pH 3, due to its configuration as



**Fig. 1** UV spectra for  $1 \times 10^{-2}$  mol/L aqueous solution samples of DL-glyceraldehyde at various irradiation doses and pH of 6.9: 1 0 kGy, 2 0.22 kGy, 3 2.2 kGy, 4 11 kGy and 5 20 kGy

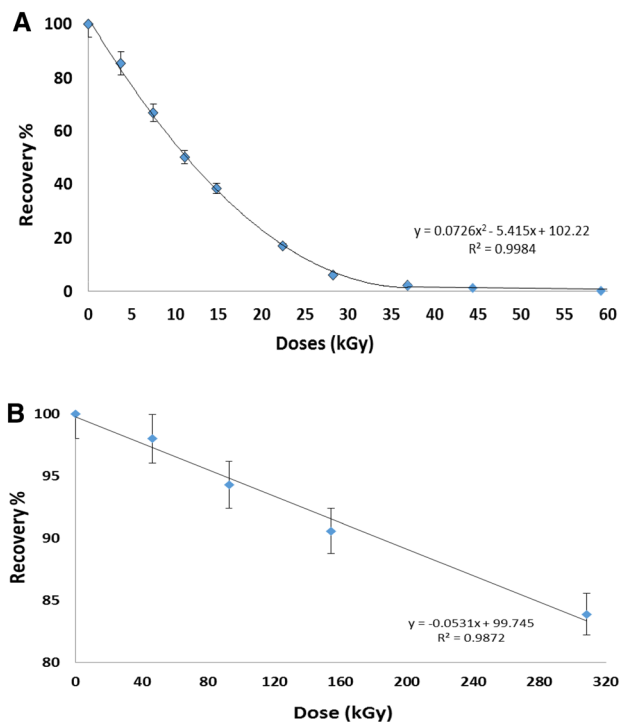
*s-cis* planar structure with an intramolecular H bond; and another one above pH 7 at 267 nm (molar absorptivity,  $\epsilon = 3.18 \times 10^4$ ) due to its enolate anion structure completely dissociated [11]. Irradiated solution change the maximum in the spectrum when the solution is measured at different pH, in a similar way that MDA. Even with a very small irradiation dose (61 Gy), the change in the spectrum is apparent. The resulting product has a very high molar extinction coefficient, and its spectral changes associated with pH may indicate that malonaldehyde is responsible for this new absorption band in irradiated carbohydrates [9, 10, 11, 12]. This change in the absorption spectrum is also observed with an aqueous solution of the irradiated solid samples. Other identified products are ethylene glycol and glycolaldehyde.

Figure 2 shows the decomposition of glyceraldehyde in an aqueous solution without clay and in a solid state as a function of an irradiation dose followed by polarography.

For irradiated solid samples an aqueous solution was prepared and the identification of products was made by HPLC–MS, based in their retention times and molecular weight (Fig. 3). Even when MDA is present in small amounts, as shown by the mass spectrum, it has a very large extinction coefficient.

### Solid samples irradiated at different temperatures

Although solid DL-glyceraldehyde is relatively stable, it produces free-radical species even at low irradiation doses



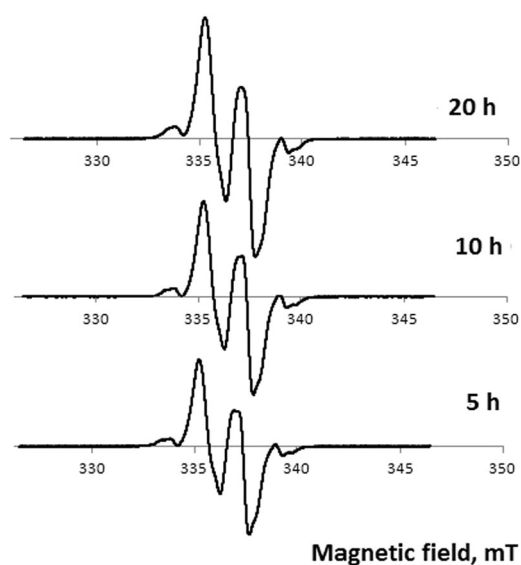
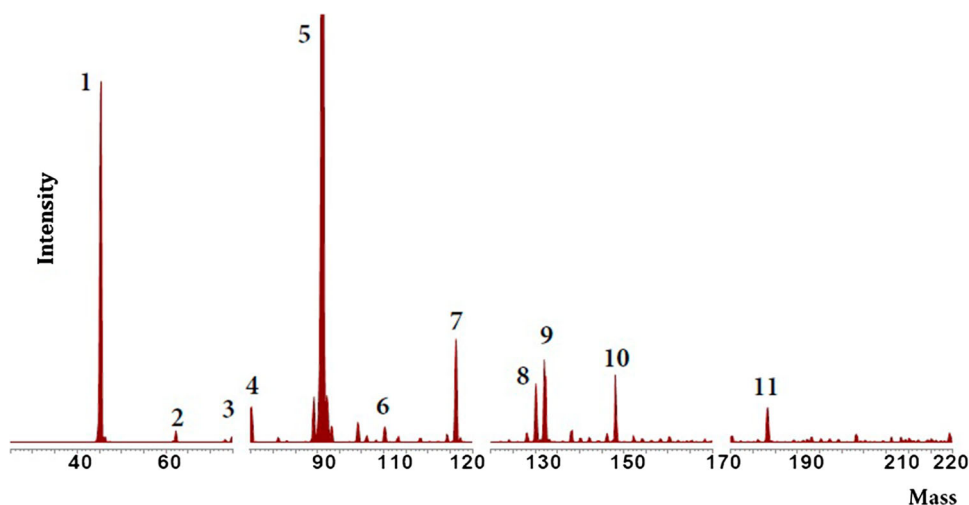
**Fig. 2** Decomposition of DL-glyceraldehyde as a function of irradiation dose: **a** aqueous solution, **b** solid-state samples

(Fig. 4). The irradiations at low temperature and at room temperature showed the same spectral patterns (Fig. 5).

Glyceraldehyde showed a composite EPR spectrum. Upon irradiation, different paramagnetic radicals formed, creating broad and overlapping lines. Polyalcohols' primary radicals are usually very unstable and are observed at low temperatures. Figure 5 shows the EPR spectra for samples irradiated at room temperature at different irradiation doses, and Fig. 6 shows the spectra for samples irradiated at room temperature and at the temperatures of dry ice and liquid nitrogen for a constant time. The same pattern of signals is present at the different temperatures and doses. The signal at  $g = 2.0090$  is the most important line in the spectrum. Steenken and Schulte-Frohlinde [12] detected two secondary radicals by EPR from the photolysis of glyceraldehyde, which was derived from the radical at C-1:  $\text{CH}_2\text{OH}^\bullet\text{CHCOOH}$  produced by 1, 2 elimination of water and  $^\bullet\text{CHOHCH}_2\text{OH}$  produced by the 1, 1 elimination of water and by decarbonylation. Those substances are stable for several weeks and are formed at low doses and temperatures.

Information about the radiation chemistry of ketones and aldehydes, whether in aqueous solution or in a solid state, is scarce [9]. In particular, the radiation-induced transformation of aldehydes is a complex problem. The entire mechanism may be elucidated by conducting a detailed analysis of the transient intermediates, identifying

**Fig. 3** HPLC-MS for dissolved solid samples irradiated at 265 kGy. Legend: 1 formic acid (reagent), 2 glycolaldehyde + ethylene glycol, 3 malonaldehyde, 4 2-hydroxypropanal, 5 glyceraldehyde, 7 ethylene glycol dimer (tetritol), 10 pentitrol, and 11–12 sugar-like compounds, 6, 8 and 9 are unknown

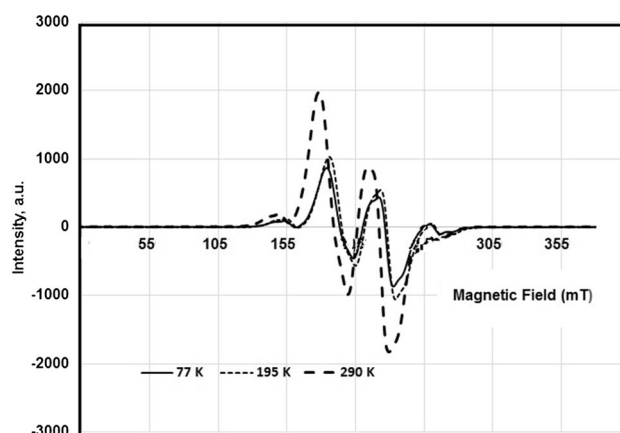


**Fig. 4** EPR spectra of glyceraldehyde irradiated at 298 K and at different radiation doses

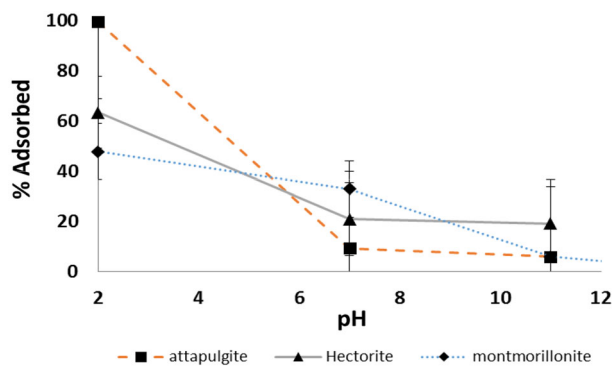
the primary stable-radiolysis products, and taking into account the kinetics and yields of their formation [9].

#### Non-irradiated aqueous samples in the presence of a clay mineral

According to chemical evolution studies, minerals (like clays) may have played an important role, such as by serving as sites for the concentration and catalysis of different reactions or possibly as a protector against external sources of energy for the molecules' adsorbed, for which dilution acts against the local conditions needed for effective prebiotic synthesis. For this reason, as a first step, the adsorption of glyceraldehyde was studied in different clay minerals and at various pH levels. The experiments with clays showed that the adsorption percentage varied for the three types of clay



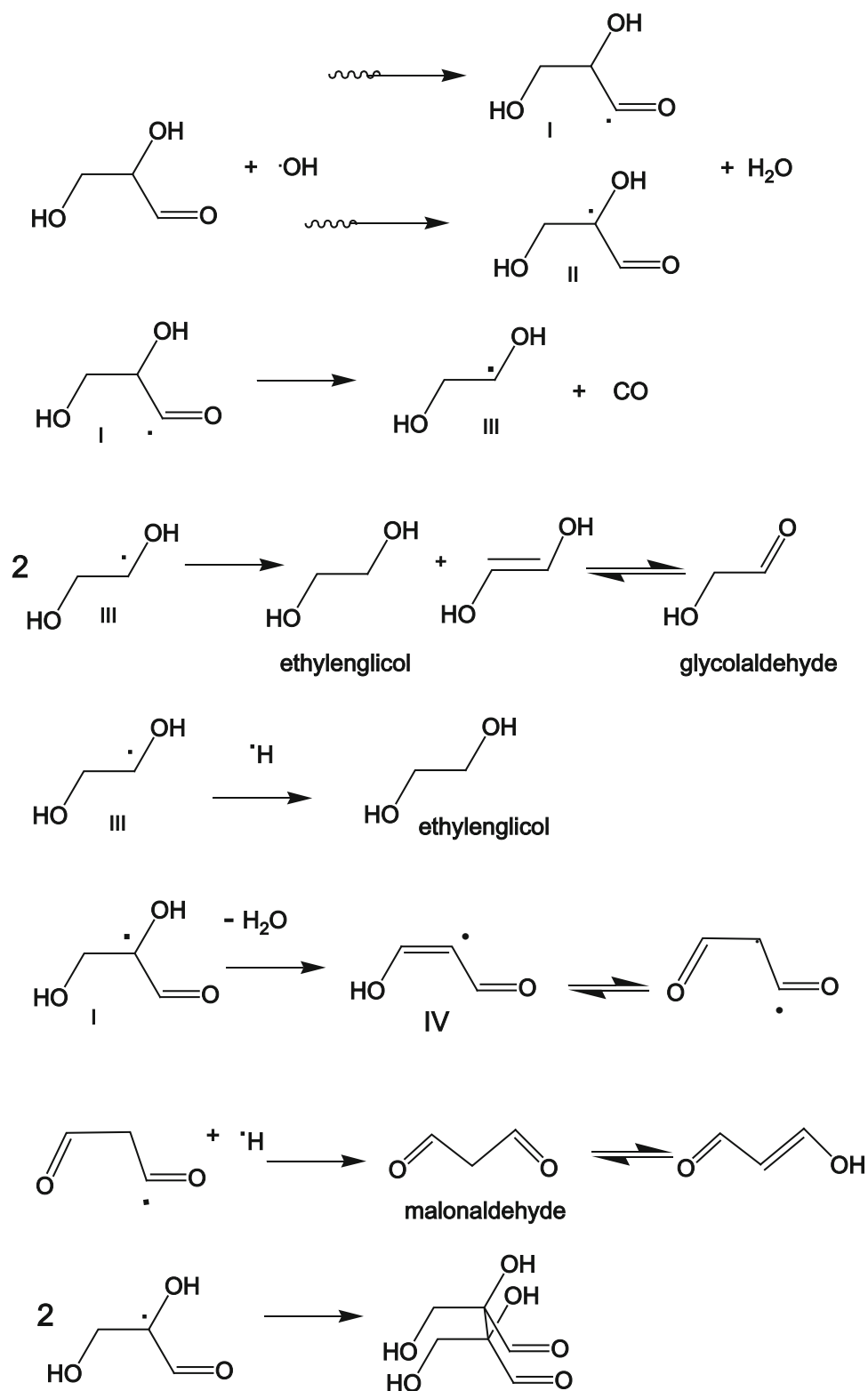
**Fig. 5** EPR spectra of glyceraldehyde irradiated at three temperatures for the same irradiation time



**Fig. 6** Effect of pH on the adsorption of glyceraldehyde ( $1 \times 10^{-2}$  mol/L) in sodium-montmorillonite, attapulgite and hectorite

used. In all cases, the maximum adsorption was at an acid pH (especially so for attapulgite). At alkaline pH, the adsorption was very low. For sodium-montmorillonite, the maximum adsorption was about 48 % at pH 1.5; the adsorption decreased as pH increased (Fig. 6). Organic compounds bind

**Fig. 7** Scheme for the possible mechanism of radiolysis from water radiolysis products



to sodium-montmorillonite in two places: the interlamellar channel and the edges of the crystal [13]. The X-ray diffraction spectrum shows that the binding of glyceraldehyde occurs in the interlamellar channel that expanded from

11.86 to 14.59 Å. The presence of the clay enhances the shift in the maximum absorption of the UV spectrum, which is accompanied by a hypsochromic shift in the peak absorption to 245 nm. This change is probably due to the decomposition

of glyceraldehyde, which is catalyzed by acid sites in the clay, forming malonaldehyde in a way that is similar to what happens with irradiation.

Glycolaldehyde, one of the products detected in this radiolysis, has been identified in interstellar space [14], where it could have been exposed to cosmic radiation and thus generated sugar-like products. Glycolaldehyde, by condensing with formaldehyde via the formose reaction, yields sugars [9, 15, 16]. Glyceraldehyde and other sugars has been detected from the ultraviolet irradiation of interstellar ice analogs [15].

The identification of the products after radiolysis reveals that oxidation is one of the predominant transformations. This process yields oxidized products with unchanged or shorter carbon chains. In the aqueous samples, the water-radiolytic products, mainly  $\cdot\text{H}$  and  $\cdot\text{OH}$ , are responsible for forming the observed products via a secondary attack. The  $\cdot\text{OH}$  radical is a powerful oxidizing agent that is very reactive with aldehydes [17, 18].



The patterns of hydroxyl radicals' reactions with a solute depends on their chemical structures. EPR and other methods have shown that OH's most typical reaction with polyhydroxy compounds is the abstraction of hydrogen atoms bound to carbon [9, 12, 16, 17]. Some possible pathways for the decomposition of DL-glyceraldehyde [9, 12, 18] via water elimination reactions and CO are shown in Fig. 7.

Our results suggest that radiation-induced reactions of glyceraldehyde may yield compounds of biological importance in both terrestrial and extraterrestrial environments.

## Conclusions

The synthesis and preservation of aldoses in prebiotic conditions is fundamental to their role in energetic functions and to the abiotic formation of nucleotides and nucleic acid components (e.g., RNA). On the primitive Earth, clay minerals may have contributed to the concentration, catalysis, or protection of organic compounds such as glyceraldehyde, which is readily absorbed in different clays, especially attapulgitite at acid pH.

Glyceraldehyde is an important molecule in chemical evolution studies. The glyceraldehyde molecule also may be formed in the ice of star-forming clouds—and thus could be a source of sugars carried to Earth on extraterrestrial bodies (such as comets). Glyceraldehyde is unstable under irradiation in aqueous solutions, even at low doses. Radiolytic decomposition forms compounds, including some sugar-like products, so decomposition may be a pathway for the formation of sugars and other compounds that are related to

bioorganic compounds under primitive Earth conditions or in icy bodies. In particular, the formation of glycolaldehyde is important because this compound has been identified in interstellar space; it could thus be an intermediate step along the path to forming more complex molecules.

**Acknowledgments** We acknowledge the support from C001-CONACYT-ANR-188689 and DGAPA Grant IN111116. We thank Benjamin Leal, M.Sc., and Francisco Flores, Phys., for their technical assistance. Finally, we are grateful to the unknown reviewers for their valuable comments.

## References

1. Miller SL, Orgel L (1974) *The origins of life on earth*. Prentice-Hall Inc, Eagle Cliffs
2. Weber AL, Pizzarello S (2006) The peptide-catalyzed stereospecific synthesis of tetroses: a possible model for prebiotic molecule evolution. *PNAS* 103:12713–12717
3. Draganic IG, Draganic ZD, Adloff JP (1990) *Radiation and radioactivity*. CRC Press Inc, Boca Raton
4. Draganic I, Draganic Z (1998) Radiation-chemical approaches to comets and interstellar dust. *J Chim Physique* 85:55–61
5. Mosqueira FG, Albarrán G, Negrón-Mendoza A (1996) A review of conditions affecting the radiolysis due to  $^{40}\text{K}$  on nucleic acid bases and their derivatives adsorbed on clay minerals: implications in prebiotic chemistry. *Origins Life Evol Bios* 26:75–94
6. Negrón-Mendoza A, Albarrán G (1993) In: Chela-Flores J, Ponnampereuma C (eds) *Chemical evolution: origin of life*. Deepak Publishing, Jalandhar, pp 147–235
7. Cataldo F, Ursini O, Angelini G, Iglesias-Groth S, Manchado A (2011) Radiolysis and radioracemization of 20 amino acids from the beginning of the solar system. *Rend Fis Acc Lincei* 22:81–94
8. Draganic IG, Draganic ZD (1971) *The radiation chemistry of water*. Academic Press, New York
9. Kochetkov NK, Kudrjashov LI, Chlenov MA (1979) *Radiation chemistry of carbohydrates*. Elsevier Ltd, Amsterdam
10. Nair V, O'Neil CL, Wang PG (2008) *Malonaldehyde*, encyclopedia of reagents for organic synthesis. Wiley, New York
11. Kwon T, Watts B (1963) Determination of malonaldehyde by ultraviolet spectrophotometry. *J Food Sci* 28:627–630
12. Steenken S, Schulte-Frohlinde D (1973) Fragmentation of radicals derived from glycolaldehyde and glyceraldehyde in aqueous solution. an EPR study. *Tetrahedron Lett* 9:653–654
13. Negrón-Mendoza A, Ramos-Bernal S (2004) In: Seckbach J (ed) *Cellular origin, life in extreme habitats and astrobiology*. Springer, Berlin, pp 181–194
14. Jørgensen JK, Favre C, Bisschop SE, Bourke TL, van Dishoeck EF, Schmalzl M (2012) Detection of the simplest sugar, glycolaldehyde, in a solar-type protostar with ALMA. *Ap JL* 757:L4
15. Meinert C, Myrgorodska I, De Marcellus P, Buhse T, Nahon L, Hoffmann SV, Le Sergeant d'Hendecourt L, Meierhenrich UJ (2016) Ribose and related sugars from ultraviolet irradiation of interstellar ice analogs. *Science* 352:208–212
16. Scherz H (1970) Formation of deoxycompounds and malonaldehyde in irradiated aqueous solutions of carbohydrates and related compounds. *Rad Res* 43:12–24
17. Steenken S (1979) Oxidation of phenolates and phenylenediamines by 2-alkononyl radicals produced from 1, 2-dihydroxy- and 1-hydroxy-2-alkoxyalkyl radicals. *Phys Chem* 83:595–599
18. von Sonntag C (1980) In: Tipson RS, Horton D (eds) *Advances in carbohydrate chemistry and biochemistry*. Academic Press, NY, pp 7–77

# Radiolysis and Thermolysis of Cytosine: Importance in Chemical Evolution

J. CRUZ-CASTAÑEDA<sup>1,2</sup>, A. NEGRÓN-MENDOZA<sup>1\*</sup>

<sup>1</sup>Instituto de Ciencias Nucleares, Universidad Nacional Autónoma de México, UNAM. Cd. Universitaria, A. P. 70-543, 04510 México, D. F. México

<sup>2</sup>Programa de Maestría y Doctorado en Ciencias Químicas, UNAM. Cd. Universitaria, A. P. 70-543, 04510 México, D. F. México

\*Email: negron@nucleares.unam.mx

Published online: August 08, 2016,

The Author(s) 2016. This article is published with open access at [www.chitkara.edu.in/publications](http://www.chitkara.edu.in/publications)

**Abstract** An important aspect of chemical evolution is the study of the stability of organic molecules with biological significance in primitive conditions, especially in the presence of constant energy sources. An example of sets of biologically important organic compounds is nitrogenous bases. The presence of these compounds in prebiotic environments is very important in forming more complex systems, such as nucleic acids, in which nitrogenous bases are an essential component. The aim of the present work is to study the stability of cytosine, a pyrimidine base, in high-radiation fields or at high temperature and to evaluate its recovery. Our results show that the cytosine ( $1 \times 10^{-4}$  M aqueous solution, oxygen-free) decomposed completely at a dose of 22 kGy, and 25% recovery was obtained with a dose of 7.4 kGy. The analysis of irradiated samples was followed by HPLC, HPLC-mass spectrometry and UV-VIS spectroscopy. The main product in both thermolysis and radiolysis was uracil, formed via a deamination reaction. Uracil is another nitrogenous base with biological significance.

**Keywords:** gamma radiation, thermolysis, nitrogenous base, chemical evolution, cytosine.

## 1. INTRODUCTION

The study of the origin of life has been divided into three main stages: chemical evolution, pre-biological evolution and biological evolution [3]. Chemical evolution is defined as the series of physical and chemical processes that led

Journal of Nuclear  
Physics, Material  
Sciences, Radiation and  
Applications  
Vol-4, No-1,  
August 2016  
pp. 183–190



---

Cruz-Castañeda, J. to the abiotic formation of organic compounds of biological importance. To  
Negrón-Mendoza, A. gain insight into these processes, laboratory simulations are carried out under  
conditions that likely existed on early Earth. The objective of these kinds of  
experiments is to find possible mechanisms by which organic molecules were  
formed and increased their complexity [4, 8, 10]. In addition, the stability of  
the products synthesized in the prevailing environment [6] is also a relevant  
topic in chemical evolution.

---

An important aspect of chemical evolution is energy sources, since energy  
is responsible for starting, promoting and directing all physicochemical  
processes. Several energy sources could plausibly have contributed to chemical  
evolution [5], including radiation and thermal energy [2, 7, 11-12].

Particularly for nitrogenous bases, cytosine is an important molecule in  
biological systems. It is part of nucleic acid molecules, which are responsible  
for storing and transmitting genetic information in living organisms, as well  
as part of energetic molecules, such as CTP and CDP. However, despite its  
importance in prebiotic environments, few articles deal with the stability of  
this compound under possible prebiotic conditions, particularly with high  
radiation fields or at high temperatures. Therefore, it is necessary to have a  
balance between the formation and destruction of these molecules to have  
them available for further use [6].

This work focuses on the stability of cytosine in aqueous solution under high  
temperatures and gamma irradiation fields. The present study contributes to a  
better understanding the behavior and stability of organic compounds of biological  
importance by simulating chemical reactions in a primitive environment.

## **2. EXPERIMENTAL**

### **2.2 Chemicals and materials**

All of the chemicals were purchased from Sigma Aldrich Co., USA and were  
of the highest purity (cytosine, uracil, ammonium acetate and formic acid). The  
HPLC-grade solvents (water and methanol) were purchased from Honeywell  
Burdick & Jacson (NJ, USA). The glassware was treated with a warm mixture  
of HNO<sub>3</sub> and H<sub>2</sub>SO<sub>4</sub> for 20 minutes, followed by a wash with distilled water  
and heating in an oven at 300 °C overnight. All of the chemical and glassware  
were handled to minimize contamination [9].

### **2.2 Preparation of samples**

A standard stock solution of cytosine 1x10<sup>-4</sup> M was prepared using triple  
distilled [1, 9] and deionized, oxygen-free water by bubbling Ar for 20

minutes. Then, 10 mL of the solution was placed in culture tubes and sealed for the irradiation experiments, and 1 mL was placed in glass vials and sealed, for experiments with thermal energy. All of the solutions were stored in a refrigerator at 4 °C when not in use.

### 2.3 Irradiation of Samples

The samples were irradiated at room temperature by a high-intensity  $^{60}\text{Co}$  gamma source (Gammabeam 651 PT) at ICN-UNAM at different doses (0 to 22 kGy) and a dose rate of 248 Gy/min. The dose was evaluated using a ferrous sulfate–copper sulfate dosimeter [13]. The samples were analyzed immediately after irradiation.

### 2.4 Thermolysis experiments

The aqueous solutions of cytosine were heated in a Parr Reactor 4838 in glass vials at 92 °C at different times (0 to 1,026 hours) and at 1 bar pressure. Afterward, the samples were cooled at room temperature and immediately analyzed by a liquid chromatographic/mass spectrometry system.

### 2.5 Analysis of samples

#### 2.5.1 LC-ESI-MS analysis

Liquid chromatographic analysis was performed on an HPLC system (515-pump from Waters Corp.) coupled with a Single Quadrupole Mass Detection system (SQ-2 manufactured by Waters Corp.), with an electrospray ionization positive mode (ESI+) source. Analysis was done within 5.0 min in Symmetry C18 column (4.6 x 75 mm, 3.5  $\mu\text{m}$  spherical particle size, by Waters Corp.) under an isocratic elution of mobile phase (0.2 M ammonium acetate solution; 80% methanol, 20% water at pH=4) at a constant flow of 0.4 mL/min. A definite sample volume (20  $\mu\text{L}$ ) was injected using a loop.

#### 2.5.2 UV spectrophotometry analysis

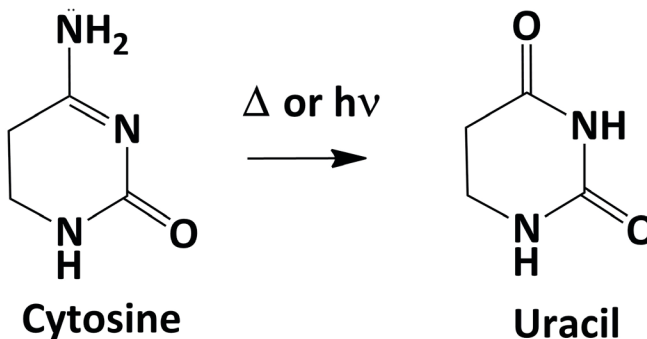
UV analysis was performance at 258 nm for uracil and 267 nm for cytosine in a Varian Cary 100 Scan Spectrophotometer using a using a 1-cm quartz cell at room temperature.

## 3. RESULTS

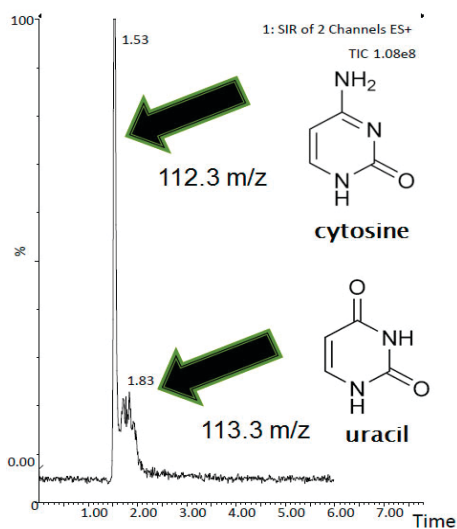
The principal reaction of the thermolysis and irradiation experiments with cytosine in aqueous solution ( $1 \times 10^{-4}$  M) was the deamination of the pyrimidine base to generate another pyrimidine base: uracil (Figure. 1).



Cruz-Castañeda, J.  
Negrón-Mendoza, A.



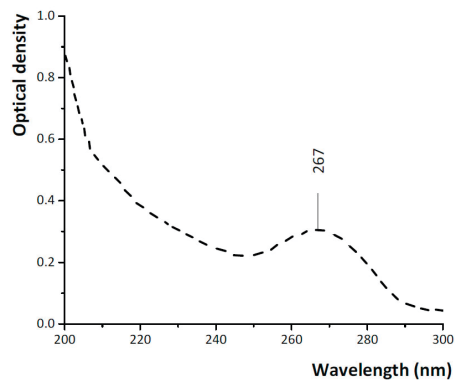
**Figure 1:** Deamination reaction of cytosine.



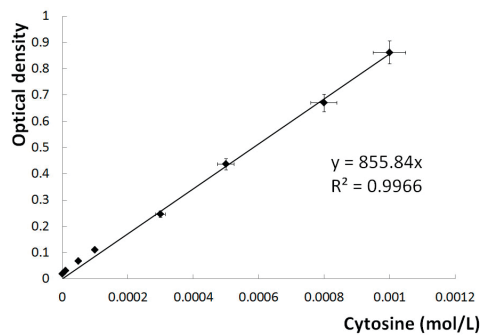
**Figure 2:** HPLC-MS analysis of cytosine.

As the principal method of decomposition identified by HPLC and MS fragmentation spectra (Figure 2), cytosine decomposition was quantified by UV spectrophotometry at 267 nm (Figure 3), with experimental  $\epsilon_{267} = 855.84 \text{ mol}^{-1} \text{ L cm}^{-1}$  (Figure 4).

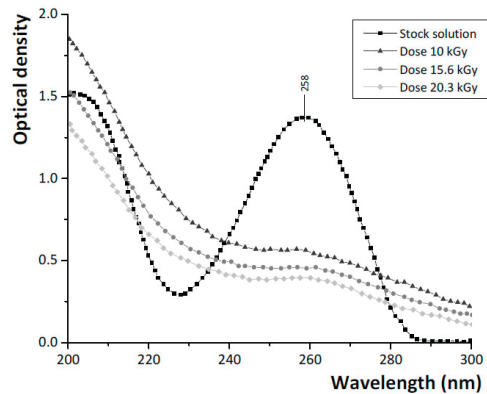
Uracil formation was quantified by UV spectrophotometry at 258 nm. Uracil formation is dose dependent, since increases in the dose showed formation of the pyrimidine base (Figure 5).



**Figure 3:** UV analysis of cytosine at 267 nm.



**Figure 4:** Cytosine decomposition quantified by UV.



**Figure 5:** UV analysis of uracil at 258 nm.

---

Cruz-Castañeda, J.  
Negrón-Mendoza, A.

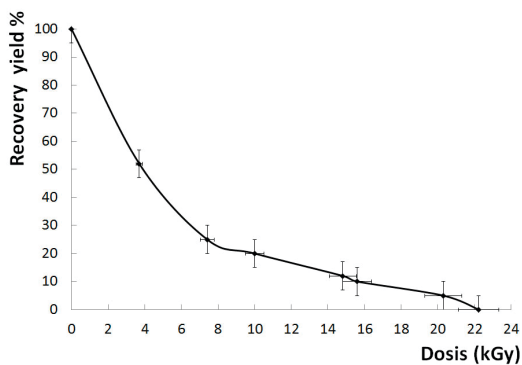
### 3.1 Gamma irradiation experiments

Cytosine decomposition was dose dependent, since with increases in the dose showed high decomposition of the pyrimidine base (Figure 6). The radiolysis showed that the cytosine ( $1 \times 10^{-4}$  M aqueous solution, oxygen free) decomposed completely at a dose of 22 kGy, while 75% decomposed with a dose of 7.4 kGy.

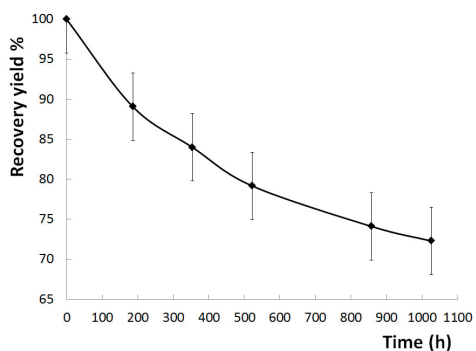
#### *Thermolysis experiments*

---

The main thermolysis product of cytosine in aqueous solution ( $1 \times 10^{-4}$  M) at 92 °C was uracil. The thermolysis reaction is time dependent; after 1,026 hours of heating, the recovery was 72%. Figure 7 shows the evolution of cytosine decomposition as a function of time. The possible reaction mechanism for the thermolysis is showed in figure 8.

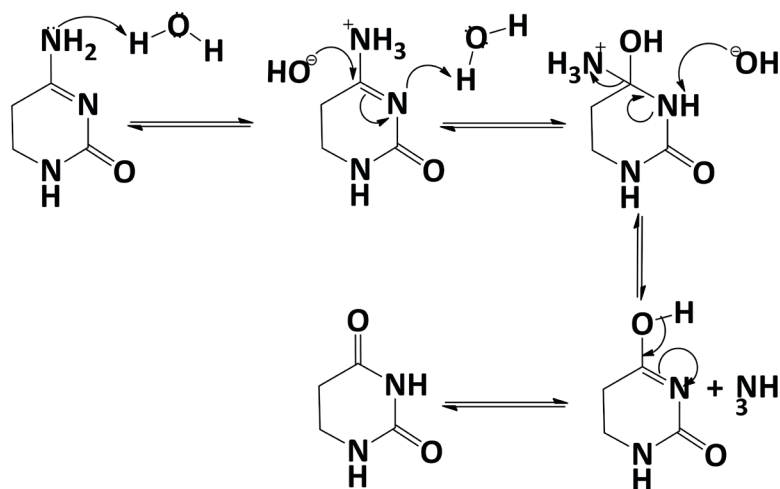


**Figure 6:** Decomposition of cytosine as a function of absorbed dose.



**Figure 7:** Dependence of cytosine deamination on time.

---



Radiolysis and  
Thermolysis  
of Cytosine:  
Importance in  
Chemical Evolution

**Figure 8:** Suggested mechanism for the formation of uracil from cytosine thermolysis.

#### 4. REMARKS

Despite the importance of nucleic acid bases in the prebiotic environment, there have been few reports on the stability of these types of compounds. Considering that the dose rate of high-radiation energy sources in the primitive Earth was low, the results presented in this paper show that cytosine in an aqueous medium was relatively stable under gamma irradiation or high temperatures, with a good yield of recovery, and its decomposition produced was another pyrimidine base. This behavior is a distinctive advantage of these types of molecules because they needed to survive to form more complex ones. The role of energy in the early Earth during the period of chemical evolution must have been important for the reactions, inasmuch as the energy was responsible for starting, promoting and directing all physicochemical processes. Many authors have proposed different energy sources on the early Earth. However, it cannot be said that one of them was the principal source; rather, only the participation of all possible sources may have contributed to the synthesis of the majority of organic compounds with biological significance.

#### 5. ACKNOWLEDGMENTS

This work was supported by PAPIIT grant No. IN111116 and the CONACyT Grant No.168579 J.C was supported by a CONACyT fellowship and the Posgrado en Ciencias Químicas, UNAM.

---

Cruz-Castañeda, J.  
Negrón-Mendoza, A.

## REFERENCES

- [1] Draganic, I. G. & Draganic Z. D. The radiation chemistry of water. New York: Academic Press, (1971).
- [2] Draganic I. G., Draganic Z. D. & Adloff J. P. Radiation and radioactivity. Boca Raton, Florida USA: CRC Press Inc., (1990).
- [3] Lemmon, R. M. Chemical evolution. *Chemical Reviews*, **70(1)**, 95-109, (1970). <http://dx.doi.org/10.1021/cr60263a003>
- [4] Meléndez, L. A., Ramos, B. S., & Ramírez, V. M. L. Stability of guanine adsorbed in a clay mineral under gamma irradiation at temperatures (77 and 298 K): Implications for chemical evolution studies. *AIP Conference Proceedings*, **1607**, 111-115, (2014). <http://dx.doi.org/10.1063/1.4890710>
- [5] Miller, S. & L. Orgel The origins of life on the Earth. New Jersey: Prentice-Hall., (1974). <http://dx.doi.org/10.1007/BF00927019>
- [6] Muller, A. W. J. & D. Schulze-Makuch. Thermal Energy and the Origin of Life. *Origins of Life and Evolution of Biospheres*, **36(2)**, 177-189 (2006). <http://dx.doi.org/10.1007/s11084-005-9003-4>
- [7] Negrón-Mendoza, A. & G. Albarran. Chemical effects of ionizing radiation and sonic energy in the context of chemical evolution. En: *Chemical Evolution. Origin of life*, 147-235 (1993).
- [8] Negrón, M. A. & Ramos, B. S. Chemical Evolution in the Early Earth. In *Astrobiology: Origins from the Big-Bang to Civilization*, Kluwer Academic Publishers, (pp. 71-84), (2000). Venezuela: Caracas.
- [9] O'Donnell, J. H. & Sangster, D. F. Principles of radiation chemistry. United Kingdom: Hodder & Stoughton Educ, (1970).
- [10] Perry, R. S. & Kolb, V. M. On the applicability of Darwinian principles to chemical evolution that led to life. *International Journal of Astrobiology*, **3(01)**, 45-53 (2004). <http://dx.doi.org/10.1017/S1473550404001892>
- [11] Russell, M. J. & Hall, A. J. The Hydrothermal Source of Energy and Materials at the Origin of Life. *Chemical Evolution II: From the Origins of Life to Modern Society*, American Chemical Society, **1025**, 45-62, (2009).
- [12] Russell, M. J., A. J. Hall, et al. Serpentinization as a source of energy at the origin of life. *Geobiology*, **8(5)**, 355-371 (2010). <http://dx.doi.org/10.1111/j.1472-4669.2010.00249.x>
- [13] Spinks, J.W.T., & Woods, R. J. Introduction to Radiation Chemistry. New York, John Wiley and Sons, Inc., (1990).

# Chemical evolution studies: the radiolysis and thermal decomposition of malonic acid

J. Cruz-Castañeda · A. Negrón-Mendoza ·  
D. Frías · M. Colín-García · A. Heredia ·  
S. Ramos-Bernal · S. Villafañe-Barajas

Received: 7 September 2014 / Published online: 2 November 2014  
© Akadémiai Kiadó, Budapest, Hungary 2014

**Abstract** In the context of chemical evolution a simulation of a hydrothermal vent was performed. The thermolysis and radiolysis of malonic acid in aqueous solution were studied. The thermolysis was done by heating the samples (95 °C) and radiolysis using gamma radiation. Products were identified by gas chromatography and gas chromatography–mass spectrometry. The thermal treatment produced acetic acid and CO<sub>2</sub>. The radiolysis experiments yield carbon dioxide, acetic acid, and di- and tricarboxylic acids. A theoretical model of the chemical process occurring under irradiation was developed; this was able to reproduce formation of products and the consumption of malonic acid.

**Keywords** Malonic acid · Radiolysis · Thermolysis · Chemical evolution

## Introduction

Chemical evolution encompasses the study of physical and chemical events leading to the formation of biologically

relevant molecules. This process is considered a preamble for the emergence of living forms [1, 2]. The early Earth was extremely dynamic and chemically complex due to the existence of different environments (the atmosphere, lithosphere and hydrosphere and the interfaces among them). All those environments were important for the chemical evolution that made the scenario more complex. For chemical processes, an energy source was also necessary. Several energy sources could plausibly have contributed to chemical evolution [3], including high-energy radiation [4, 5] and thermal energy [6–8].

On Earth, many environments, such as volcanic hot springs and in hydrothermal vents (black and white) on the bottom of the ocean, present temperature gradients, which allow the synthesis of organic molecules in these locations. In the 1970s, hydrothermal vents were discovered, and scientists have proposed that these systems could have been plausible geological sites for the origin of life [9–15]. However, there is an intense debate regarding the possible contribution of these systems to chemical evolution [16]. White vents are distant from the ascending magma that heats the fluids, and they do not reach the temperatures present in black smokers, approximately 300 °C, where most organic compounds can be altered. In white vents, the vent fluids are at 40–90 °C, and water is heated by convection currents that originate from hot rocks underneath [17]. Baross and Hoffman [18] have suggested that submarine hydrothermal vents are contemporary geological environments that can be classified as truly primeval because of their nature as a source of gases and dissolved elements for both Achaean oceans and modern ones.

In addition to thermal energy in these environments, radionuclides are also present as local sources of chemical activity contributing to the synthesis and/or degradation of chemical compounds. Therefore, radioactivity should have

---

J. Cruz-Castañeda · A. Negrón-Mendoza (✉) · A. Heredia ·  
S. Ramos-Bernal · S. Villafañe-Barajas  
Instituto de Ciencias Nucleares, Universidad Nacional  
Autónoma de México, Ciudad Universitaria, D.F.,  
A.P. 70-543, Mexico, DF, Mexico  
e-mail: negron@nucleares.unam.mx

D. Frías  
Departamento de Ciências Exatas e Tecnológicas, Universidade  
do Estado da Bahia, Salvador, Brazil

M. Colín-García  
Instituto de Geología, Universidad Nacional Autónoma de  
México, C.P. 04510, Mexico, DF, Mexico

been important in the early Earth, since the levels of radioactivity were much higher than the present value, for example,  $^{40}\text{P}$  is still dissolved in the oceans [4, 19].

Malonic acid is an important molecule in chemical evolution studies, because it can yield by chemical reactions, products related to metabolism, such as acetic, citric and succinic acids, and it might serve as an inhibitor of important metabolic pathways. The synthesis of malonic acid has been previously reported in several prebiotic experiments such as those performed by Miller and Urey [20, 21] in their classic experiments with electric discharges. Both, gamma radiolysis [22] and photolysis of acetic acid [23] generate malonic acid in relatively high yields. Furthermore, dicarboxylic acids have been detected in carbonaceous chondrites such as the Murchison meteorite [24]. For this reason, the radiation chemistry and thermolysis of malonic acid is important in chemical evolution studies.

Our aim is to study the radiolysis and thermolysis of malonic acid in aqueous solution, simulating chemical reactions occurring in a primordial hydrothermal system. Malonic acid was chosen because it is readily formed in several prebiotic experiments, because it is also present in natural samples as meteorites, and because its decomposition generates other polycarboxylic acids of biological importance such as molecules present in metabolic processes (i.e., Krebs cycle).

## Experimental procedure

### Chemicals

All the chemicals used were of the highest purity available. Malonic acid and other acids used as standards were purchased from Sigma-Aldrich Chemical Company (USA). The water was triple distilled according to standard techniques in radiation chemistry [25, 26].

### Preparation of samples

The aqueous solutions of malonic acid were 0.01–0.1 mol dm<sup>-3</sup>. The solutions were at a natural pH (2.4), except in certain competition experiments where the pH was adjusted by adding HClO<sub>4</sub>. The oxygen was removed by bubbling argon through the solutions.

### Irradiation

The irradiations were conducted at room temperature (22 °C) using a high-intensity  $^{60}\text{Co}$  gamma source (Gammabeam 651-PT, at ICN-UNAM). The absorbed doses were from 0.3 to 300 kGy (dose rate of 13 kGyh<sup>-1</sup>). The

dosimetry of the source was performed by a ferrous sulfate–cupric sulfate dosimeter [25, 26]. For the gas analysis, the samples were irradiated in a Gammacell 200 unit at 0.2 kGyh<sup>-1</sup>. The doses were from 3 to 160 kGy. This source, with low dose/rate value was used mainly for the analysis of gaseous products that can be better analyzed at low doses.

### Thermal treatment

Sealed tubes containing malonic acid were used for the thermal decomposition experiments. The thermolysis of malonic acid was studied in a static system at temperatures up to 95 °C for different periods from 0.5 to 192 h, simulating a white hydrothermal vent. After heating, they were immediately analyzed.

### Analysis of products

The gas products were analyzed using a Töepler pump according to Negrón-Mendoza et al. [27]. For the non-volatile products, a measured amount of the irradiated solutions was evaporated to dryness. Next, methyl esters were prepared according to Negrón-Mendoza et al. [28]. The analysis was performed in a gas chromatograph HP-5890 (Hewlett-Packard, USA) using a glass column (1.82 m in length and an internal diameter of 4 mm) packed with Silar 7C (Supelco Co., USA). The identification of the products was based on their retention times in gas chromatography (GC), co-injections with standards and by their fragmentation pattern in mass spectrometry (MS). For the GC–MS analysis, an HP-5890 (Hewlett-Packard, USA) gas chromatograph was coupled to a mass spectrometer HP model 5970. The separation was performed in a capillary column of methyl silicon (12 m in length and 0.33 μm of inner diameter). For the acetic acid analysis, a SRI 8610C gas chromatograph equipped with a capillary column was used. The column was MXT (length 30 m) with an isothermal regimen of 130 °C.

### Computational framework for radiation-induced reactions

The model was developed using Scilab ([www.scilab.org](http://www.scilab.org)), which is a free, open-source software package that provides a platform for diverse scientific computations (French National Institute for the Research in Computer Science and Control, INRIA).

The chemical reactions are translated to differential equations creating a model that describes the closed domain kinetics of a reaction mechanism. The model consists of a system of nonlinear ordinary differential equations (ODE); that is, all the equations must be solved

simultaneously [29]. The program reads a formatted file containing the list of chemical species, as well as the reaction constants and stoichiometric constants for each feasible reactions of two, not necessarily different, reactants. With those data, it constructs a 2-dimensional matrix representing the right-hand side (RHS) of the differential equations, one line for each chemical species to be computed. By evaluating, the RHS at each integration time-step the time derivative of the molar concentrations of the chemical species are calculated, allowing then estimating the current molar concentration, using such time derivatives and their previous concentrations.

More specifically, one differential equation consists of a mass balance for a single species, which predicts the expected change in the molar concentration of the species over time. All the reaction rates leading to the production (source term) and destruction (sink terms) of the given species must be considered. In choosing the species to be included in the overall mass balance for simulation purposes, two criteria were considered: (a) the species must react with at least one of the other species, and the reaction, whatever its rate, must lead to the production or consumption of a certain species; and (b) the species concentration is monitored as the experiment progresses. Therefore, for the species involved in the reaction mechanism, we included a differential equation of the general form:

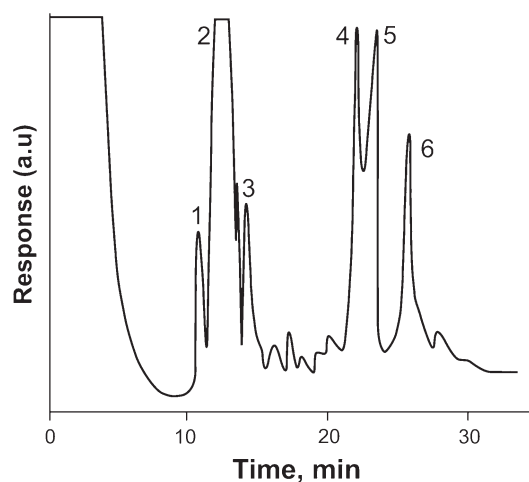
$$\frac{d\chi_i(t)}{dt} = f_i + \sum_n \sum_m \aleph_{n,m}^{(i)} \chi_n(t) \chi_m(t) - \chi_i(t) \sum_j \aleph_{i,j}^{(i)} \chi_j(t), \quad (1)$$

where  $\chi(t)$  denotes the molar concentration at time  $t$  of the  $i$ -th species, based on the numbering of the species, and the first term in the RHS,  $f_i$ , is its yield-by-radiolysis; that is, the number of molecules of species  $i$  produced by the radiolysis process by a unit of radiation energy absorbed by the medium. The second and third terms in the RHS of Eq. (1) are the internal production rate and consumption rate, respectively. In these terms,  $\aleph$  denotes the rate constant for the reaction of the two species indicated by its double subscript that produces or consumes the species indicated by its superscript. In these calculations, we only included reactions with reported rate constants. A more detailed description of the method can be found in Sanchez-Mejorada et al. [30].

## Results and discussion

### Radiolysis of malonic acid in aqueous medium

The pH of the solutions was naturally acidic, and in this condition, the  $e_{aq}^-$  formed by the radiolysis of water was



**Fig. 1** Gas chromatogram of methyl esters of carboxylic acids formed by the irradiation of malonic acid at 10 kGy. 1 oxalic, 2 malonic, 3 succinic, 4 2,3 dicarboxy-succinic, 5 tricarballic, and 6 citric acids

**Table 1** Estimated  $G^\circ$  values for the gaseous products from the radiolysis of malonic acid ( $0.1 \text{ mol dm}^{-3}$ )

Compound	$G^\circ$
H <sub>2</sub> (pH 1 HClO <sub>4</sub> adjusted)	3.5
H <sub>2</sub> (pH 2.4)	2.1
CO	0.03
CO <sub>2</sub>	2.9

$G$  number of molecules formed for 100 eV given to the system

converted ( $\sim 98\%$ ) into a  $\bullet\text{H}$  radical by a reaction with  $\text{H}_3\text{O}^+$ .



The concentration of malonic acid was sufficiently high to ensure complete scavenging of  $\bullet\text{OH}$  and  $\bullet\text{H}$  radicals. At pH of 2, approximately 88 % of the malonic acid is in an undissociated form, which is known to react efficiently with the radiolytic products of water ( $\bullet\text{H}$ ,  $\bullet\text{OH}$  and  $e_{aq}^-$ ) with  $k_{\text{H}} = 4.2 \times 10^5 \text{ dm}^3 \text{ mol}^{-1} \text{ s}^{-1}$ ,  $k_{\text{OH}} = 2.6 \times 10^7 \text{ dm}^3 \text{ mol}^{-1} \text{ s}^{-1}$ , and  $k_{e_{aq}^-} = 1.45 \times 10^9 \text{ dm}^3 \text{ mol}^{-1} \text{ s}^{-1}$  [31]. The yield of molecular hydrogen at a pH 2.4 was 2.1, which shows that, in addition to the reaction of  $\text{H}_3\text{O}^+$  with  $e_{aq}^-$ , it also reacts with malonic acid because it is known that the undissociated forms of carboxylic acids react with  $e_{aq}^-$  [31]. The gas analysis indicated the formation of H<sub>2</sub> and CO<sub>2</sub>. The yield of molecular hydrogen was measured at two different pH values. Only traces of CO were detected. For non-volatile radiolytic products, chromatograms obtained at different radiation doses revealed the presence of several carboxylic acids (Fig. 1). An analysis of the non-volatile radiolytic products showed that they increased in



**Table 2** Estimated  $G^\circ$  values for the non-volatile products from the radiolysis of malonic acid

Compound	$G^\circ$
Acetic acid	2.97
Oxalic acid	0.0
	1
Malonic acid (target)	6.0
Succinic acid	0.1
Carboxysuccinic acid	
Tricarballic acid	0.03
1,2,4-Butanetricarboxylic acid	
2,2,3,3-Ethanetetracarboxy acid	1.6
Citric acid	0.08
1,2,3,4-Butanetetracarboxylic acid	0.03

$G$  number of molecules formed for 100 eV given to the system

molecular weight with respect to the target compound. This result suggests that dimerization/condensation reactions occurred. The main product was a result of an  $\cdot\text{H}/\cdot\text{OH}$  abstraction reaction yielding  $\alpha,\alpha$ -dicarboxy methyl radical ( $\cdot\text{CH}(\text{COOH})_2$ ), that reacted further to produce the observed products. The non-volatile acids formed are as follows: 2,3 dicarboxy-succinic, the dimeric product  $(\text{HOOC})_2\text{-CH-CH-}(\text{COOH})_2$ , oxalic  $(\text{HOOC-COOH})$ , succinic  $(\text{HOOC-CH}_2\text{-CH}_2\text{COOH})$ , carboxy-succinic  $(\text{HOOC})_2\text{-CH-CH}_2\text{-COOH}$ ,

tricarballic  $(\text{HOOC-CH}_2\text{-CH}(\text{COOH})\text{-CH}_2\text{COOH})$ , and citric  $(\text{HOOC-CH}_2\text{-C}(\text{OH})(\text{COOH})\text{-CH}_2\text{COOH})$ .

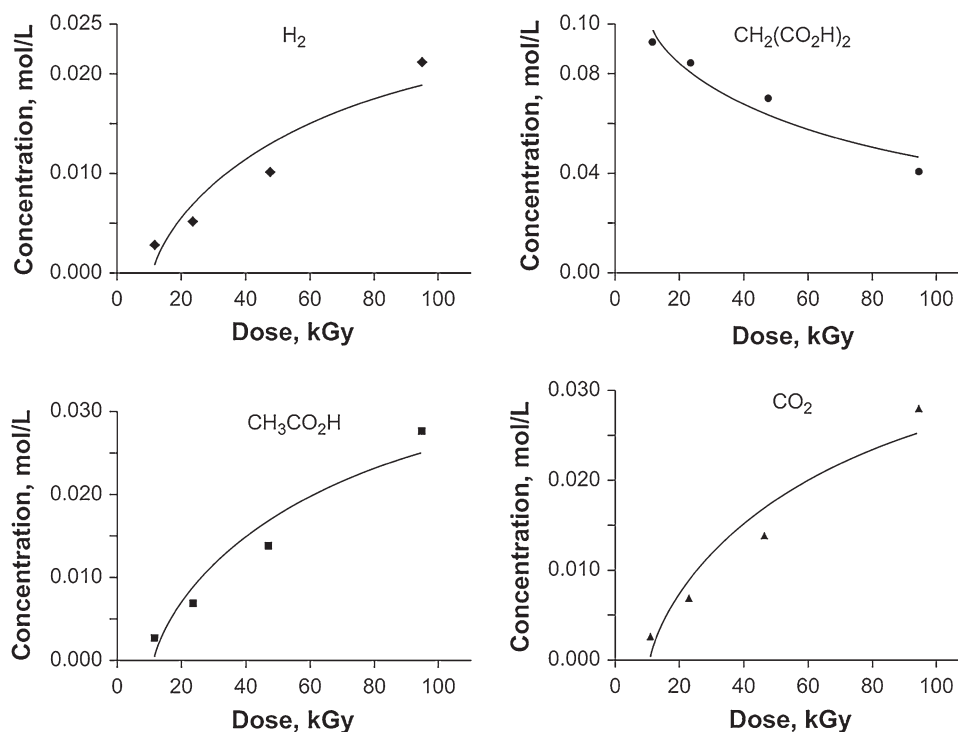
Changes in the concentration of malonic acid show the same distribution of products. Table 1 summarizes the detected gaseous products, and Table 2 the yield of the non-volatile products formed. Within the limits of accuracy for the determination of products, the observed yield of decomposition corresponded to water molecules that had undergone radiolysis. Figure 2 shows the formation of the radiolytic products from malonic acid as a function of the absorbed dose.

### Computational modeling

The results for the mathematical model via water radiolysis showed an exponential relationship between concentration of products and dose at high dose. At low doses (10–50 kGy), results might be better fitted to a straight line, at these conditions the radiolytic behavior is simpler since products do not participate in secondary reactions. These findings allowed for the study of the effect of dosage in such contexts only in the case where the rate constant was known.

A survey of the radiolytic products and their yields (determined by plotting the number of molecules formed/destroyed by 100 eV, called  $G$  value, vs. dose) enabled us to consider one of some possible pathways for their formation (Figs. 3, 4). However, further studies are required

**Fig. 2** Formation of some products from the radiolysis of malonic acid ( $0.1 \text{ mol dm}^{-3}$ ). The lines correspond to the calculated values, and the symbols to the experimental points





These radiation chemistry approaches are particularly encouraging by the possibilities offered by the existence of natural nuclear reactors on the Precambrian Earth [39] and by the chemical action of both cosmic rays and radioactive materials in terrestrial and extraterrestrial environments [4]. Additionally, the action of ionizing radiation in malonic acid aqueous solution is accompanied by the formation of various products. The main products of the radiolysis were carbon dioxide, acetic acid, and di- and tricarboxylic acids such as 2,3 dicarboxy-succinic, succinic, carboxy-succinic, tricarballic and citric acids, and the yield of formation of carboxylic acids was estimated. The accuracy of the theoretical and the experimental results suggests that the mathematical simulation is reliable for predicting the behavior of irradiated, simple, diluted aqueous solutions. Finally, we should remark that the kinetic model is very simple, and the numerical solver is robust, making it attractive for its use in different systems.

The present study of radiolysis of malonic acid contributes to a better understanding of the radiolytic behavior of dicarboxylic acids at large doses. It shows the formation of larger molecules formed by dimerization/condensation-type reactions that are important for chemical evolution. These types of reactions could have occurred in primitive hydrothermal vents.

The experiments of thermolysis show that although malonic acid is relatively stable at temperatures of approximately 90–100 °C, (typical temperature in white smokers) the synthesis of potential biologically relevant molecules may occur, for example the formation of acetic acid.

The results obtained in this research show that energy sources, thermal and radiation, generate important prebiotic molecules. This suggests that the action of both in hydrothermal vents could have generated a complex chemical system favoring the production of organics. Of course, it is necessary to continue the experiments and to explore the effect of both energy sources acting synergistically in order to have a better model.

**Acknowledgments** PAPIIT Grant No. IN110712 and CONACYT Grant No. 168579 supported this work. JCC was supported by a CONACYT fellowship. The support of the “Posgrado en Ciencias Químicas” through the invitation to Prof. D. Frías is acknowledged. We also thank C. Camargo, B. Leal and F. Flores for their technical support. We thank to the reviewers for their very useful comments and suggestions to improve the manuscript.

## References

- Perry RS, Kolb VM (2004) On the applicability of Darwinian principles to chemical evolution that led to life. *Int J Astrobiol* 3(1):45–53
- Negrón-Mendoza A, Ramos-Bernal S (2000) In: Chela-Flores J, Lemarchand G, Oró J (eds) *Astrobiology: origins from the Big Bang to civilization*. Kluwer Academic Publisher, Dordrecht, pp 71–84
- Miller SL, Orgel L (1974) *The origins of life on earth*. Prentice-Hall, Inc., Eagle Cliffs
- Draganic IG, Draganic ZD, Adloff JP (1990) *Radiation and radioactivity*. CRC Press Inc, Boca Raton
- Negrón-Mendoza A, Albarrán G (1993) In: Ponnampereuma C, Chela-Flores J (eds) *Chemical evolution: origin of life*. Deepak Publishers, Hampton, pp 147–235
- Muller AWJ, Schulze-Makuch D (2006) Thermal energy and the origin of life. *Orig Life Evol Biosph* 36:177–189
- Russell MJ, Hall AJ (2009) A hydrothermal source of energy and materials at the origin of life. *Chemical evolution II: from origins of life to modern society*. American Chemical Society, Washington, DC, pp 45–62
- Russell MJ, Hall AJ, Martin W (2010) Serpentinization and its contribution to the energy for the emergence of life. *Geobiology*. doi:10.1111/j.1472-4669.2010.00249.x
- Corliss JB, Baross JA, Hoffman SE (1981) An hypothesis concerning the relationship between submarine hot springs and the origin of life on Earth. *Oceanol Acta* 4:59–69
- Wächtershäuser G (1988) Before enzymes and templates: theory of surface metabolism. *Microbiol Rev* 52:452–484
- Holm NG, Charlou JL (2001) Initial indications of abiotic formation of hydrocarbons in the rainbow ultramafic hydrothermal system, Mid-Atlantic Ridge. *Earth Planet Sci Lett* 191:1–8
- Holms N, Andersson E (2005) Hydrothermal simulation experiments as a tool for studies of the origin of life on earth and other terrestrial planets: a review. *Astrobiology* 5(4):444–460
- Martin W, Baross J, Kelley D, Russell MJ (2008) Hydrothermal vents and the origin of life. *Nat Rev Microbiol* 6:805–814
- Wächtershäuser G (2010) In: Barton LL, Mandl M, Loy A (eds) *Geomicrobiology: molecular and environmental perspective*. Springer, Dordrecht
- Stüeken EE, Anderson RE, Bowman JS, Brazelton WJ, Colangelo-Lillis J, Goldman AD, Som SM, Baross JA (2013) Did life originate from a global chemical reactor? *Geobiology* 11(2): 101–126
- Miller SL, Bada JL, Friedmann N (1989) What was the role of submarine hot springs in the origin of life? *Orig Life Evol Biosph* 19:536–537
- Kelley DS, Karson JA, Früh-Green GL, Yoerger DR, Shank TM et al (2005) A serpentinite-hosted ecosystem: the Lost City hydrothermal field. *Science* 307:1428–1434
- Baross JA, Hoffman SE (1985) Submarine hydrothermal vents and associated gradient environments as sites for the origin and evolution of life. *Orig of Life* 15:327–345
- Draganic I, Bjergbake E, Draganic Z, Sehested K (1991) Decomposition of ocean waters by <sup>40</sup>K radiation 3800 Ma ago as a source of oxygen and oxidizing species. *Precambrian Res* 52: 337–345
- Miller S (1953) A production of amino acids under possible primitive Earth conditions. *Science* 117:528–529
- Miller S, Urey H (1959) Organic compound synthesis on the primitive Earth. *Science* 130:245–251
- Negrón-Mendoza A, Ponnampereuma C (1978) In: Noda H (ed) *Origins of life*. Center of Scientific Publications, Tokyo, pp 101–104
- Negrón-Mendoza A, Ponnampereuma C (1982) Prebiotic formation of higher molecular weight compounds from the photolysis of aqueous acetic acid. *Photochem Photobiol* 36:595
- Lawless JG, Zeitman B, Pereira WE, Summons RE, Duffield AM (1974) Dicarboxylic acids in the Murchison meteorite. *Nature* 251:40–42
- O'Donnell JHO, Sangster DF (1970) *Principles of radiation chemistry*. Elsevier, New York

26. Draganic ID, Draganic ZD (1971) The radiation chemistry of water. Academic Press, New York
27. Negrón-Mendoza A, Castillo S, Torres JL (1984) Micro-determinación de gases disueltos en soluciones acuosas por cromatografía de gases (in Spanish). *Rev Soc Quím Mex* 28:21–24
28. Negrón-Mendoza A, Draganic Z, Navarro R, Draganic IG (1983) Aldehydes, ketones and carboxylic acids formed radiolitically in aqueous solutions of cyanides and nitriles. *Radiat Res* 95:248–261
29. Shampine LF (1994) Numerical Solution of Ordinary Differential Equations. Chapman and Hall, New York
30. Sanchez-Mejorada G, Frias D, Negrón-Mendoza A, Ramos-Bernal S (2008) A comparison between experimental results and a mathematical model of the oxidation reactions induced by radiation of ferrous ions. *Radiat Meas* 43:287–290
31. Simic M, Neta P, Hayon E (1969) Pulse radiolysis of aliphatic acids in aqueous solutions. II. Hydroxy and polycarboxylic acids. *J Phys Chem* 73:4214–4219
32. Sagstuen E, Lund A, Itagaki Y, Maruani J (2000) Weakly coupled proton interactions in the malonic acid radical: single crystal ENDOR analysis and EPR simulation at microwave saturation. *J Phys Chem A* 104:6362–6371
33. Kang J, Tokdemir S, Shao J, Nelson WH (2003) Electronic g-factor measurement from ENDOR-induced EPR patterns: malonic acid and guanine hydrochloride dihydrate. *J Magn Reson* 165:128–136
34. Yamamoto S, Back RA (1985) The photolysis and thermolysis of pyruvic acid in the gas phase. *Can J Chem* 63:549–553
35. Yamamoto S, Back RA (1985) The gas phase photochemistry of oxalic acid. *Can J Chem* 63:622–625
36. Back RA, Yamamoto S (1985) The gas phase photochemistry and thermal decomposition of glyoxylic acid. *Can J Chem* 63:542–548
37. Cao JR, Back RA (1986) The thermolysis and photolysis of malonic acid in gas phase. *Can J Chem* 64:967–968
38. Mosqueira FG, Albarran G, Negrón-Mendoza A (1996) A review of conditions affecting the radiolysis due to  $^{40}\text{K}$  on nucleic acid bases and their derivatives adsorbed on clay minerals: implications in prebiotic chemistry. *Orig Life Evol Biosph* 26:75–94
39. Draganic IG, Draganic ZD, Altiparmako D (1983) Natural nuclear reactors and ionizing radiation in the Precambrian. *Precambrian Res* 20:283–298

# The Possible Role of Hydrothermal Vents in Chemical Evolution: Succinic Acid Radiolysis and Thermolysis

J. Cruz-Castañeda<sup>1</sup>, M. Colín-García<sup>2</sup>, A. Negrón-Mendoza<sup>1\*</sup>

<sup>1</sup>*Instituto de Ciencias Nucleares, Universidad Nacional Autónoma de México, UNAM.  
Cd. Universitaria, A. P. 70-543, 04510 México, D. F. México*

<sup>2</sup>*Instituto de Geología, Universidad Nacional Autónoma de México,  
México, D.F., C.P. 04510, México*

**Abstract.** In this research, the behavior under a high radiation field or high temperature of succinic acid, a dicarboxylic acid clue in metabolic routes, is studied. For this purpose, the molecule was irradiated with gamma rays in oxygen-free aqueous solutions, and the thermal decomposition was studied in a static system at temperatures up to 90 °C, simulating a white hydrothermal vent. Our results indicate that a succinic acid is a relatively stable compound under irradiation. The gamma radiolysis yields carbon dioxide and di- and tricarboxylic acids such as malonic, carboxysuccinic, and citric acids. The main products obtained by the thermal treatment were CO<sub>2</sub> and propionic acid.

**Keywords:** gamma radiation, succinic acid, thermolysis, hydrothermal vents, chemical evolution.  
PACS: 82.50.-m, 82.30.Lp

## INTRODUCTION

The Earth since its formation has undergone and continues to undergo many changes. Probably one of the most important was the origin of life. This event occurred in the Precambrian period, at about 3.5 Ga, the date of the oldest fossils. Oparin and Haldane proposed that the origin of life could be understood based on abiotic physical and chemical events [1] and preceded by a preamble now known as chemical evolution. In this scenario, the presence of matter and energy was fundamental for the chemical reactions, which form organics that eventually generated the first system that could be considered alive.

Different energy sources could have formed organic compounds in the early Earth; one of the most important and conspicuous is thermal energy. Heat is widely distributed in volcanoes, volcanic hot springs, and the hydrothermal vent seabed [2, 3]. At these sites, the temperature gradients (from 90 to 400 °C) were relevant to prebiotic synthesis because the gradients could have provided the energy to promote chemical reactions [4]. Another type of energy source is high-energy radiation from radionuclides and cosmic radiation [5]. Ionizing radiation may have been of great importance to generate the chemical reactions that took place in the early Earth due to its high penetration, its efficiency in inducing the synthesis of organic compounds, and its abundance. Cosmic rays are another probable source of this type of energy [6, 7].

It has been suggested that life on our planet originated not only on the Earth's surface, but also in the oceans. This idea has prompted new proposals on the origins of life on Earth and other planets [8]. In the 1970s, the discovery of hydrothermal vent systems created the discussion; such vents were likely a suitable place for the synthesis of organic compounds through non-biological processes by Fischer-Tropsch type reactions. These reactions involve the participation of gases at high pressures and temperatures in the

presence of minerals such as carbonates, iron oxides, metal sulfides, and clays [9]. These sites could also have had high levels of radiation due to the presence of radioactive nuclides imbedded in minerals.

This research focuses on the study of the stability of succinic acid as an example of carboxylic acids related to metabolic routes, such as the Krebs cycle. This compound was exposed to high temperatures in addition to the presence of a gamma radiation field, and both energy sources can be found near hydrothermal vents.

## MATERIALS AND METHODS

### *Preparation of Material*

The glassware was treated with a mixture of HNO<sub>3</sub>/H<sub>2</sub>SO<sub>4</sub> (1:1) for 30 minutes at 30 °C, followed by an abundant rinsing with distilled water, and it was later heated in an oven (300 °C) overnight. This procedure was followed to avoid contamination of samples, eliminating all organic matter that could be present.

### *Preparation of Samples*

40 mL of an oxygen-free solution of succinic acid 0.1 mol.L<sup>-1</sup> (pH= 2.7) were placed in glass syringes for the irradiation experiments. For the experiments with thermal energy, 20 mL of the solution were placed in sealed glass culture tubes.

### *Irradiation of Samples*

The samples were irradiated in two <sup>60</sup>Co-gamma sources: Gammabeam 651 PT and Gammacell-200 at ICN-UNAM (Mexico). The dose was evaluated using a ferrous sulfate–copper sulfate dosimeter. The dose rate was 193 Gy/min, and samples were irradiated at different doses, from 46.29 to 277.78 kGy. The samples were analyzed immediately after irradiation.

### *Thermolysis Experiments*

Succinic acid aqueous solutions in a sealed culture tube (saturated with argon) were heated in an oven at 105 °C for 0.5, 1, 2, 4, 8, 12, 24, 72, and 100 h. After heating, the samples were cooled and analyzed by gas chromatography (GC).

### *Analysis of Non-volatile Products*



The carboxylic acids were analyzed as their methyl esters by GC in a Chromatograph Varian 3400 instrument with a flame ionization detector, using a glass column (1.82 m in length and an internal diameter of 4 mm) packed with Silar 7C.

Gas chromatography/mass spectrometry (GC-MS) was used to identify the reaction products. The instrument was a Gas Chromatograph HP-5890A with a capillary column filled with methyl silicon (12 m length and internal diameter of 0.2 mm).

### *Analysis of CO<sub>2</sub>*

Volatiles were analyzed by extraction using a Toepler gauge coupled to chromatograph Varian-1400 gas chromatograph equipped with a thermal conductivity detector. A stainless steel column (4 m in length and 3.2 mm outer diameter) packed with silica gel (mesh 40/60) was used, with helium as a carrier gas and at a flow of 30 mL/min.

## RESULTS AND DISCUSSION

### *Gamma Irradiation Experiments*

Many carboxylic acids were formed from the gamma-radiolysis of succinic acid in an oxygen free aqueous solution. They were identified by their retention times with GC and by their fragmentation pattern using GC-MS. The principal feature of succinic acid in the irradiation experiments was the dimer formation: 1, 2, 3, 4-butanetetracarboxylic acid. Succinic acid decomposition is dose-dependent (Fig. 1) with a  $G_0 = 4.6 \text{ mol.mL}^{-1}$

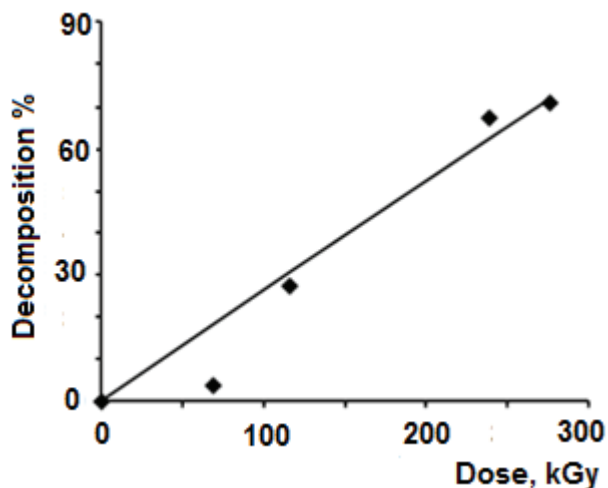


Figure 1. Succinic acid decomposition as a function of dose.

Figure 2 shows the gas chromatogram of methyl esters of carboxylic acids formed by gamma irradiation of succinic acid in an aqueous solution (the samples were analyzed in triplicate). The identified products are oxalic, malonic, malic, tricarballic, citric, and 1, 2, 3, 4-butanetetracarboxylic acids (succinic acid dimer). Malonic acid, an important inhibitor in the Krebs cycle, is formed at low and high doses, but in concentrations of about 1%. A similar case presents the citric acid, another important molecule for organisms.

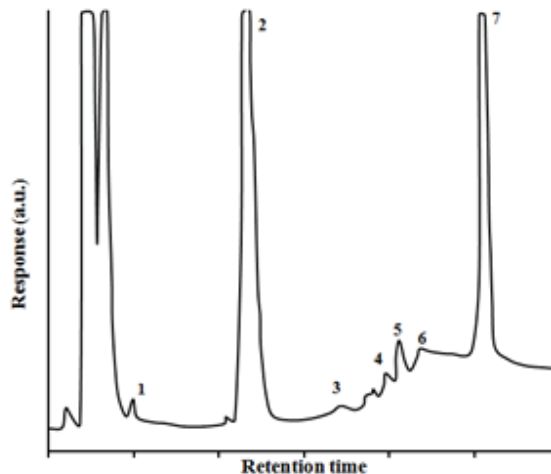
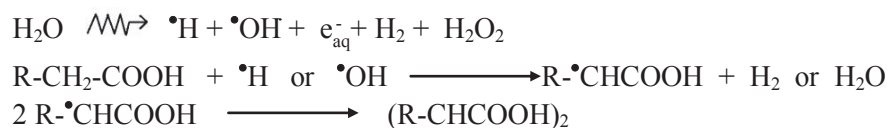


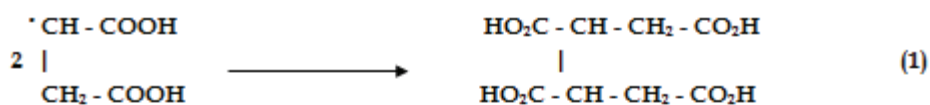
Figure 2. Gas chromatogram of methyl esters of carboxylic acids formed by gamma irradiation (69.4 kGy). (1) Malonic, (2) Succinic, (3) Malic, (4) 1, 2, 3-butanetricarboxylic, (5) Tricarballic + aconitic, (6) Citric (7) Dimer of succinic acid.

When ionizing radiation interacts with water, several phenomena occur. The first is physical and refers to interaction-matter radiation and energy transfer, causing excited molecules. These excited molecules are in turn capable of undergoing changes and reaching a steady state (the physicochemical stage) that results in the formation of highly reactive species (the chemical stage) [10]. In our system, when a diluted aqueous solution interacts with radiation, most of the energy is deposited in the water molecules, forming reactive radicals:

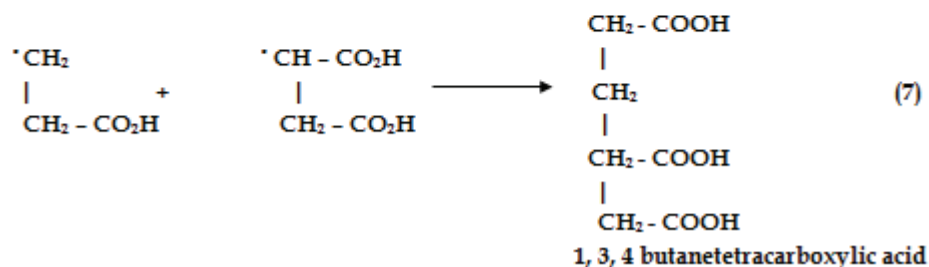
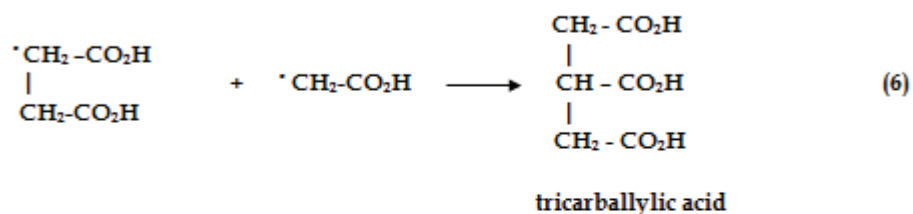
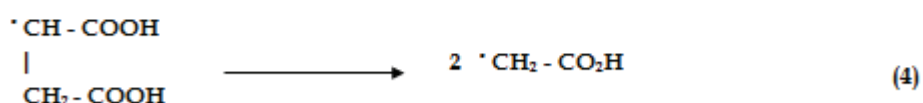
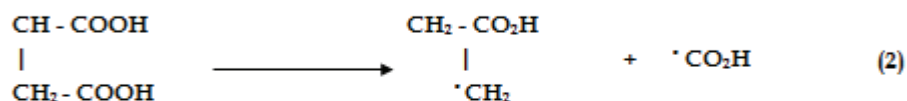




These radicals, through secondary reactions, react with the solute (succinic acid) and yield the observed products. For example, the following mechanism explains the dimer



1, 2, 3, 4 butanetetra-carboxylic acid (dimer)



formation:

Other products may be explained by reactions among the free radicals generated. Radiolysis produces a wide variety of non-volatile compounds with and without biological relevance, which means that if these reactions occurred close to hydrothermal vents, new products should have been available. However, depending on their stability under these conditions, they could have also been decomposed, generating other molecules, which in turn react with others.

Succinic acid appeared to be stable at high radiation doses, and it is formed under different prebiotic experiments, especially the radiolysis of Krebs cycle components [11]. This observation may be important, considering that succinic acid has been identified as one of the most abundant compounds in carbonaceous chondrites [12].

### *Thermolysis Experiments*

In the thermolysis at 105 °C, the decarboxylation is the main reaction, generating propionic acid and carbon dioxide as the more abundant products. Figure 3 shows the MS-fragmentation spectrum for propionic acid and the following reactions shows the proposed mechanism:

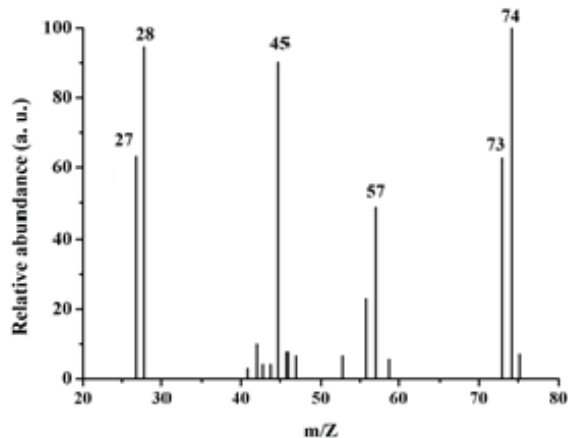
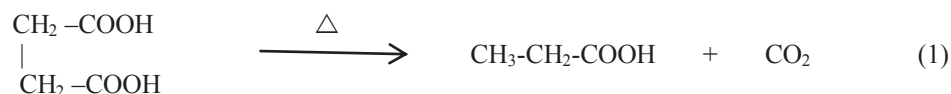


Figure 3. MS fragmentation pattern of propionic acid, product of the thermolysis of succinic acid.

These and previous experiments [11, 13] demonstrated that carboxylic acids can undergo interconversion in other members of the Krebs cycle, enhancing their importance in prebiotic processes. Due to this property, a single acid can yield several others, just by the action of an energy source. Another essential feature is that carboxylic acids can also be transformed into other molecules, such as amino acids, through a combination of their ammonium salts.

### **REMARKS**

In the early Earth, energy must have been essential for the reactions to take place during the period of chemical evolution in which simple molecules led to those that are more complex. The results presented in this paper focus on the role of ionizing radiation and heat as important sources of energy for prebiotic processes. Regardless of the nature of this energy (radiation or heat), it can induce chemical changes in organics, as in the case of succinic acid.

Within a hydrothermal vent, heat must be fundamental, but radiation is also important because radionuclides are included in minerals associated with these places, and the level of radiation was three to four times higher than at the present [13]. Radiolysis can generate a wide variety of compounds; these could have been the new raw materials for subsequent reactions.

## ACKNOWLEDGMENTS

This work was supported by PAPIIT grant No. IN110513 and the CONACyT Grant No. 168579/11. J.C. was supported by a CONACyT fellowship. We thank the Posgrado en Ciencias Químicas, UNAM; and Mr. Saúl Villafañe, M. Sc. Benjamin Leal, and Phys. Francisco García, for their technical support.

## REFERENCES

1. Lal, A., Origin of Life, *Astrophys Space Science* 317, 267–27, (2008).
2. Lathe, R., Fast Tidal Cycling and the Origin of Life, *Icarus* 168, 18-22, (2004).
3. Russell M., and Hall, A.J., The Emergence of Life From Iron Monosulphide Bubbles at a Submarine Hydrothermal Redox and pH Front, *J. Geol. Soc. London* 154, 377-402, (1997).
4. Muller A.W.J., and Schulze-Makuch D., Thermal energy and the origin of life, *Origins of Life and Evolution of the Biosphere* 36, 177-189, (2006).
5. Draganic, I. G., and Draganic Z. D., Radioactivity and Radiation-Chemistry on the Early Earth. *Lectura plenaria en el Segundo Simposium de Química Nuclear, Radioquímica y Química de Radiaciones, México*, (1978).
6. Negrón-Mendoza, A., and Albarrán, G., Chemical effects of ionizing radiation and sonic energy in the context of chemical evolution In: *Chemical Evolution. Origin of life*, 147-235, (1993).
7. Draganic, I., Bjergbake, E., Draganic, Z., and Sehested, K., Decomposition of ocean archean waters by  $^{40}\text{K}$  radiation 3800 Ma ago as a source of oxygen and oxidizing species. *Precambrian Res.*, 52, 337-345, (1991).
8. Wächtershäuser, G., Before enzymes and templates: Theory of surface metabolism, *Microbiological Rev.* 52, 452-84, (1988).
9. Miller, S.L. Bada, J.L., and Friedmann N., What Was the Role of Submarine Hot Springs in the Origin of Life? *Origins of Life and Evolution of the Biosphere* 19, 536-537, (1989).
10. Donnell, O., and Sangster, J., *Principles of Radiation Chemistry*. United Kingdom: Edward Arnold, (1970).
11. Ramos-Bernal, S. and Negrón-Mendoza, A., Radiation Heterogeneous Processes of  $^{14}\text{C}$ -Acetic Acid Adsorbed in Na-Montmorillonite. *Journal of Radioanalytical and Nuclear Chemistry* 160, 487-492, (1992).
12. Peltzer, E. T., Bada, J. L., Schlesinger, G. and Miller, S. L., The chemical conditions on the parent body of the Murchison meteorite: Some conclusions based on amino, hydroxy and dicarboxylic acids *Advances in Space Research* 4, 69-74, (1984).
13. Negrón-Mendoza, A. and Ponnampuruma, C., Intercoversion of biologically important carboxylic acids by radiation. *Origin of life; Second ISSOL Meeting and Fifth ICOL Meeting; April 5-10, 1977; Center for Academic Publications Japan Tokyo*, 101-104, (1978).

# Formation of Hydrocarbons from Acid–Clay Suspensions by Gamma Irradiation

J. Cruz-Castañeda, A. Negrón-Mendoza\*, S. Ramos-Bernal

*Instituto de Ciencias Nucleares, Universidad Nacional Autónoma de México, UNAM.  
Cd. Universitaria, A. P. 70-543, 04510 México, D. F. México*

**Abstract.** The adsorption of certain organic compounds by clays gives rise to the transformation of the adsorbate through the action of the clays. This phenomenon can be enhanced using ionizing radiation. In this context, these kinds of reactions play an important role in many natural and industrial processes. For example, in oil and gas exploration, the source and trap of petroleum hydrocarbons is frequently clay-rich rocks. Clay–water-based muds are also seen as environmentally friendly alternatives to toxic oil-based fluids.

The principal processes that occur in sediments are usually held to be of bacterial action and thermal transformation, which may include thermally induced catalytic alteration of the organic debris. On the other hand, radioactive materials are widely distributed throughout Earth. They were more abundant in the past, but are present in petroleum reservoirs. Their presence induced radioactive bombardment, which may have altered these sediments. This important subject has not been extensively studied.

The aim of this work is to study the behavior of fatty acids—like behenic acid—and dicarboxylic acids—like fumaric acid—as model compounds, which are adsorbed in a clay mineral (Na-montmorillonite) and exposed to gamma radiation. The results show that the radiation-induced decomposition of the clay–acid system goes along a definitive path (oxidation), rather than following several modes of simultaneous decomposition, as happens in radiolysis without clay or by heating the system. The main radiolytic products for fatty acids are their corresponding hydrocarbons, with one C-atom less than the original acid.

**Keywords:** clay minerals, gamma radiation, hydrocarbon, carboxylic acids  
PACS: 82.50.-m, 82.30.Lp

## INTRODUCTION

Fatty acids are abundant organic compounds in sediments. The decarboxylation of fatty acids into hydrocarbons catalyzed by clay minerals has been proposed as a possible pathway for the conversion of lipids into petroleum hydrocarbons. The thermal decomposition of fatty acids in the presence of clay minerals has been studied by several investigators [1]. Although the adsorption of fatty acids by clay minerals is an important geochemical reaction, very little is known about its mechanisms. The adsorption of fatty acids from aqueous solutions in clays (which depends on the pH of the system) is mainly due to their interactions with the edges of clay pellets.

On the other hand, radioactive materials are widely distributed throughout Earth but were more abundant in the past [2]; they are present in petroleum reservoirs. In this geological condition, the action of high energy radiation affects the organic material present. Thus, the behavior of certain organic compounds adsorbed onto clays gives rise to the transformation of the adsorbate by the action of clays and can be enhanced through ionizing radiation.

In this paper, we simulated a geological environment in which an organic compound adsorbed onto a clay mineral is exposed to a high energy source or a thermal process. Our aim is to enhance the decarboxylation of fatty acids via the irradiation of the system's fatty acid–clay and compare these results with that of the decomposition induced by heating. The study of the lipid fraction of biological material in sediments is important in organic geochemistry because lipids may be considered as a major precursor of petroleum.

## MATERIALS AND METHODS

### Preparation of Material

Since the presence of impurities in samples that are irradiated can give rise to critical errors, all chemical and glassware were handled in ways that minimized contamination. The glass materials were treated with a warm

RADIATION PHYSICS

AIP Conf. Proc. 1544, 49-52 (2013); doi: 10.1063/1.4813459  
© 2013 AIP Publishing LLC 978-0-7354-1169-2/\$30.00

mixture of HNO<sub>3</sub> and H<sub>2</sub>SO<sub>4</sub> for 30 minutes, followed by a wash with distilled water and heating in an oven at 300 °C overnight.

The clay used in each reaction (SWy-1 sodium montmorillonite) was obtained from the Clay Minerals Repository of the Clay Minerals Society at the University of Missouri, which was sterilized by autoclaving at 2 Kg/cm<sup>2</sup> for 30 minutes at 121 °C.

#### *Preparation of the Mono-cationic Clays (Na<sup>+</sup> and Fe<sup>3+</sup>)*

The mono-cationic clays were prepared by ion exchange. For these purposes, solutions of FeCl<sub>3</sub>·5H<sub>2</sub>O and NaCl with 1 N concentration were prepared and mixed with clay, in order to exchange the cation present for the desired cation. The montmorillonite used has an ion exchange capacity of 101 meq of Na<sup>+</sup> / 100 g of clay. The procedure used to prepare the Na<sup>+</sup> and Fe<sup>3+</sup> clays was the same; 10 g of clay were mixed with 100 ml of the corresponding dissolution in continuous agitation on a plate at 120 rpm for 30 min. Then, the sample was centrifuged at 10,000 rpm for 10 minutes and was washed with distilled water and deionized water several times; finally, it was dried in an oven at 50 °C for 24 hours. X-ray diffraction was used to characterize the clay.

Samples were prepared with 500 mg of mono-cationic clay mixed with 50 mg of behenic acid or fumaric acid in a closed culture tube, saturated with argon and then irradiated at room temperature for different doses

#### *Analysis of Linear Hydrocarbons and Carboxylic Acids*

The hydrocarbons were analyzed by gas chromatography (GC). We used a gas chromatograph Alltech SRI8610C with flame ionization detector, with a capillary column MXT – (length of 30 m). The temperature program was from 100 to 200 °C at 10 °C/min, followed by an isotherm of 200 °C for 40 minutes, the gases used were: nitrogen (carrier gas) 10 ml/min, 25 ml/min hydrogen and air 250 ml/min. In order to determine and possibly quantify linear hydrocarbons, two pattern curves were prepared: one to identify the hydrocarbons formed (carbon number vs. retention time), and the second to quantify the identified hydrocarbons (area vs. concentration). Standards for pure hydrocarbons from C10 to C22 in concentrations from 10<sup>-2</sup> to 0.2 M were used.

The carboxylic acids were analyzed as their methyl esters by gas chromatography [4]. Gas chromatography/mass spectrometry was used to determine the reaction products and confirm the structure of each compound.

#### *Irradiation of Samples*

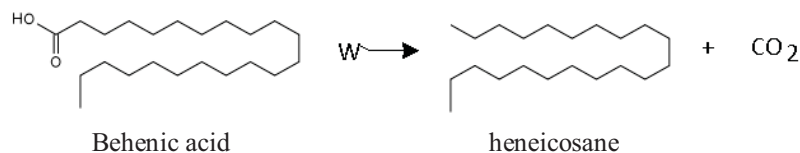
The samples were irradiated in <sup>60</sup>Co gamma irradiator (Gammabeam 651 PT) at ICN-UNAM. The dose was evaluated using an iron sulfate–copper sulfate dosimeter. The dose rate was 143 Gy/min for the experiments with behenic acid and the samples were irradiated at different doses (0 to 62 kGy). Fumaric acid was irradiated from 0 to 363 kGy at 189 Gy/min and was analyzed immediately.

#### *Thermolysis experiments*

Behenic acid samples (50 mg) were mixed with the clay (500 mg), in a closed culture tube (saturated with argon), and were heating in an oven at 250 °C for 0.5, 1, 2, 4, 8, 12, 24, 96, 480, and 960 hours. After the samples were cooled and analyzed by GC. For fumaric acid the samples were heated at 180°C from 0.5 to 120 h.

## **RESULTS**

The principal feature of the experiments with behenic acid by thermolysis or irradiation was to observe the decarboxylation reaction of the acid, as the principal method of decomposition for the target compound, by forming a hydrocarbon with one carbon atom less and CO<sub>2</sub>.



In the radiolysis other hydrocarbons with small numbers of carbon atoms were also formed. In the presence of clay, the number of products decreased (9 for the Na-montmorillonite and 4 for Fe-montmorillonite), while 13 products were formed in the system without clay. However, the decomposition of the target compound was higher in the system without clay. Figure 1 show the formation of the C-21 hydrocarbon from the irradiation of behenic acid in solid state.

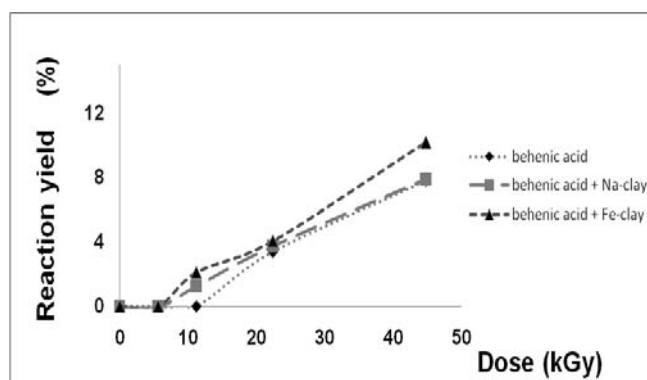


Figure 1. Formation of heneicosane (C21) from the irradiation of behenic acid

The decomposition induced by radiation of behenic acid is shown in Figure 2.

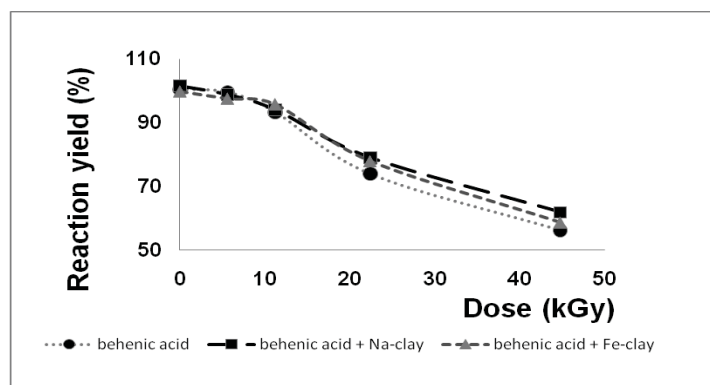
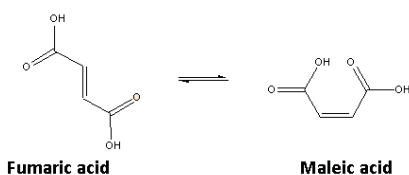


Figure 2. Decomposition of behenic acid induced by gamma radiation.

For the thermolysis experiments the formation of C21 hydrocarbon was very low, for the samples heated 960 h the yield was 4.1 % in the presence of Fe-montmorillonite and the C21 was not formed without clay. In the case of fumaric acid, a dicarboxylic acid, the main pathways of the reaction were the decarboxylation and isomerization reaction. The product formed by isomerization is maleic acid: Table 1 show some features of these experiments.



As shown in Table 1, the number of products in the presence of the clay is less than in the system without the clay. Figure 3 show the decomposition of fumaric acid after heating the samples at 250 °C.

**TABLE 1.** Radiation-induced decomposition of fumaric acid (62 kGy)

System	Fumaric acid	Fumaric acid + Na-montmorillonite
Main reaction	decarboxylation	decarboxylation
Other products	2	1
Products	✓maleic acid ✓succinic acid	✓maleic acid
Remaining acid	60.6 %	53.7 %

In this case the decomposition in the presence of clay was very high and the number of products is increased

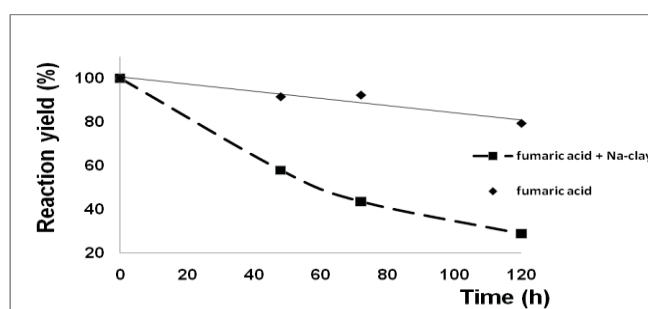


Figure 3. Thermolysis of Fumaric Acid at 180 °C during 120 h

## REMARKS

The results showed that radiation-induced reactions in carboxylic acids are an example of preferential synthesis, when adsorbed onto a solid surface. The presence of a solid surface alters the formation and distribution of radiolytic products, as fewer products are formed. In the case of thermal treated samples, the number of products is higher. The irradiation of the clay–acid system goes along a definitive path (oxidation), rather than following several modes of simultaneous decomposition. This behavior is important for petroleum genesis because solid surfaces can drive the reaction towards a more preferable path. These experiments prove that non-random products are produced under plausible geological conditions. These results appear to support the hypothesis that radiation and clays played a role as natural catalysts in the genesis of petroleum. The present study was a further attempt to gain more insight into the role played by radiation-induced reactions in solid surfaces and to compare them with thermal decomposition.

## ACKNOWLEDGMENTS

This work was supported by PAPIIT Grant No. IN110712-3 and CONACyT Grant No. 168579/11. We thank Posgrado en Ciencias Químicas-UNAM. The technical support from C. Camargo, B. Leal, and F. García-Flores is also acknowledged.

## REFERENCES

1. W.D. Johns, *Ann. Rev. Earth Planet. Sci.* 7, 183 (1979).
2. A. Negrón-Mendoza, and S. Ramos, The role of clays in the origin of life, in ed. J. Chela-Flores, G. Lemarchand and J.. Oró, Kluwer Academic Publisher Amsterdam, pp. 183-194, 2004.
3. A. Negrón-Mendoza, and C. Ponnemperuma, *Photochem. Photobiol.* 36: 595-597 ( 1982).